University of South-Eastern Norway

www.usn.no

FMH606 Master's Thesis 2021

EET

Recommended guideline for allocation simulation

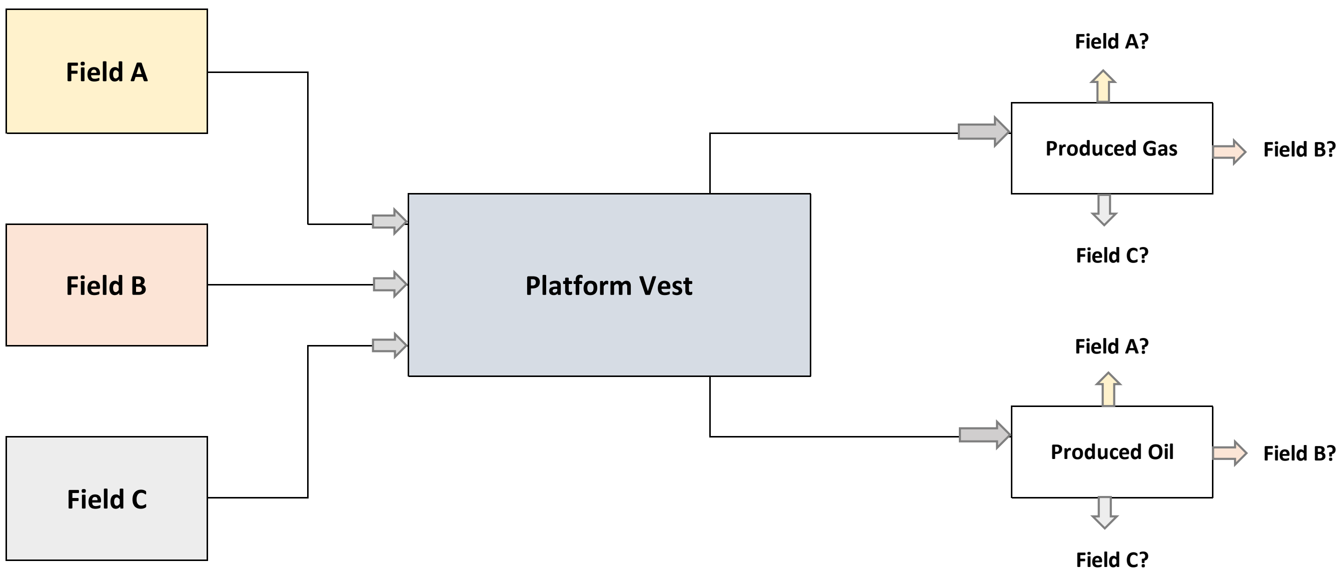

Madelen Smedsli

Faculty of Technology, Natural Sciences and Maritime Sciences
Campus Porsgrunn

University of South-Eastern Norway

www.usn.no

Course: FMH606 Master's Thesis, 2021

Title: Recommended guideline for allocation simulation

Number of pages: 93 + Appendices

Keywords: Allocation, UniSim, ProMax, PVTsim

Student: Madelen Smedsli

Supervisor: Britt M. E. Moldestad

External partner: Equinor ASA, Trine Amundsen Madsen

Availability: Open

Summary:

A platform often has oil and gas production from more than one field. The determination of how much oil and gas originates from the different fields is called allocation. The platform studied in this report is called Platform Vest, located in the North Sea, with production from field A, field B (high GOR) and field C (low GOR). The current allocation method for Platform Vest is based on oil recovery factors (ORF) for each component. Other allocation methods evaluated are allocation by difference, process simulation and pro-rata allocation.

The main objective for the report is to recommend the most fair and prudent allocation for Platform Vest and allocation in general.

The objective is studied using different process simulations created in UniSim and ProMax, with varying fluid characterisations (obtained from PVTsim) and different process input parameters and utilities.

When comparing the different allocation methods, the current established ORF method was the method that gave the fairest allocation of gas and oil to the different fields, especially when considering the different GOR values of the fields.

Inclusion of aromatics in the fluid characterisation and the case using the ProMax model gave the highest deviation from the initial case when comparing the estimated ORFs. Both cases should be investigated further to determine the impact this can have on the allocation.

In conclusion, the newest fluid characterisation and up-to-date process input (a process simulation will never be more accurate than the accuracy of the input parameters) should always be used when possible. The C20+ lumping and the allocation utility method can be safely used with the ORF estimation with approximately the same result as the initial case. The C10+ lumping scheme can be considered for ORF estimation without too large deviations from the initial case.

Preface

This Master's thesis is written as the result for the FMH606 course at the University of South-Eastern Norway, Faculty of Technology, Natural Sciences and Maritime Sciences (TNM) at campus Porsgrunn. The thesis is written in collaboration with Equinor ASA as an external partner, and Trine Amundsen Madsen as an external supervisor representing the company.

I would like to thank Trine Amundsen Madsen at Equinor for the opportunity to write my thesis in collaboration with them, and for the great supervision and guidance she has given throughout the thesis work.

I would also like to thank Britt M. E. Moldestad for great supervision and help during the thesis work.

The scope of work for this thesis is given in Appendix A – Scope of work.

Porsgrunn, 19.05.21

Madelen Smedsli

Contents

Table of figures

Nomenclature

Symbol	Description
B_n	Estimated quantity to user n [ton/h]
c	Volume correction [m^3/mol]
EOS	Equation of state
GL	Gas lift
GOR	Gas-oil-ratio
$m_{AG, i}$	Allocated gas for component i [ton/h]
$m_{AO, i}$	Allocated oil for component i [ton/h]
$m_{GB, i}$	Gas basis for component i [ton/h]
$m_{HC, i}$	Hydrocarbon inflow of component i [ton/h]
m_{IBG}	Gas imbalance [ton/h]
m_{IBO}	Oil imbalance [ton/h]
$m_{OB,i}$	Oil basis for component i [ton/h]
$m_{oil,i}$	Oil flow of component i in the export [ton/h]
m_{TG}	Total gas export, dry basis [ton/h]
m_{TO}	Total oil export, dry basis [ton/h]
n	Moles [mol]
ORF	Oil recovery factor [%]
P	Pressure [Pa]
P_c	Critical Pressure [Bar]
PNA	Paraffin, naphthene and aromatic
PVT	Pressure, volume and temperature
Q	Total quantity to be allocated [ton/h]
Q_1	Quantity allocated to user 1 [ton/h]
Q_2	Quantity allocated to user 2 [ton/h]
Q_n	Quantity allocated to user n [ton/h]

R	Gas constant [J/°K*mol]
T	Temperature [°C]
$\mathbf{T_c}$	Critical Temperature [°C]
$\mathbf{T_r}$	Reduced temperature [°K]
UBA	Uncertainty based allocation
V	Volume [m^3]
$\hat{V}$	Molar volume [m^3/mol]
$\hat{V}_t$	Translated molar volume [m3/mol]
VF	Vapour fraction [-]
$\mathbf{Z_{RA}}$	Rackett compressibility factor [-]
ω	Acentric factor [-]

1 Introduction

Offshore oil and gas platforms are costly installations with a long-life expectancy, typically 20 to 30 years [1, p.12]. It is, therefore, expected that one platform has oil and gas production from more than one field. If fields are coproducing over one platform, it is essential to understand the commingling effects and how this will affect the total production from the different fields. The determination of how much oil and gas originates from the different fields is called allocation. [2]

Different methods can be used to allocate the oil and gas products, including process simulation, allocation by difference and pro-rata allocation. The most important aspect is that the allocation is fair and prudent for all the different producers and owners on the platform.

The platform used for the cases in this report is called Platform Vest. This platform, located in the North Sea, has production from three fields, all having different owners.

Figure 1.1 shows a simple overview of Platform Vest. The platform produces oil and gas from fields called field A, field B and field C. The outflow streams from the platform are fuel gas, flare gas, export gas, export oil and produced water. The gas lift to field B and field C is provided from Platform Øst. The fuel and flare gas are set to zero in this scope for simplifications, meaning that the total produced gas is the gas export stream.

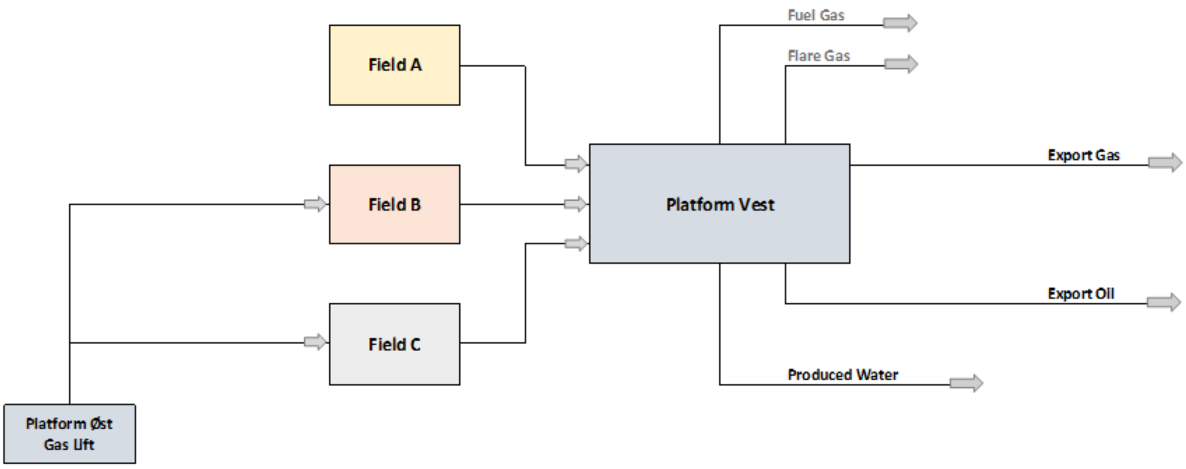

Figure 1.1: Simple overview of Platform Vest

The main objective of this report is to investigate and recommend the most fair and prudent allocation for Platform Vest and allocation in general. The fluid characterisations for the different fields are studied using PVTsim, and phase envelopes are generated. Different simulation models are built using the simulation software UniSim, to investigate the effect variations in the fluid characterisation and setup will have on the simulated results. A simple simulation model is also built with the simulation software ProMax and compared to a simple case in UniSim, to study differences between the software.

The current allocation agreement for Platform Vest is based on ORFs (oil recovery factors) obtained from standalone simulations for each field. The ORFs obtained from the different cases is thus essential parameters to study and compare. Other allocation methods are also evaluated and compared to the current allocation agreement for Platform Vest.

This report contains 8 chapters. The first chapter is the introduction.

Chapter 2 gives a description of Platform Vest, the different fields, and the process description.

Chapter 3 includes theory on allocation in general, different allocation methods and a description of the current allocation agreement for Platform Vest.

Chapter 4 includes the fluid characterisation for the different fields, a description of the selected equation of state, the phase envelopes, and an introduction to the software PVTsim.

Chapter 5 includes theory on the simulation software UniSim, and how it is used for allocation.

Chapter 6 includes theory on the simulation software ProMax, and how it is used for allocation.

Chapter 7 includes the results for the different cases and discussion around them. A recommended guideline based on the results from the different cases is also included in the last chapter.

Chapter 8 includes the conclusion of the report.

2 Platform Vest

Platform Vest is a platform located in the North Sea with gas and condensate production from three different fields. These fields are called A, B and C. After arriving on the platform, the three fields are commingled together and separated into gas and condensate for export out of Platform Vest. A platform with condensate production needs to be able to handle gas, condensate, and water. The difference between condensate and oil is that condensate is technically gas that has gone from the vapour phase to the liquid phase due to cooling. This condensation process happens when the fluid enters the platform. The downside related to condensate is that it is a much more unstable fluid than oil; therefore, it is essential to stabilise the condensate as much as possible before it is exported from the platform. [3]

To be able to produce from a field, the pressure in the reservoir needs to be adequate to lift the fluid from the reservoir to the platform. As a reservoir is producing, the reservoir pressure will decrease due to the reduction of the total fluid amount in the reservoir. If the production flow should be kept at a sufficient level, there is a need for artificial driving forces to the production. Two efficient methods used for oil recovery are water injection and gas injection. [4] With water injection, water is inserted into the reservoir to increase the reservoir pressure. Gas injection uses the same principle only with inserting gas instead of water. [5]

2.1 The fields

Platform Vest has production from three different fields. These fields are further described in the sections below.

2.1.1 Field A

The A field was the initially intended producer on Platform Vest and is the oldest field to produce on the platform of the three fields. The field is produced by pressure depletion, meaning that the pressure in the reservoir is the driving force to get the fluid from the reservoir and up to the platform. [3] The reservoir is a high-pressure and high-temperature reservoir and is at a depth of 4600 metres. The A field’s production is in the tail phase, meaning that the recovery from the fields is declining each year. The field is a gas and condensate field, but the condensate is sold as oil. The typical GOR (gas-oil ratio) value for field A is 2500 Sm^3/Sm^3. Equinor is the owner of 55% of the field, while Company A, Company B and Company C own 20%, 19% and 6%, respectively. [6]

2.1.2 Field B

The B field was the second field to produce on Platform Vest together with Field A. The B field produces by pressure depletion and gas cap expansion, meaning that the gas above the oil in the reservoir will expand and put pressure on the oil. The field has previously produced with water and gas injection. Field B is also equipped with a gas lift (provided from Platform Øst), a process where compressed gas is injected into the production stream from the reservoir to lift the oil up to the surface. [7] The reservoir is at a depth of 3500 metres. The field is a gas, condensate, and oil field with high GOR (typically 5000 Sm^3/Sm^3). Equinor is the owner of 59% of the field, while Company C and Company B own 23% and 18%, respectively. [6]

2.1.3 Field C

The C field is the latest field to join the production on Platform Vest. The C field produces by water injection and is also equipped with a gas lift (provided from Platform Øst). The reservoir is at a depth of 3800 metres. The field is a gas and oil field with low GOR (typically 120-130 Sm^3/Sm^3). In this field, Equinor is not an owner. Field C is owned by Company D, Company A and Company E with 50%, 30% and 20% shares, respectively. [6]

2.2 Process description

The products from field A, B and C are arriving at Platform Vest from the different reservoirs. The fluid from field B and C are combined at the inlet manifold, while the field A fluid are routed to the test manifold. Initially, the platform had only production from field A, and later field A and field B together; the platform has thus not the capacity to route all the field streams to the same separator. Field A is permanently routed through the test separator, so that field B and C can be combined in the inlet separator. Field B is a high GOR field, and field C is a low GOR field; the commingled stream will try to adjust these differences. This can result in field C getting less of the products out in the oil export when producing together with field B. Field B can, on the other hand, get more of the products out in the oil phase when producing with field C.

The naming of the process equipment is based on the NORSOK standard [8]. The prefix 20 means that the purpose of the equipment is to separate and stabilise the fluid, prefix 21 means crude handling, prefix 23 is gas recompression and scrubbing, 24 means gas treatment, and 27 is gas pipeline compression. The item function codes used are VA for separators, VE for columns, VG for scrubbers, HA for shell and tube heat exchangers, HB for plate heat exchangers, HJ for printed circuit heat exchangers, KA for centrifugal compressors and PA for centrifugal pumps.

Achieving good separation between the liquid and gas phase is accomplished with the use of multiple separation stages. The different stages in the separation process will have decreasing pressure to ensure high stability of the gas and liquid leaving the last separator. Three-stage separation is most common for the separation of fields with medium to high GOR and moderate inlet pressure. The three-stage separation process is also seen as the most optimum for instalment cost. The gas streams out of the second and third stage separators need to be recompressed to meet the pressure of the first stage separation. [9, p. 197-198] A more thorough process description is described in the sections below.

The first separation stage is shown in Figure 2.1 [10]. The inlet separator (20VA001) and the test separator (20VA004) are both 3-phase-separators which separates the gas at the top, the condensate in the middle, and the water out at the bottom. The condensate downstream of the inlet separator is heated to the desired temperature in a heat exchanger (20HA101). This is to separate water and gas from the oil in a more efficient way. The heated commingled stream is then mixed with the test separator's condensate in the mixer (MIX-107). [3]

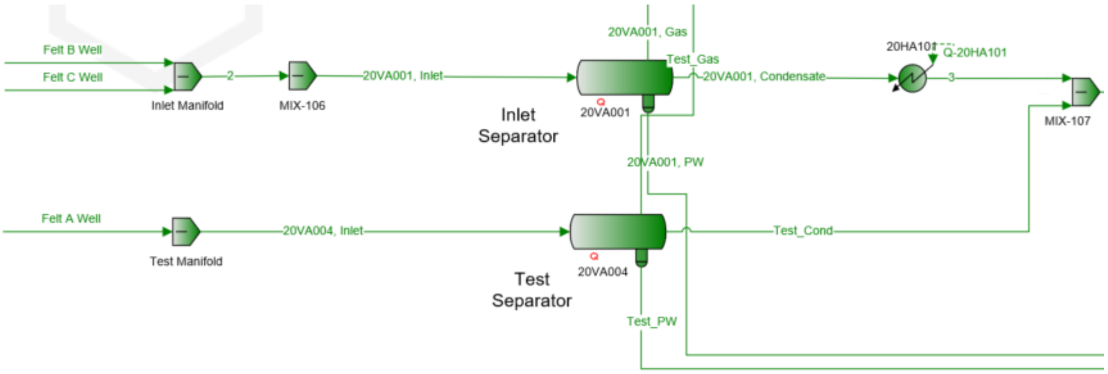

Figure 2.1: Illustration of the first separation stage

The second and third stage separation process is illustrated in Figure 2.2 [10]. The mixed stream with both condensate streams is then routed to the second stage separator (20VA002). The second stage separator is a two-phase separator that separates the gas at the top and the liquid out at the bottom. The second stage separator operates at a lower pressure than the inlet and the test separators. The second stage liquid outlet is then routed to the third stage separator (20VA003), a three-phase separator operating at an even lower pressure than the second stage separator. This separator separates the remaining water at the bottom, the gas out in the top and the condensate out in the middle. [3]

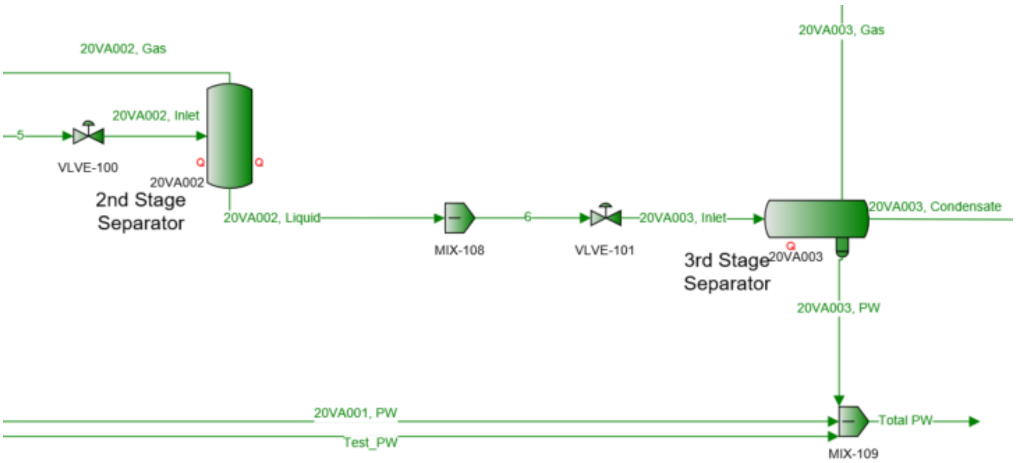

Figure 2.2: Illustration of the second and third separation stage

The outlet condensate stream from the third stage separator is then heated and pumped to meet the condensate export specification, as shown in Figure 2.3 [10].

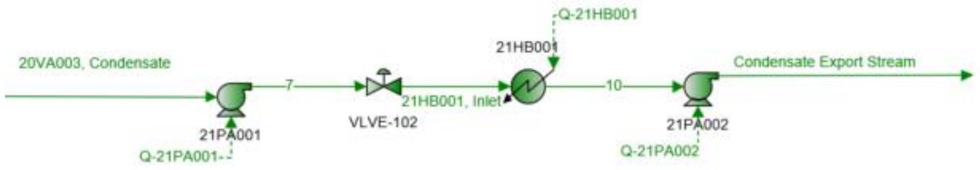

Figure 2.3: Illustration of the condensate export

The first and second stage recompression is illustrated in Figure 2.4 [10]. The gas out of the third stage separator is cooled (23HB001) and routed through a scrubber (23VG001) that separates the liquid from the vapour. The liquid out of the first scrubber is pumped (23PA 001) and mixed into the inlet stream to the third stage separator. The vapour out of the first scrubber is compressed (23KA001) and cooled (23HB002) right after to remove the heat of compression from the fluid. This is called the first stage of recompression. The fluid is then routed through a second scrubber (23VG002) to remove even more liquid from the vapour. The liquid out of the second scrubber is mixed into the inlet stream to the third stage separator. The vapour out of the scrubber is compressed (23KA002) to meet the outlet vapour pressure of the second-stage separator. This is the second stage of recompression. The vapour from the second stage separator is mixed (MIX-110) with the second stage recompression vapour. [3]

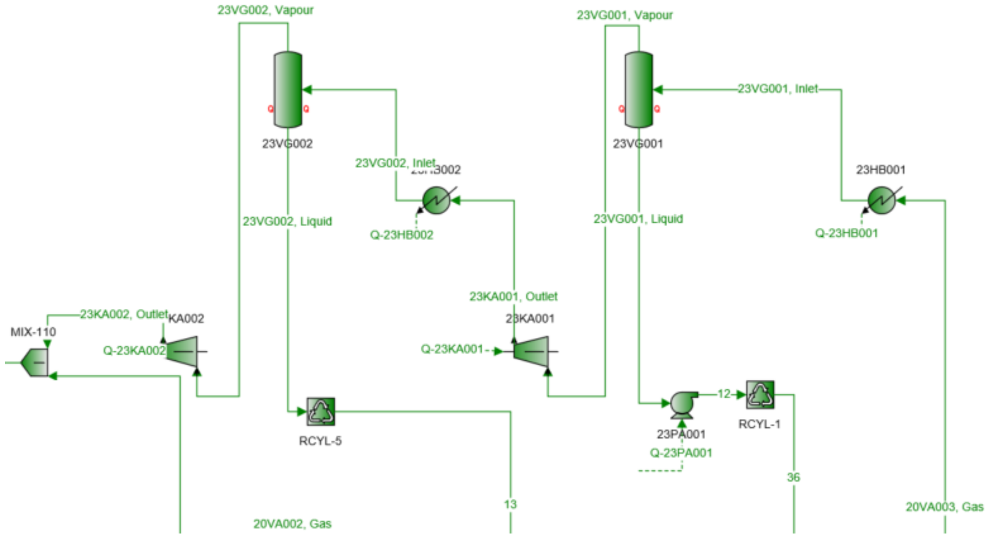

Figure 2.4: Illustration of the first and second recompression stage

The third stage of recompression is illustrated in Figure 2.5 [10]. The combined stream, including the second recompression stage vapour and the second stage separator vapour, is cooled (23HJ001) and routed through a third scrubber (23VG003) to remove even more of the liquid from the vapour. The liquid from the third scrubber is pumped (23PA002) and mixed into the inlet stream to the second stage separator. The vapour out of the third scrubber is compressed (23KA003). [3]

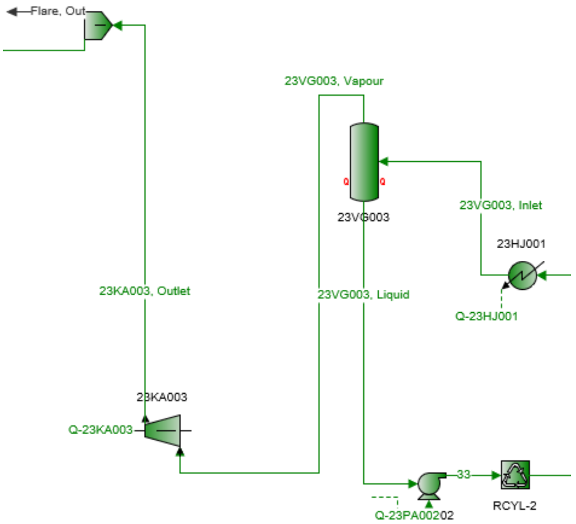

Figure 2.5: Illustration of the third recompression stage

The low-pressure recompression is illustrated in Figure 2.6 [10]. The vapour out of the inlet separator and the test separator are combined, and the mixed stream is cooled (23HJ600) and routed through a scrubber (23VG600) to remove the liquid from the vapour. The liquid out of the scrubber is mixed into the inlet stream to the second stage separator. The vapour out of the scrubber is compressed (23KA600) to meet the third stage recompression vapour. This is called low-pressure compression. The vapour out of the low-pressure compression and the third stage recompression are mixed (MIX-112) and then cooled (24HJ001) before being routed through another scrubber (24VG001) for additional liquid removal from the vapour. The liquid stream from this scrubber is mixed into the inlet stream to the inlet separator. [3]

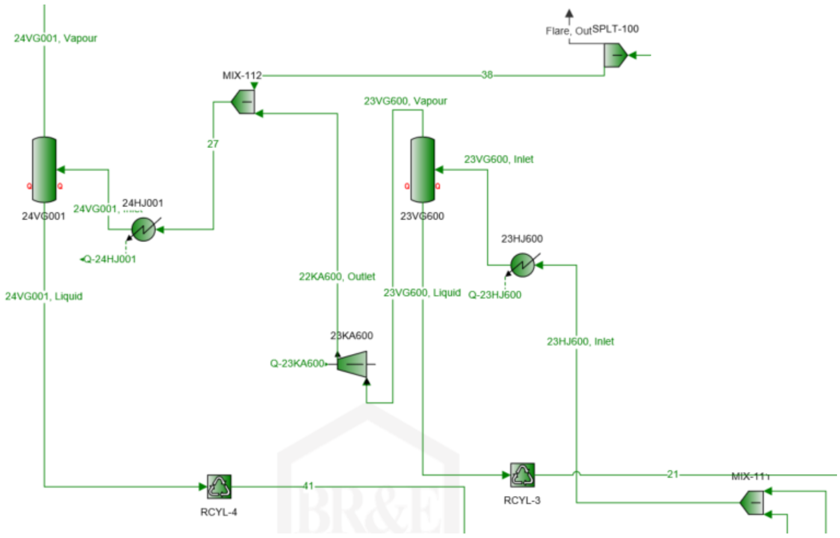

Figure 2.6: Illustration of the low-pressure compression

The final step in the process is illustrated in Figure 2.7 [10]. The vapour stream is cooled (24HA001) and dried from the remaining water. Gas drying methods could include adsorption or absorption with, for instance, glycol. [3] The dried gas is then cooled (27HJ001) before it is sent to the last scrubber (27VG001), where the last bit of liquid is separated out. The liquid outlet from this last scrubber is mixed into the inlet of the second stage separator. The gas outlet is compressed (27KA001) and cooled (27HJ002) to meet the gas export specifications. [3]

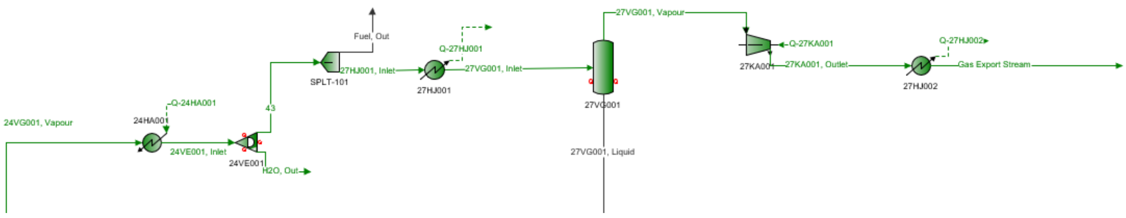

Figure 2.7: Illustration of the gas export

A total illustration of the process on Platform Vest is illustrated in Figure 2.8. [10].

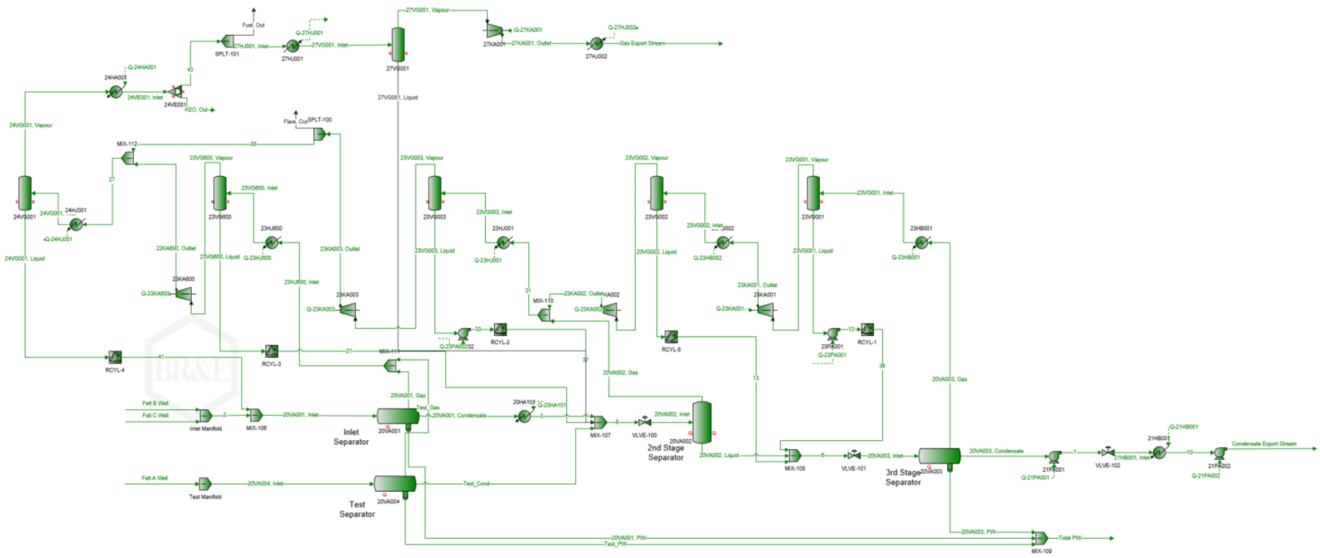

Figure 2.8: Illustration of the total process on Platform Vest

Phase envelops for each field is given in Chapter 4.3 to better illustrate the effect the different pressures and temperatures have on each fluid.

3 Allocation

The fluid that comes out of a reservoir is a mixture of gas, oil, and water. The exact amount of gas and oil cannot be determined until the fluid is separated at a platform. On the platform, the export gas and export oil can be measured.

An offshore platform is a costly installation to install for gas and oil separation. Therefore, it is expected that one single platform produces from more than one field. When a platform has production from several fields, it is hard to accurately know how much of the produced oil and gas is from a specific field. The determination of which field the produced gas and oil is from is called allocation. [11]

An offshore platform is often built initially to produce from a few known fields, but often newer fields are routed to the existing platform. This can lead to restrictions for allocation options and platform installation modification. Which can further lead to higher uncertainties in measured values. [11]

The allocation practice may seem like a straightforward process, but the implementation is often a complex matter. Getting the allocation as accurate and fair as possible is a common problem. The allocation result is a function of the input data, meaning that the allocation's quality depends on the uncertainty of the input data. Different types of allocation methods are presented in the next section. [11]

3.1 Allocation methods

Some methods used for allocation is described in the sub-chapters below.

3.1.1 Equity-based allocation

Equity-based allocation is a method that shares the production between the different fields to their share of the equity. The claim is often given in percentage. This method does not consider the quality and the quantity of the fluids from the different fields. The technique is, therefore, more used if all the fields have the same owner. [11] There are several different owners for the Platform Vest case, and the equity-based allocation method is thus seen as not reasonable.

3.1.2 Allocation by difference

Allocation by difference is another allocation method that is suitable if one field is unmeasured. Then the unmeasured field gets the products that have not been allocated to any of the measured fields. The uncertainty with using this method increases with a higher number of fields that are allocated. This method reduces the need for measuring instrumentation in the process. For the Platform Vest case, the A and B fields were previously allocated using this method before the C field was routed through the platform. The formula for calculating allocation by difference is: [11]

$$Q_2 = Q - Q_1 \tag{3.1}$$

Where Q_2 is the unknow quantity allocated to user 2, Q is the total quantity to be allocated and Q_1 is the known quantity for user 1.

3.1.3 Pro-rata allocation

Pro-rata allocation (or Proportional allocation) is allocation based on measured or estimated field quantities. This means that each field gets the amount of production proportional to the estimated quantity of the specific field. This method is less affected by biases since the uncertainties are evenly distributed between the fields. The formula for calculating allocation pro-rata is: [11]

$$Q_n = Q * \frac{B_n}{\sum_n B_n} \tag{3.2}$$

Where Q_n is the quantity allocated to user n and B_n is the measured/estimated quantity to user n.

3.1.4 Uncertainty-based allocation

Uncertainty-based allocation (UBA) uses the accuracy of the input to give a fairer allocation. The input data with the lowest uncertainty is emphasised more than data with higher uncertainty. This method requires that the uncertainties in the system are highly evaluated. [11]

3.1.5 Simulation-based allocation

Allocation can also be done by making a model in a process simulation software, such as UniSim or ProMax. A simulation model needs sufficient input data for the simulation to be solvable. The input data is often pressure and temperature specifications for the different process equipment, field compositions and stream flows. A process simulation can provide information on the hydrocarbons after being separated and experiencing thermodynamic changes in the process. Normally, the simulation model is built from a process flow diagram from the real platform process. However, it is better for just allocation purposes to construct a model that favours stability and solvability, assuming that the process specification is achieved. The uncertainty of the simulation model is dependent on the uncertainty of the input data and the quality of the model. [11]

A process simulation software has basic hydrocarbons defined in the component library. If the library components are used for a simulation with more than one fields, it is impossible/challenging to measure how much of the hydrocarbons in the export belonging to which field. One way of solving this problem is to define hypothetical components for each field. In this way, the user can track the hydrocarbons from different fields throughout the process and know which field the product is originated from.

Simulation-based allocation is always used for new fields to get an understanding of the commingling effect, limitations or if there is a need for modifications.

3.2 Current allocation method for Platform Vest

This chapter describes the current allocation method used for Platform Vest.

3.2.1 Input and production streams

The hydrocarbon mass flow to Platform Vest from the A field is not directly measured but determined by other measurements and calculations. Field A is routed through the test separator alone, making measurements from the test separator useful to decide flow from the field. The field's hydrocarbon flow is determined using updated well performance curves and densities from sample analysis and validated with measurements from the test separator. The uncertainty for this method can be set to ± 5%. [12]

The hydrocarbon flow from field B and field C are measured separately with topside multiphase flow metres. The uncertainty with this type of meter is set to ± 5%. [13] Backup flow determination for field B and C is subsea multiphase flow metres or well performance curves. [14]

The production streams are measured with fiscal metres on a mass basis. The parameter to be measured on the gas export is the accumulated monthly mass. The parameters measured for the oil export are the daily mass and the accumulated monthly mass. [14]

3.2.2 Oil export allocation

The oil export allocation is based on standalone ORFs. The ORF (oil recovery factor) determines how much of a specific component is recovered in the oil production. ORFs need to be calculated for each component in every field. The ORFs also need to be free of any gas lift, only pure component from the specific field. The formula for the calculation is: [14]

$$ORF_{i,Field\ x} = \frac{m_{Oil_{i,Field\ x}}}{m_{HC_{i,Field\ x}}} \tag{3.3}$$

ORF is calculated for the following components (i = N2, CO2, C1, C2, C3, iC4, nC4, iC5, nC5, C6, C7, C8, C9 and C10+), where m_{Oil} is the oil in the liquid product for the specific component (i) and m_{HC} is the total hydrocarbon feed of that specific component. Platform Vest has production from three fields, meaning that the specific ORFs needs to be calculated for each field, resulting in 14 ORFs for each field and a total of 42 ORFs for each Platform Vest case. The ORFs is based on a standalone simulation for the fields. A standalone simulation is a simulation where only the production from one field is simulated, resulting in three different simulation models. This gives a non-commingled result for the simulation. The input to the simulations is given from the fluid characterisation of the fields and typical process input. The ORFs are kept and used for the allocation until a new fluid characterisation or other changes requires for a new simulation. This is often done once every year. [14]

The formula for calculating the basis for the oil production for each field is:

$$m_{OB_{i,Field\,x}} = m_{HC_{i,Field\,x}} * ORF_{i,Field\,x} \tag{3.4}$$

The oil production using this formula is used for the oil allocation from the A field, meaning that the calculated oil from this formula is the oil allocated to field A. For field B and field C, this formula is just used as a base for further calculations. The reason for doing this is because field A was the original field on the platform so that it does not "lose" any production (meaning that part of the oil production will not be recovered as oil due to the commingling effect) with the addition of the new fields to the platform.[14]

Further, for field B and C, a correction factor is added to even out the imbalance and make it fairer. The formula for calculating this imbalance is as follows:

$$m_{IBO_i} = \left[m_{TO_i} - m_{OB_{i,Field\,A}}\right] - \left[m_{OB_{i,Field\,B}} + m_{OB_{i,Field\,C}}\right] \tag{3.5}$$

Where m_{IBO} is the imbalance for the oil for each component on a mass basis, m_{TO} is the total export oil on a dry mass basis (no water), m_{OB} is the oil basis for each component for each field calculated from the formula above. [14]

When the imbalance factor is calculated, it is used in the following formula to calculate allocated oil from field B and field C. The x in the formula represents either B or C.

$$m_{AO_{i,Field\,x}} = m_{OB_{i,Field\,x}} + \left[\frac{m_{OB_{i,Field\,x}}}{m_{OB_{i,Field\,B}} + m_{OB_{i,Field\,C}}}\right] * m_{IBO_i} \tag{3.6}$$

The formula gives the allocated oil products for each component for each field (a calculation example is included in Chapter 7.9.1). [14]

3.2.3 Gas export allocation

The basis for the gas allocated is subtracting the allocated oil from the hydrocarbon flow into the platform using the following formula: [14]

$$m_{GB_{i,Field\,x}} = m_{HC_{i,Field\,x}} - m_{AO_{i,Field\,x}} \tag{3.7}$$

After the basis for the gas allocation is determined, the imbalance is calculated using the following formula: [14]

$$m_{IBG_i} = m_{TG_i} - \left[m_{GB_{i,Field\,A}} + m_{GB_{i,Field\,B}} + m_{GB_{i,Field\,C}}\right] \tag{3.8}$$

Where mTG is the total gas export excluding gas lift. The final gas allocation for each component for each field is calculated with the following formula: [14]

$$m_{AG_{i,Field\,x}} = m_{GB_{i,Field\,x}} + \left[\frac{m_{GB_{i,Field\,x}}}{m_{GB_{i,Field\,B}} + m_{GB_{i,Field\,B}} + m_{GB_{i,Field\,C}}}\right] * m_{IBG_i} \tag{3.9}$$

4 Fluid characterisation

Fluid characterisation defines how a fluid will behave in correlation to other fluids and how it will be affected by different PVT changes. The fluid characterisation and the process model for Platform Vest are based on the equation of state called SRK (Soave-Redlich-Kwong).

4.1 Equation of state

An equation of state is an equation describing the relation between the pressure, the temperature, and the volume of a gas. The most used EOS for simple gases is the ideal gas law (PV = nRT); this equation is adequate for calculations at low pressures. If the gas is at high pressure or low temperature, the gas will deviate from the ideal behaviour, making the ideal gas law insufficient. A more complex equation such as the Soave-Redlich-Kwong (SRK) equation is needed for the PVT calculations in this case. [15, p. 191]

The SRK equation of state is a cubic equation of state because it can be written as a third-order equation for the specific volume. [15, p. 203] This EOS is dependent on the critical temperature and the critical pressure of the fluid. The critical temperature is the highest temperature at which the fluid is in both the vapour phase and the liquid phase, while the critical pressure is the highest pressure at which the fluid is in both phases. [15, p. 200]. The equation is as follows: [15, p. 203]

$$P = \frac{RT}{\hat{V} - b} - \frac{\alpha a}{\hat{V}(\hat{V} + b)} \tag{4.1}$$

Where:

$$a = 0.42747 \frac{(RT_c)^2}{P_c} \tag{4.2}$$

$$b = 0.08644 \frac{RT_c}{P_c} \tag{4.3}$$

$$\alpha = [1 + m(1 - \sqrt{T_r}\,)]^2 \tag{4.4}$$

$$T_r = \frac{T}{T_c} \tag{4.5}$$

$$m = 0.48508 + 1.55171\omega - 0.1561\omega^2 \tag{4.6}$$

The saturated-liquid volumes predicted by the SRK EOS will have an average deviation of 16%. This can be improved by incorporating the Peneloux volume translation. This method used the knowledge that the predicted volumes by SRK is too large and will be improved by being reduced the predicted volume by a value c (the volume correction). The formula for this is: [16]

$$\hat{V}_t = \hat{V} - c \tag{4.7}$$

This incorporated into the SRK EOS gives the following formulas:

$$P = \frac{RT}{\hat{V} - b} - \frac{\alpha a}{(\hat{V} + c)(\hat{V} + b + 2c)} \tag{4.8}$$

$$b = 0.08644 \frac{RT_c}{P_c} - c \tag{4.9}$$

$$c = \frac{RT_c}{P_c}(0.1156 - 0.4077 * Z_{RA}) \tag{4.10}$$

Where ZRA is the Rackett compressibility factor. [16]

The EOS used for simulation with simulation software in Equinor is the SRK and the SRK Peneloux for fluid characterisation.

4.2 Fluid characterisation using PVTsim

The fluid characterisation for a mixture can be found and calculated from different methods. The method used for the scope in this report is a calculation using software called PVTsim.

The input values to PVTsim are the mol% (or weight%), the density and the molar weight of a fluid mixture. PVTsim includes a variety of EOS to choose from, and the equation used for this scope is the SRK. The output from PVTsim is multiple state values, including critical pressure, critical temperature, and critical volume for all the components in the fluid mixture. See Appendix B – PVTsim procedure for an elaborated procedure for the different fields in PVTsim.

For a new fluid characterisation in PVTsim, the input values to PVTsim are given from an analysis of fluid samples from the test separator. It is essential that these samples are taken when production is under normal operating conditions to get a sample that best represents the reality. The separator samples are sent to a non-associated company responsible for doing the tests needed for the sample. This company uses gas chromatography to determine the composition, a densitometer to determine the density and a cryoscopy to determine the molecular weight. The results are given back to Equinor in a report, and the results can be used as the input values to PVTsim to characterise the fluid. [17]

For the scope of this report, there was a given fluid characterisation that has been used for a few years. This characterisation is defined from PVT analysis taken from separator samples a few years ago. Part of the results will compare this old fluid characterisation and a new fluid characterisation based on new separator samples.

4.2.1 Lumping method

PVTsim has an option for lumping hydrocarbons together to form a hypothetical hydrocarbon with the average fluid characterisation for all the hydrocarbons set to be in that hydrocarbon lump. For the A field, a hydrocarbon lump is set to C19-C23; this means that this hypothetical component has the average characterisation of the hydrocarbons with 19 carbons to 23 carbons. The lumping scheme for the different fields is already predefined based on earlier fluid characterisations. It is recommended to keep this the same each year to avoid modifications to the allocation model. The set lumping scheme is shown in Table 4.1.

Table 4.1: Lumping scheme for field A, B and C

Field A	Field B	Field C
A - N2*	B - N2*	C - N2*
A - CO2*	B - CO2*	C - CO2*
A - C1*	B - C1*	C - C1*
A - C2*	B - C2*	C - C2*
A - C3*	B - C3*	C - C3*
A - iC4*	B - iC4*	C - iC4*
A - nC4*	B - nC4*	C - nC4*
A - iC5*	B - iC5*	C - iC5*
A - nC5*	B - nC5*	C - nC5*
A - C6*	B - C6*	C - C6*
A - C7*	B - C7*	C - C7*
A - C8*	B - C8*	C - C8*
A - C9*	B - C9*	C - C9*
A - C10*	B - C10-C11*	C - C10-C12*
A - C11*	B - C12*	C - C13-C14*
A - C12*	B - C13-C14*	C - C15-C17*
A - C13-C14*	B - C15-C16*	C - C18-C20*
A - C15-C16*	B - C17-C18*	C - C21-C25*
A - C17-C18*	B - C19-C22*	C - C26-C30*
A - C19-C23*	B - C23-C29*	C - C31-C37*
A - C24-C34*	B - C30-C40*	C - C38-C47*
A - C35-C80*	B - C41-C80*	C - C48-C80*

4.2.2 Comparison old and new well composition

The well composition of the C10+ hydrocarbons can be determined using the old fluid characterisation or with a new fluid characterisation. If using the old fluid characterisation, the distribution of the C10+ hydrocarbons will have the same ratio. If using a new characterisation, the C10+ distribution would be determined based on the lower hydrocarbons (done in PVTsim). Table 4.2, Table 4.3 and Table 4.4 shows the well composition with old and new characterisation and the percentage deviation for field A, field B and field C, respectively.

Table 4.2: Field A well composition new vs. old characterisation

Field A	New	Old	Deviation (%)
A - N2*	0.00449	0.00449	0.00 %
A - CO2*	0.03994	0.03994	0.00 %
A - C1*	0.72172	0.72172	0.00 %
A - C2*	0.08927	0.08927	0.00 %
A - C3*	0.04346	0.04346	0.00 %
A - iC4*	0.00898	0.00898	0.00 %
A - nC4*	0.0164	0.0164	0.00 %
A - iC5*	0.00688	0.00688	0.00 %
A - nC5*	0.00792	0.00792	0.00 %
A - C6*	0.00947	0.00947	0.00 %
A - C7*	0.01332	0.01332	0.00 %
A - C8*	0.01237	0.01237	0.00 %
A - C9*	0.00707	0.00707	0.00 %
A - C10*	0.00449	0.00418	-6.85 %
A - C11*	0.00297	0.00281	-5.51 %
A - C12*	0.00205	0.00201	-2.41 %
A - C13-C14*	0.00315	0.00310	-1.49 %
A - C15-C16*	0.00188	0.00196	4.24 %
A - C17-C18*	0.00120	0.00124	3.97 %
A - C19-C23*	0.00157	0.00159	0.86 %
A - C24-C34*	0.00109	0.00110	0.25 %
A - C35-C80*	0.00031	0.00071	126.72 %

Table 4.3: Field B well composition new vs. old characterisation

Field B	New	Old	Deviation (%)
B - N2*	0.00691	0.00691	0.00 %
B - CO2*	0.02402	0.02402	0.00 %
B - C1*	0.81959	0.81959	0.00 %
B - C2*	0.05805	0.05805	0.00 %
B - C3*	0.03273	0.03273	0.00 %
B - iC4*	0.00487	0.00487	0.00 %
B - nC4*	0.01047	0.01047	0.00 %
B - iC5*	0.00333	0.00333	0.00 %
B - nC5*	0.00445	0.00445	0.00 %
B - C6*	0.00475	0.00475	0.00 %
B - C7*	0.00685	0.00685	0.00 %
B - C8*	0.00588	0.00588	0.00 %
B - C9*	0.00344	0.00344	0.00 %
B - C10-C11*	0.00332	0.00439	32.06 %
B - C12*	0.00137	0.00148	7.88 %
B - C13-C14*	0.00226	0.00241	6.55 %
B - C15-C16*	0.00175	0.00165	-5.67 %
B - C17-C18*	0.00135	0.00111	-17.88 %
B - C19-C22*	0.00185	0.00128	-31.04 %
B - C23-C29*	0.00163	0.00103	-36.87 %
B - C30-C40*	0.00085	0.00081	-4.08 %
B - C41-C80*	0.00027	0.00050	85.15 %

Table 4.4: Field C well composition new vs. old characterisation

Field C	New	Old	Deviation (%)
C - N2*	0.00247	0.00247	0.00 %
C - CO2*	0.02336	0.02336	0.00 %
C - C1*	0.26983	0.26983	0.00 %
C - C2*	0.0696	0.0696	0.00 %
C - C3*	0.0861	0.0861	0.00 %
C - iC4*	0.01607	0.01607	0.00 %
C - nC4*	0.05074	0.05074	0.00 %
C - iC5*	0.0181	0.0181	0.00 %
C - nC5*	0.02853	0.02853	0.00 %
C - C6*	0.03307	0.03307	0.00 %
C - C7*	0.05277	0.05277	0.00 %
C - C8*	0.05056	0.05056	0.00 %
C - C9*	0.03487	0.03487	0.00 %
C - C10-C12*	0.06561	0.07001	6.71 %
C - C13-C14*	0.03442	0.03498	1.64 %
C - C15-C17*	0.04077	0.03981	-2.37 %
C - C18-C20*	0.03065	0.02884	-5.91 %
C - C21-C25*	0.03512	0.02960	-15.72 %
C - C26-C30*	0.02183	0.01992	-8.74 %
C - C31-C37*	0.01742	0.01739	-0.20 %
C - C38-C47*	0.01130	0.01346	19.07 %
C - C48-C80*	0.00680	0.00992	45.81 %

The deviation between the different predicted well compositions is considerable. This verifies that it would be interesting to see how the different compositions influence the predicted results when incorporated into a process simulation.

4.2.3 Comparison old and new PVTsim characterisation

The two parameters compared in this section are the predicted critical pressure and the predicted critical temperature for the new and old characterisation. These parameters are essential for the fluid behaviour of the components. Figure 4.1, Figure 4.2 and Figure 4.3 show a comparison between the critical pressure with new and old characterisation and a comparison for the critical temperature for field A, field B and field C, respectively. The x-axis illustrates the molecular weight of the hydrocarbon. Critical pressure and critical temperature

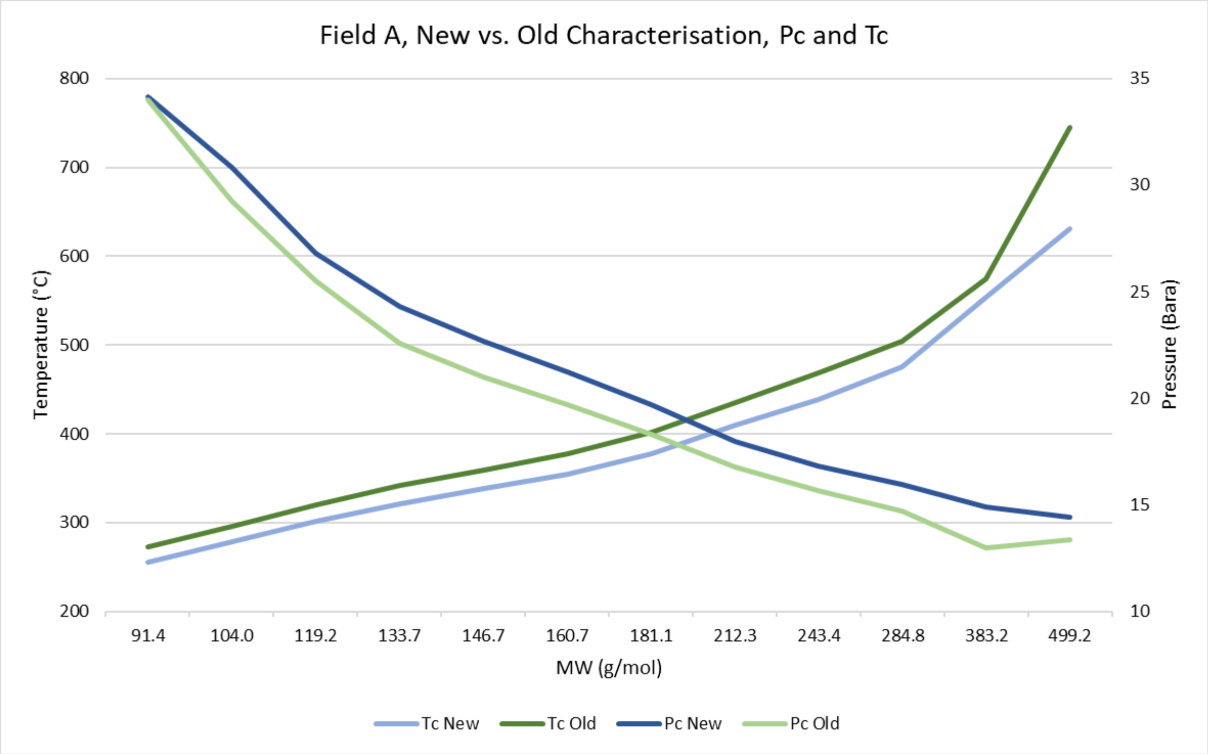

Figure 4.1: Critical parameters for field A, new vs. old characterisation

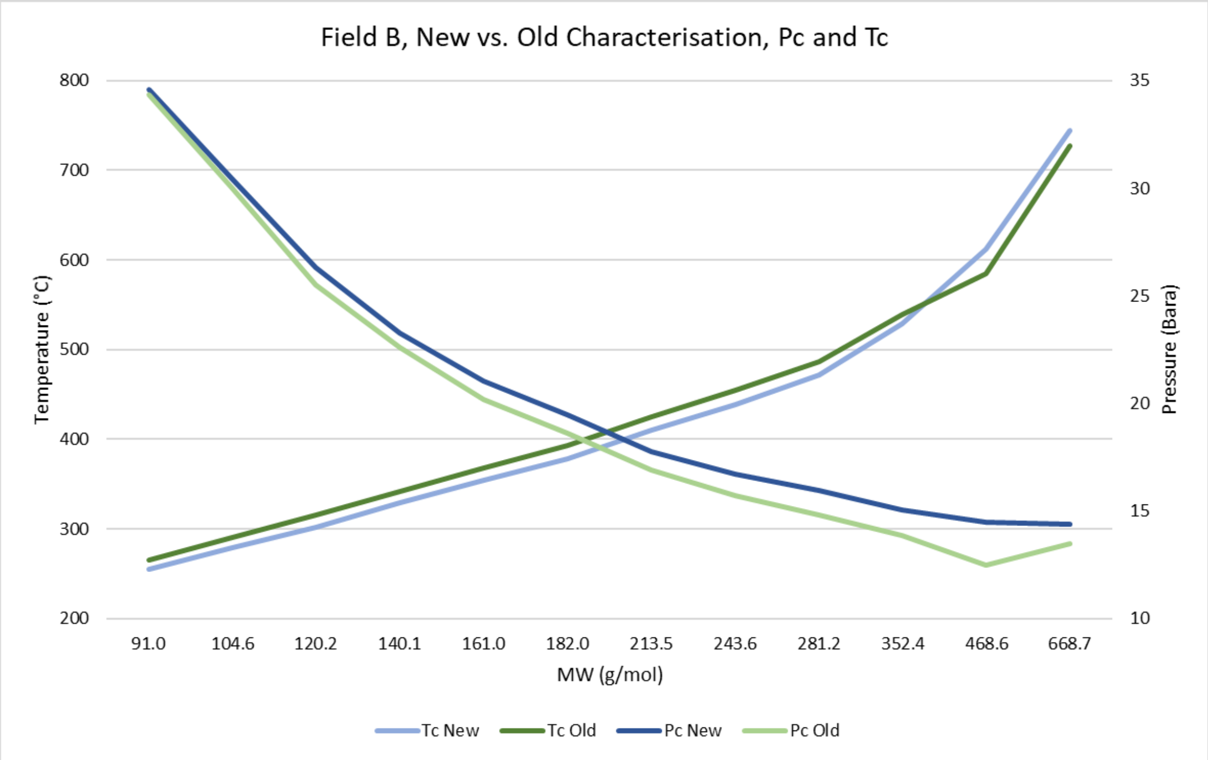

Figure 4.2: Critical parameters for field B, new vs. old characterisation

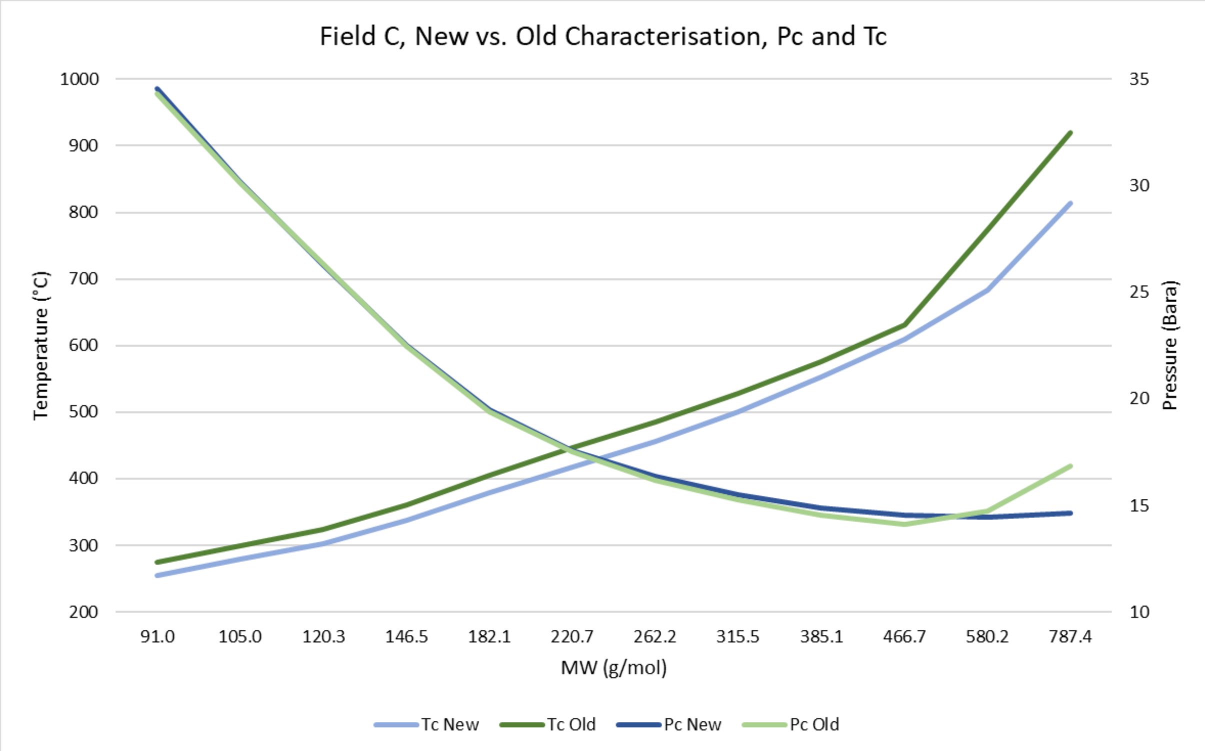

Figure 4.3: Critical parameters for field C, new vs. old characterisation

These figures show that there is a deviation between the old and new characterisation for the hydrocarbons. Based on this finding, a more detailed simulation analysis (chapter 7.1) shows the effect of the deviations and what this will mean for the simulation results.

The total fluid characterisation for all fields with old and new characterisation is given in Appendix C – Old fluid characterisation and Appendix D – New fluid characterisation.

4.3 Phase envelope

The phase envelope is the pressure and temperature prediction of the phase diagram for a fluid consisting of multiple components. The phase envelope predicted for a fluid is determined for a fixed fluid composition. The area inside the phase envelope is identified as the two-phase area where both liquid and gas are present. [9, p.43] The phase envelopes predicted for the results in this report are solely included to confirm that the phase diagram is predicted the same in the characterisation and simulation and determine if the phase diagram is the same between the different cases in the result. According to [18], the predicted phase envelope will change if PNA (paraffin, naphthene and aromatic) is included in the fluid. According to [19, p.86], the phase envelopes will be broader and higher with extended fluid characterisation, and narrower and downscaled with a lower degree of fluid characterisation (for instance, with C20+ or C10+ characterisation).

4.3.1 Phase envelope for the new characterisation

The phase envelopes for the different fields are obtained from the PVTsim results and shown in Figure 4.4, Figure 4.5 and Figure 4.6 for field A, field B, and field C, respectively.

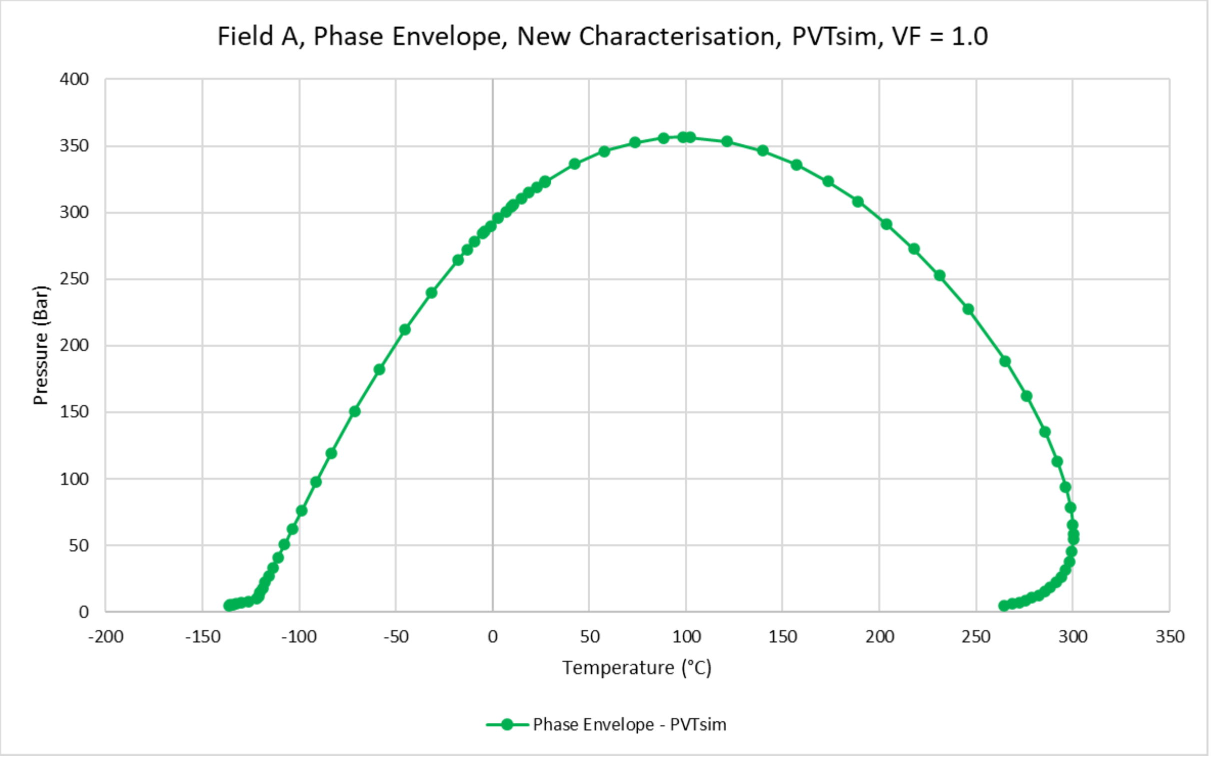

Figure 4.4: Phase envelope, new characterisation, PVTsim, Field A

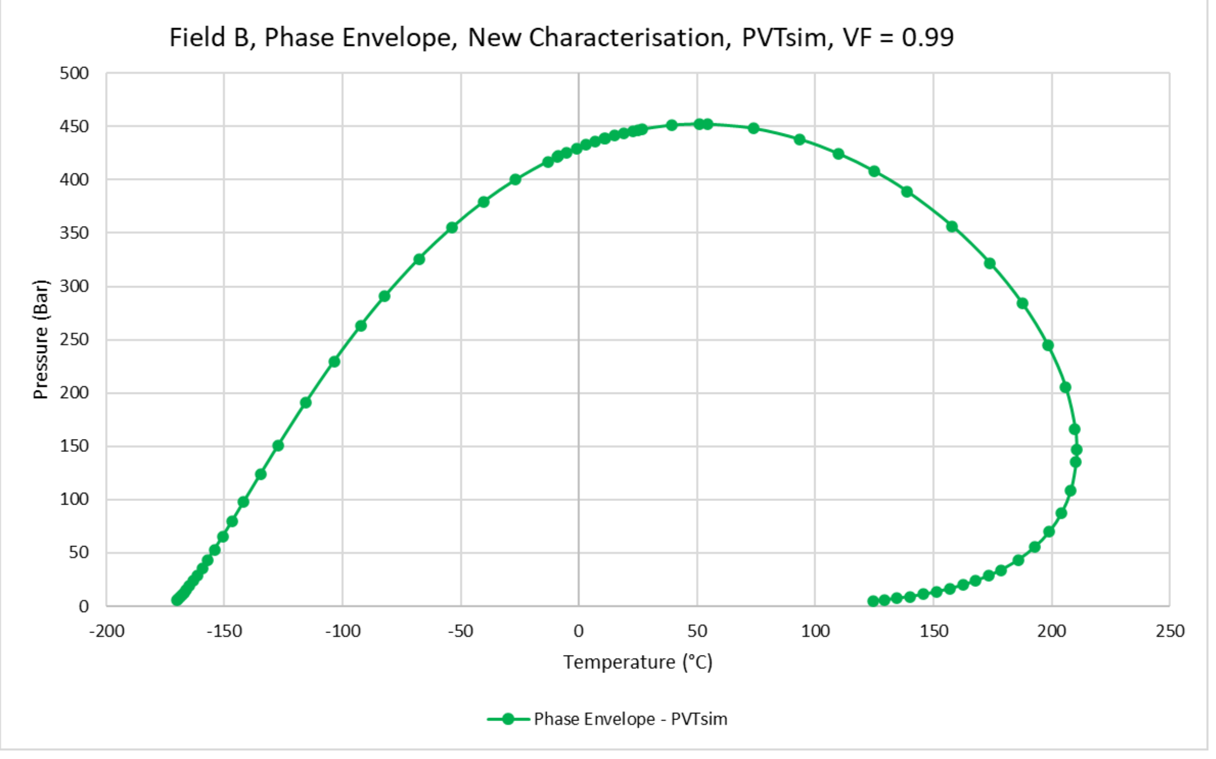

Figure 4.5: Phase envelope, new characterisation, PVTsim, Field B

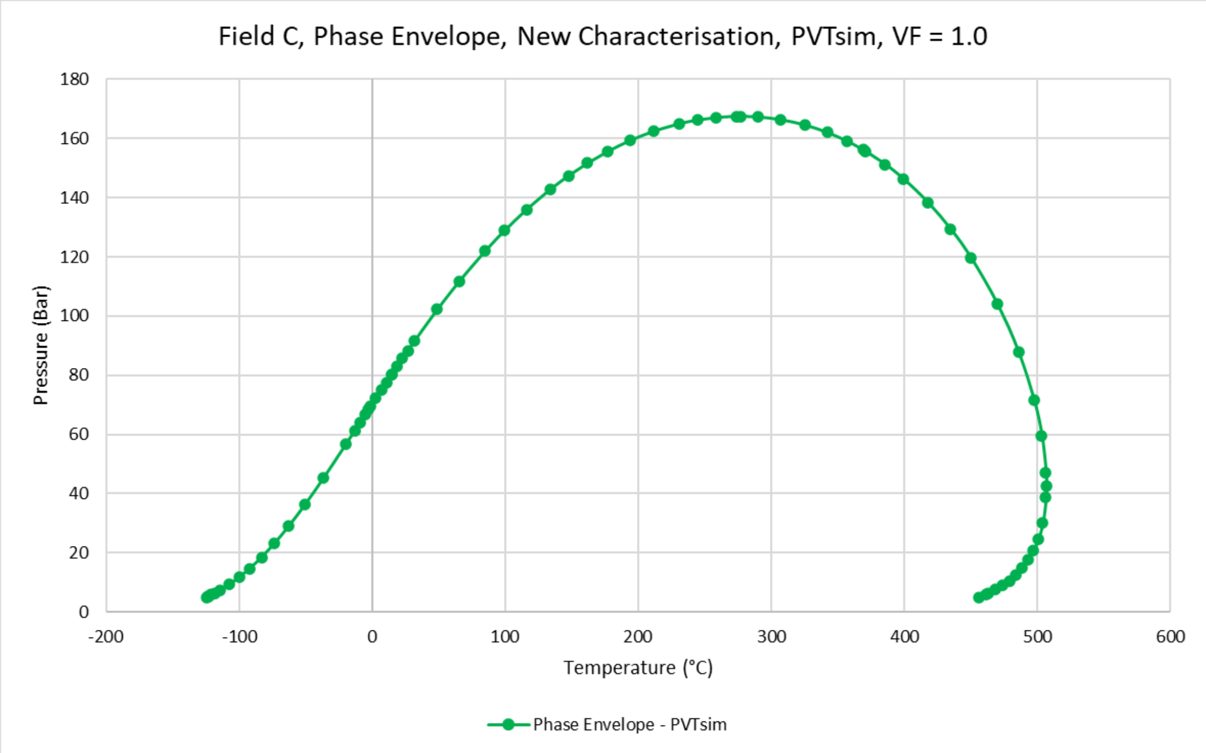

Figure 4.6: Phase envelope, new characterisation, PVTsim, Field C

These phase envelopes will be compared to the simulation models to determine if the fluid characterisation is incorporated successfully into the simulation model. The different phase envelops also show that the fields are very different when looking at the properties.

4.4 Value adjustment

The oil produced from an offshore platform consists of different qualities. These qualities can be defined from the normal boiling point of the hydrocarbon obtained from the fluid characterisation. The cut description for the normal boiling points is described in Table 4.5. together with the value for the product. The prices and dollar exchange rate are retrieved 3rd of March 2021. The exchange rate used for the calculation is 8.49 NOK/USD [20].

Table 4.5: Oil products NBP range and value

Oil product	NBP range	Value
	°C	USD/ton
Naphtha	20 - 165 °C	588.2 [21]
Jet kerosene	165 - 250 °C	455.4 [22]
Gasoil	250 - 375 °C	537.9 [23]
Atmospheric residue	375+ °C	264.1 [24]

The products with NBP (normal boiling point) lower than 20 °C is cut as gas and will not be included in the value estimation. The value of the gas export will also not be included for value estimation. This is to limit the number of results to be discussed for this scope. A value adjustment for the oil products mentioned will indicate value for the profit to each field.

The oil production cuts will be the same for both new and old characterisation. The cuts are given in Table 4.6, based on NBPs given in Appendix C – Old fluid characterisation and Appendix D – New fluid characterisation.

Table 4.6: Oil product cuts for the different fields

Field A		Field B		Field C	
Component	Cut	Component	Cut	Component	Cut
A - iC5*	Naphtha	B - iC5*	Naphtha	C - iC5*	Naphtha
A - nC5*		B - nC5*		C - nC5*	
A - C6*		B - C6*		C - C6*	
A - C7*		B - C7*		C - C7*	
A - C8*		B - C8*		C - C8*	
A - C9*		B - C9*		C - C9*	
A - C10*	Kerosene	B - C10-C11*	Kerosene	C - C10-C12*	Kerosene
A - C11*		B - C12*		C - C13-C14*	
A - C12*		B - C13-C14*		C - C15-C17*	Gasoil
A - C13-C14*		B - C15-C16*	Gasoil	C - C18-C20*	
A - C15-C16*	Gasoil	B - C17-C18*		C - C21-C25*	
A - C17-C18*		B - C19-C22*		C - C26-C30*	Residue
A - C19-C23*		B - C23-C29*	Residue	C - C31-C37*	
A - C24-C34*	Residue	B - C30-C40*		C - C38-C47*	
A - C35-C80*		B - C41-C80*		C - C48-C80*	

5 UniSim

UniSim is a process simulation software developed by Honeywell International Inc. The UniSim Design version used for the results in this report is R460.2.

5.1 Allocating components

To allocate different hydrocarbons in a process simulation using UniSim, the software recommends using hypothetical components for the different fields. This means that there is separate methane for each field with supposedly the same fluid characterisation. These components are defined in the environmental design for the simulation. The fluid characterisation for these components is described in Appendix C – Old fluid characterisation and Appendix D – New fluid characterisation. UniSim needs the value for normal boiling point, molecular weight, liquid density, critical temperature, critical pressure, critical volume, and the acentric factor to define a hypothetical component.

5.2 EOS

The standard EOS used for process simulations in Equinor is the SRK equation of state. For UniSim simulations, the company standard is to use SRK with Peneloux volume correction. The SRK-Peneloux is thus chosen as the EOS for the simulations for this report.

5.3 The simulation model

The simulation model is built according to the process described in the Process description chapter. The only difference is the addition of heat exchangers before the inlet and test separators. These are added to ensure that the equipment has the same thermodynamic properties according to the given process parameters. A figure of the model is given in Figure 5.1 [25].

A closer illustration of the model is given in Appendix E – UniSim model.

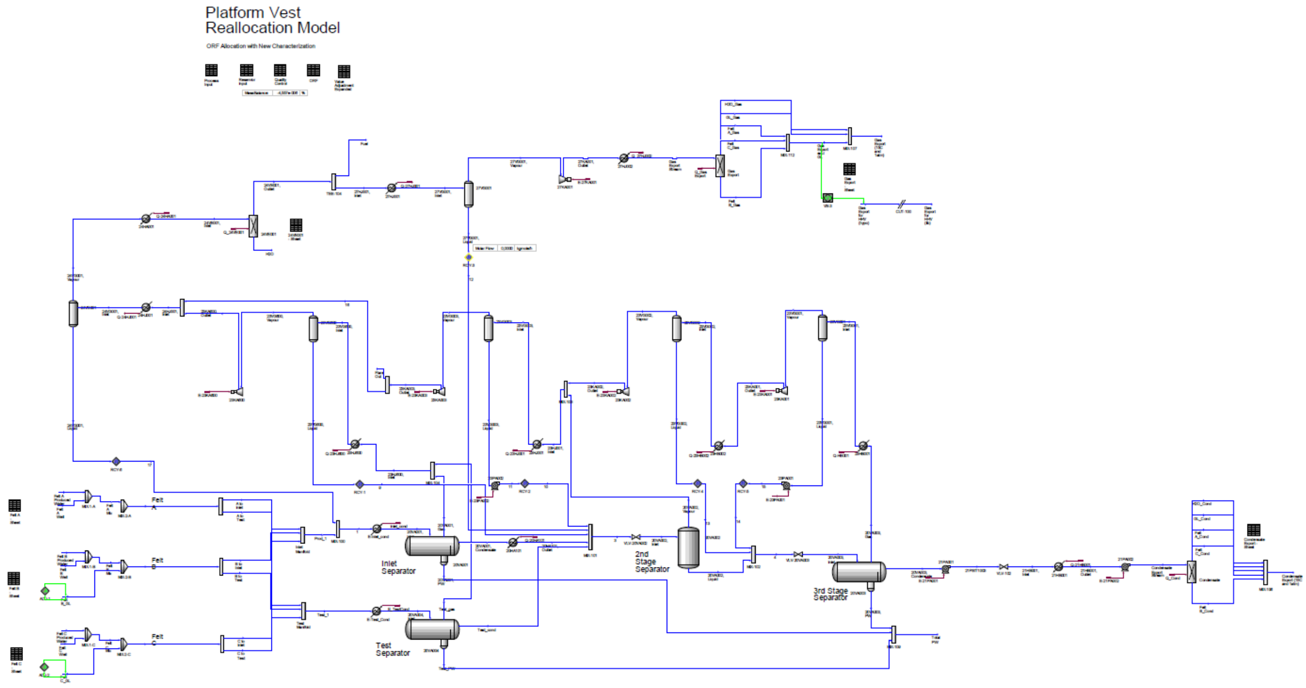

Figure 5.1: Complete UniSim model

The process input (temperature and pressure) for given process equipment are given in Appendix F – Process equipment input and the profiles are given in Appendix G – Inflow data for reallocation. The input composition is given in Appendix C – Old fluid characterisation and Appendix D – New fluid characterisation.

5.4 Allocated production streams

To easier know which field the product is allocated from, the export streams are divided into products from field A, field B, field C and the GL. This is done by using dividers in UniSim, which allows the user to divide all the components into different product streams. These dividers are marked with an X in Figure 5.1.

6 ProMax

ProMax is a process simulation software developed by Bryan Research & Engineering, LLC. The ProMax version used for the results in this report is 5.0.

6.1 Allocating components

ProMax offers an allocation method called mixed species or allocation by full account. This gives the opportunity to use library components (not defining hypotheticals) for different hydrocarbons in the simulation and still know which field they are coming from. Giving the opportunity to just have one methane in the simulation instead of three hypothetical methane like in UniSim. ProMax claims that this gives a more thermodynamically correct commingling compared to just using hypothetical components.

For the Platform Vest case, the fluid characterisation for the lightest hydrocarbons (C1 to C6) was the same for the different fields. These hydrocarbons were thus only added as library components. The hydrocarbons from C7 and heavier were defined as hypothetical. ProMax uses single oils to represent the hypothetical components, where the only needed fluid characterisation input is the molecular weight and the specific gravity. The fluid characterisation for the single oils is described in Appendix C – Old fluid characterisation and Appendix D – New fluid characterisation.

6.2 EOS

The EOS used for Promax is SRK.

6.3 The simulation model

The simulation model is built according to the process described in the Process description chapter, with added heat exchangers as the UniSim model. A figure of the model is given in Figure 6.1 [10].

A closer illustration of the ProMax model is given in Appendix H – ProMax model.

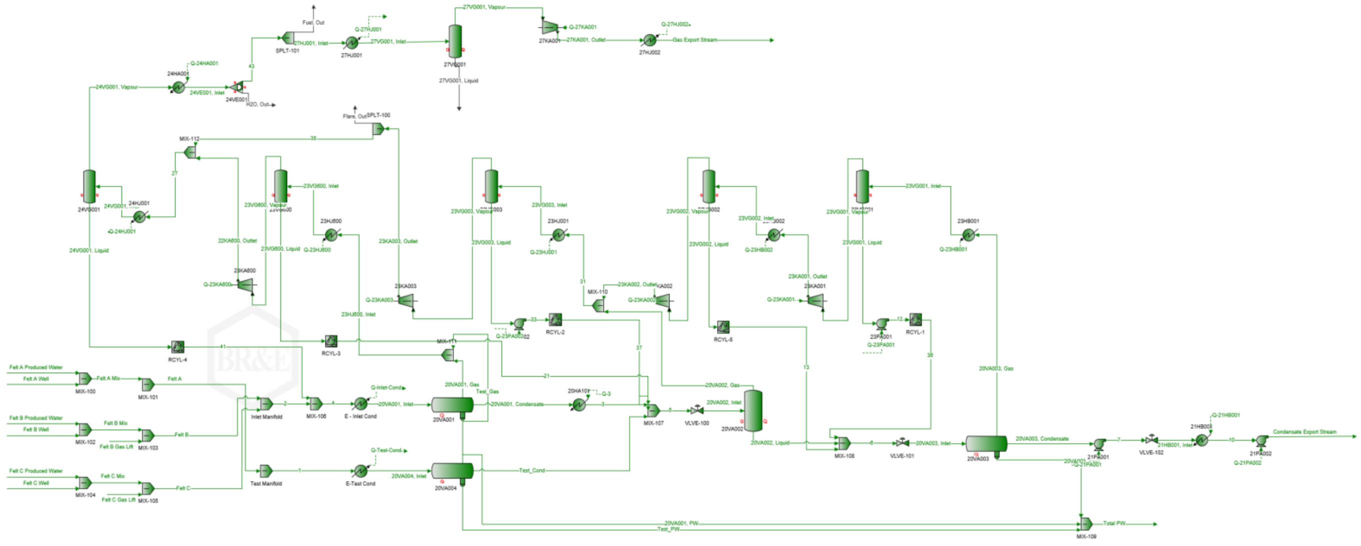

Figure 6.1: Complete ProMax model

The process input (temperature and pressure) for given unit operators are given in Appendix F – Process equipment input and the profiles are given in Appendix G – Inflow data for reallocation. The input composition is given in Appendix C – Old fluid characterisation and Appendix D – New fluid characterisation. Same as the UniSim model.

6.4 Allocated production streams

Due to the mixed-species option in ProMax, there is no need to split the product streams into different fields. Instead, there is an option for mixed species analysis that can be incorporated into the stream. This analysis gives the opportunity to see what and how much product is coming from which field.

7 Results and discussion

The results in this report are divided into; a fluid characterisation part where simulations with new and old characterisation are compared, a reallocation part to specifically look at how the ORFs change with different changes in the UniSim model and the characterisation, an UniSim future allocation part with tuning on oil, gas and GOR, and a simple ProMax model comparison. Different allocation methods are also compared to the current allocation agreement for Platform Vest. The last section in this chapter includes a recommended guideline for allocation simulation based on the results from the different cases in the results.

7.1 Simulation with new characterisation vs. old characterisation

For this comparison part, two different UniSim simulation models are developed. Where one model has the new characterisation, and one model has the old characterisation. The lumping scheme, EOS, and the model in total were kept the same, with the only changes being the fluid properties for the hypothetical components and the well composition. A detailed description of how the model is made is given in Appendix I – Building the UniSim model.

7.1.1 Phase envelope comparison

The phase envelops from PVTsim are compared to the phase envelops in UniSim to see if the estimated curves match. This is a necessary quality assurance for proper setup in UniSim, to ensure that the fluid will behave the same as the estimated fluid in PVTsim. The VF (vapour fraction) is 1.0 for field A and field C and 0.99 for field B. The inlet conditions for the different fields are also included on the phase envelopes. Figure 7.1, Figure 7.2 and Figure 7.3 show the phase envelope comparison for field A, field B and field C, respectively.

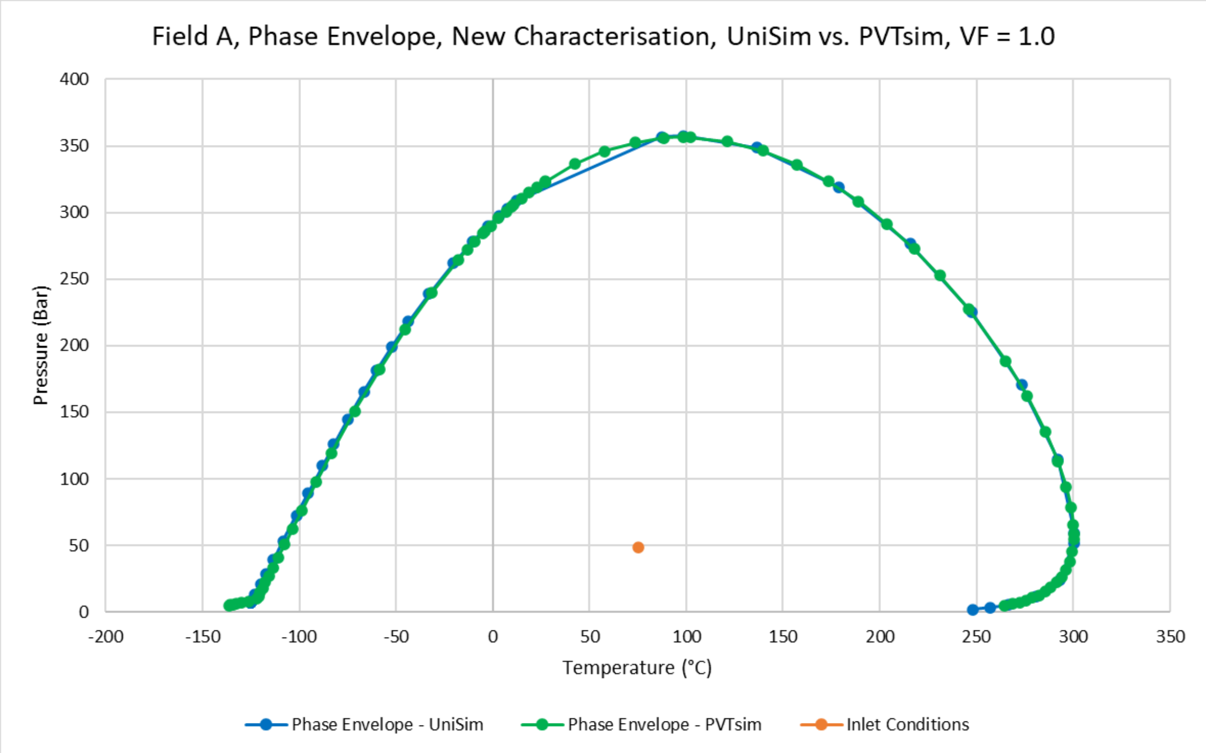

Figure 7.1: Phase envelope, new characterisation, UniSim vs. PVTsim, Field A

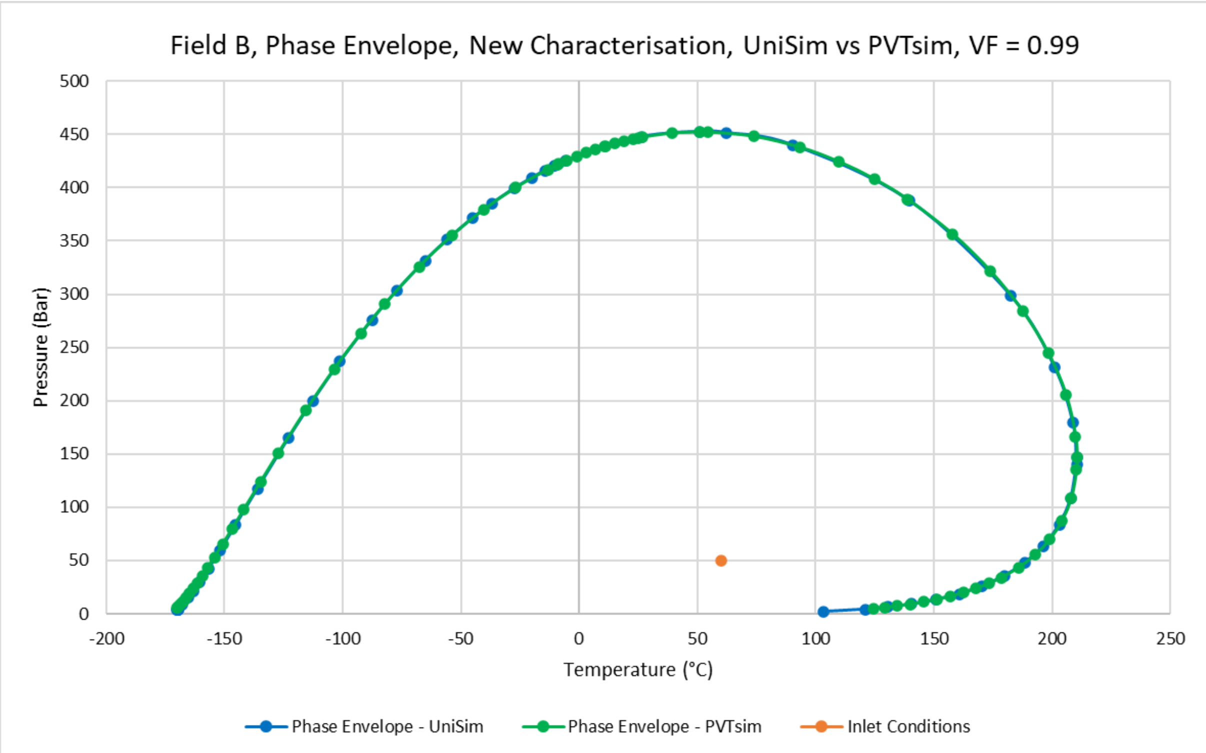

Figure 7.2: Phase envelope, new characterisation, UniSim vs. PVTsim, Field B

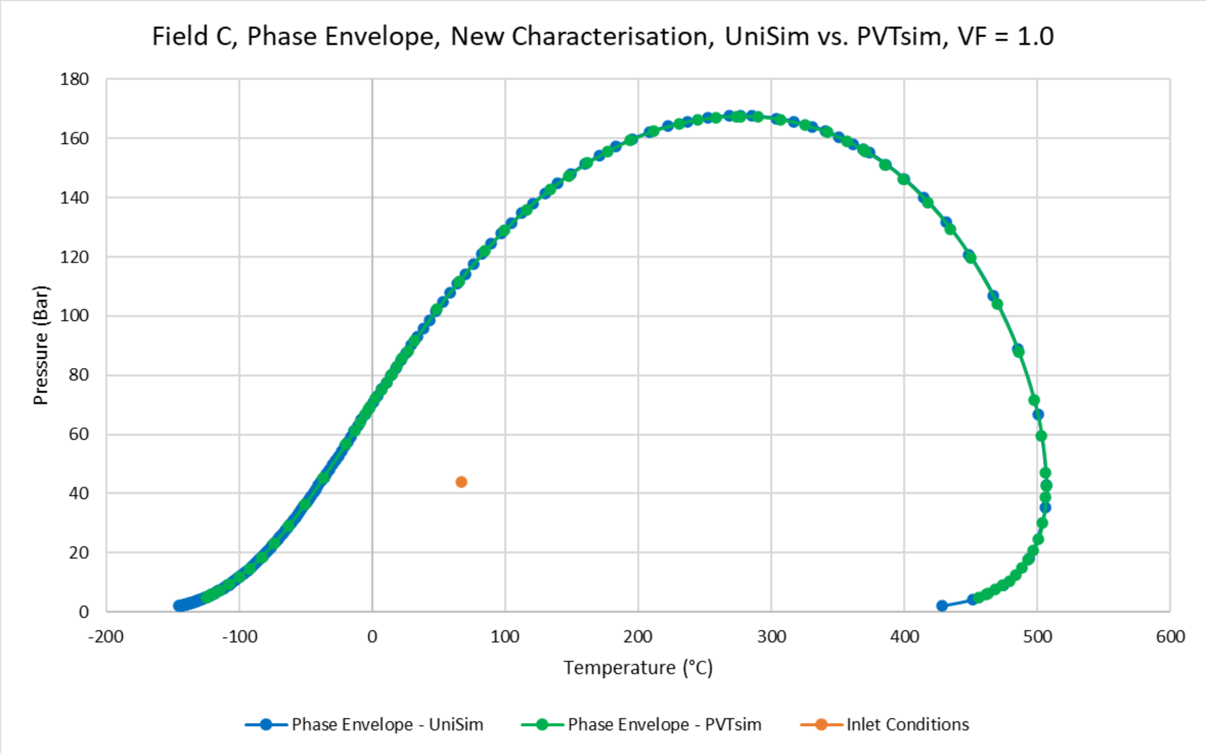

Figure 7.3: Phase envelope, new characterisation, UniSim vs. PVTsim, Field C

The curves show that the phase envelope determined from PVTsim matches the phase envelope determined from UniSim. This indicates that the new fluid characterisation is incorporated correctly into the simulation model. The inlet conditions are inside the two-phase area for all the fields.

For the old fluid characterisation, the component properties and the fluid composition are different from the new characterisation. The phase envelopes for the old and new characterisation are thus expected to deviate for the different fields. For the old characterisation, a PVTsim analysis is not included. The phase envelopes are thus predicted by UniSim. The phase envelopes from the UniSim model with the old characterisation is compared to the predicted UniSim phase envelopes with new characterisation. The VF is 0.99 for all the fields specified in both the new and old model to get a comparable result. Inlet conditions are also included in the figures. Figure 7.4, Figure 7.5 and Figure 7.6 show the phase envelopes for the new and old characterisation for field A, field B and field C, respectively.

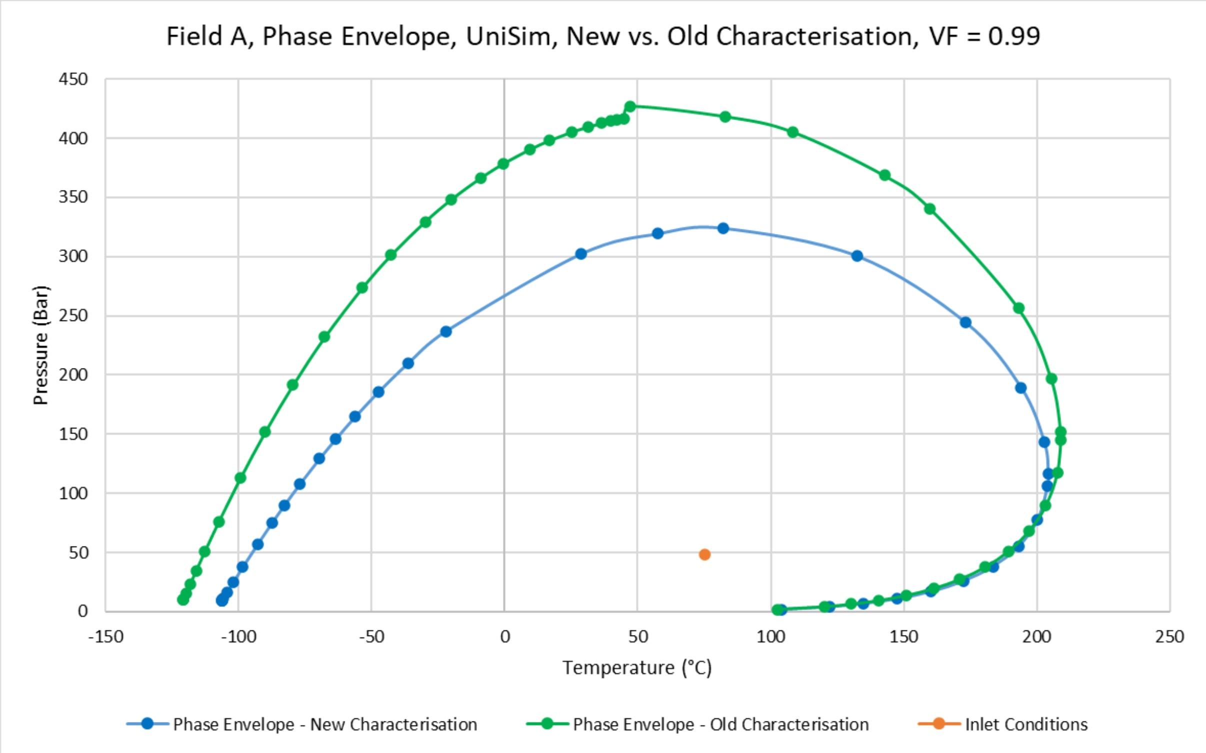

Figure 7.4: Phase envelope, new vs. old characterisation, UniSim, Field A

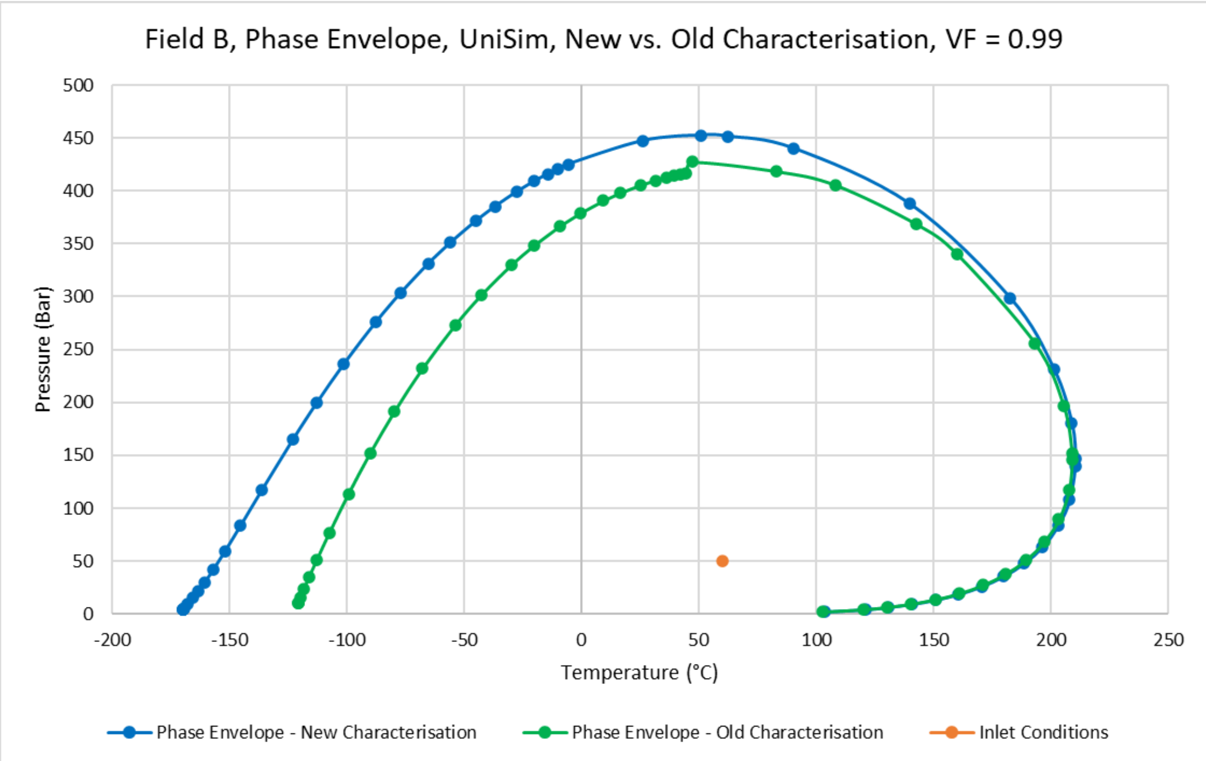

Figure 7.5: Phase envelope, new vs. old characterisation, UniSim, Field B

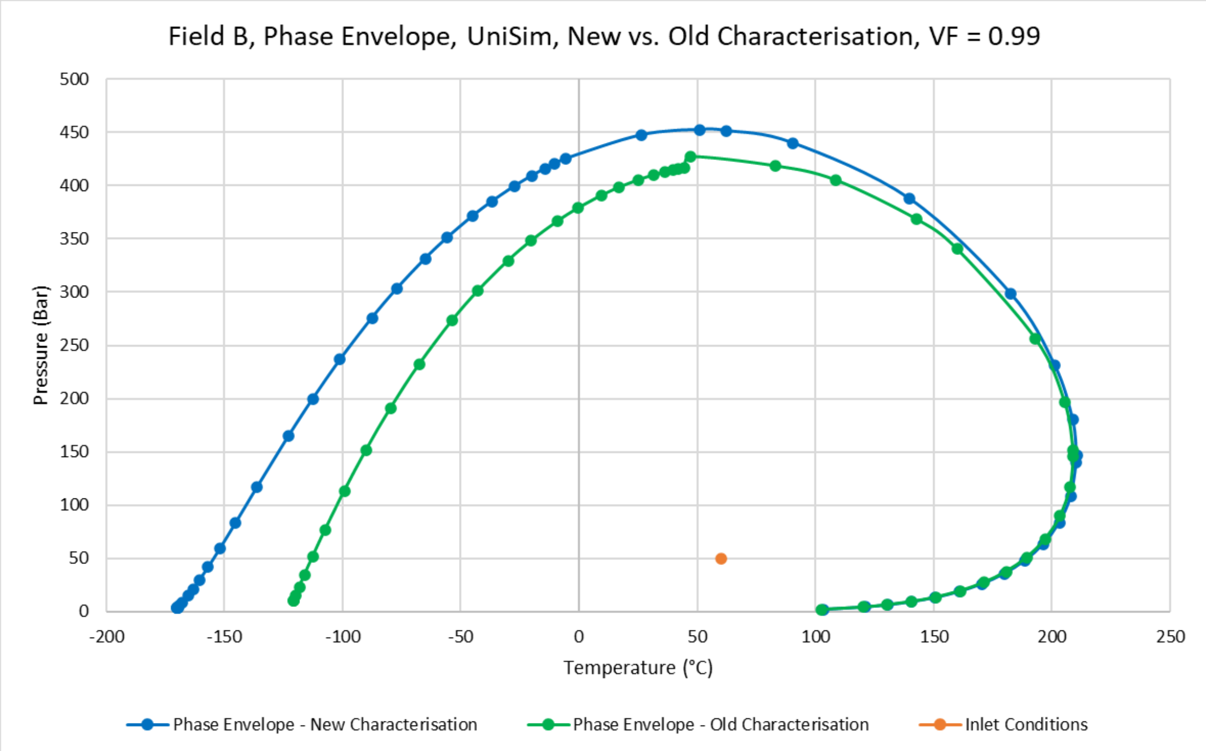

Figure 7.6: Phase envelope, new vs. old characterisation, UniSim, Field C

The phase envelopes from the new and old characterisation deviate significantly from each other. This indicates that the fluids from the new characterisation will not behave the same way as the fluids with the old characterisation. This indicates that the results from the different simulation models will deviate.

7.1.2 UniSim simulation results for new vs. old characterisation

The simulation is performed with the old and new fluid characterisation to evaluate the predicted results and study the deviations. The results predicted by the UniSim models are the oil and gas production (both total and for each field) and the estimated value for the oil products from each field, and the total value. The result values are taken both from an all-in simulation, meaning that all the fields are producing to the platform simultaneously, and from standalone cases where one field is routed through the platform alone. Both standalone cases and all-in are included to observe the commingling effect between the fields and see the difference when the field is producing alone. This is done for both the new fluid characterisation case and the old fluid characterisation case. The simulation results from the standalone cases are shown in Table 7.1, and the simulation results with the all-in case are shown in Table 7.2.

Table 7.1: Standalone simulation results for all fields with new and old characterisation

Standalone simulation	Field A	Field B	Field C
Oil production, Sm3/d:			
New characterisation	1148	2991	2747
Old characterisation	1163	2979	2749
Approximate deviation	-15	11	-2
Gas production, MSm3/d:			
New characterisation	2.1	9.6	0.3
Old characterisation	2.1	9.7	0.3
Approximate deviation	0.0	0.0	0.0
Value adjustment, MNOK/yr:			
New characterisation	1301	3457	3067
Old characterisation	1310	3415	3020
Approximate deviation	-9	42	47

Table 7.2: All-in simulation results for all fields with new and old characterisation

All-in simulation	Field A	Field B	Field C	Total
Oil production, Sm3/d:				
New characterisation	1130	3147	2557	6834
Old characterisation	1148	3121	2570	6839
Approximate deviation	-18	26	-13	-6
Gas production, MSm3/d:				
New characterisation	2.1	9.6	0.3	12.0
Old characterisation	2.1	9.7	0.3	12.1
Approximate deviation	0.0	-0.1	0.0	0.0
Value adjustment, MNOK/yr:				
New characterisation	1297	3564	2959	7821
Old characterisation	1309	3509	2923	7741
Approximate deviation	-11	55	36	80

The oil production is given in Sm^3/d, the gas production is given in MSm^3/d, and the value is given in MNOK/year. The new and old fluid characterisation predicts approximately the same gas production (with the chosen unit) for all the fields and in total for both the standalone cases and the all-in case.

For the oil production, field A and field C are getting less oil production with the new characterisation compared to the old, while field B is getting more oil production with the new characterisation than the old characterisation. For the value adjustment, field A is predicted less value with the new characterisation, while field B and field C is gaining more value with the new characterisation. These trends are current for both all-in simulation and standalone cases.

Field B is gaining oil production when producing in an all-in simulation compared to standalone. This means that the fluids from A and C are helping the fluids from B to go out in the oil phase instead of the gas phase. For the C field and the A field, this is reversed with more oil production on a standalone basis than all-in.

When evaluating the total production, the new characterisation predicts less oil production compared to the old characterisation. The total gas production is approximately the same, while the estimated values are 80 MNOK/year higher with the new characterisation compared to the old characterisation.

The ORFs are illustrated in the form of a bar chart for each field. The ORF values are shown inside the bars, and the lowest hydrocarbons are skipped to illustrate the deviations between the higher hydrocarbons better. The ORFs are determined on a standalone basis since standalone is used in the current allocation method for Platform Vest.

Figure 7.7 shows the ORFs estimated in percentage for the hydrocarbons for field A.

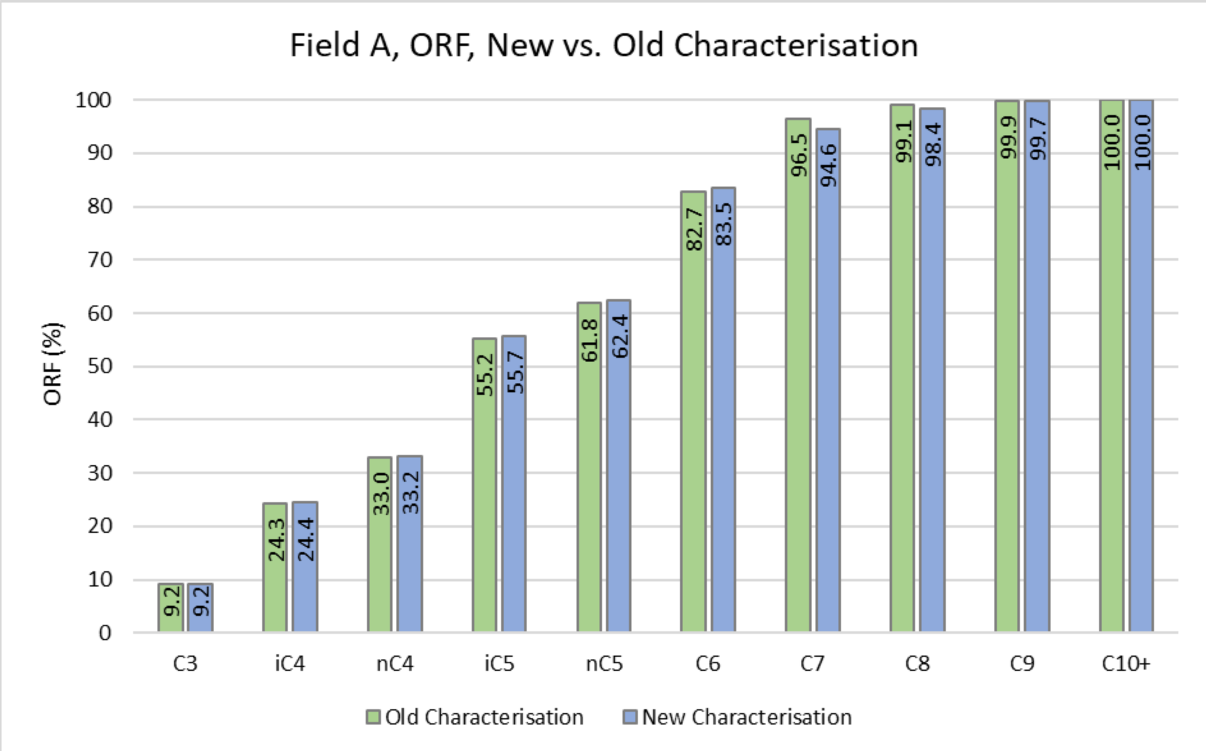

Figure 7.7: Field A ORFs, new vs. old characterisation

The ORFs predicted for field A are similar but with a slight overestimation of the C7 component with the old characterisation compared to the new characterisation. The deviation for the C7 component is 1.9 %.

Figure 7.8 shows the ORFs estimated for field B.

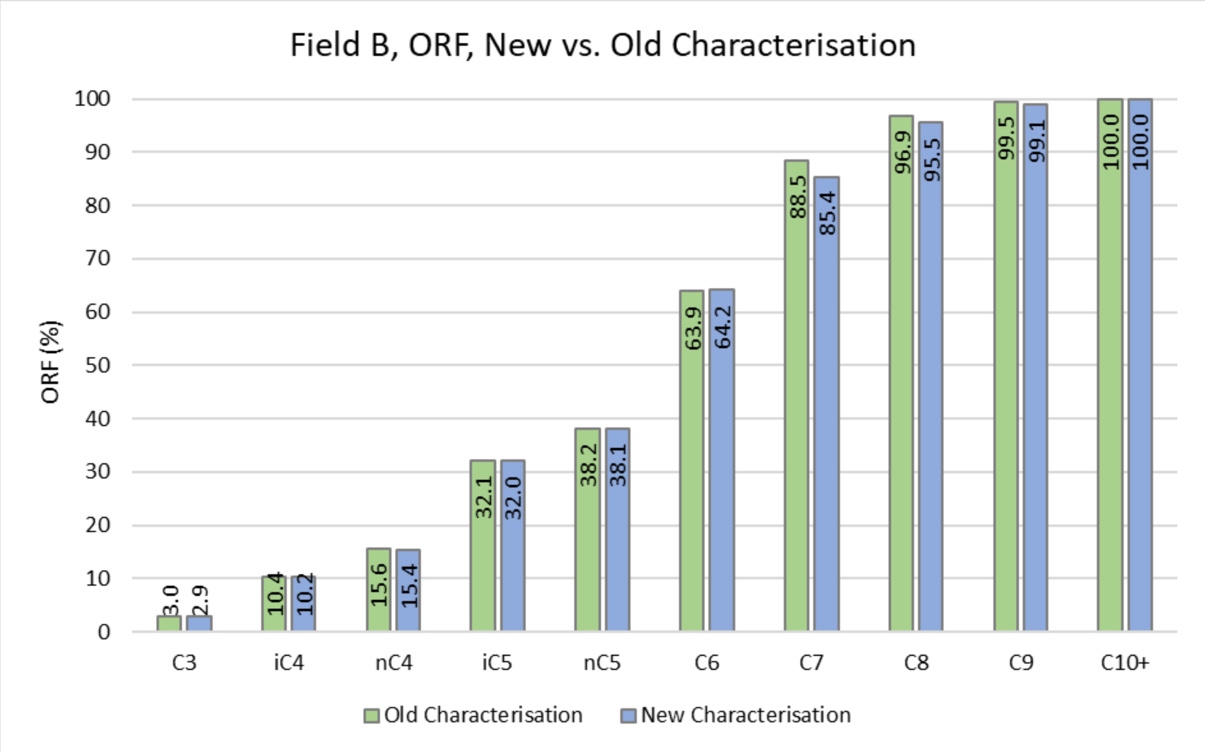

Figure 7.8: Field B ORFs, new vs. old characterisation

The ORFs predicted for field B are similar but with an overestimation for the C7+ hydrocarbons with the old characterisation compared to the new. The highest deviation is 3.1% overestimation with the old characterisation compared to the new characterisation for the C7 component.

Figure 7.9 shows the ORFs estimated for field C.

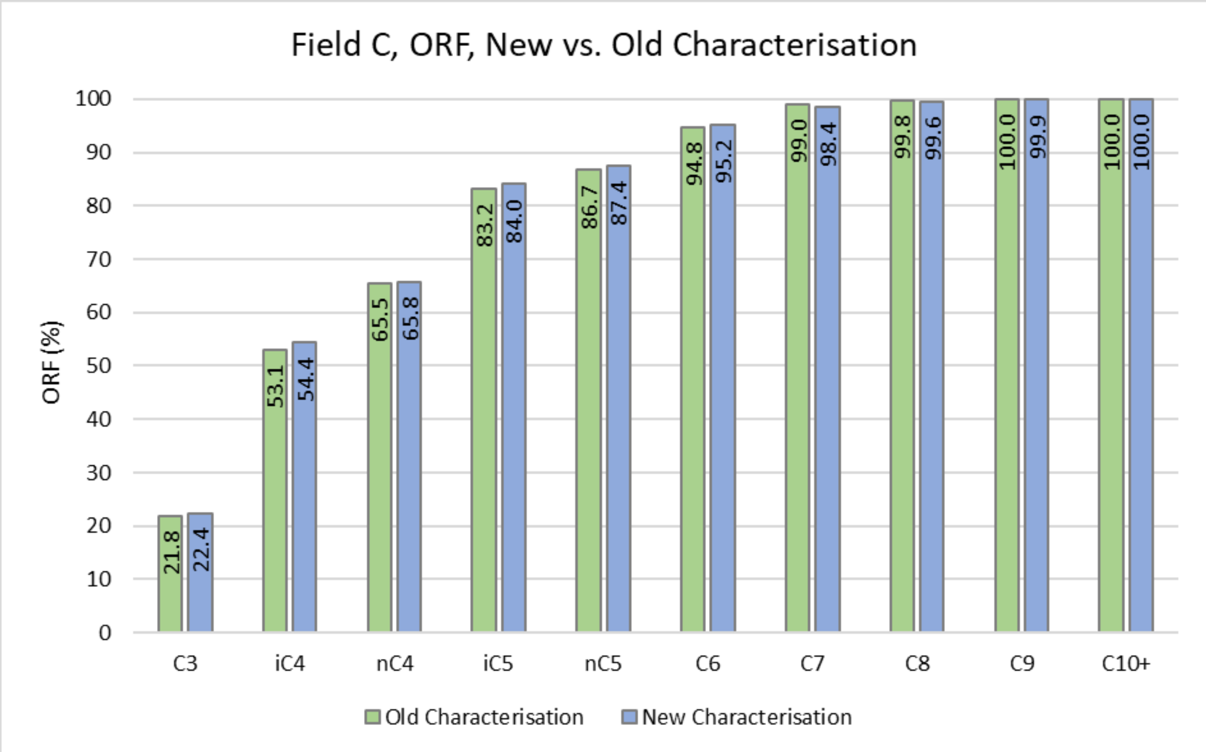

Figure 7.9: Field C ORFs, new vs. old characterisation

The ORFs estimated for field C is the most similar when comparing the new and old characterisation, with the highest deviation of 0.8 % for the iC5 component.

The consequence of keeping the old characterisation instead of switching to the new is 11 MNOK/year favouring field A, 55 MNOK/year less to field B and 36 MNOK/year less to field C when looking at the all-in simulation case. The most crucial allocation principle is that the allocation between the producers should always be as fair and prudent as possible. The ORFs are also important parameters used for the current allocation agreement. Therefore, it is important that this parameter is up to date and representative of the current fluids in production. The new characterisation is based on newer test samples and is therefore seen as the more up-to-date characterisation. Keeping the old characterisation will give different values compared to the new characterisation; it is recommended to switch to the new characterisation. The new characterisation will be used as a reference for correct allocation results for Platform Vest for the following cases. The new characterisation simulation results will be referred to as the initial/original results when compared to other cases.

7.2 Hypothetical components vs. UniSim allocation utility

UniSim offers a utility that gives the user the possibility to track a component from one input stream to one outlet stream. This gives the possibility to use library components for the lighter hydrocarbons where the fluid characterisation is estimated equally. The higher (C6+) hydrocarbons often have varying characterisation depending on the field and will be defined as hypothetical components like the initial case.
The results gained from an allocation utility in UniSim is the flow in either mass, mol or

volume (no option to get the std volume flow). This reduces the opportunity to compare the predicted results to the results from the initial case. The standalone ORFs are the only result obtained from the UniSim simulation using the allocation utility method. The Appendix J – Utility method in UniSim shows how the utility allocation is used and set up in the UniSim model.

Figure 7.10, Figure 7.11 and Figure 7.12 show the ORFs estimated for field A, field B and field C, respectively.

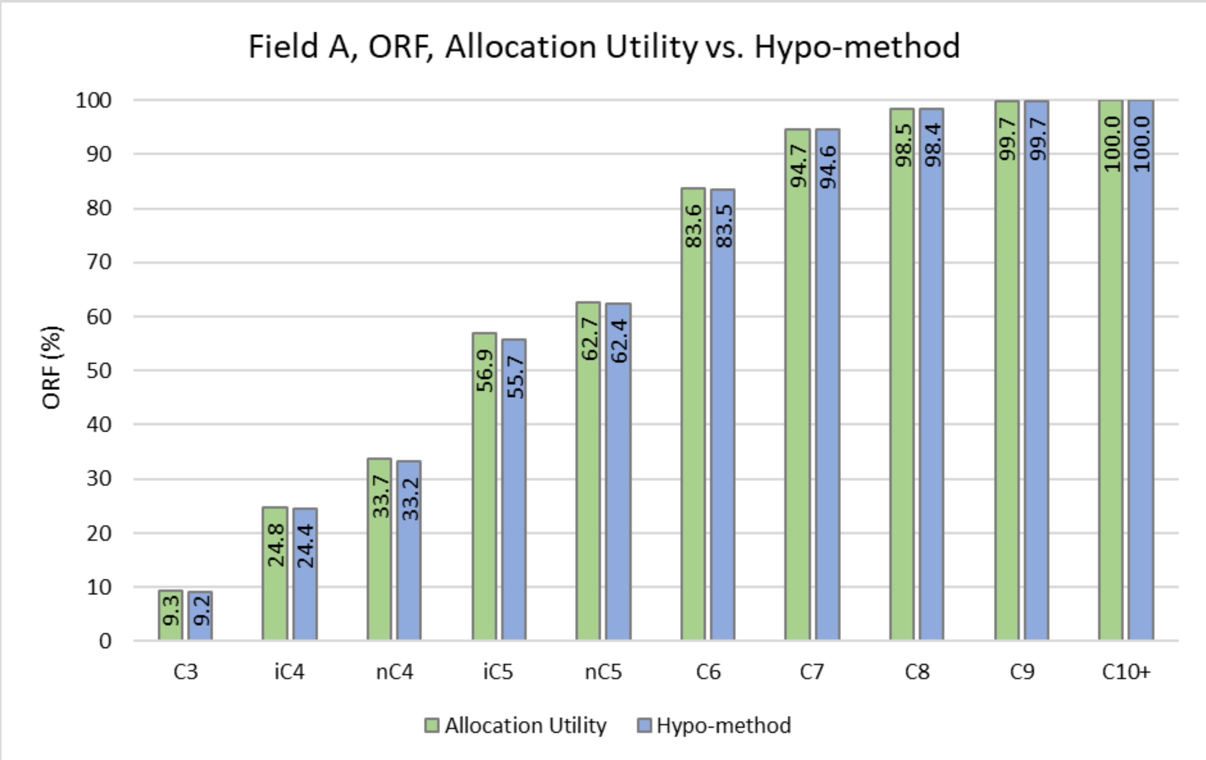

Figure 7.10: Field A ORFs, Hypo-method vs. Allocation utility

The ORFs predicted for field A are estimated slightly higher for the library components in the utility allocation compared to the hypo-method. The highest deviation is 1.2% for the iC5 component. The higher hydrocarbons (C6+) are estimated approximately the same when comparing the values from the two methods.

.

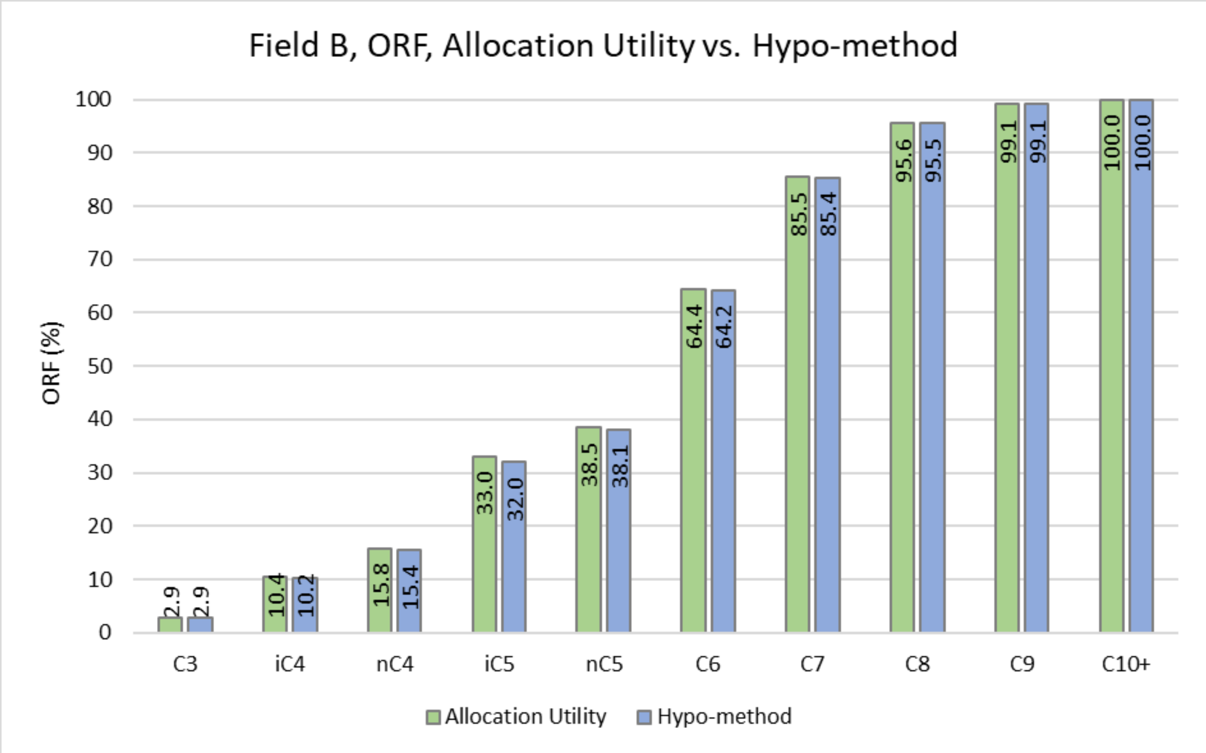

Figure 7.11: Field B ORFs, Hypo-method vs. Allocation utility

The estimated ORFs for field B follow the same trend as the field A results, with slightly higher predictions with the utility allocation compared to the hypo-method for the lower hydrocarbons. The highest deviation is 1.0% for the iC5 component.

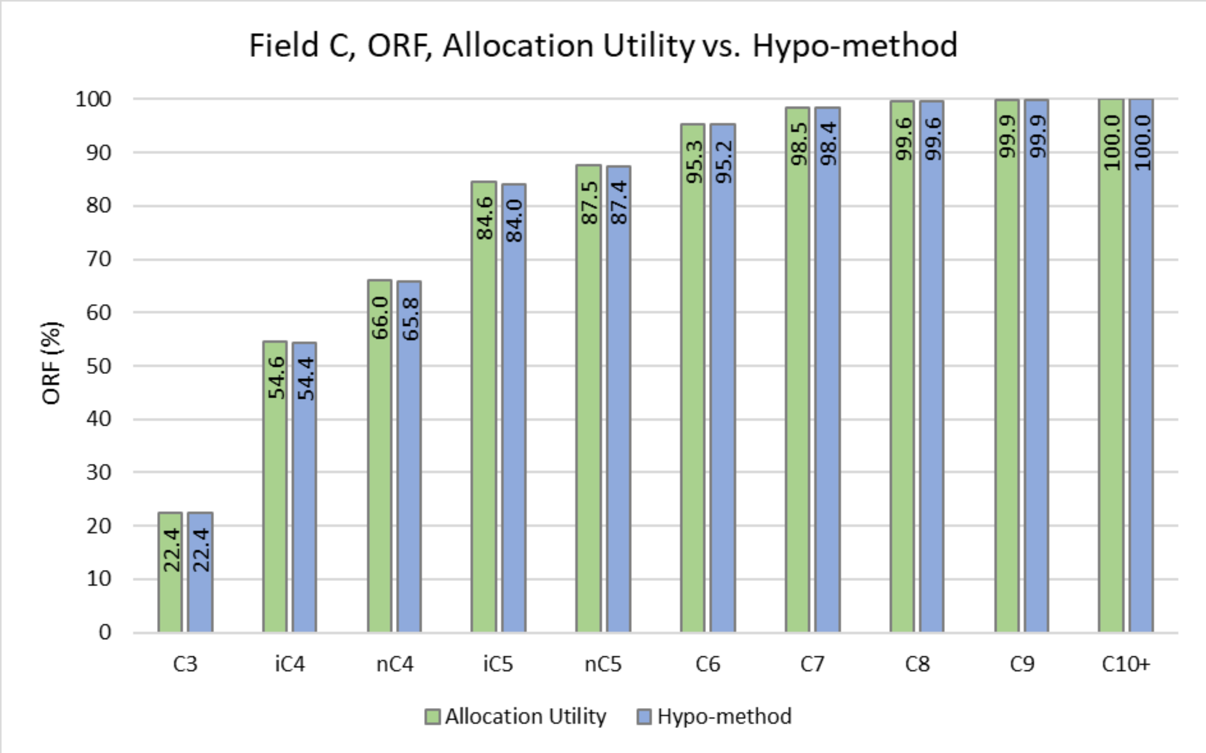

Figure 7.12: Field C ORFs, Hypo-method vs. Allocation utility

The field C ORFs are estimated approximately the same for the two methods, with a slightly higher value estimation for the allocation utility compared to the hypo-method. The highest deviation is 0.6% for the iC5 component.

Comparing the results shows that field A is the field that has the highest deviation between the allocation utility and the hypo-method. Overall, the results are very similar, with the highest deviation being 1.2% for iC5 in field A. The negative with using the allocation utility method is the limitation of the possible results. If ORFs are the only needed result for a simulation, the utility method is a good enough method. The utility method is also timesaving since the lower hydrocarbons can be added as library components.

7.3 Benzene in the fluid setup

This part of the result illustrates how the ORFs change when an aromatic is incorporated into the well composition. The PVT analysis reports that approximately 1 wt.% of the well fluid is aromatics, and this section will investigate how this will affect the results from the simulations. Benzene is used as an aromatic for this case, and 1 wt.% of the total flow from each field is the basis for the benzene flow. Benzene is added as a library component to the fluid setup, and all other parameters are kept the same as in the initial simulation case.

7.3.1 Phase envelope with incorporated benzene to the fluid setup

Figure 7.13, Figure 7.14 and Figure 7.15 show the phase envelope for the initial case compared to the phase envelope where benzene is added to the fluid setup for field A, field B and field C, respectively. The VF is 1.0 for field A and field C and 0.989 for field B. The inlet conditions are also included.

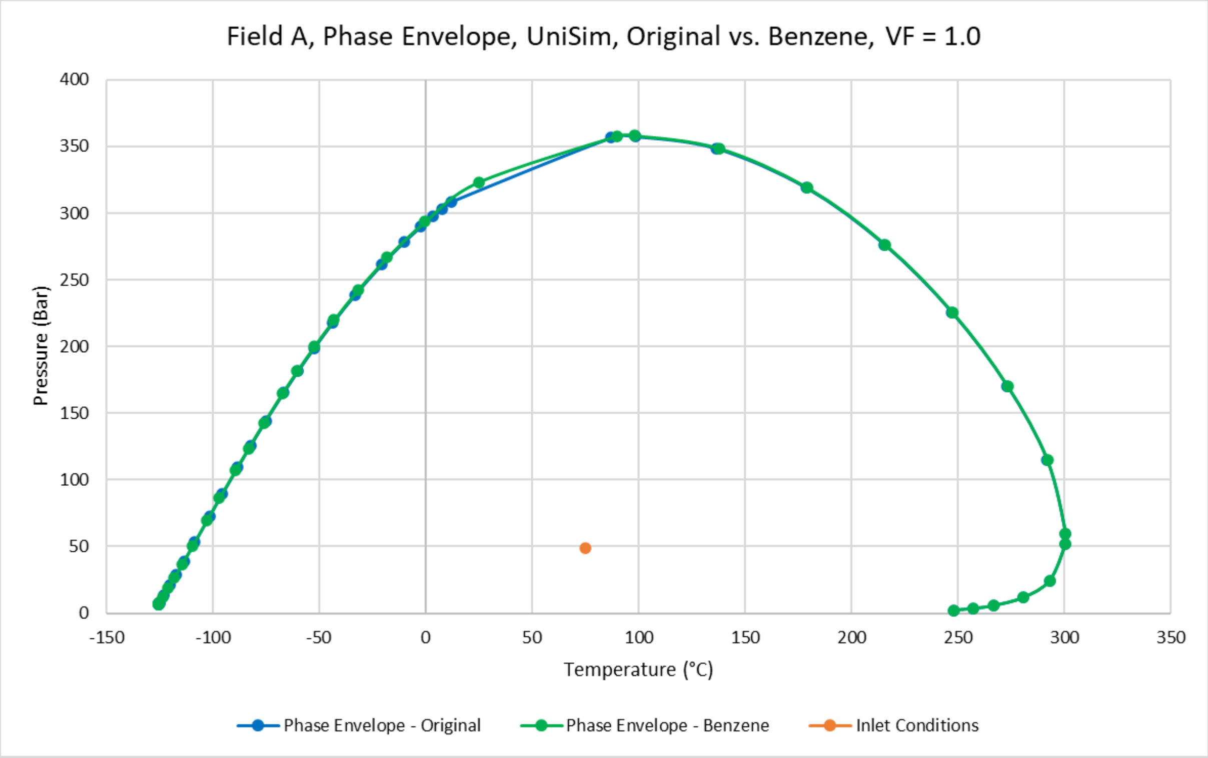

Figure 7.13: Phase envelope, Initial vs. benzene, UniSim, Field A

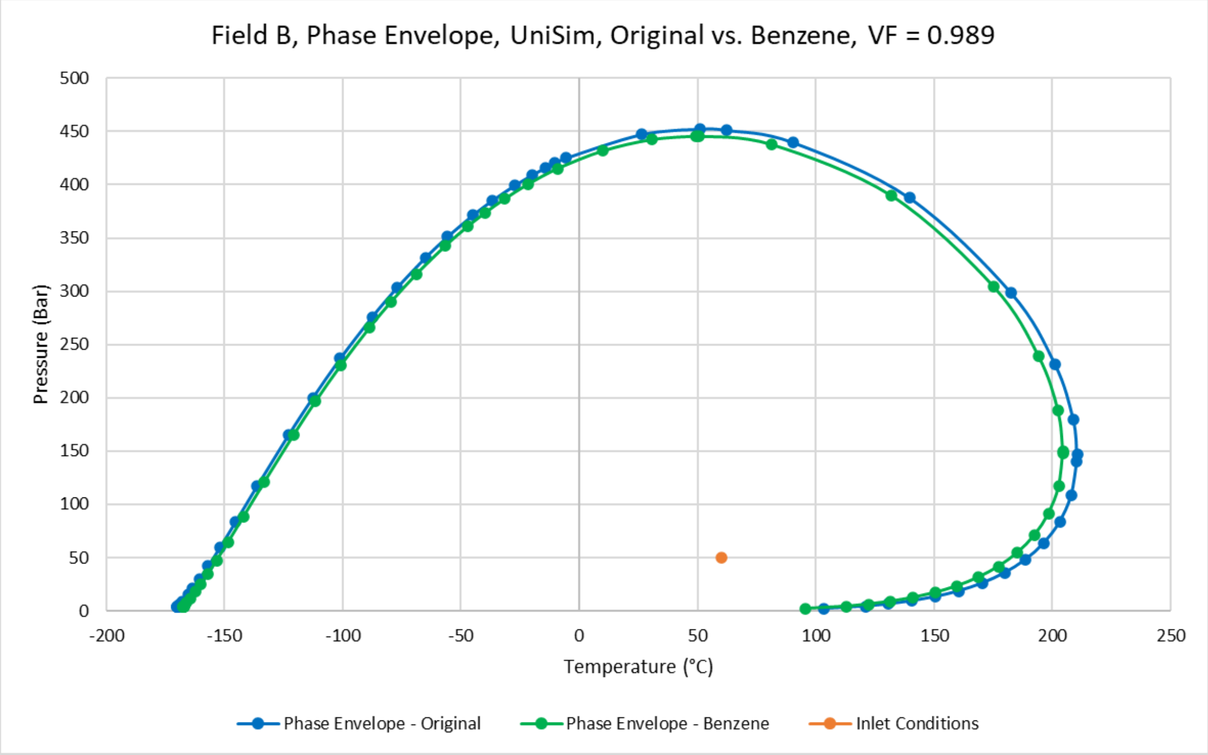

Figure 7.14: Phase envelope, Initial vs. benzene, UniSim, Field B

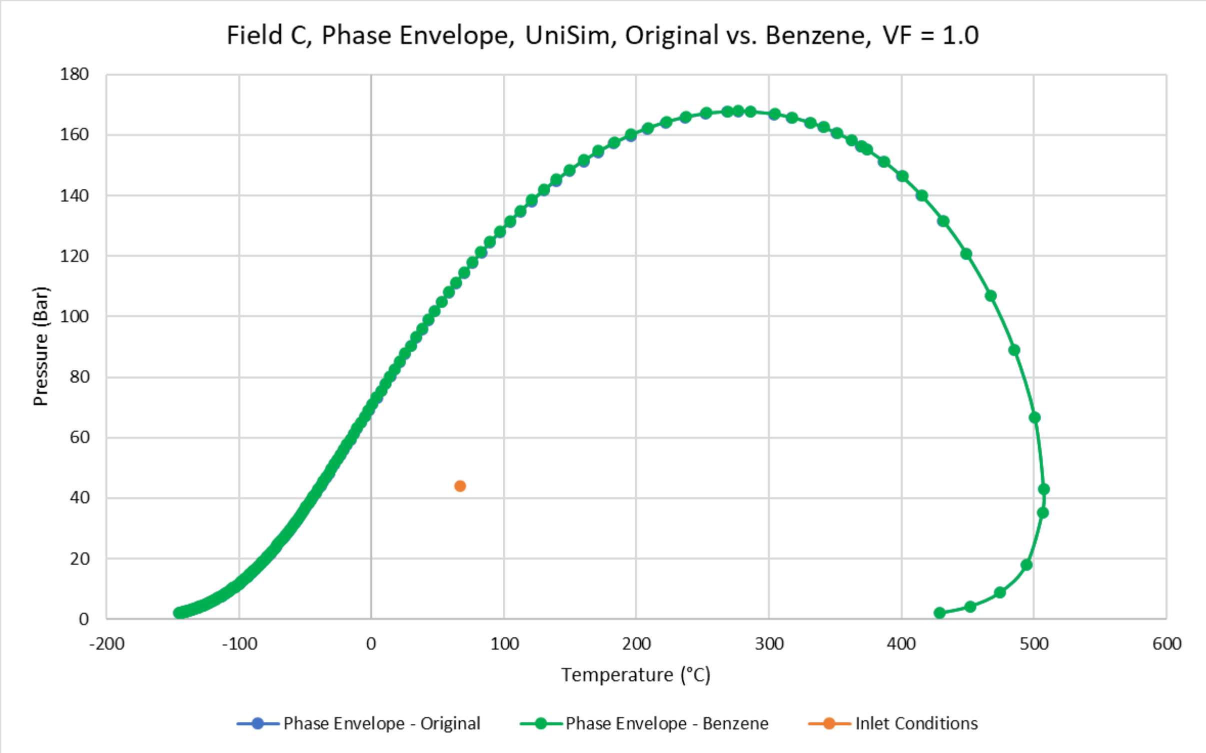

Figure 7.15: Phase envelope, Initial vs. benzene, UniSim, Field C

These results show similar phase envelop curves when comparing the initial case and the case with benzene for field A and field C. The phase envelopes predicted for field B is slightly deviation, indicating that the fluids in the different simulation models will behave slightly deviating from each other.

7.3.2 UniSim simulation result with added benzene

The simulation results are based on standalone for the different fields to be able to get the correct ORF values and be able to track the benzene to the different fields. Table 7.3 shows the total estimated results for oil and gas production on a standalone basis.

Table 7.3: Standalone simulation results for all fields with the initial case and the benzene case

Standalone simulation	Field A	Field B	Field C
Oil production, Sm3/d:			
Initial case	1148	2991	2747
Benzene case	1182	3104	2776
Approximate deviation	-34	-114	-28
Gas production, MSm3/d:			
Initial case	2.1	9.6	0.3
Benzene case	2.1	9.6	0.3
Approximate deviation	0.0	0.0	0.0

The gas production is estimated approximately the same for the two cases (with the given unit MSm^3/d), but the oil production with benzene is much higher than in the initial case. This suggests that the benzene influences how much of the inlet fluid is going out in the oil instead of the gas. Note that for this case, only 1 wt.% of benzene was added to the inlet streams and gives high deviations in the resulting when comparing to the initial simulation case. Field B has the highest deviation with 114 Sm^3/d more oil production with benzene added compared to the initial case.

Figure 7.16, Figure 7.17 and Figure 7.18 show the ORFs estimated for field A, field B and field C, respectively.

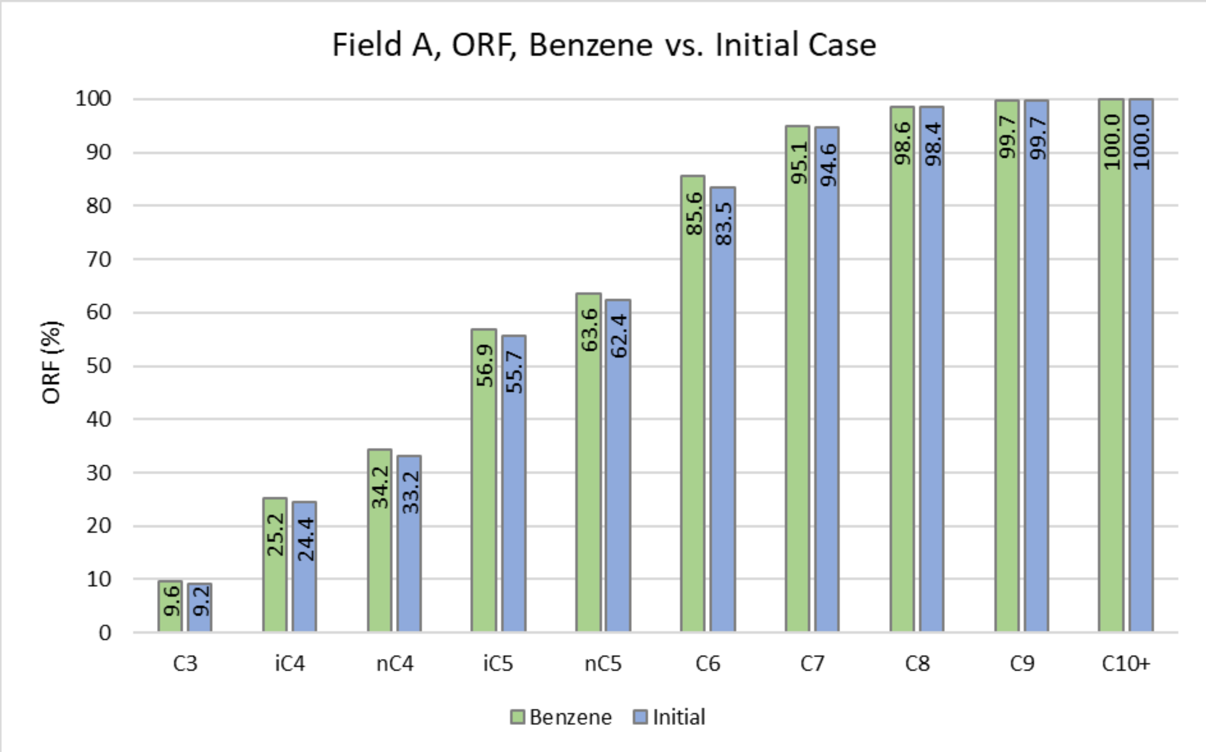

Figure 7.16: Field A ORFs, Initial vs. benzene

The estimated ORFs for field A for the benzene case is noticeably higher than the initial case. The highest deviation is 1.9 % higher ORF estimation for the C6 component.

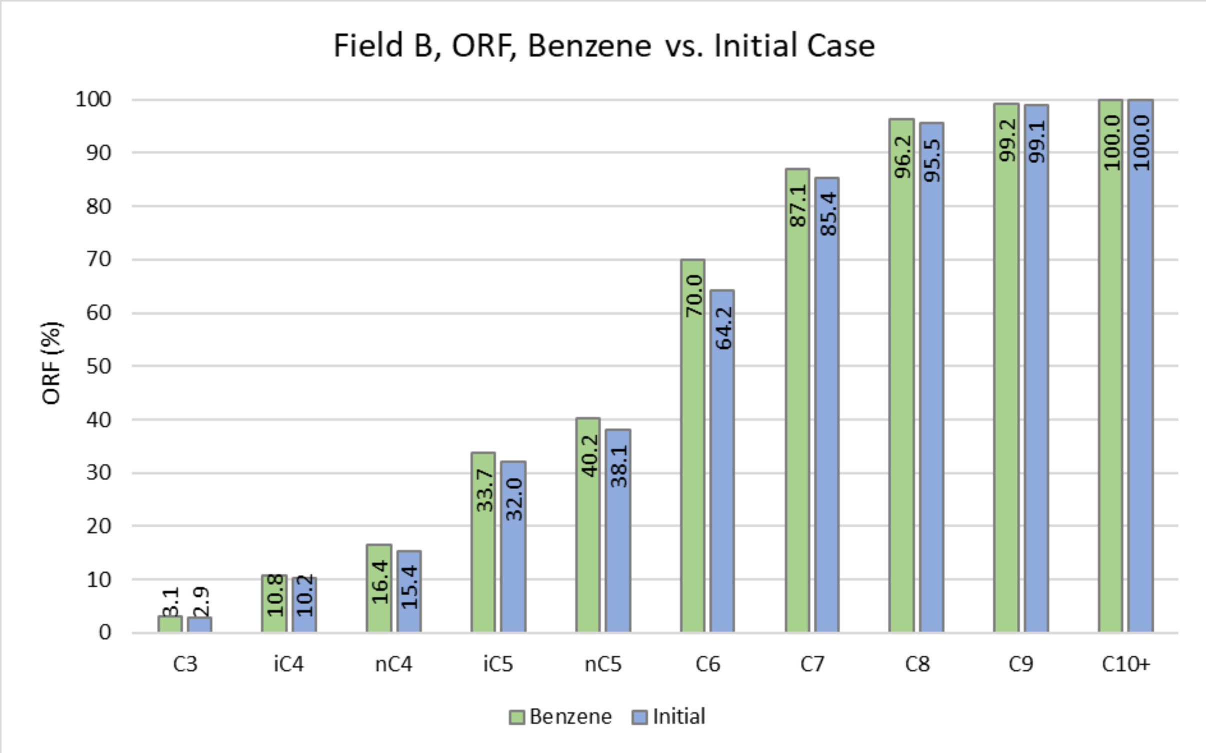

Figure 7.17: Field B ORFs, Initial vs. benzene

The estimated ORFs for field B with benzene is higher than the initial case. The most significant deviation is 5.8 % for the C6 component.

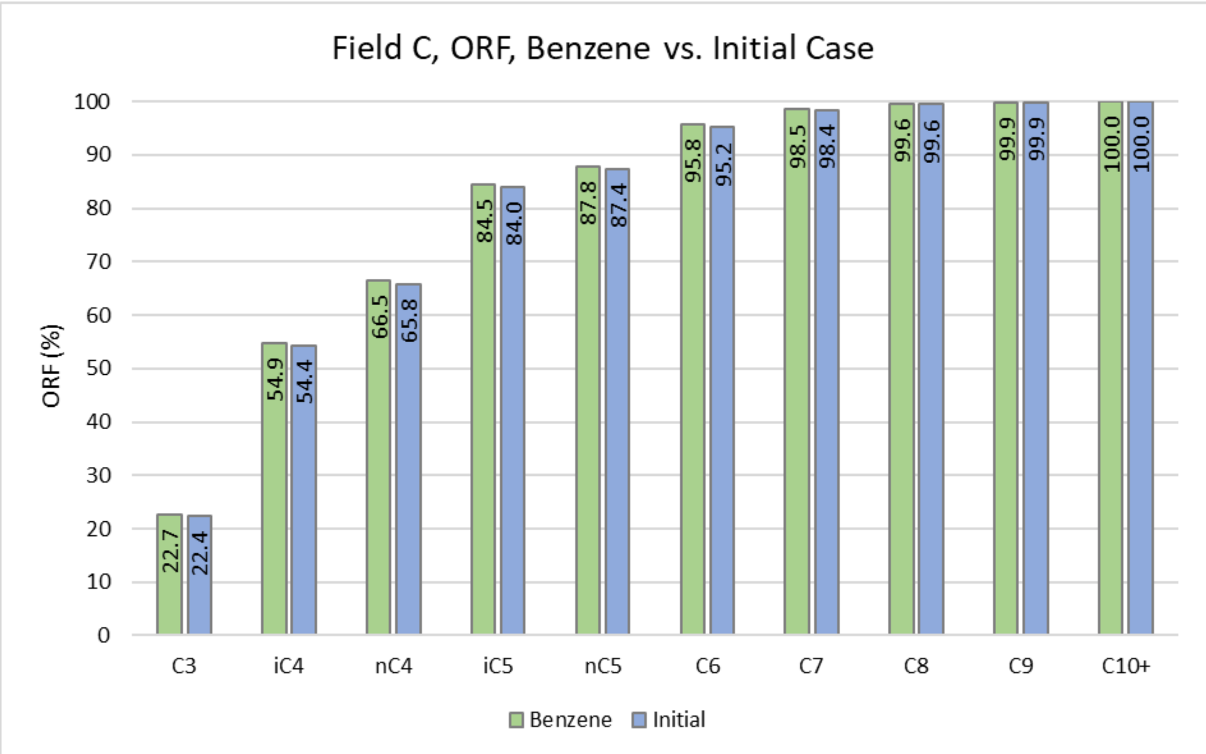

Figure 7.18: Field C ORFs, Initial vs. benzene

The estimated ORFs for field C are the most similar between the two cases compared to the field A and field B results. The most significant deviation is 0.6 % for the C6 component.

The predicted ORF results for all the fields estimate a higher result for the benzene case compared to the initial case. The most noticeable deviation is 5.8 % for the C6 hydrocarbon for field B. This deviation is only due to the addition of 1 wt. % benzene to the inflow. From the results estimated in this section, the addition of aromatics in the fluid setup will affect the estimated results noticeably in a process simulation.

7.4 Pressure and temperature adjustment in the first stage separator

For this part of the results, the importance of using process input with high certainty is studied by adjusting the temperature and the pressure for the first stage separation. The first stage of separation consists of the inlet separator and the test separator. The adjustment is made the same for the two separators (e.g., if the temperature in the test separator is adjusted, the temperature in the inlet separator is also adjusted the same quantity). The temperature is adjusted ±1°C, and the pressure is adjusted ±1bar, resulting in 8 different cases. The cases are shown in Table 7.4.

Table 7.4: Pressure and temperature adjustment cases

Case name	Pressure adjustment	Temperature adjustment
P-	- 1 bar	Initial
T-	Initial	- 1 °C
P-T-	- 1 bar	- 1 °C
P+	+ 1 bar	Initial
T+	Initial	+ 1 °C
P+T+	+ 1 bar	+ 1 °C
P-T+	- 1 bar	+ 1 °C
P+T-	+ 1 bar	- 1 °C

Figure 7.19 shows the total oil production over the platform with the adjusted temperature and pressure cases.

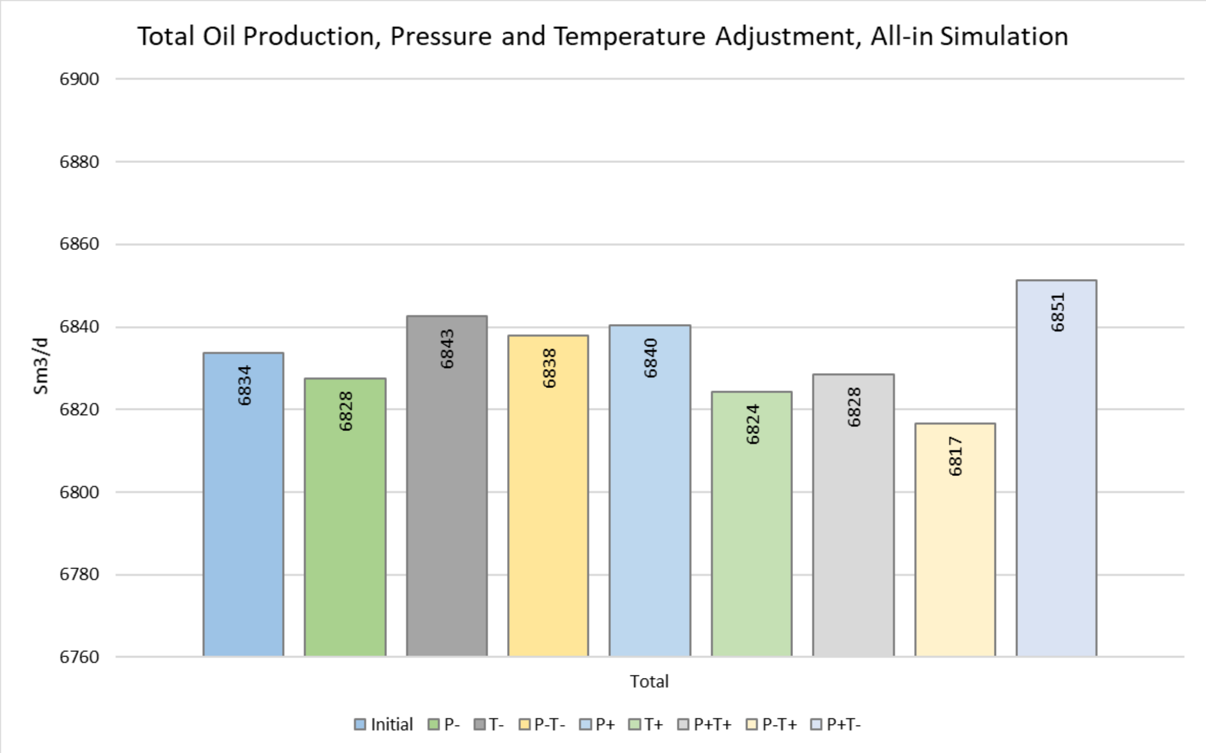

Figure 7.19: Total oil production, all T and P adjustments

The results show that the oil production is similar, but the P+T- case and the P-T+ case gives the highest deviation with 17 Sm^3/d. The result for gas production is not included due to approximately the same predictions for all the cases.

Figure 7.20, Figure 7.21 and Figure 7.22 show some selected ORF estimations for field A, field B and field C, respectively. These ORFs are selected due to having the highest deviation compared to the ORFs for the other components.

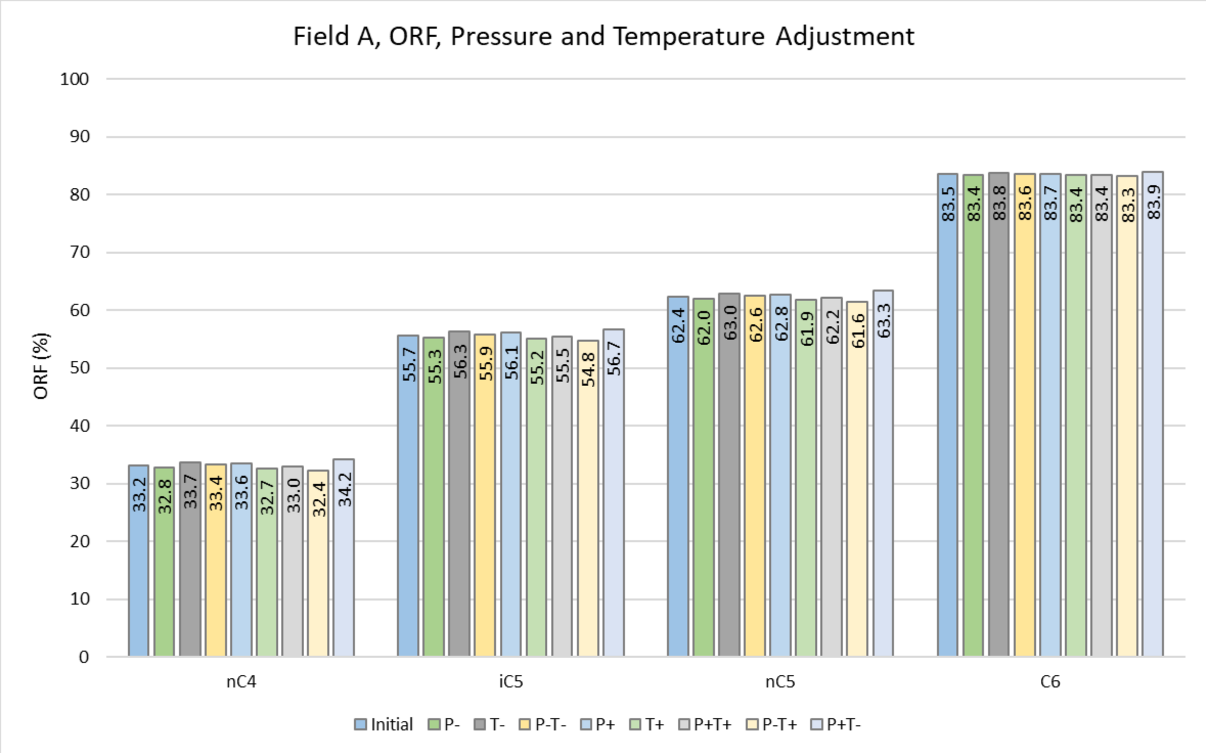

Figure 7.20: Field A ORFs, all T and P adjustments

The results show that the ORFs estimated for field A is similar, but the P+T- case deviates the highest with 1.0 % for the nC4 and iC5 component compared to the initial case.

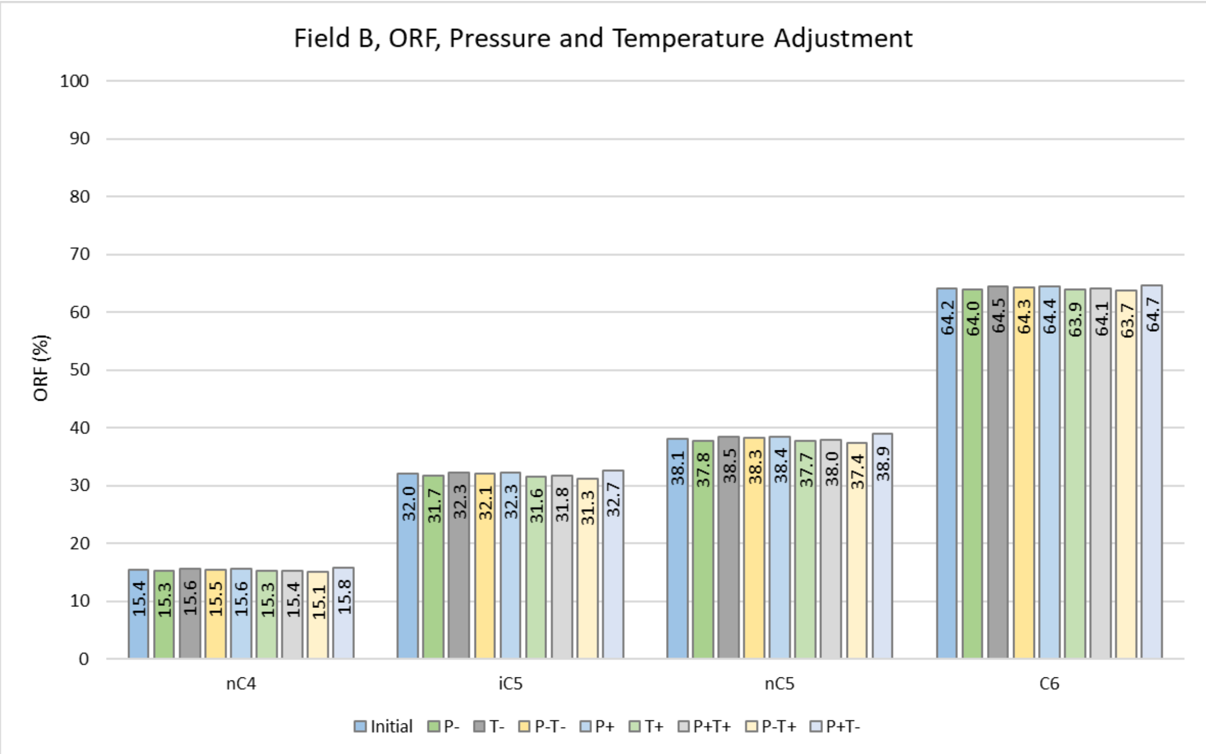

Figure 7.21: Field B ORFs, all T and P adjustments

The results show that the ORFs estimated for field B is similar, but the P+T- case deviates the highest with 0.8 % for the iC5 component compared to the initial case.

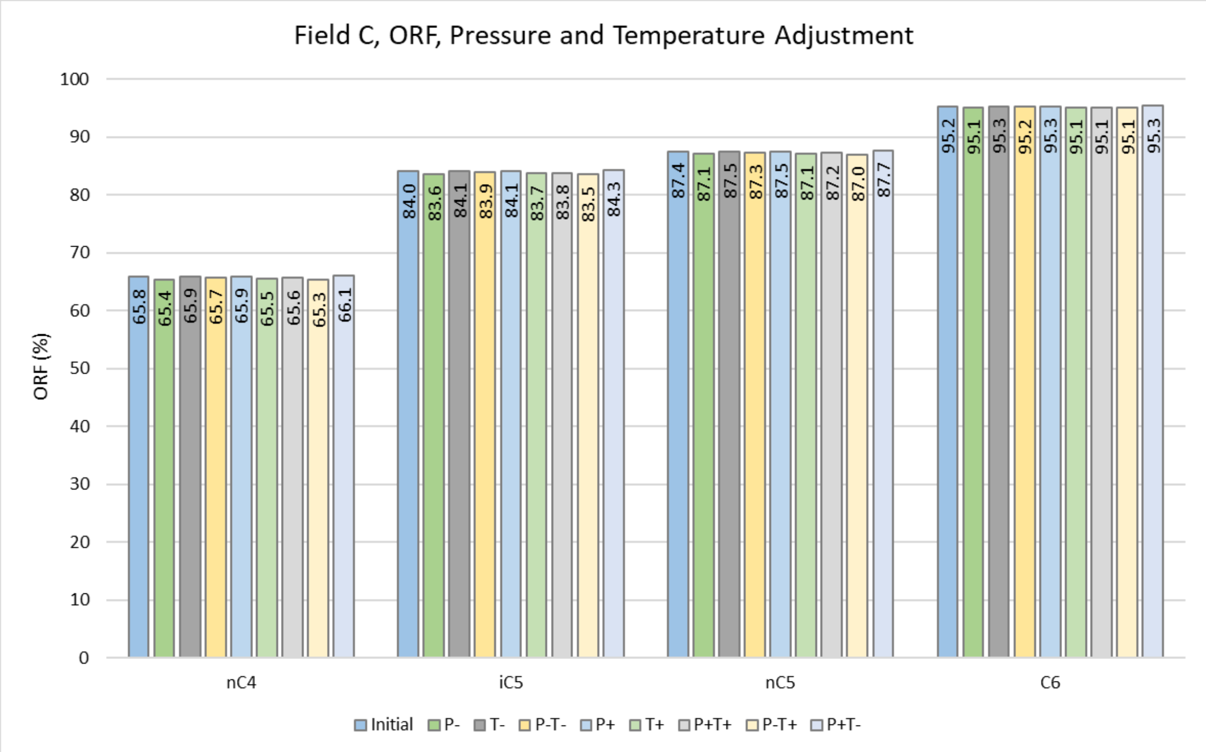

Figure 7.22: Field C ORFs, all T and P adjustments

The results show that the ORFs estimated for field C are similar, but the P-T+ case deviates the highest with 0.5 % for the nC4 and iC5 component compared to the initial case.

These comparisons show that the P+T- case and the P-T+ case give the highest deviations compared to the initial case. The estimated results for the total oil production and the ORFs for the different fields show that it is essential always to use quality process input with a low uncertainty as input to the simulations to get the most certain simulation results. The deviations are not extremely large when compared to the initial case, but only two process input parameters are adjusted in these cases. A process simulation will never be more accurate than the accuracy of the input parameters; thus, the accuracy of the parameters is essential for the correctness of the results.

7.5 C20+ lumping for the fluid characterisation and input

The fluid characterisation for the different fields uses lumping schemes up to C80. In this section, the fluid characterisation is lumped together in new brackets so that C20+ includes all components from C20 and up to C80. This chapter is included to see the importance of fluid characterisation and determine how partite a fluid characterisation must be. For this section, there was a need to characterise the fluid again using PVTsim with the new fluid test samples as the input to form a new characterisation for the new lumping scheme. With the new lumping scheme, the value adjustment cuts from the initial case cannot be used. Therefore, the value adjustment is not included in the results in this section since the comparison would not be legitimate. A detailed description of the C20+ characterisation is given in Appendix K – C20+ fluid characterisation.

7.5.1 Phase envelope for the C20+ characterisation

The phase envelope from PVTsim is compared to the phase envelope from UniSim to assure the quality of the proper UniSim setup for the C20+ simulation. The phase envelope for the initial case is also included to see how it deviates from the phase envelope predicted for the C20+ case. Figure 7.23, Figure 7.24 and Figure 7.25 show the phase envelops for field A, field B and field C, respectively. The VF is 1.0 for field A and field C and 0.96 for field B. The inlet conditions are also included in the figures.

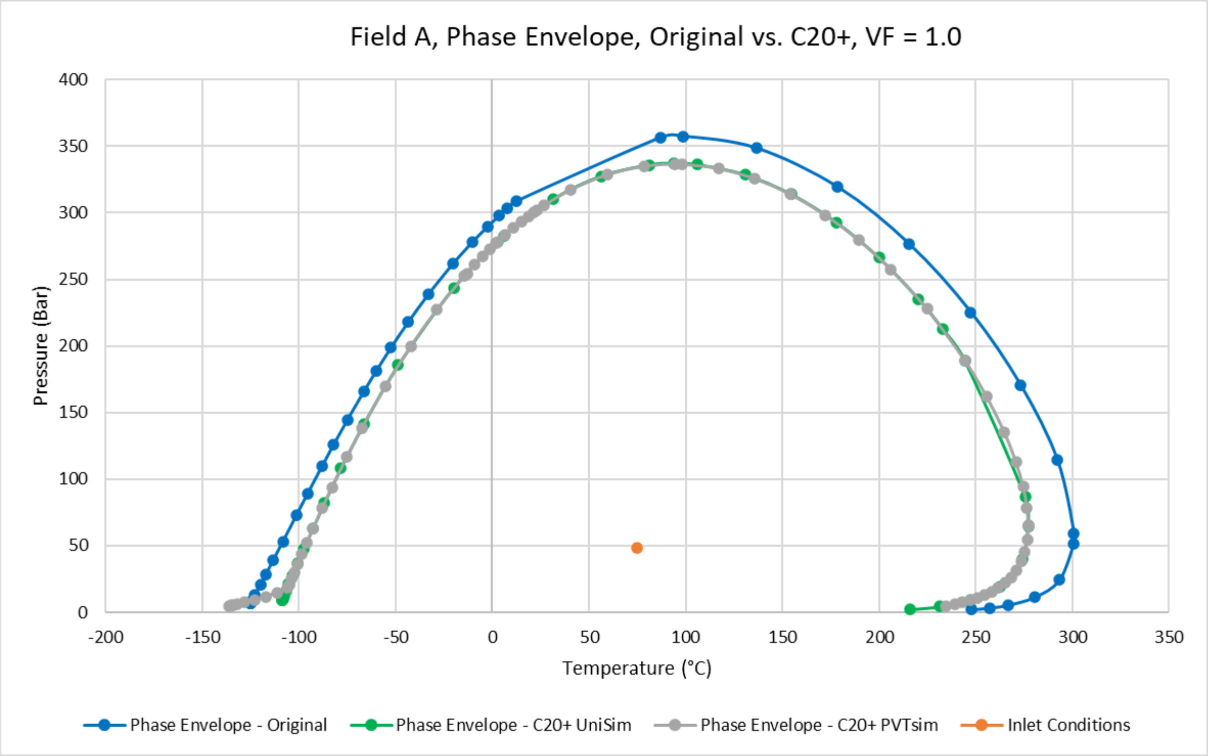

Figure 7.23: Phase envelope, Initial vs. C20+, UniSim and PVTsim, Field A

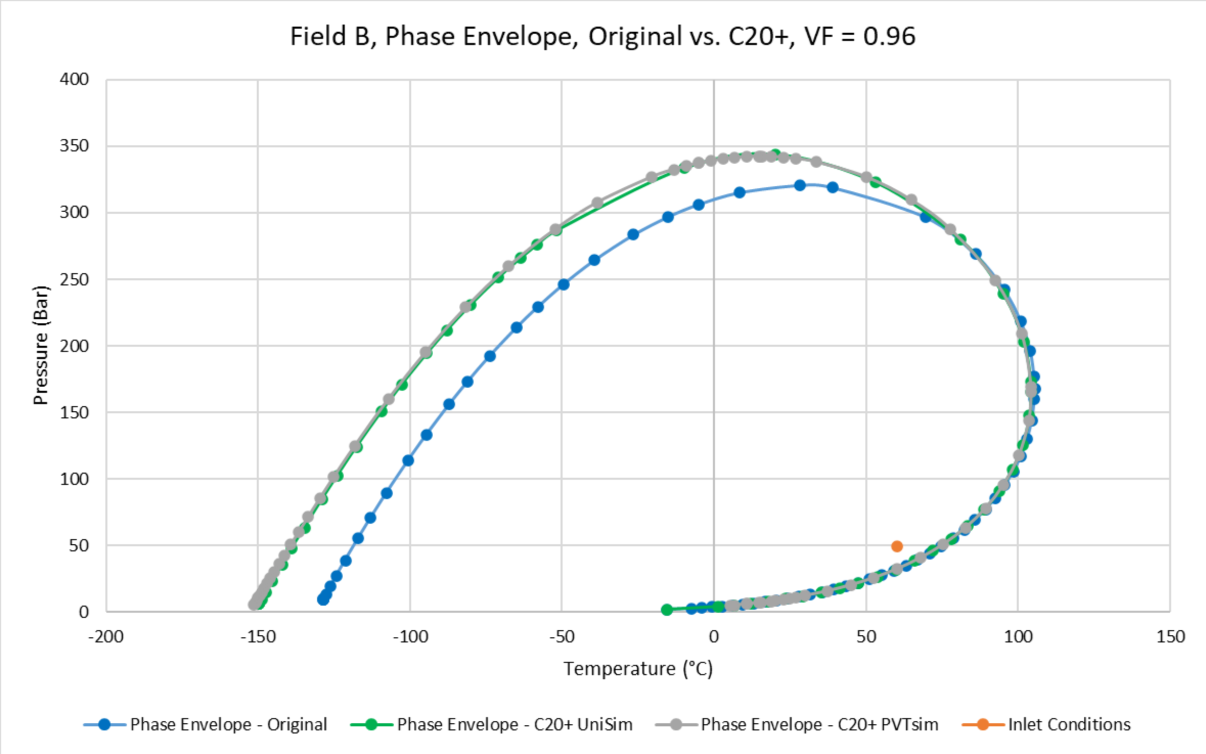

Figure 7.24: Phase envelope, Initial vs. C20+, UniSim and PVTsim, Field B

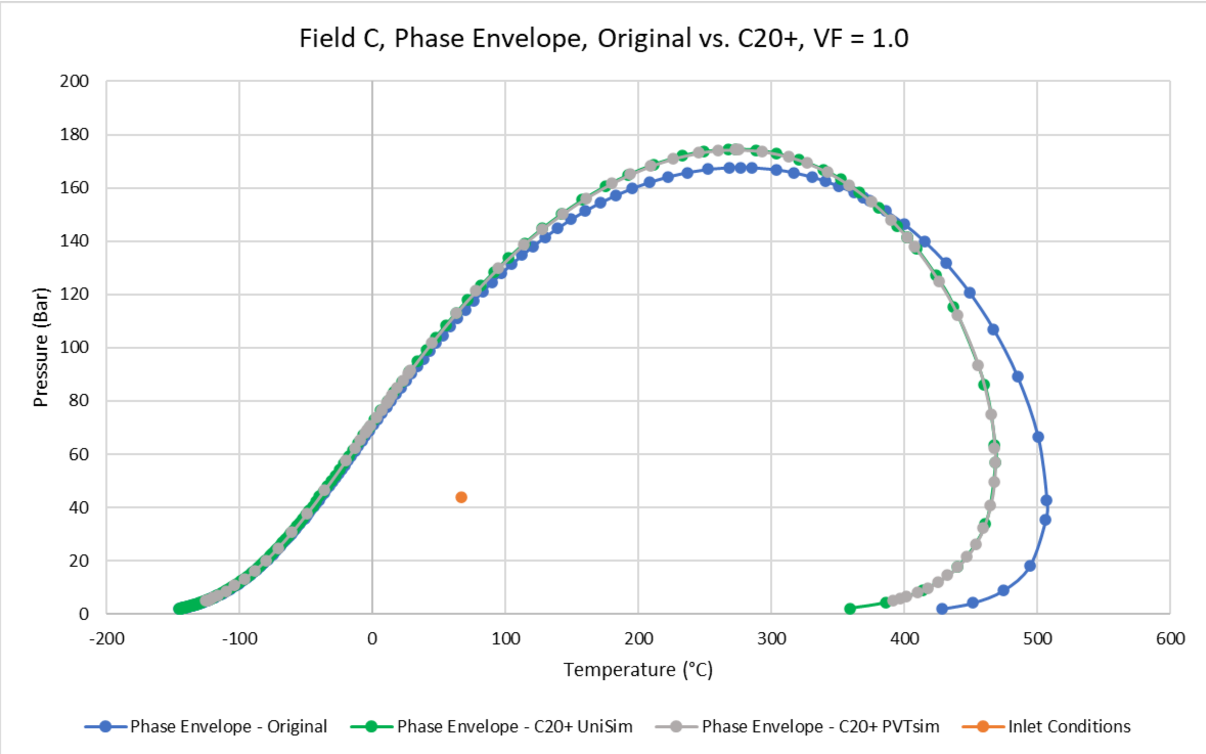

Figure 7.25: Phase envelope, Initial vs. C20+, UniSim and PVTsim, Field C

The curves show that the phase envelope determined from PVTsim for the C20+ lumping scheme matches the phase envelope determined from the UniSim model with C20+ lumping.

This indicates that the C20+ fluid characterisation is incorporated correctly into the C20+ simulation model. The inlet conditions are inside the two-phase area for all the fields.

The phase envelopes from the initial case and the C20+ case deviate significantly from each other. This indicates that the fluids from the C20+ characterisation will not behave the same way as the fluids in the initial case, resulting in possible deviations between the simulation results.

7.5.2 UniSim results for the C20+ characterisation

The results given from the UniSim models are the oil and gas production, both total and for each field. The results are estimated both from an all-in simulation and from the standalone cases. The standalone cases and the all-in case are included to observe the commingling effect between the fields and see the difference when the field is producing alone. This is done for the C20+ case, which is compared to the initial case. The simulation result with the standalone cases is shown in Table 7.5, and the simulation result with the all-in case is shown in Table 7.6.

Table 7.5: Standalone simulation results for all fields with the initial case and the C20+ case

Standalone simulation	Field A	Field B	Field C
Oil production, Sm3/d:			
Initial case	1148	2991	2747
C20+ case	1148	2993	2754
Approximate deviation	0	-3	-6
Gas production, MSm3/d:			
Initial case	2.1	9.6	0.3
C20+ case	2.1	9.6	0.3
Approximate deviation	0.0	0.0	0.0

Table 7.6: All-in simulation results for all fields with the initial case and the C20+ case

All-in simulation	Field A	Field B	Field C	Total
Oil production, Sm3/d:				
Initial case	1130	3147	2557	6834
C20+ case	1130	3148	2565	6843
Approximate deviation	0	-2	-7	-9
Gas production, MSm3/d:				
Initial case	2.1	9.6	0.3	12.0
C20+ case	2.1	9.6	0.3	12.0
Approximate deviation	0.0	0.0	0.0	0.0

The initial case and the C20+ case predict approximately the same gas production for all the fields and in total with the standalone cases and the all-in case. For field A the estimated oil production is approximately the same for both cases and simulations. Field B and field C have a slightly lower oil prediction in the initial case compared to the C20+ case, with 2 Sm^3/h and 7 Sm^3/d difference, respectively. When evaluating the total production, the initial case predicts less oil production compared to the C20+ case.

The commingling effect for the C20+ case follows the same prediction as the initial case, with higher oil prediction for field B with all-in, and higher predictions for field A and field C with standalone simulation.

The simulation results show that the difference with using C20+ lumping instead of the initial lumping does not give high deviations.

The ORFs are determined on a standalone basis and compared to the predicted ORF values in the initial case.

Figure 7.26, Figure 7.27 and Figure 7.28 show the ORFs estimated for field A, field B and field C, respectively.

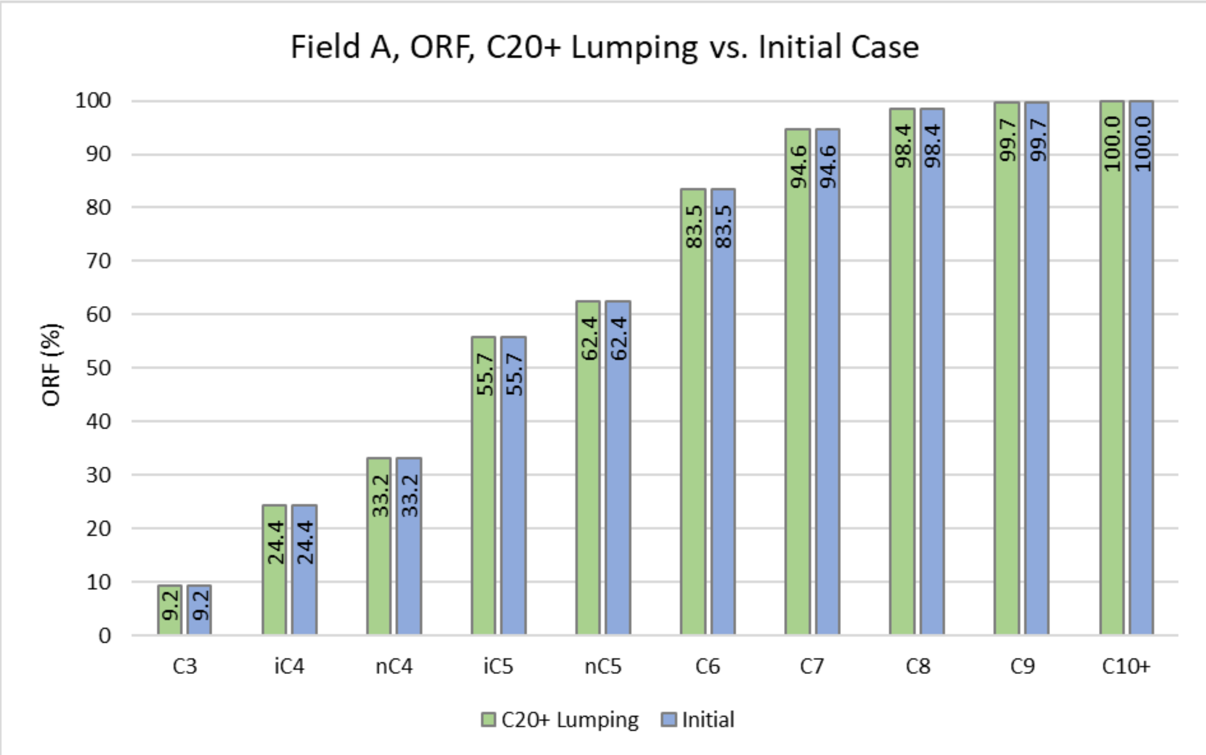

Figure 7.26: Field A ORFs, C20+ lumping vs. initial case

The ORF estimates for field A predicts approximately the same values when comparing the C20+ case with the initial case.

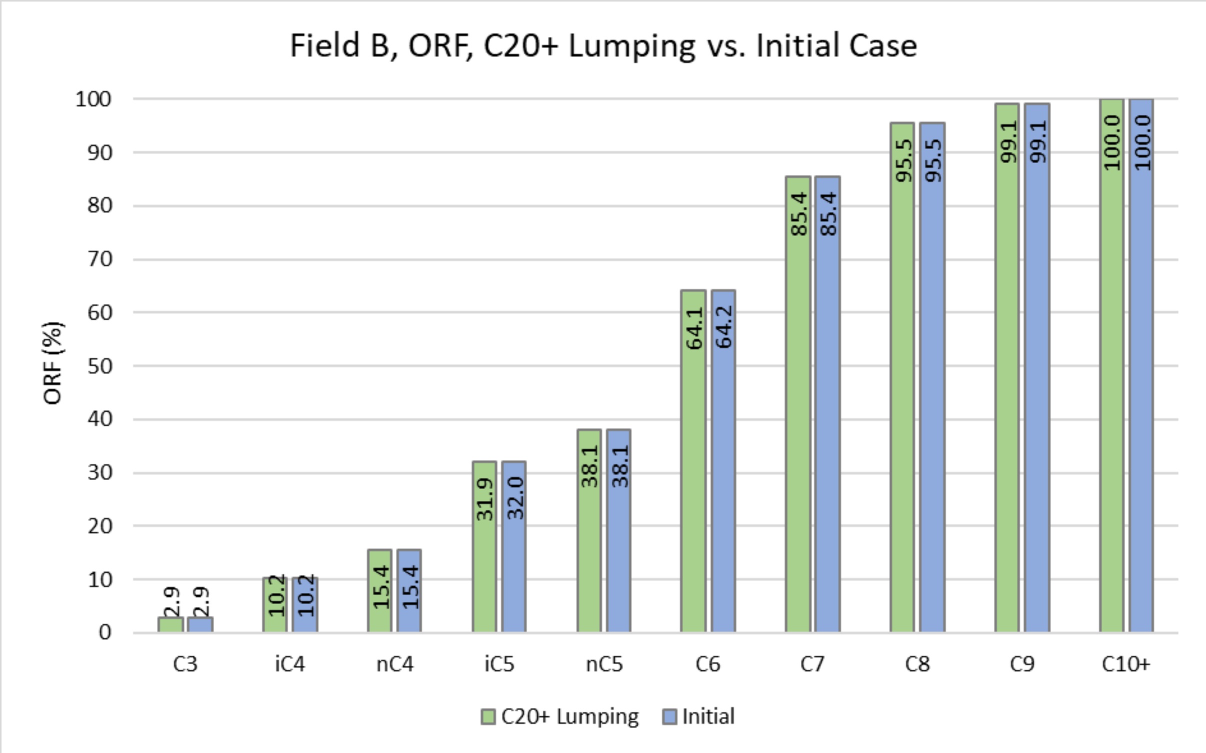

Figure 7.27: Field B ORFs, C20+ lumping vs. initial case

The ORF estimates for field B predicts approximately the same values when comparing the C20+ case with the initial case.

.

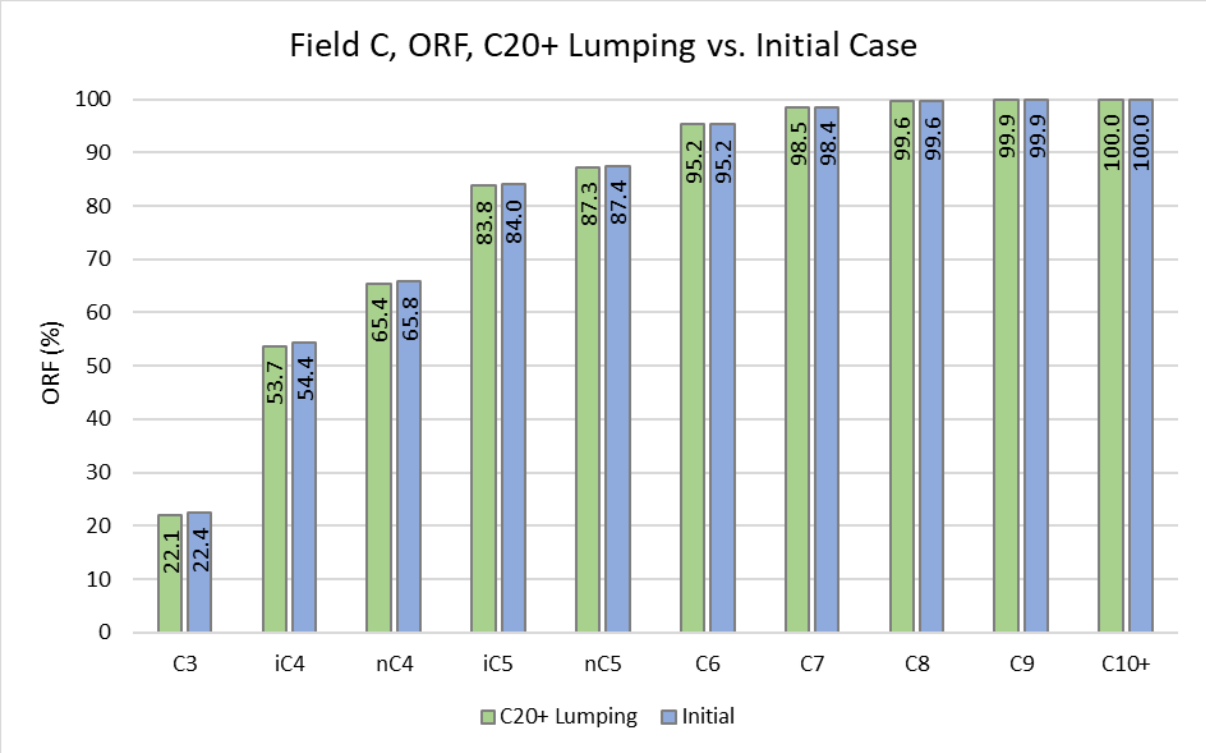

Figure 7.28: Field C ORFs, C20+ lumping vs. initial case

The ORF estimates for field C predict similar values when comparing the C20+ case with the initial case, but slightly more deviating than the deviations for field A and field B. The highest deviation is 0.7 % for the iC4 component.

The results from the C20+ case shows that the estimates from the simulations and the ORFs are very similar to the initial case, despite the phase envelopes dissimilarities.

7.6 C10+ lumping for the fluid characterisation and input

In this section, the fluid characterisation is lumped together in even fewer brackets so that C10+ includes all components C10 and higher up to C80. This case is investigated since the result with C20+ lumping showed very similar results to the initial case. This case is also interesting since the C10+ characterisation is often a more easily obtained analysis than an in-depth laboratory analysis for the total composition (which often is expensive). For this section, there was also a need to characterise the fluid again using PVTsim with the new fluid test samples as the input. A detailed description of the C10+ characterisation is given in Appendix L – C10+ fluid characterisation.

7.6.1 Phase envelope for the C10+ characterisation

The phase envelope from PVTsim is compared to the phase envelope from UniSim to assure the quality of the proper UniSim setup for the C10+ simulation. The phase envelope for the initial case is also included to see how it deviates from the phase envelope predicted for the C10+ case. Figure 7.29, Figure 7.30 and Figure 7.31 show the phase envelops for field A, field B and field C, respectively. The VF is 1.0 for field A and field C and 0.88 for field B.

The inlet conditions are also included for field A and field C but excluded from field B since the inlet conditions are outside the phase envelope with the set vapour fraction.

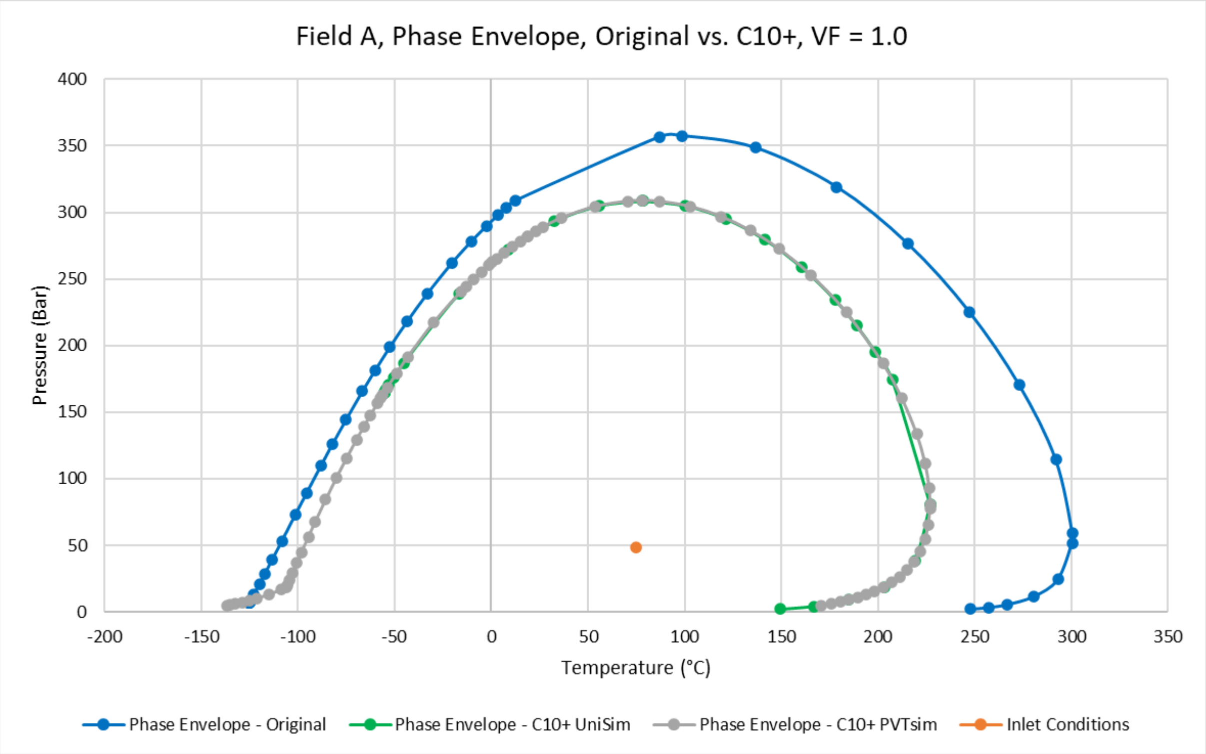

Figure 7.29: Phase envelope, Initial vs. C10+, UniSim and PVTsim, Field A

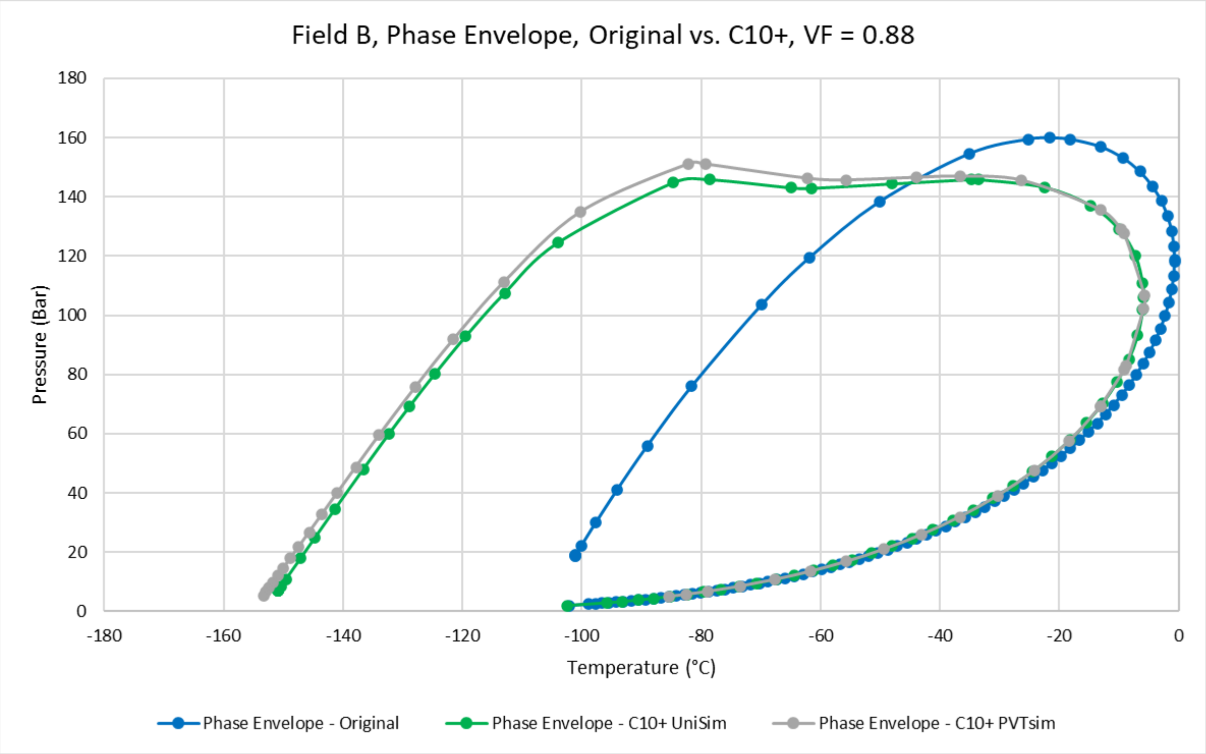

Figure 7.30: Phase envelope, Initial vs. C10+, UniSim and PVTsim, Field B

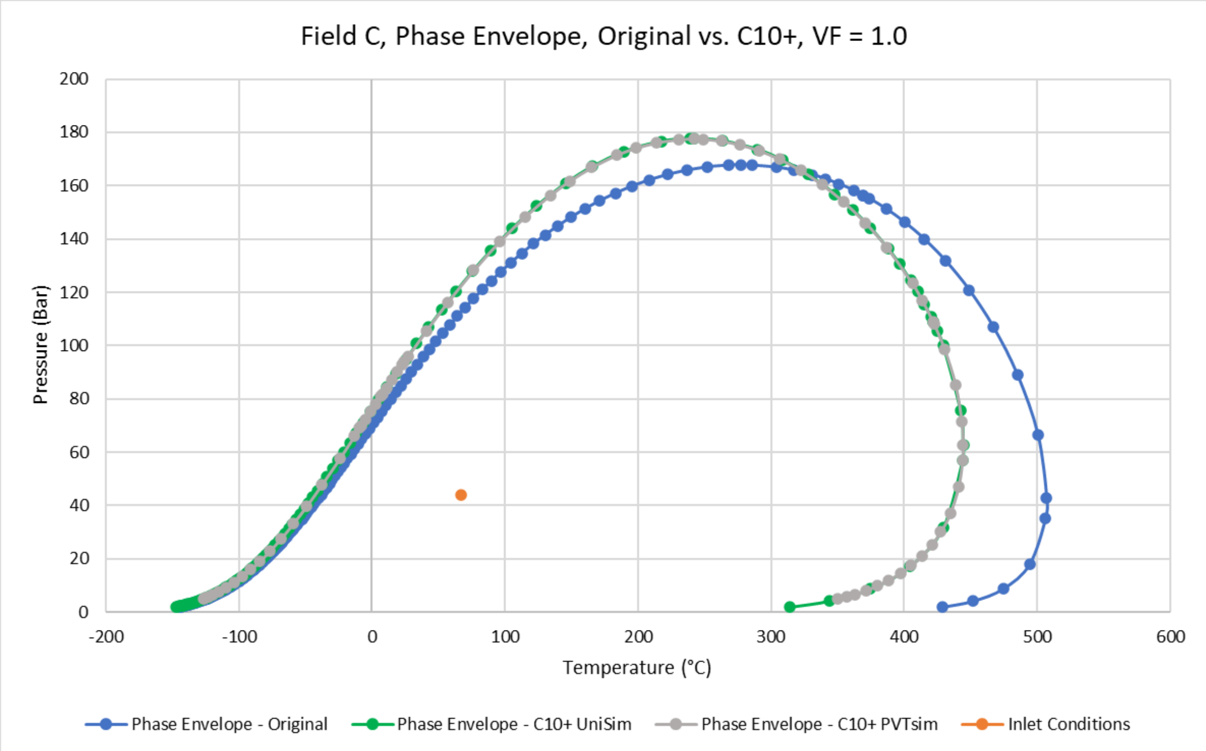

Figure 7.31: Phase envelope, Initial vs. C10+, UniSim and PVTsim, Field C

The curves show that the phase envelope determined from PVTsim for the C10+ lumping scheme matches the phase envelope determined from the UniSim model with C10+ lumping. This indicates that the C10+ fluid characterisation is incorporated correctly into the C10+ simulation model.

The phase envelopes from the initial case and the C10+ case deviate significantly from each other. This indicates that the fluids from the C10+ characterisation will not behave the same way as the fluids in the initial case, resulting in possible deviations between the simulation results.

7.6.2 UniSim results for the C10+ characterisation

The results given from the UniSim models are the oil and gas production, both total and for each field. The results are estimated both from an all-in simulation and from standalone cases. Standalone cases and an all-in case are both included to observe the commingling effect between the fields and see the difference when the field is producing alone. This is done for the C10+ case, which is compared to the initial case. The simulation result with the standalone cases is shown in Table 7.7, and the simulation result with the all-in case is shown in Table 7.8.

Table 7.7: Standalone simulation results for all fields with the initial case and the C10+ case

Standalone simulation	Field A	Field B	Field C
Oil production, Sm3/d:			
Initial case	1148	2991	2747
C10+ case	1145	2980	2749
Approximate deviation	3	10	-2
Gas production, MSm3/d:			
Initial case	2.1	9.6	0.3
C10+ case	2.1	9.6	0.3
Approximate deviation	0.0	0.0	0.0

Table 7.8: All-in simulation results for all fields with the initial case and the C10+ case

All-in simulation	Field A	Field B	Field C	Total
Oil production, Sm3/d:				
Initial case	1130	3147	2557	6834
C10+ case	1127	3134	2557	6819
Approximate deviation	3	12	0	15
Gas production, MSm3/d:				
Initial case	2.1	9.6	0.3	12.0
C10+ case	2.1	9.6	0.3	12.0
Approximate deviation	0.0	0.0	0.0	0.0

The initial case and the C10+ case predict approximately the same gas production for all the fields and in total with the standalone cases and the all-in case. For field A and field B, the estimated oil production is slightly higher for the initial case compared to the C10+ case, with 3 Sm^3/h and 12 Sm^3/d difference, respectively. Field C has a slightly lower oil production prediction for the standalone case when comparing the C10+ case to the initial case. In the all-in simulation, the predicted oil production for field C is approximately the same, with 2 Sm^3/h higher in the C10+ case.

The commingling effect for the C10+ case follows the same prediction as the initial case, with higher oil prediction for field B with all-in and higher for field A and field C with standalone.

The simulation results show that using C10+ lumping instead of the initial lumping the deviations is not excessively high.

The ORFs are determined on a standalone basis and compared to the predicted ORF values in the initial case.

Figure 7.32, Figure 7.33 and Figure 7.34 show the ORFs estimated for field A, field B and field C, respectively.

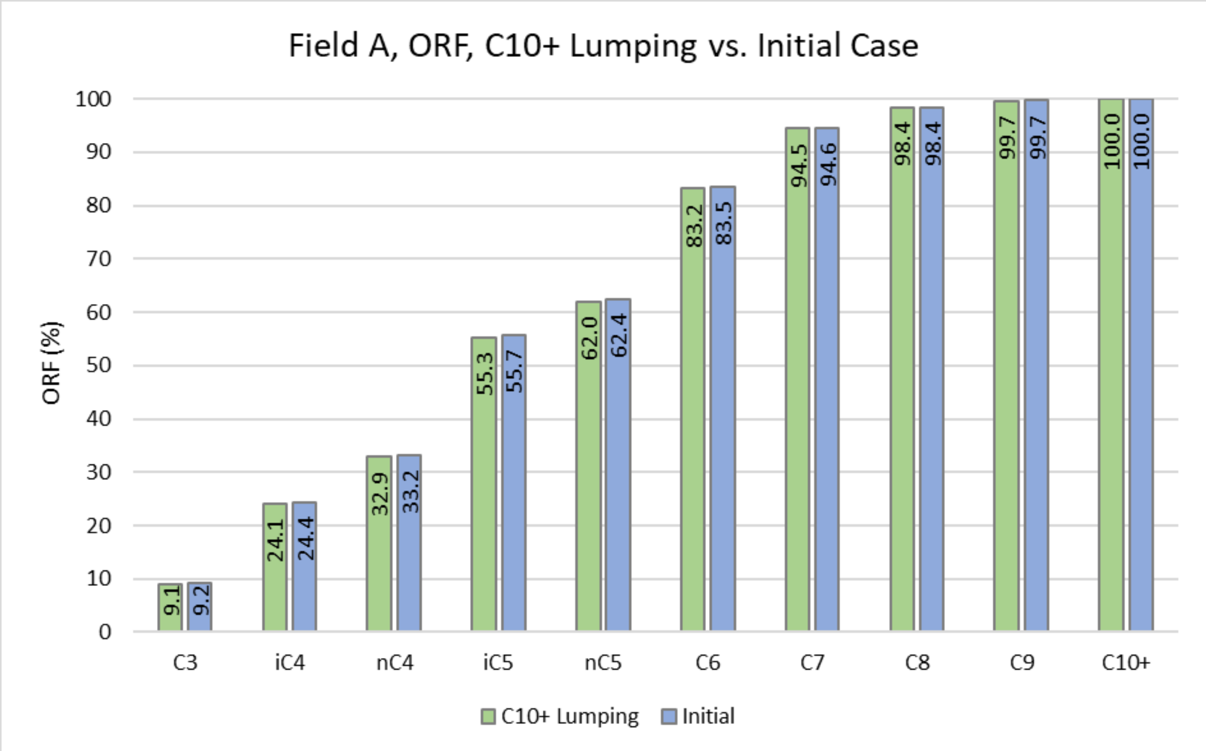

Figure 7.32: Field A ORFs, C10+ lumping vs. initial case

The ORF estimates for field A are similar, with the highest deviation being 0.4% for the iC5 and nC5 components.

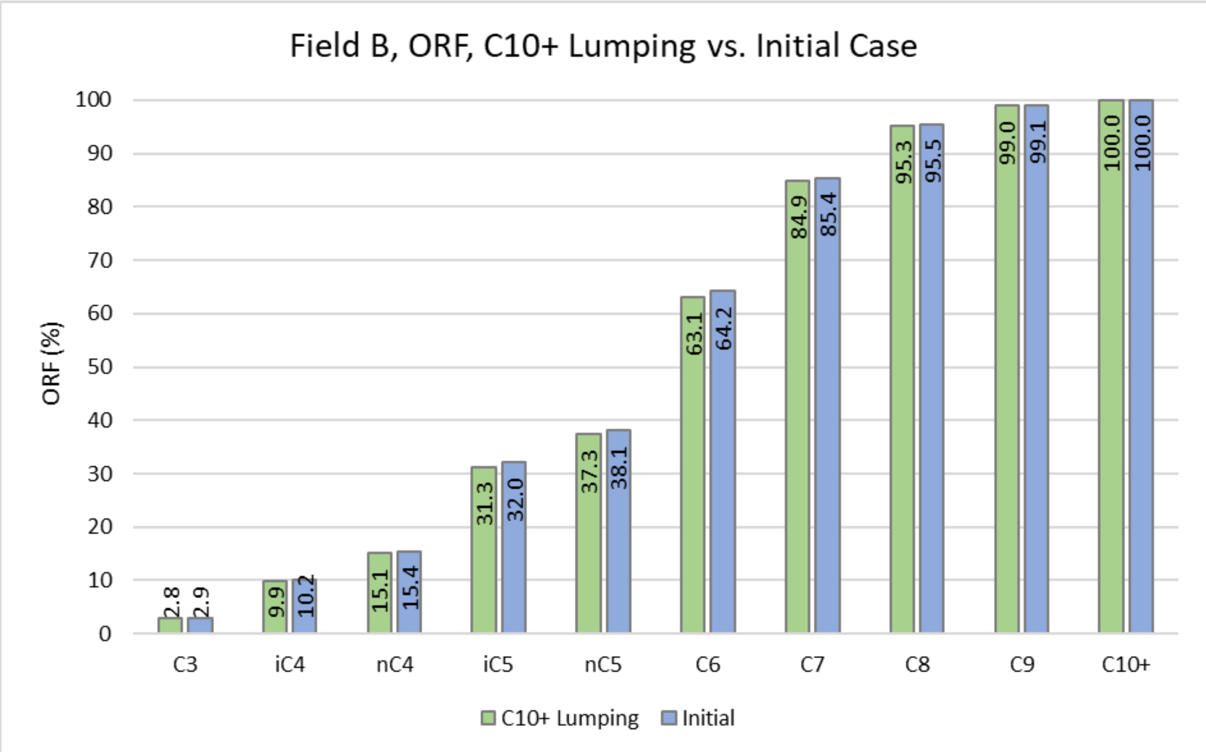

Figure 7.33: Field B ORFs, C10+ lumping vs. initial case

The ORF estimates for the field B results are slightly more deviating than the A field ORF result, with the most significant deviation for the C6 hydrocarbon at 1.1 %.

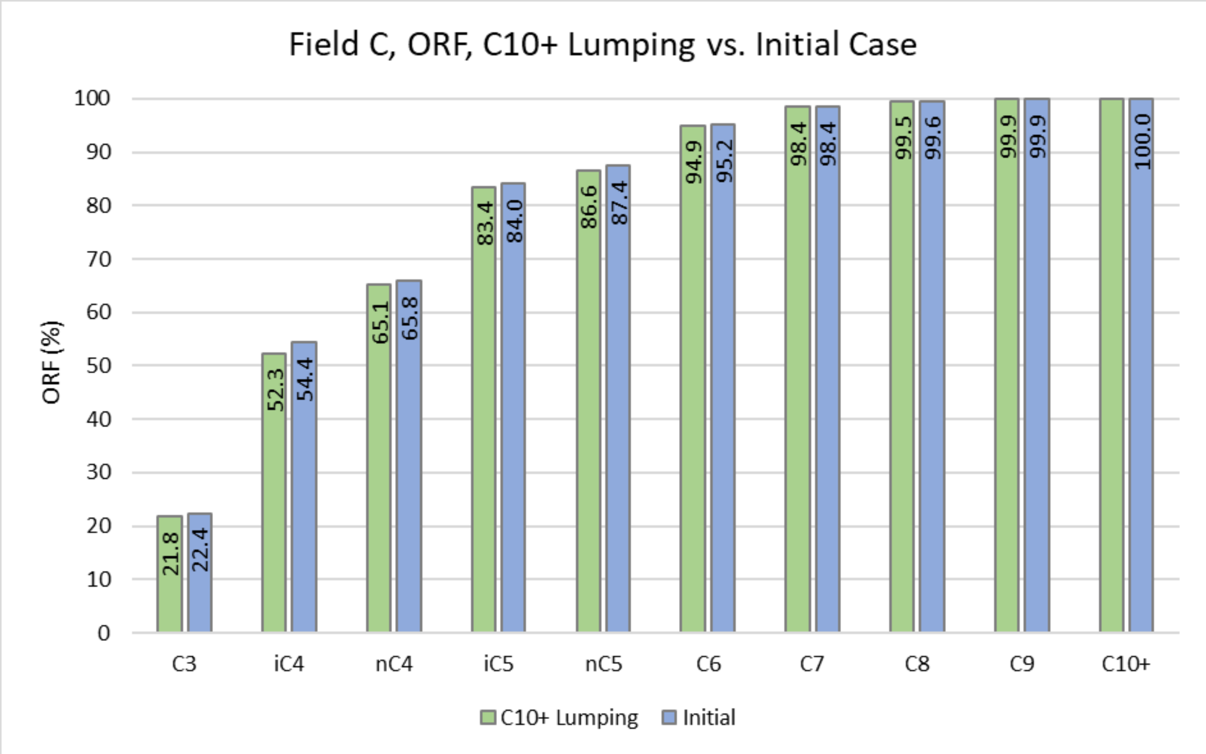

Figure 7.34: Field C ORFs, C10+ lumping vs. initial case

The ORF estimates for the C field are more deviating than the A and B field ORF result, with the most significant deviation for the iC4 hydrocarbon with 2.1 %.

The results from the C10+ lumping case shows that the estimates are not too far from the initial case but more divergent than the C20+ case results. The current allocation method for Platform Vest is based on ORFs, meaning that the ORF estimate should be accurate.

On the other hand, a detailed laboratory analysis with a total lumping scheme is expensive; thus, maybe an ORF estimation with C10+ lumping is sufficient for some allocations.

7.7 Future allocation in UniSim

Future allocation is the practice of allocating the predicted production to the different fields over a period, often a few years or even longer, with commonly an allocation for each year in the set period. It is necessary to perform future allocation as a foundation for the allocation agreement that should be fair for all users. The future allocation is also important to estimate the production and allocation in the future and better understand the commingling between the different fields. The years allocated in the future allocation for this case are year 8, 10 and 12, and the profiles are given in Appendix M – Future allocation profiles. Estimates for gas, oil, and water production, predicted GOR, inlet pressure and gas lift are given in the profile for the selected years.

A few different methods can be used to match the simulation model to these predicted estimates. For this scope, the predicted results for standalone simulation, all-in simulation and field A with field B will be evaluated for all three years. These are selected to evaluate how the results change with different commingling and different approaches. The A with B field is studied since the C field is the newest field on the platform; to estimate how the production would be if field C were not routed through the platform.

For future allocation, the new characterisation with the initial lumping scheme is used.

7.7.1 Future allocation with tuning on the oil

One way to do the future allocation is to tune the inflow from each field to match the predicted oil production from that specific field. This tuning is done on a standalone basis, meaning that the tuning is done with no commingling between the different fields. This tuning method is a chosen approach based on the assumption that the predicted profiles are on a standalone basis. The tuned inflow for each field on a standalone basis is kept when inserted into the all-in simulation case and the field A with field B simulation case. The tuning is done on the oil instead of the gas; since the allocation method is ORF-based, it is essential to have the estimated oil production as authentic to the actual case as possible. Appendix M – Future allocation profiles give the profiles, and Appendix N – Future allocation ORF result for year 10 and 12 gives complementary results that are not included in the sections below.

Figure 7.35 shows the oil production for field A with the different simulation cases for the three years.

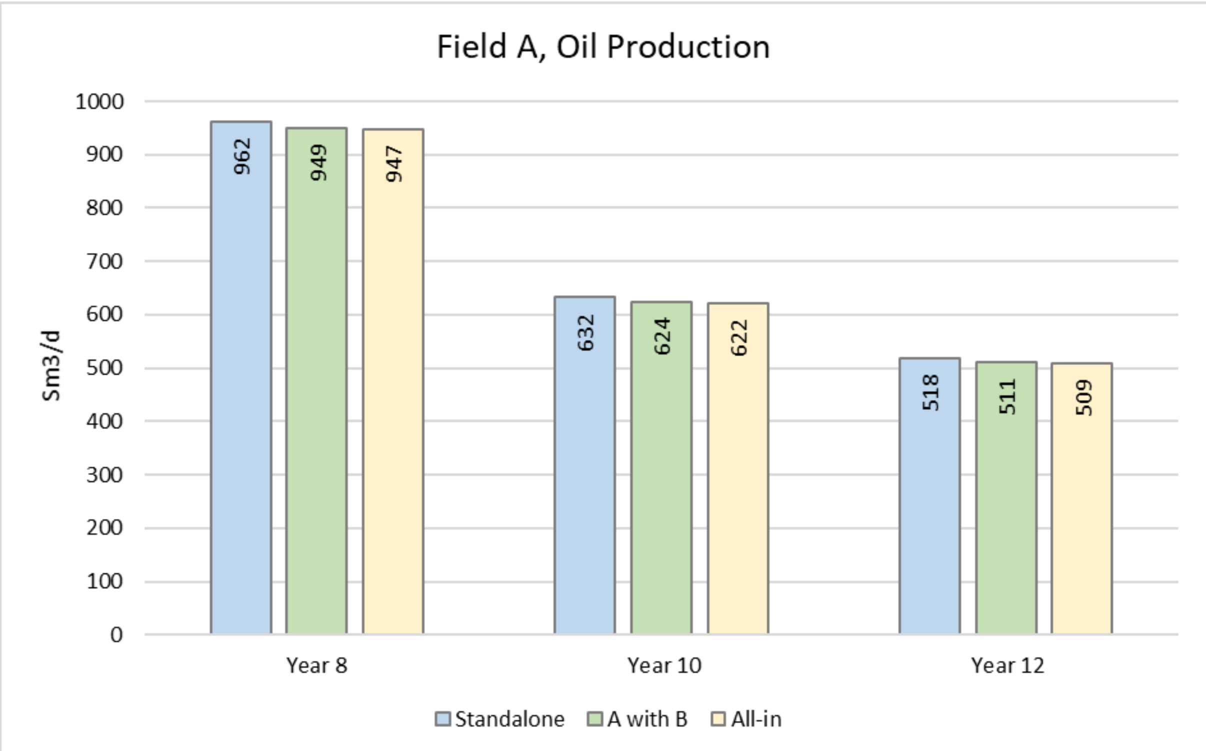

Figure 7.35: Field A, Oil production, standalone, A with B and all-in

The results for field A show slightly lower oil production when field A is producing together with the B field, and even lower when all fields are producing together. The oil production from field A is negatively impacted when producing with the B field and all-in. From the decline in the oil production over the years from field A, it is noticeable that the production from the A field is in the tail phase.

Figure 7.36 shows the oil production for field B with the different simulation cases for the three years.

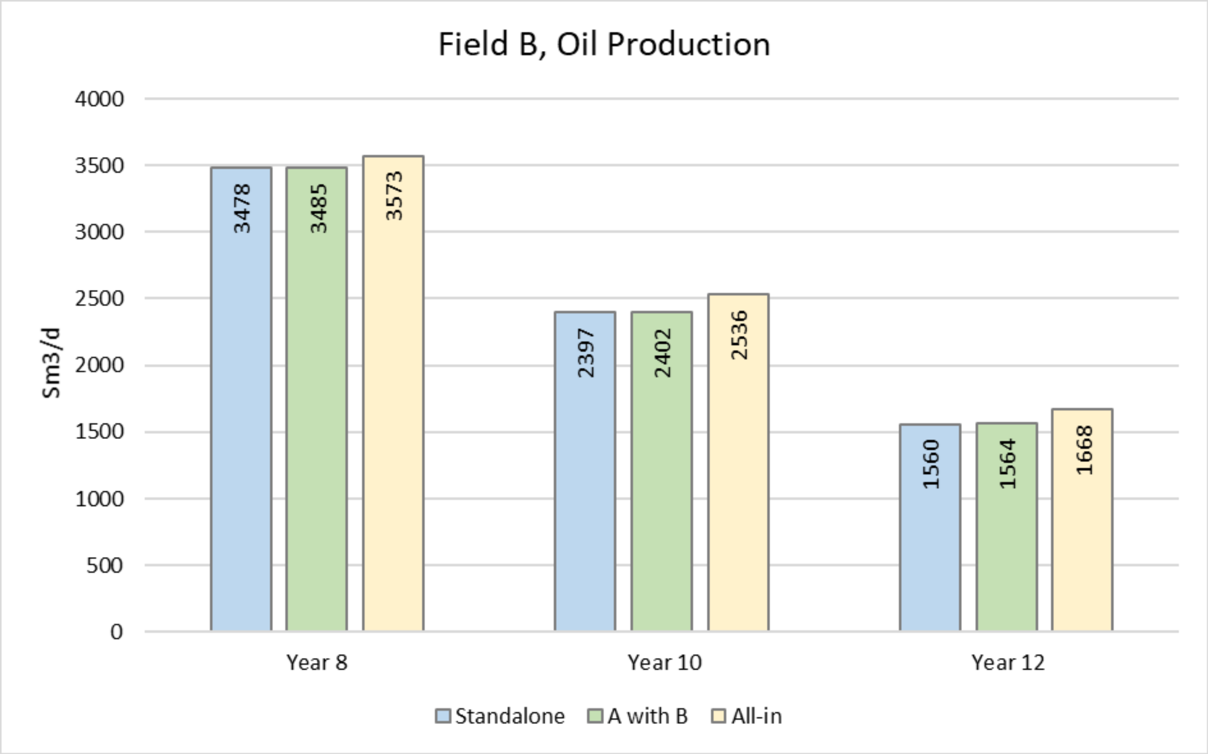

Figure 7.36: Field B, Oil production, standalone, A with B and all-in

The results for field B show slightly higher oil production when field A is producing together with the B field, and even higher when all fields are producing together. The oil production from field B is positively impacted when producing with the A field and all-in. From the decline in the oil production from field B it is noticeable that the production from the B field is declining, but the amount is over three times higher than the oil production from field A.

Figure 7.37 shows the oil production for field C with the different simulation cases for the three years.

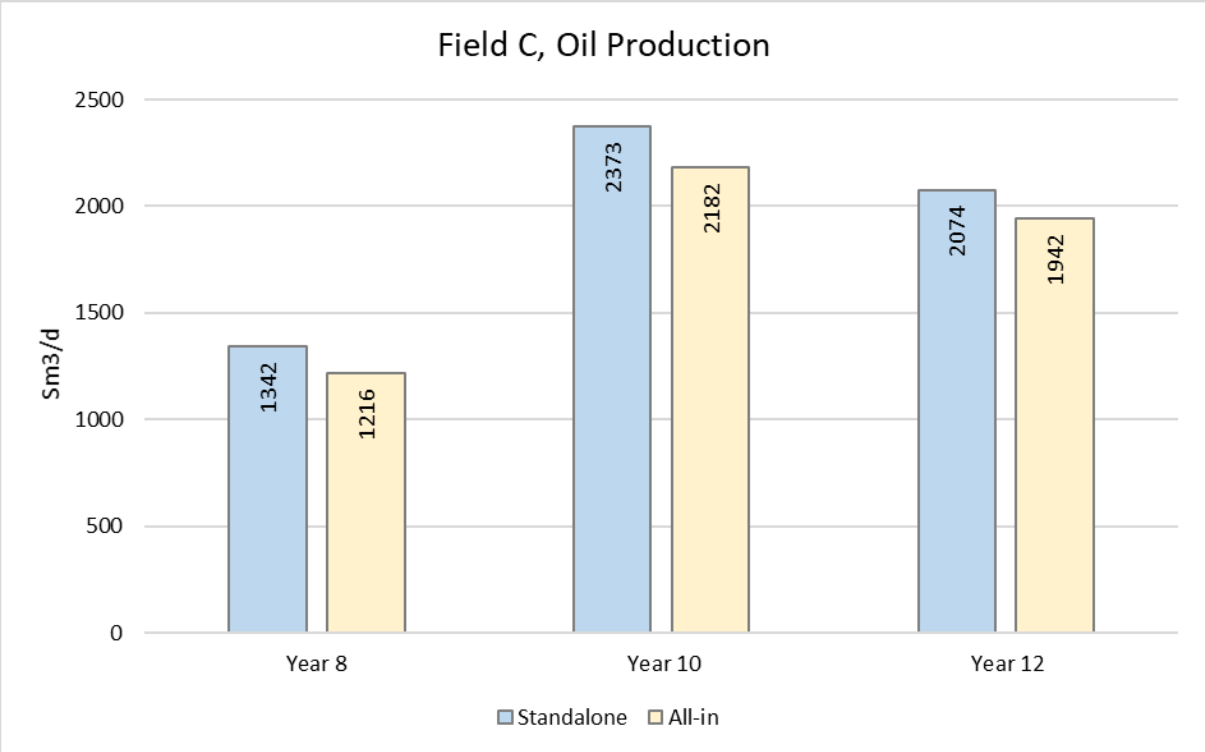

Figure 7.37: Field C, Oil production, standalone, A with B and all-in

Field C shows higher oil production when field C is producing alone on the platform compared to all-in. The oil production from field C is negatively impacted when producing with all-in simulation. The oil production from field C increases from year 8 to year 12, indicating a steady production.

Figure 7.38 shows the ORFs estimated for the three simulation cases for field A in year 8.

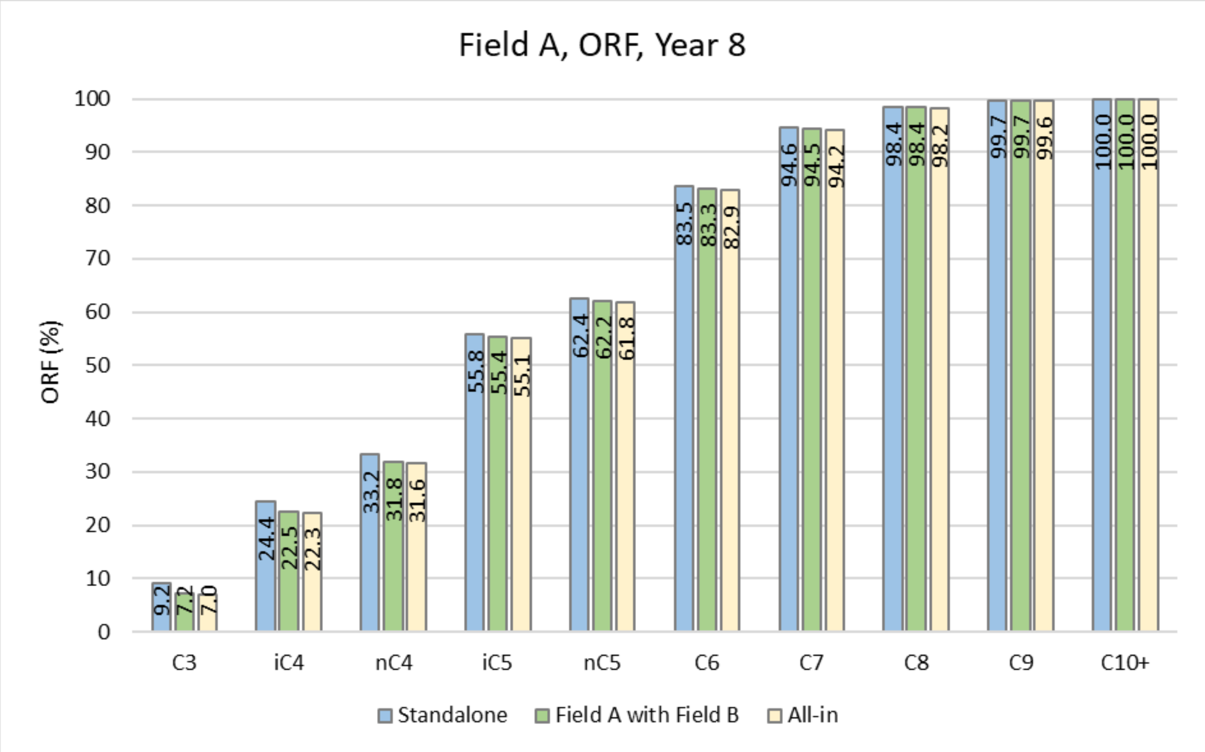

Figure 7.38: Field A ORFs, standalone, A with B and all-in

The standalone predicts slightly higher ORFs, following by field A with field B and then the all-in with the lowest estimated ORFs. This indicates that less oil is predicted in the oil production stream when not producing on a standalone basis.

Figure 7.39 shows the ORFs estimated for the three simulation cases for field B in year 8.

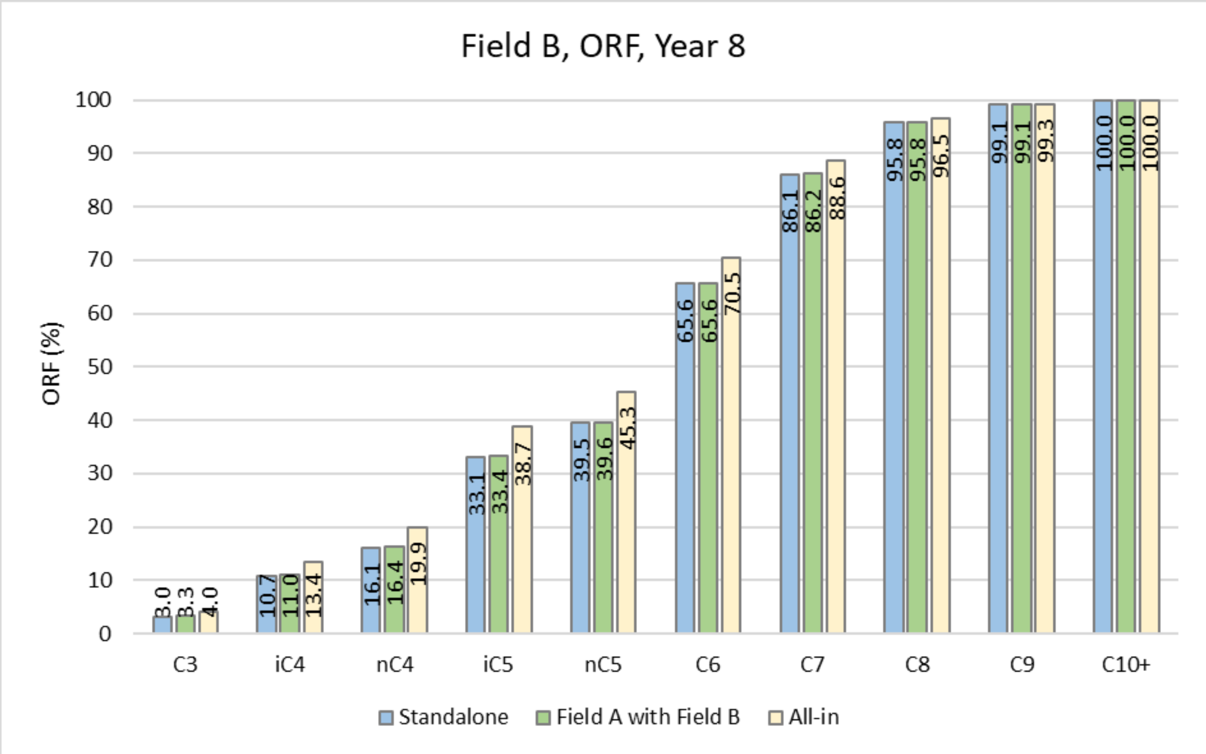

Figure 7.39: Field B ORFs, standalone, A with B and all-in

The standalone predicts the lowest ORFs, following by field A with field B and then the all-in case with the highest estimated ORFs. This indicates that more oil is predicted in the oil production stream when producing with the other fields, compared to standalone.

Figure 7.40 show the ORFs estimated for the two simulation cases for field C in year 8.

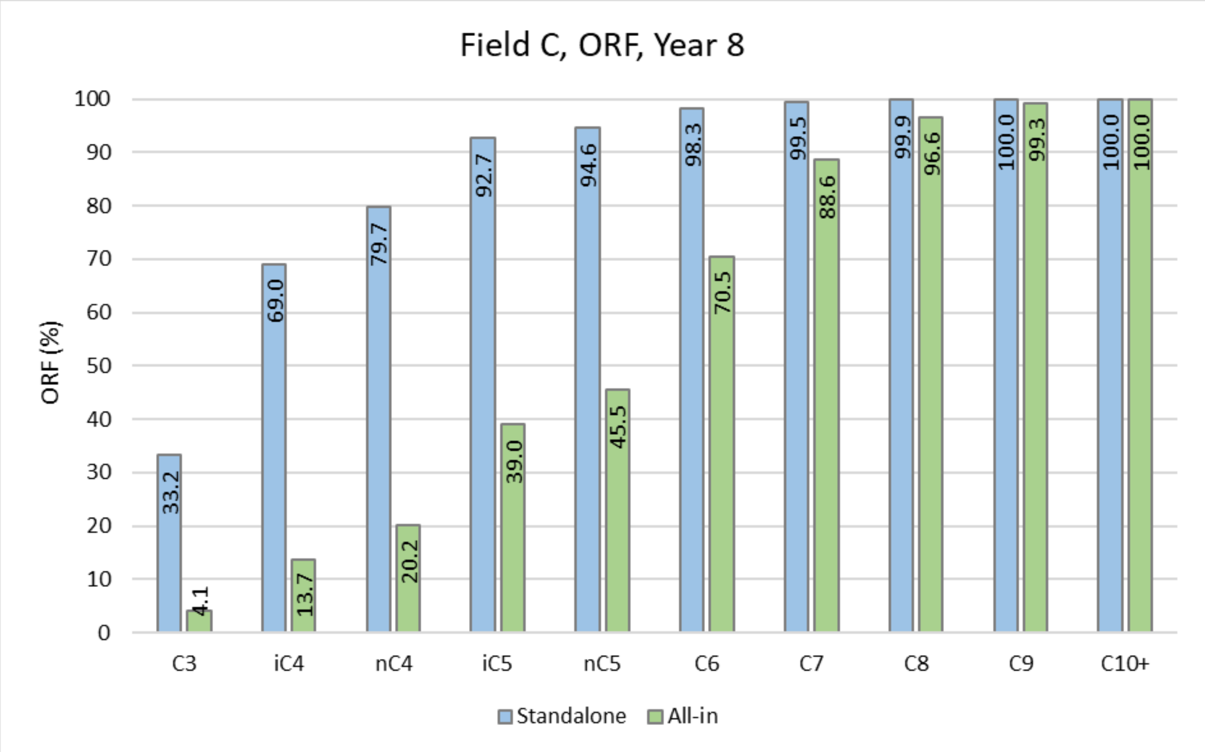

Figure 7.40: Field C ORFs, standalone and all-in

The standalone predicts a shockingly high ORF estimate compared to the all-in case for field C. This indicates that a lot more oil is predicted in the oil production stream when producing standalone than all-in with the other fields.

Field C is a low GOR field, indicating that the field contains a higher oil to gas ratio compared to the other fields. When a low GOR field coproduces with a high GOR field, the high amount of gas will prevent oil products from the low GOR field to go out in the oil production stream.

Field A (medium GOR) and Field C (low GOR) are the two fields negatively impacted fields when producing all-in compared to standalone for the oil production. Field B (high GOR) is the only field with a better oil production estimate with all-in simulation compared to standalone simulation. This is due to the oil components from field A and field C attracting the oil from field B, making more of it go out in the oil production stream.

The ORF results show the same trend for all three years. ORFs for year 8 are presented below, while ORFs for year 10 and 12 can be seen in Appendix N – Future allocation ORF result for year 10 and 12.

7.7.2 Year 8 with GOR tuning

The GOR (Gas-oil-ratio) is another parameter that can be tuned to match the predicted GOR for the different years. In this method the inlet flow and composition are adjusted for each field to match the GOR prediction for the production. A new UniSim model is built to predict this new composition and inflow. A detailed description of how the model is built and how it works can be found in Appendix O – UniSim GOR model.

The estimated ORFs are predicted for year 8 for the standalone approach for the three fields. These ORFs are compared to the ORFs estimated with the standalone oil tuning method done in Chapter 7.7.1.

Figure 7.41 shows the field A standalone ORFs estimated for two methods in year 8

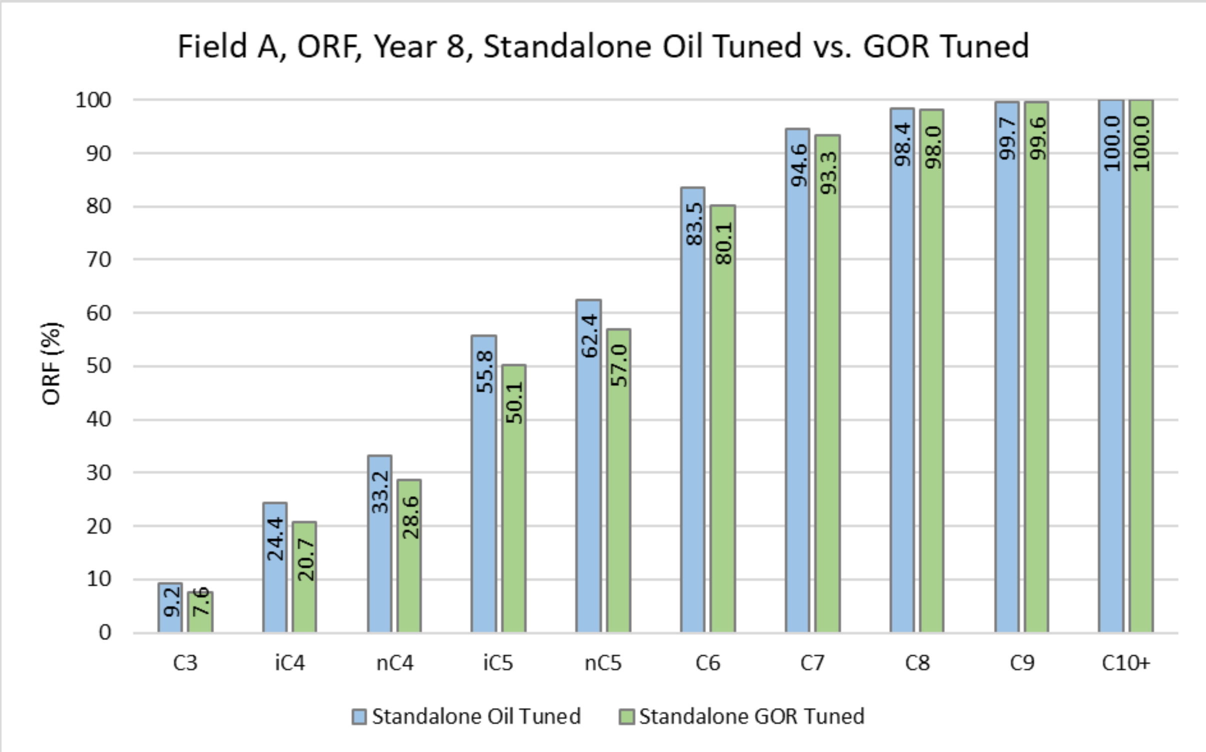

Figure 7.41: Field A, standalone ORFs, oil tuned vs. GOR tuned

The oil tuning method predicts higher ORFs compared to the GOR tuning method for field A.

Figure 7.42 shows the field B standalone ORFs estimated for the two methods in year 8.

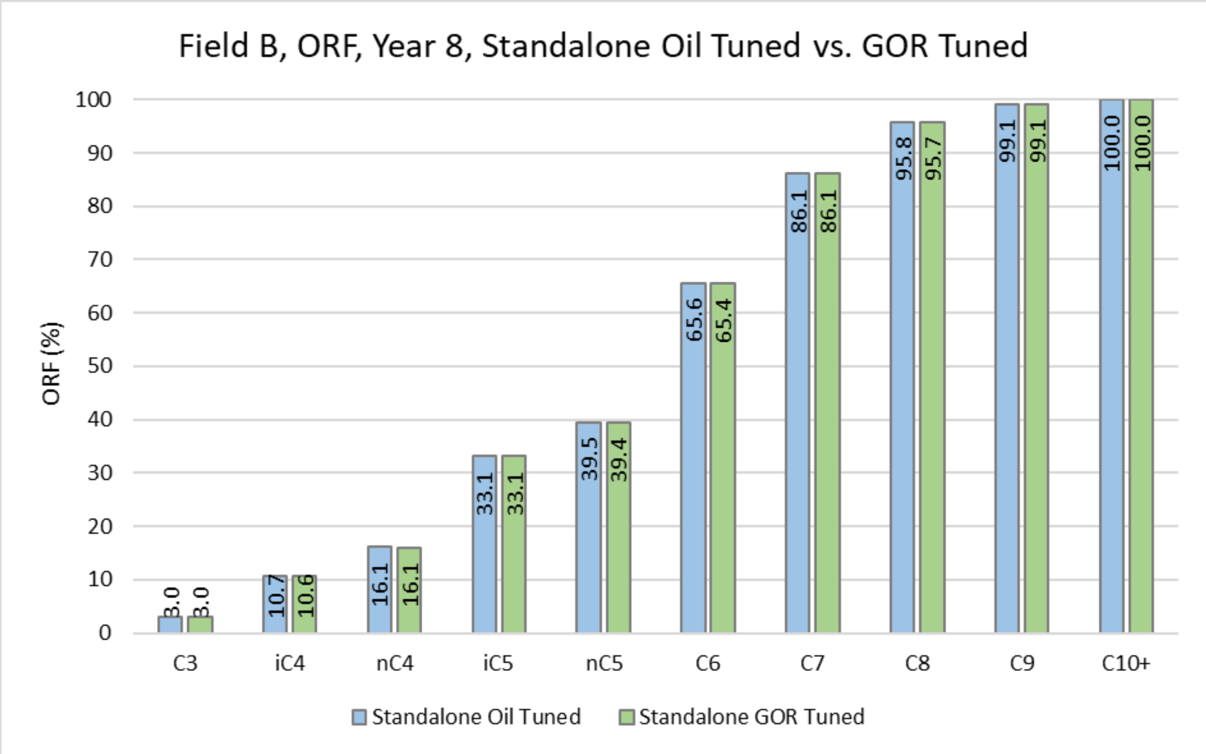

Figure 7.42: Field B, standalone ORFs, oil tuned vs. GOR tuned

The ORFs show similar values for the oil tuning compared to the GOR tuning for field B.

Figure 7.43 shows the field C standalone ORFs estimated for two methods for year 8.

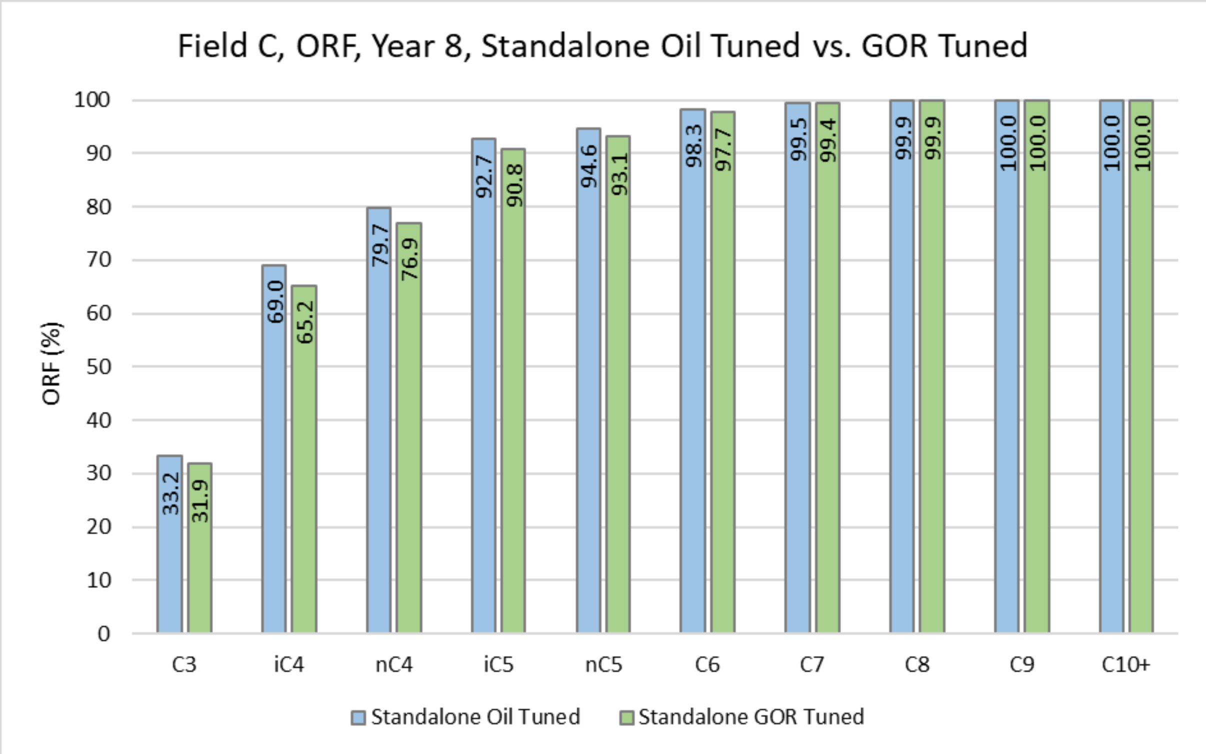

Figure 7.43: Field C, standalone ORFs, oil tuned vs. GOR tuned

The oil tuning method predicts higher ORFs compared to the GOR tuning method for field C.

The low and mediate GOR fields A and C predict a lower ORF estimate with the GOR tuning method compared to the oil tuning method. The high GOR field B estimates similar ORFs when comparing the two tuning methods.

GOR tuning is a method that can be used when the composition is uncertain, estimated from old samples, or if the predicted GOR value is more valid than other tuning parameters.

7.7.3 Year 8 with gas tuning

Instead of tuning the model to the oil production, it can be tuned to match the predicted gas production. This tuning is done the same way as the oil tuning method, on a standalone basis. The ORFs are predicted and compared to the estimated ORFs from the oil tuning method.

Figure 7.44, Figure 7.45 and Figure 7.46 show the standalone ORFs estimated for the two methods in year 8 for field A, field B and field C, respectively.

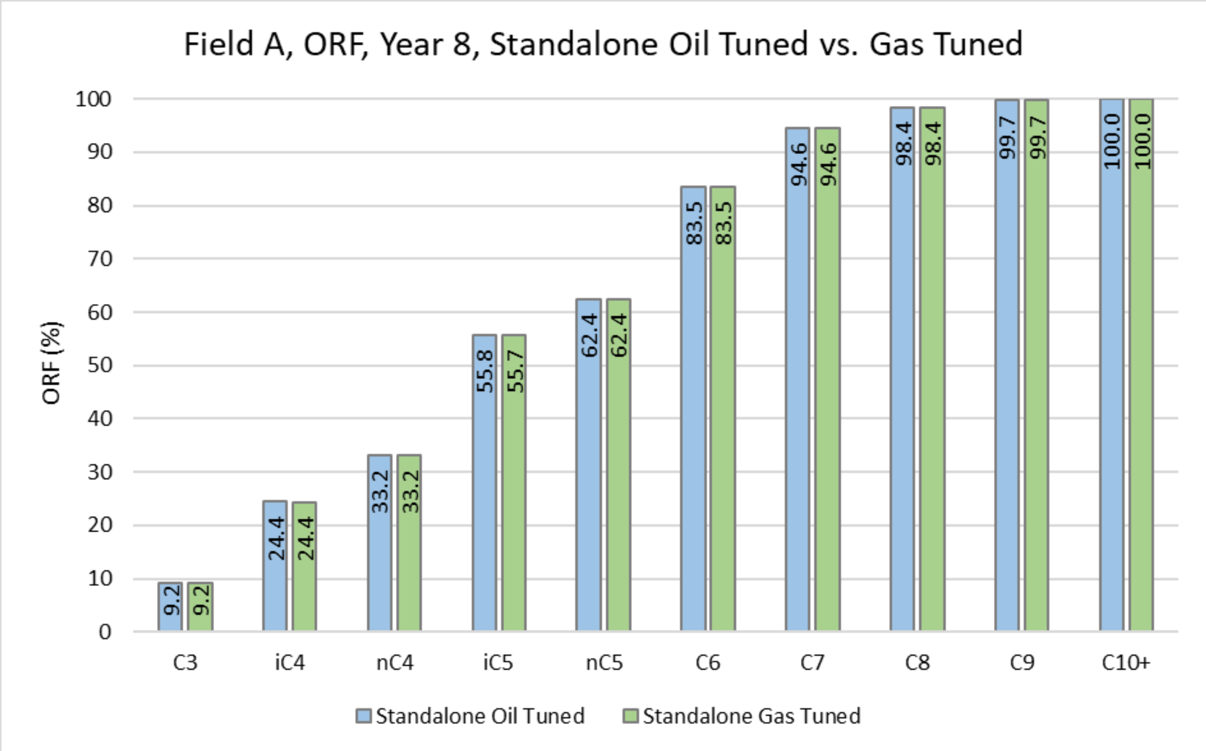

Figure 7.44: Field A, standalone ORFs, oil tuned vs. gas tuned

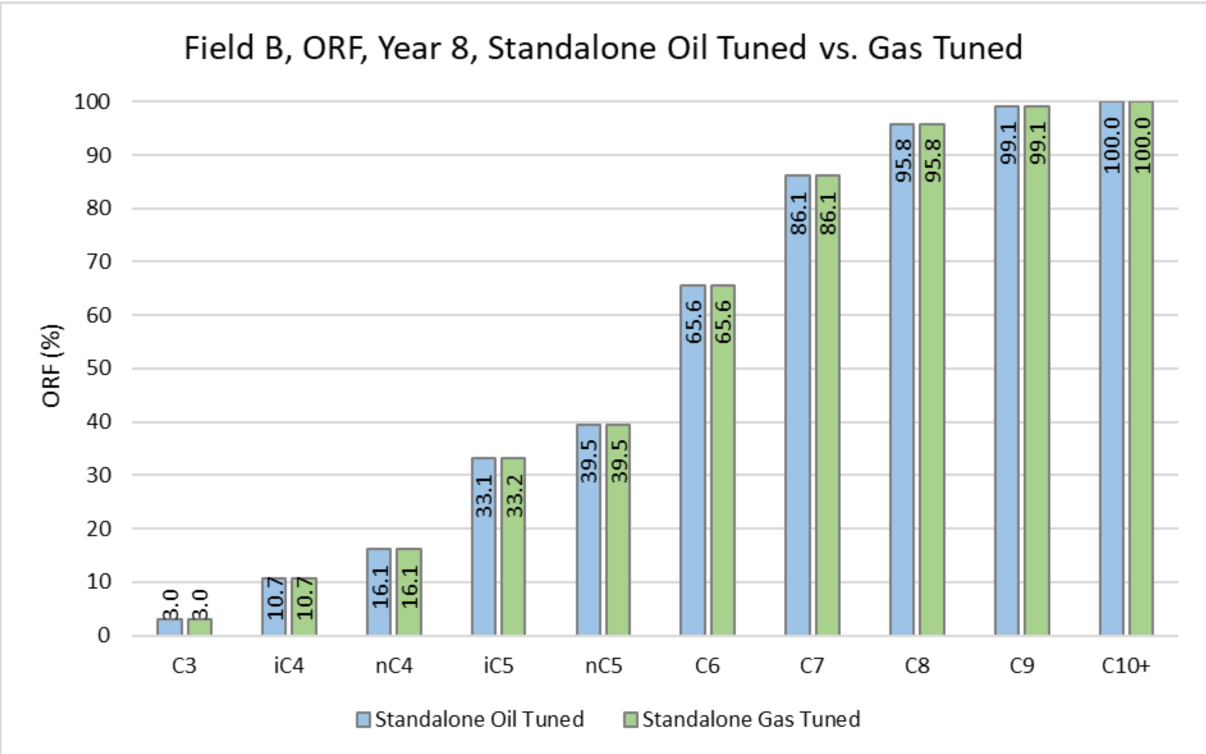

Figure 7.45: Field B, standalone ORFs, oil tuned vs. gas tuned

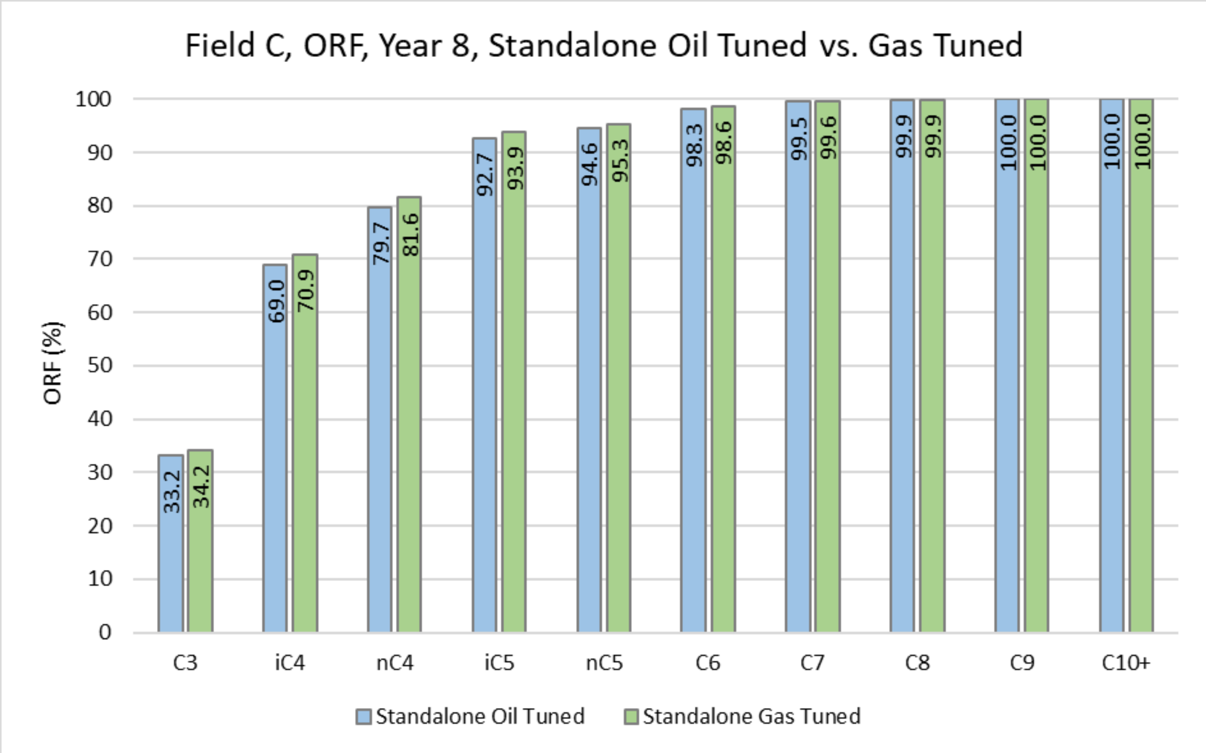

Figure 7.46: Field C, standalone ORFs, oil tuned vs. gas tuned

Field A and field B have similar ORF predictions when comparing the results from the two tuning methods. For field C gas tuning method estimates slightly higher ORFs compared to the oil tuning method. The highest deviation is 1.9 % for the iC4 and nC4 components.

The differences between the oil tuning method and gas tuning methods are because the simulations are only tuned to match one of the phases. In the oil tuning method, the predicted gas is not matched, and for the gas tuning method, the predicted oil is not matched. Since ORF values are essential for the current allocation agreement, the tuning on the predicted oil is deemed more correct than tuning on the predicted gas.

7.8 ProMax vs. UniSim for Platform Vest reallocation

For this comparison part, a ProMax model was developed with the new fluid characterisation as input. The result from the ProMax simulation case is compared to the UniSim simulation case with the new characterisation, also called the initial case. A detailed description of how the model is made is given in Appendix P – Building the ProMax model.

7.8.1 Phase envelope prediction

Figure 7.47, Figure 7.48 and Figure 7.49 show the phase envelope estimated by UniSim and Promax for field A, field B and field C, respectively. The VF is set to 1.0 for field A and field C and 0.97 for field B. The inlet conditions are also included in the figures.

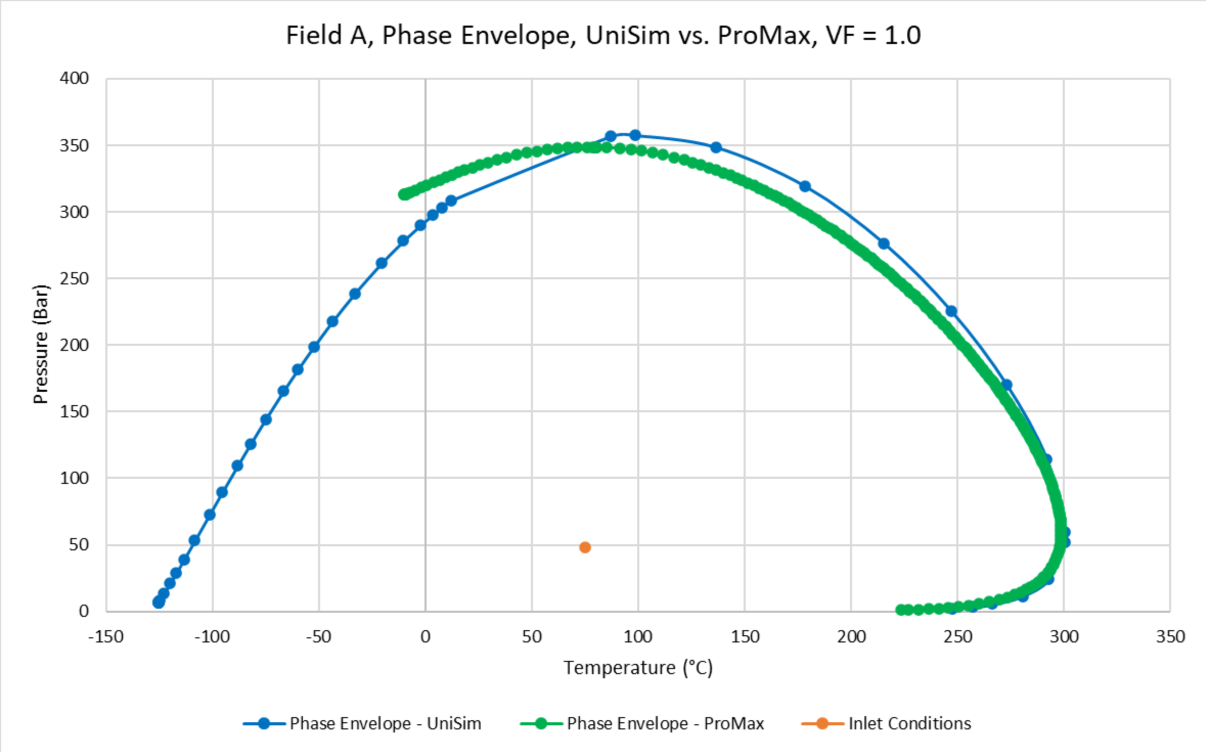

Figure 7.47: Phase envelope, UniSim vs. ProMax, Field A

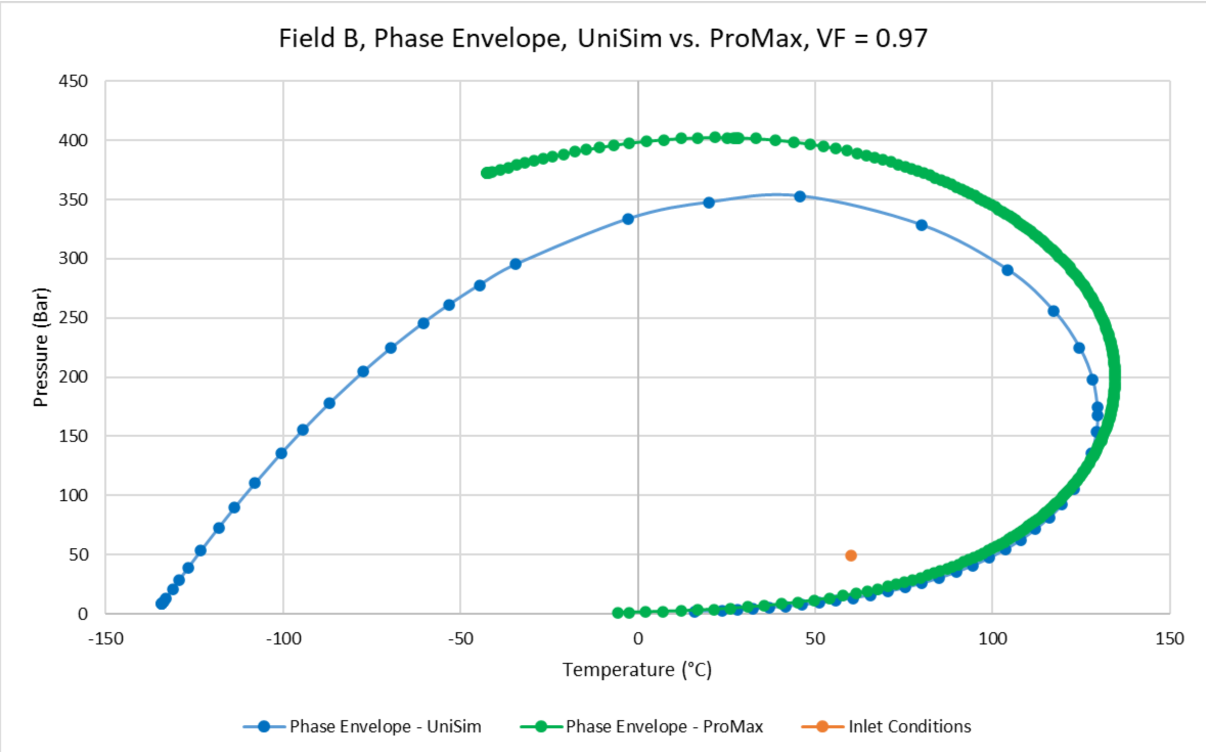

Figure 7.48: Phase envelope, UniSim vs. ProMax, Field B

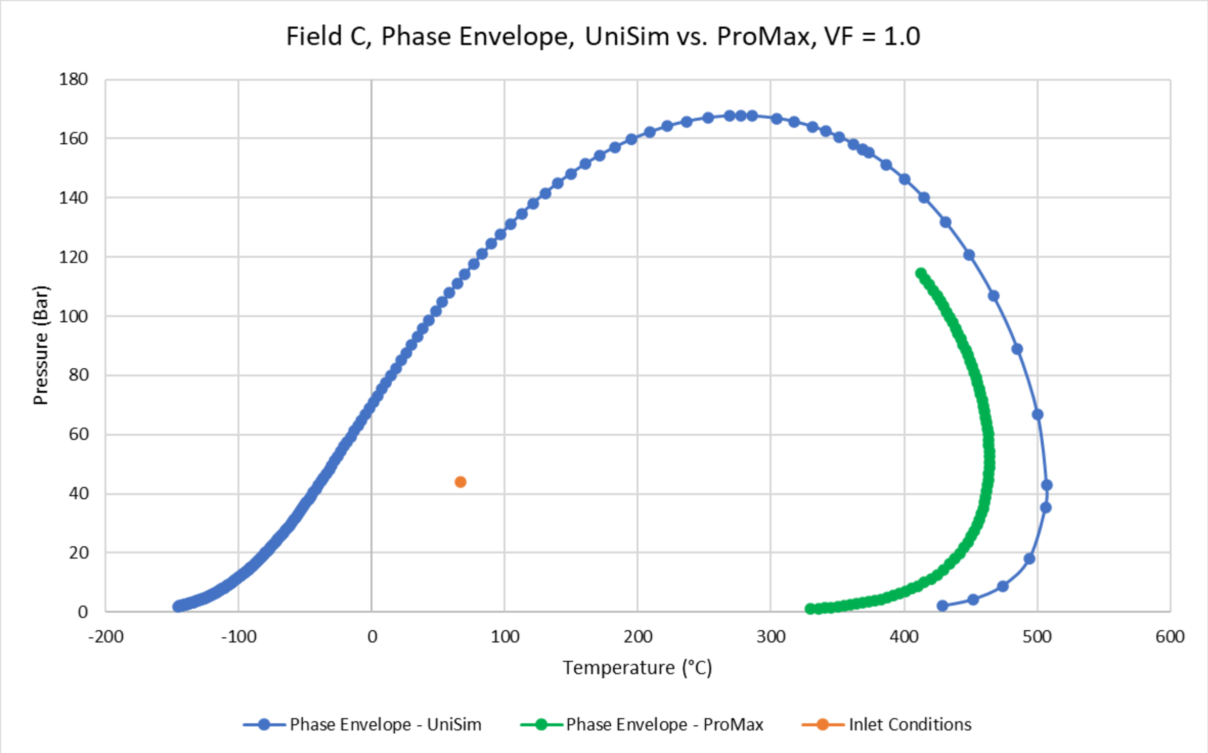

Figure 7.49: Phase envelope, UniSim vs. ProMax, Field C

The phase envelopes for ProMax are predicted differently than the phase envelopes from UniSim. The phase envelopes deviate significantly from each other, indicating that the fluids in the ProMax model will not behave the same way as the fluids in the UniSim model, resulting in possible deviations between the simulation results.

7.8.2 Oil and gas prediction

The oil and gas production (both total and for each field), the estimated value for the oil products from each field and total, and the ORFs for each field are compared. The results are predicted from an all-in simulation, meaning that all the fields are producing to the platform simultaneously. The ORFs are estimated from standalone simulations. The all-in simulation results are shown in Table 7.9.

Table 7.9: All-in simulation results for all fields with the initial UniSim case and the ProMax case

All-in simulation	Field A	Field B	Field C	Total
Oil production, Sm3/d:				
UniSim	1130	3147	2557	6834
ProMax	1118	3087	2530	6735
Approximate deviation	11	60	27	98
Gas production, MSm3/d:				
UniSim	2.1	9.6	0.3	12.0
ProMax	2.1	9.6	0.3	12.1
Approximate deviation	0.0	0.0	0.0	0.0
Value adjustment, MNOK/yr:				
UniSim	1297	3564	2959	7821
ProMax	1289	3380	3062	7731
Approximate deviation	9	184	-103	89

The UniSim model is predicting a higher oil production and value for all fields and in total. The deviation on oil production is 11 Sm^3/d, 60 Sm3/d and 27 Sm^3/d for field A, field B and field C, respectively. The value deviation is 9 MNOK/year, 184 MNOK/year and 103 MNOK/year for field A, field B and field C, respectively.

The predicted gas production is approximately the same for the UniSim case compared to the ProMax case.

Figure 7.50, Figure 7.51 and Figure 7.52 show the ORFs estimations for field A, field B and field C, respectively.

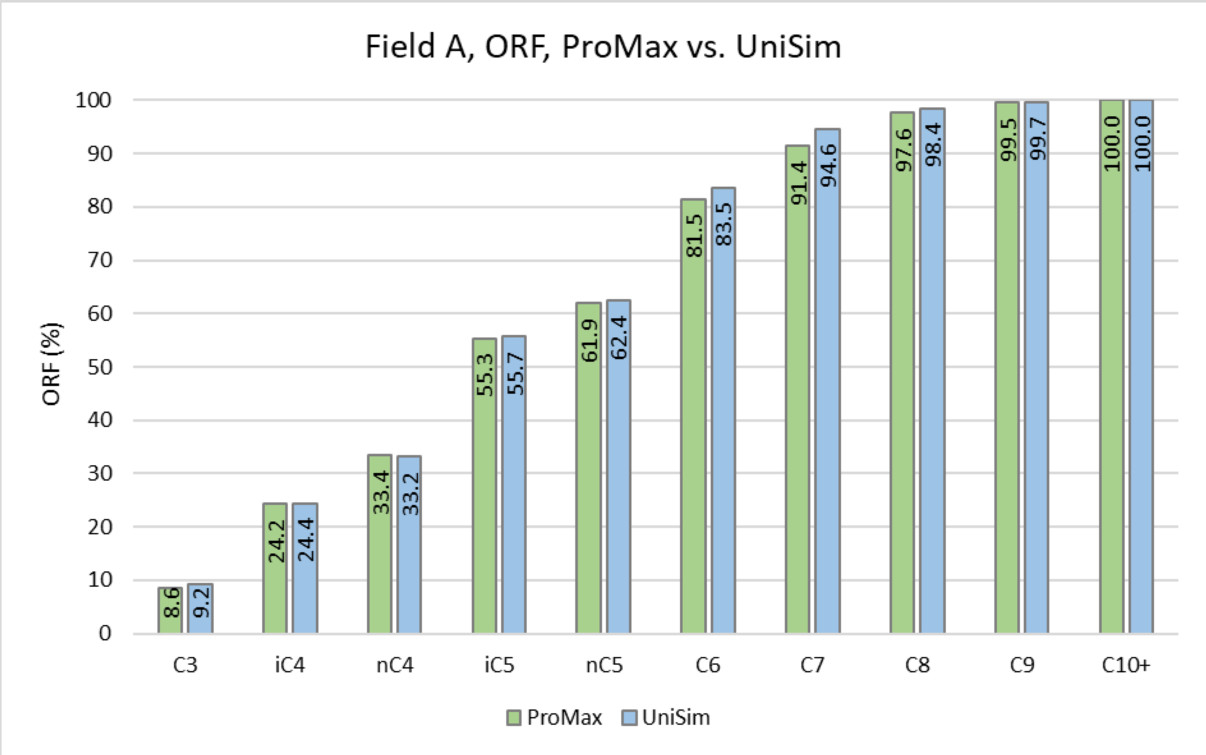

Figure 7.50: Field A ORFs, ProMax vs. UniSim

The ORFs predicted for field A in ProMax are slightly higher than the UniSim ORFs. With the highest deviation being 3.2 % for the C7 component.

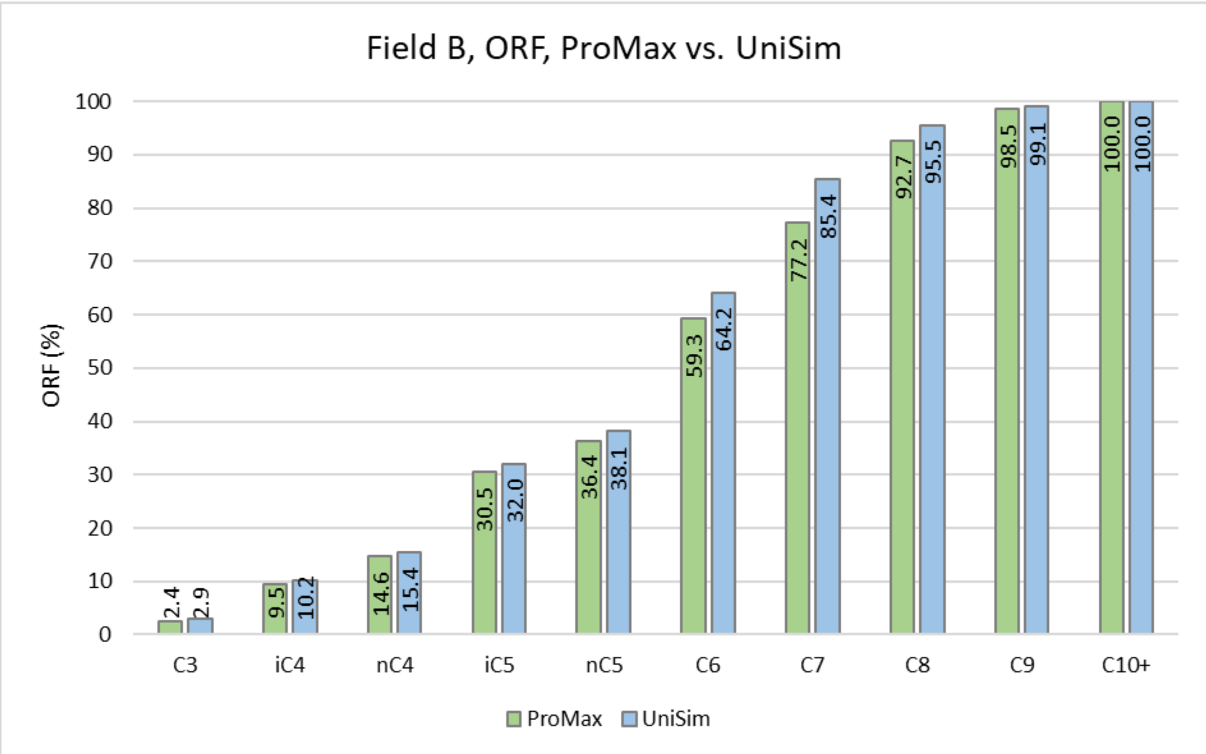

Figure 7.51: Field B ORFs, ProMax vs. UniSim

The ORFs predicted for field B in the ProMax model is estimated higher than the ORFs for the UniSim model. With the highest deviation being 8.2 % for the C7 component.

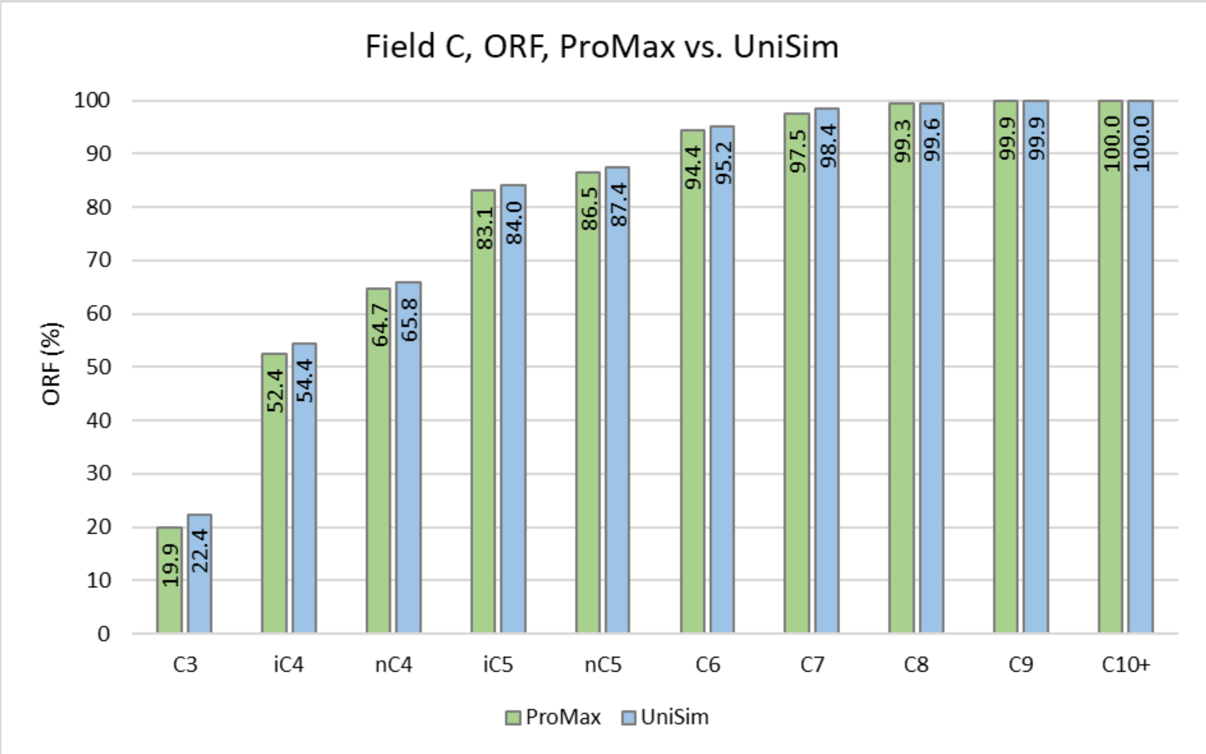

Figure 7.52: Field C ORFs, ProMax vs. UniSim

The ORFs predicted for field C in the ProMax model is estimated higher than the ORFs for the UniSim model. With the highest deviation being 2.5 % for the C3 component.

The comparison results between the two simulation models show differences, especially when looking at the estimated value and oil production. The ORFs are also important parameters used in the current allocation agreement, and it is essential that these parameters are representative.

The discussion on which of the simulation tools gives the most correct estimations is not clear. The ProMax creators claim that the thermodynamic is more correct when creating a mixed-species instead of using hypothetical components. The result clearly shows that there are differences when using the two models, even when the input is supposed to be the same. The procedure for definition hypothetical components (single oils) in ProMax is to use the molecular weight and the specific gravity as input and let the software calculate the other properties based on that. The set procedure for defining hypothetical components in UniSim is to trust the total fluid characterisation given from the PVTsim analysis and use these parameters as input. The question then is if the properties calculated from ProMax are more correct than the properties from PVTsim. To get a clear conclusion on the topic on which simulation tool is the most correct, there is a need for further analyses.

7.9 Different allocation methods

Year 8 from future allocation is used as a base for the comparison of the different allocation methods. The equity-based allocation is not included since the total number of different companies with ownership in the different fields is high. The uncertainty-based allocation is also not studied since the accuracy of the parameters is not measured or given. The methods looked more into in this section are the allocation by difference and the pro-rata allocation. The measurement values for the allocation are given in Table 7.10.

Table 7.10: Results from the year 8 simulations on a mass basis

	Field A (Standalone)	Field B (Standalone)	Field C (Standalone)	Commingled (All-in)
Dry feed rate, (ton/d):	2307.5	12045.5	1233.6	15586.6
Typical produced gas, (ton/d):	1586.4	9271.9	127.7	11012.0
Typical produced oil, (ton/d):	721.2	2773.7	1106.6	4575.3

7.9.1 The ORF method (the current allocation agreement)

The calculation for the ORF method is done following the formulas (3.3) to (3.9). The results are given in Table 7.11.

Table 7.11: Allocated quantity with ORF method

	Field A	Field B	Field C
Typical produced gas, (ton/d):	1586.4	9291.1	134.5
Typical produced oil, (ton/d):	721.2	2755.0	1099.2

7.9.2 Allocation by difference

For the Platform Vest case, the C field was the last field to produce from the Platform. This field is therefore chosen as the field to be allocated by difference. Field A and field B will be allocated first, and then the rest is assumed to be from field C. The formula used for the allocation is (3.1). The result from the by difference allocation is given in Table 7.12.

Table 7.12: Allocated quantity with by difference method

	Field A	Field B	Field C
Typical produced gas, (ton/d):	1586.4	9271.9	153.8
Typical produced oil, (ton/d):	721.2	2773.7	1080.4

7.9.3 Pro-rata allocation

The pro-rata allocation is calculated using (3.2). The result from this allocation method is given in Table 7.13.

Table 7.13: Allocated quantity with pro-rata allocation method

	Field A	Field B	Field C
Typical produced gas, (ton/d):	1590.1	9293.9	128.0
Typical produced oil, (ton/d):	717.1	2757.9	1100.3

7.9.4 Allocation by process simulation

The simulation model used is all-in year 8 in UniSim. The result from this allocation method is given in Table 7.14.

Table 7.14: Allocated quantity with all-in simulation allocation method

	Field A	Field B	Field C
Typical produced gas, (ton/d):	1594.9	9213.5	203.7
Typical produced oil, (ton/d):	712.7	2832.3	1030.4

7.9.5 Allocation method results

Illustrations of the result with the different allocation methods are given in the figures below. Figure 7.53, Figure 7.54 and Figure 7.55 show the allocated oil and gas production for field A, B and C, respectively. The y-axis for all the figures has the same range of 120 ton/d for oil production and 100 ton/day for gas production. The green column illustrates the input values used for the allocation obtained from standalone simulations.

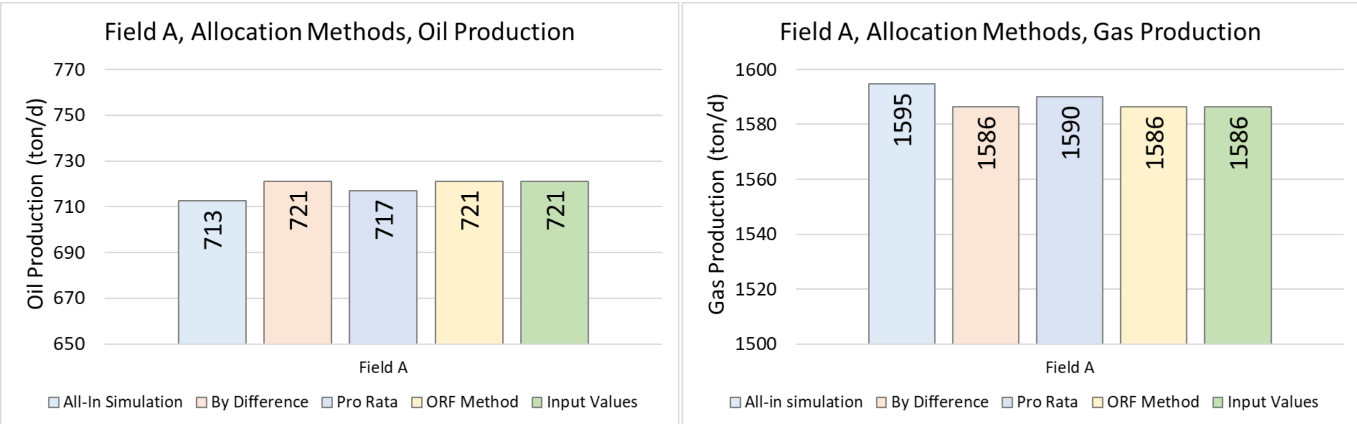

Figure 7.53: Field A, Allocation methods, Gas and oil production

For field A, the different allocation methods predict similar values for both gas production and oil production. The highest allocated value for the oil production is 721 ton/day (by difference and ORF method) and the lowest is 713 ton/day (all-in simulation), resulting in a deviation of 7 ton/day when comparing the methods. For the gas production allocation, the highest value is 1595 ton/day (all-in simulation) and the lowest is 1586 ton/day (by difference and ORF method), resulting in a deviation of 9 ton/day when comparing the methods. For field A, the allocation method that gives the highest prediction, and the prediction equal to the input values, are the by difference allocation and ORF method.

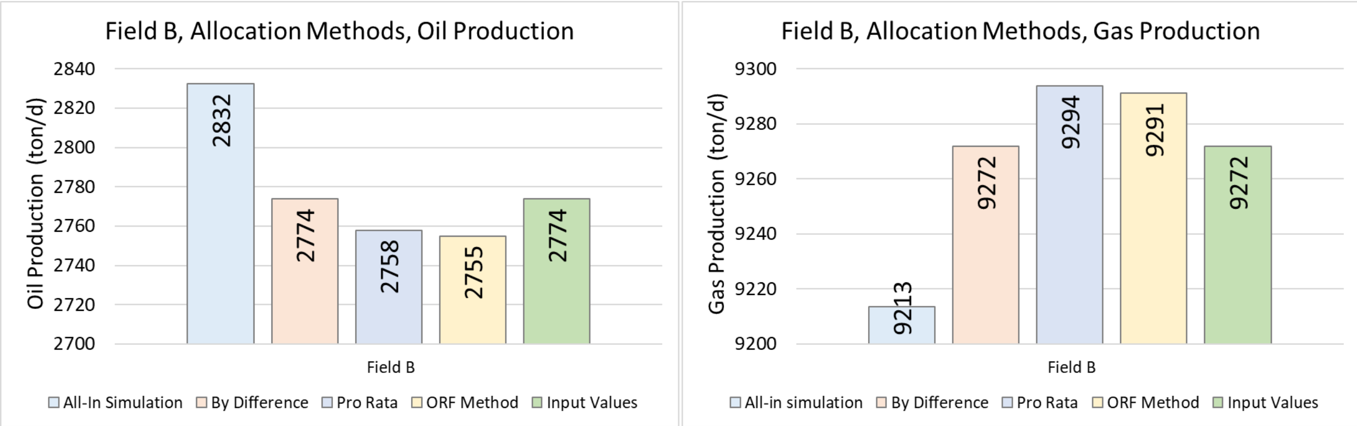

Figure 7.54: Field B, Allocation methods, Gas and oil production

For field B, the different allocation methods predict deviating values for both gas production and oil production. The highest allocated value for the oil production is 2832 ton/day (all-in simulation) and the lowest is 2755 ton/day (ORF method), resulting in a deviation of 77 ton/d when comparing the methods. For the gas production allocation, the highest value is 9294 ton/day (pro-rata allocation) and the lowest is 9213 ton/day (all-in simulation), resulting in a deviation of 81 ton/day when comparing the methods. For field B, the allocation method that gives predictions like the input values is the by difference allocation followed by the ORF method and the pro-rata allocation.

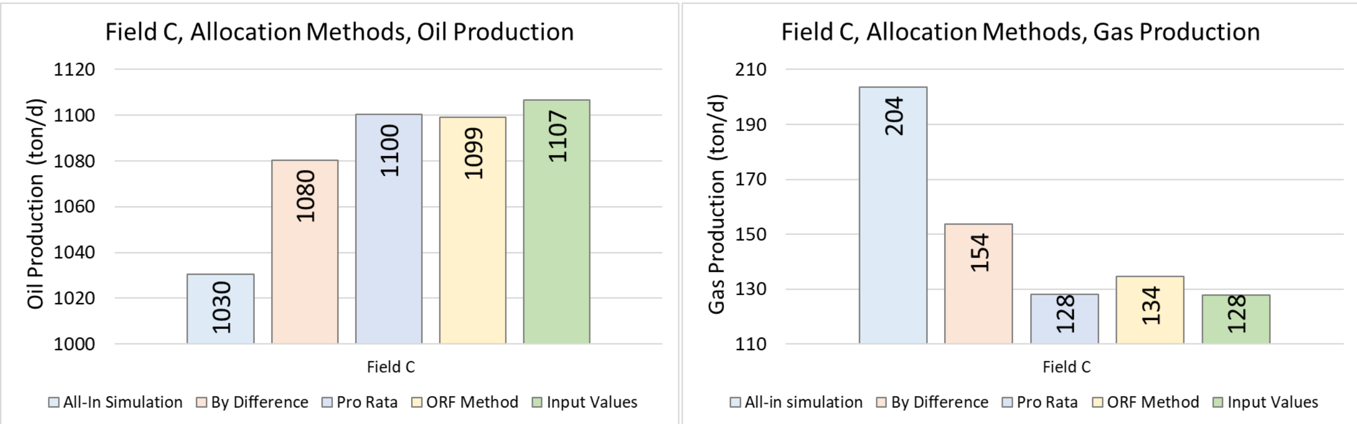

Figure 7.55: Field C, Allocation methods, Gas and oil production

For field C, the different allocation methods predict deviating values for both gas production and oil production. The highest allocated value for the oil production is 1100 ton/day (pro-rata allocation) and the lowest is 1030 ton/d (all-in simulation), resulting in a deviation of 70 ton/day when comparing the methods. For the gas production allocation, the highest value is 204 ton/day (all-in simulation) and the lowest is 128 ton/day (pro-rata allocation), resulting in a deviation of 76 ton/day when comparing the methods. For field C, the allocation method that gives predictions closest the input values are the pro-rata allocation followed by the ORF method.

The results from the comparison between the different allocation methods show that there are significant differences depending on which method that is used. The results from field A give similar allocation values for the different methods, while the results from field B and field C deviate considerably.

The GOR values for the different fields are also essential to consider when selecting an allocation method for the platform. The all-in simulation method gives a much higher oil production to field B than any other methods and much lower oil production to field C than the other methods. For the gas production, this trend is reversed with a much lower prediction with the all-in simulation for field B and higher with the all-in simulation for field C. The all-in simulation method for allocation is thus not a suitable allocation method for Platform Vest.

The by difference allocation predicts similar values to the input values for field A and field C but deviates considerably for field C. The allocation by difference is thus not optimal for Platform Vest. Then the ORF method and the pro-rata allocation method remains.

The input values are obtained from standalone simulations for the fields, making it not reasonable that these input values are accurately representative when all the fields are producing together. For field C, the pro-rata allocation predicts the same values as the input values for gas production. When considering that field C is a low GOR field, the realistic gas production would be a little higher than the standalone prediction. For gas production, the ORF method and the pro-rata allocation predicts approximately the same oil allocation. This results in the ORF method being the fairest for field C.

For field B, the pro-rata allocation and the ORF method are approximately equally deviation compared to the input values, making both methods applicable for allocation for the field.

Based on the evaluation of the different allocation methods, the current ORF method is the most fair and prudent allocation on Platform Vest when considering all the fields.

The evaluation is only based on and concluded for the result for year 8. When selecting an allocation method, a complete conclusion cannot be made until predictions are calculated for more years to study the future and historically production trends.

The calculations for the results are given in Appendix Q – Allocation methods calculation.

7.10 Recommended guideline for allocation simulation

The recommended guideline for allocation simulation based on the results in this report can be summarised in the following points.

- Always use the newest fluid characterisation to assure a fair and prudent allocation.
- The allocation utility in UniSim is good enough if the only needed output is the ORFs.
- Aromatics in the fluid setup can impact the allocation, but this needs to be investigated further to see the full effect.
- C20+ lumping scheme gives insignificant deviation compared to the original lumping scheme. This new lumping scheme can be used instead of the original without noticeable deviations.
- The PVT analysis for a C10+ lumping is much cheaper compared to a finer lumping scheme analysis. When only comparing the estimated ORFs, the deviation between the C10+ case and the initial case is not too large. In comparison, the results between the new and old characterisation gave a much higher deviation. This indicates that it is better to use C10+ lumping than to keep an old fluid characterisation.

- Future allocation can be done with different tuning methods.
  The GOR tuning method is preferred if the fluid composition is uncertain or the GOR value is the most valid estimated value for the different fields.
  Tuning to match the estimated oil production is preferred if the allocation is dependent on accurate oil simulation. This is the case for Platform Vest, where ORF is the current allocation agreement.
  Tuning to match the estimated gas production is preferred if the allocation is dependent on accurate gas simulation. This is not the case for Platform Vest.
- Allocation simulation using ProMax compared to UniSim gave noticeable deviations. The decision on which simulation software is the most correct needs to be researched more thoroughly before a conclusion regarding the different simulation software can be made.
- When looking at the different allocation methods, the most significant deviation between the methods occurred for the high GOR field B and the low GOR field C. For field A the allocation methods were not too deviating.
- Based on evaluations of the different allocation methods, the current ORF method is the most fair and prudent allocation on Platform Vest for all fields.

8 Conclusion

Allocation simulation is a complex and complicated process, where the most crucial aspect is to get the allocation as fair and prudent as possible. The possible allocation methods depend on the different fields, the production platform and the owners and users. Many different parties shall be satisfied with the established allocation method.

Platform Vest is a platform with production from three fields, where each field has different owners. Field A is the original field on the platform, and it is important that this field is not negatively impacted by allowing production from other fields through the same platform. However, the allocation cannot be biased towards the A field either. The allocation method needs to be unbiased towards all involving parties but also fair and prudent.

When comparing the different allocation methods, the current established ORF method was the method that gave the fairest allocation of gas and oil to the different fields, especially when considering the different GOR values of the fields. If any of the other methods were to be used, at least one field would get an unfair allocation with either too low predictions or too high predictions.

For future allocation, the tuning method recommended when the allocation method is ORF based is to tune to match the predicted oil production.

Predicting the ORFs for the allocation should be as close to the initial case as possible. The result from this report ranks the ORF deviation from highest to lowest, with the highest occurred when incorporating benzene to the fluid inflow (5.8 %), followed by using the old characterisation (3.1 %), using the C10+ lumping (2.1 %), allocation utility method (1.2 %), adjusting the process input for the first stage separation (1.0 %) and lastly using the C20+ lumping (0.7 %).

The deviation between the predicted ORF in ProMax and UniSim was 8.2 %, but the conclusion on which software is the most correct needs to be further analysed to obtain a fair decision.

The addition of benzene to the inflow gave the most significant deviation if the ProMax comparison is disregarded. PNA in the fluid characterisation should thus be further investigated to determine the impact this can have on the allocation.

To summarise, the newest fluid characterisation should always be used when possible. The C20+ lumping and the allocation utility method can safely be used with approximately the same result as the initial case if only the ORFs are the required result. The process input should always be representative of the actual case to get the most up-to-date simulation for the allocation. The C10+ lumping scheme can be considered without too large deviations for the ORFs when a complete fluid analysis is not created and acquired.

In conclusion, for Platform Vest the most fair and prudent allocation method for all fields is the current allocation method using standalone ORFs achieved from process simulations.

References

[1] S. Chakrabarti, *Handbook of Offshore Engineering*, Illinois: Elsevier Science & Technology, 2005.

[2] S. Kanshiro, "A review of hydrocarbon allocation methods in the upstream oil and gas industry," *Journal of Petroleum Science and Engineering*, volume 184, January 2020. [Online]. Available: doi: 10.1016/j.petrol.2019.106590

[3] J. H. Johnsen. "Gass- og kondensatbehandling." ndla. https://ndla.no/nb/subject:6/topic:1:182061/topic:1:151959/resource:1:157189/346?filters=urn:filter:01c27030-e8f8-4a7c-a5b3-489fdb8fea30 (accessed Mar. 3, 2021).

[4] A. Aabø. "Drivmekanismer i reservoaret." ndla. https://ndla.no/subject:6/topic:1:182061/topic:1:155237/resource:1:153039?filters=urn:filter:01c27030-e8f8-4a7c-a5b3-489fdb8fea30 (accessed Mar. 5, 2021).

[5] J. Lavis. "What's the difference between gas lift and gas injection." Drillers. https://drillers.com/whats-difference-gas-lift-gas-injection/ (accessed Mar. 5, 2021).

[6] Equinor, Field information for A, B and C, Jan. 2021.

[7] L. V. Lidal. "Gassløft og kjemikalieinjeksjon." ndla. https://ndla.no/subject:6/topic:1:182061/topic:1:151959/resource:1:181801?filters=urn:filter:01c27030-e8f8-4a7c-a5b3-489fdb8fea30 (accessed Mar. 5, 2021).

[8] NORSOK STANDARD, *Design principles: coding system*, Jan. 1995.

[9] S. Mokhatab, W. A. Poe and J. Y. Mak, Handbook of Natural Gas Transmission and Processing: Principles and Practices, 4th ed. Oxford: Elsevier Science & Technology, 2018. [Online]. Available:https://ezproxy1.usn.no:2452/lib/ucsn-ebooks/reader.action?docID=5560017

[10] Bryan Research & Engineering, *ProMax*, version 5.

[11] The Energy Institute (EI), "Guidelines for the allocation of fluid streams in oil and gas production," London, England, 1st ed. 2012

[12] Equinor, Mail correspondence with uncertainties, Mar. 2021.

[13] E. Åbro *et al*. *"Experience with the multiphase meter system used for allocation of Visund South tie-in to Gullfaks C."* [Online]. Available: https://nfogm.no/wp-content/uploads/2019/02/2015-25-Experiences-with-the-multiphase-meter-system-%C3%85bro-Statoil.pdf (accessed April. 7, 2021).

[14] Equinor, Provided current allocation method for Platform Vest, Jan. 2021.

[15] R.M. Felder and R. W. Rousseau, Elementary principle of chemical processes, 3rd ed. New Jersey; Wiley, 2005.

[16] J.N. Jaubert, R. Privat, Y.L. Guennec and L. Coniglio, "Note on the properties altered by application of a Peneloux-type volume translation to an equation of state", Fluid Phase Equilibria, vol. 419, pp. 88-95, 2016. [Online]. Available: doi: 10.1016/j.fluid.2016.03.012

[17] Equinor. Provided fluid analysis reports for field A, B and C. Jan. 2021.

[18] E. Skouras, "Thermodynamics in Gas Processing – Phase Envelope Predictions and Process Design," presented at 1st Trondheim Gas Technology Conference, Trondheim, Norway, 21-22 October 2009. [Online]. Available: https://www.sintef.no/globalassets/upload/energi/arrangementer/tgtc09/a4_1_skouras.pdf

[19] J. M. Campbell, Gas conditioning and processing: volume 1: The basic principles, 7th ed. Oklahoma: Campbell Petroleum Series, 1992.

[20] Norges bank. "Exchange rates." https://www.norges-bank.no/en/topics/Statistics/exchange_rates/?tab=currency&id=USD (accessed Mar. 3, 2021)

[21] Markets insider. "Naphthapreis (European)." https://markets.businessinsider.com/commodities/naphthapreis (accessed Mar. 3, 2021)

[22] Commodity3. "Jet Fuel Kerosene in US$/mt." https://www.commodity3.com/swaps/7/jet-fuel-kerosene-in-us$-mt (accessed Mar. 3, 2021)

[23] Kurzycz. "Gas oil." https://eng.kurzy.cz/commodities/gas-oil-price-development-chart/ (accessed Mar. 3, 2021)

[24] Equinor, Provided calculation example, Jan. 2021.

[25] Honeywell International Inc., *UniSim,* Version R460.2.

Appendices

Appendix A – Scope of work

University of
South-Eastern Norway

Faculty of Technology, Natural Sciences and Maritime Sciences, Campus Porsgrunn

FMH606 Master's Thesis

Title: Recommended guideline for allocation simulation

USN supervisor: Britt M. E. Moldestad

External partner: Equinor ASA, Trine Amundsen Madsen

Task background:
Oil and gas fields are typically owned by different companies. To determine the quantity and quality of the feed and product stream belonging to each user/partner, the oil and gas product are allocated between the partners. Allocation simulations are performed to allocate the values between partners for ongoing production, and for evaluating commingling effects for new tie-ins fields to define the allocation method fair and prudent for all producers. Allocation simulation are important for all oil and gas companies, and Equinor allocate for 50 billion NOK every month.

Task description:
A recommended guideline for allocation includes evaluation from fluid sampling, fluid characterization, process simulation and evaluation. The following scope are recommended:

1. What is allocation and what are the basic allocation principles?

2. Evaluate PVT description of different wells. How are PVT samples taken and measured?

3. Evaluate the fluid characterization and the EOS model prediction for component properties, and the transfer from PVTsim to the process simulation tool.

4. Evaluate the overall uncertainties in allocation simulation. Compare UniSim process simulation tool to ProMax process simulation tool for allocation simulations for different fields. Data from fields will be provided and case study to be performed. Evaluate the different allocation methods.

5. Summarize the findings in a report and recommend a guideline for allocation simulation.

Student category: EET, Madelen Smedsli

The task is suitable for online students (not present at the campus): No

Practical arrangements:

The Covid-19 pandemic effects the location of workplace. There is unfortunately no capacity at the local Equinor office due to regulations. The work will be carried out at the University or home office with close collaboration with supervisor via Teams.

Software's to be used depend on the availability for the student. Unisim/Aspen Hysys and ProMax (to checked) will be used during this study. If access to PVTsim, this tool will also be used to evaluate fluid characterization. If no access, the evaluation will be carried out in collaboration with supervisor.

Supervision:

As a general rule, the student is entitled to 15-20 hours of supervision. This includes necessary time for the supervisor to prepare for supervision meetings (reading material to be discussed, etc).

Signatures:

17.02.21

Britt M. E. Moldestad, USN Supervisor, date

18.02.21

Trine A. Madsen, External Supervisor, date

17.02.21

Madelen Smedsli, Student, date

Appendix B – PVTsim procedure

The PVTsim procedure is described as follows:

1) When opening PVTsim, the software opens as the following figure.

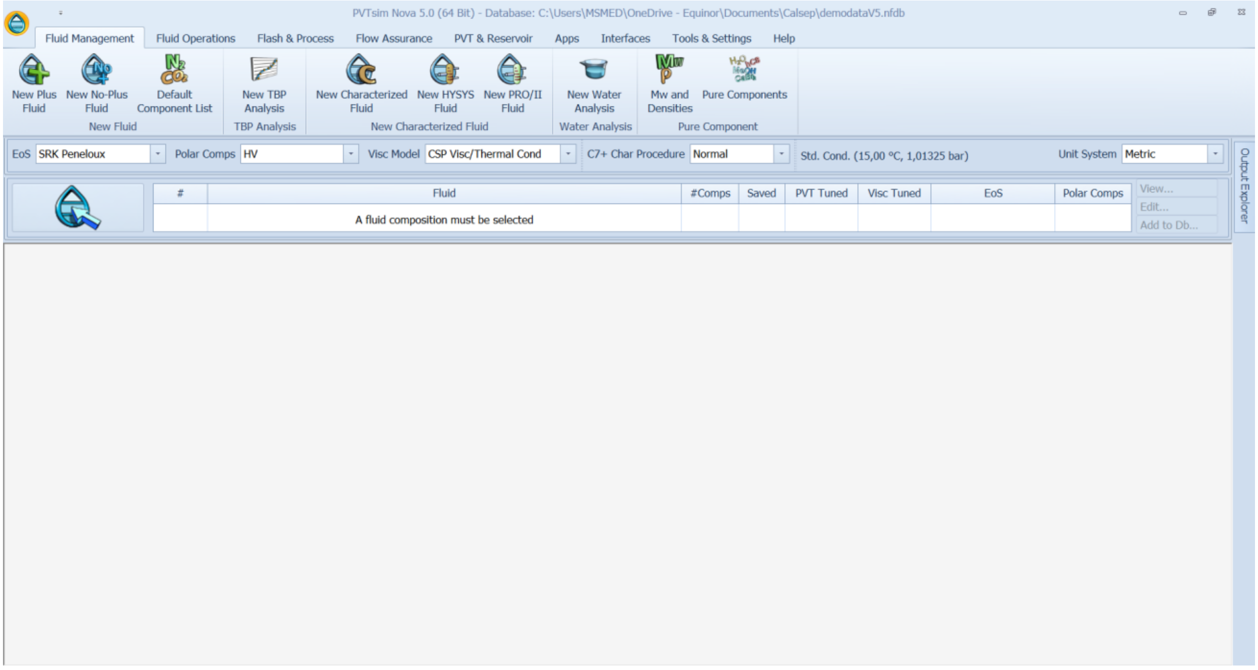

2) When defining the EOS as SRK Peneloux, click on new plus fluid and the following page will open:

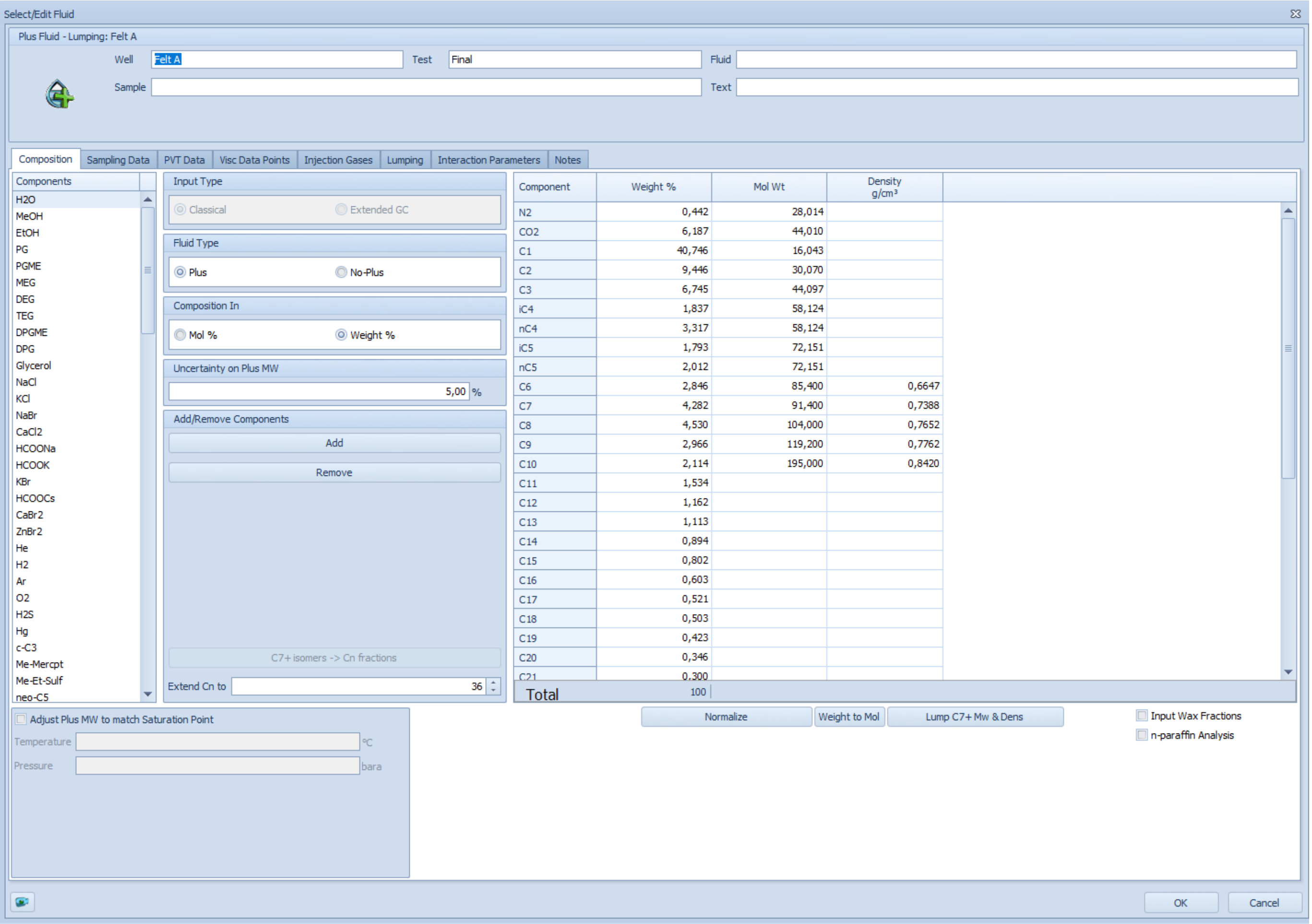

3) The input to the figure above is found from the analysis reports (not added as an appendix due to confidentiality). The input is mol % or weight % (from N2 to C36+ for field A, and from N2 to C10+ for field B and C), the mol weight (from N2 to C10) and the density (C6 to C10). The Cn is extended to 36 as shown above (for all field).
4) The lumping scheme is defined in the lumping fane as illustrated in the figure below (for field A):

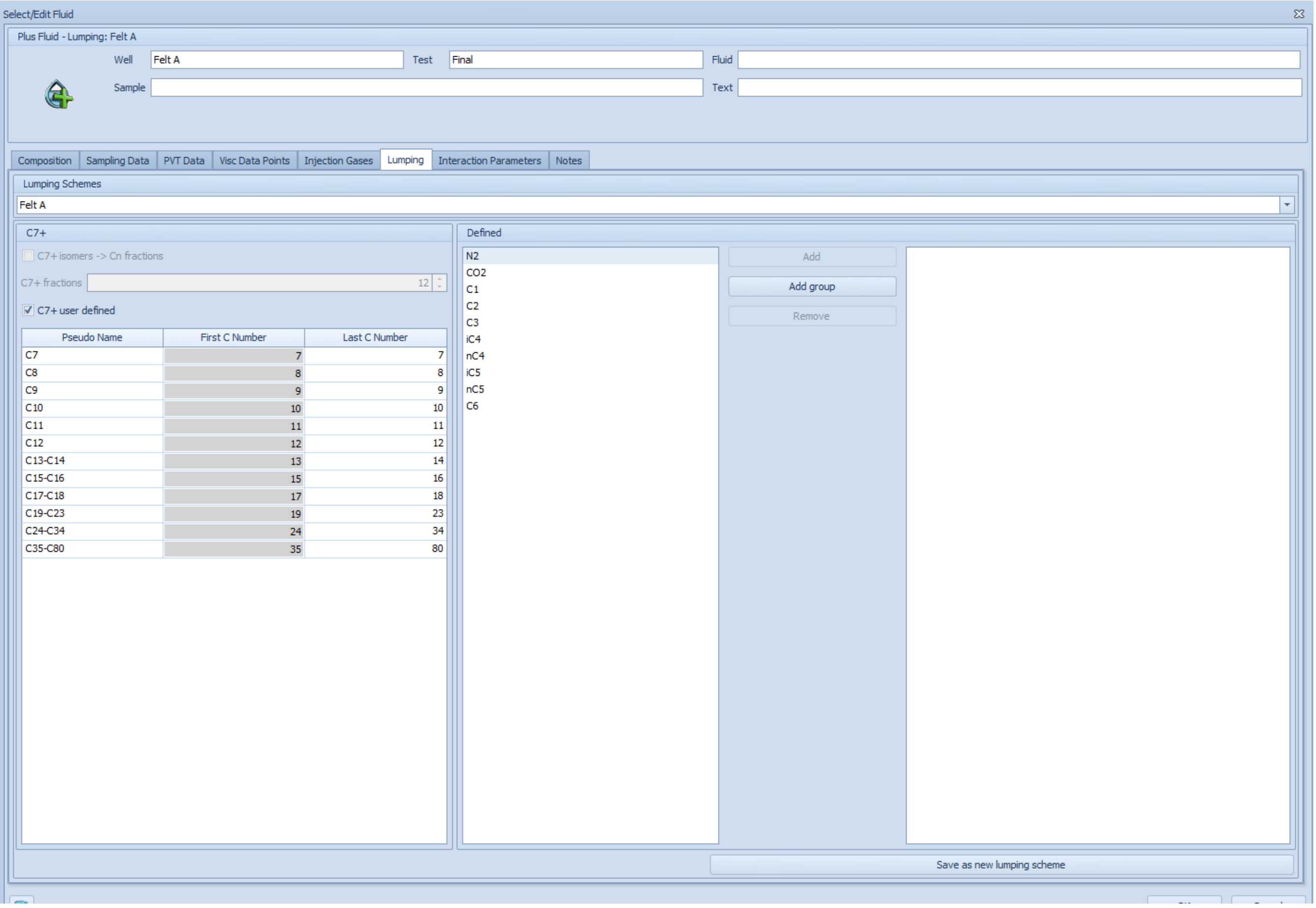

5) Click the OK button, and the following output is given:

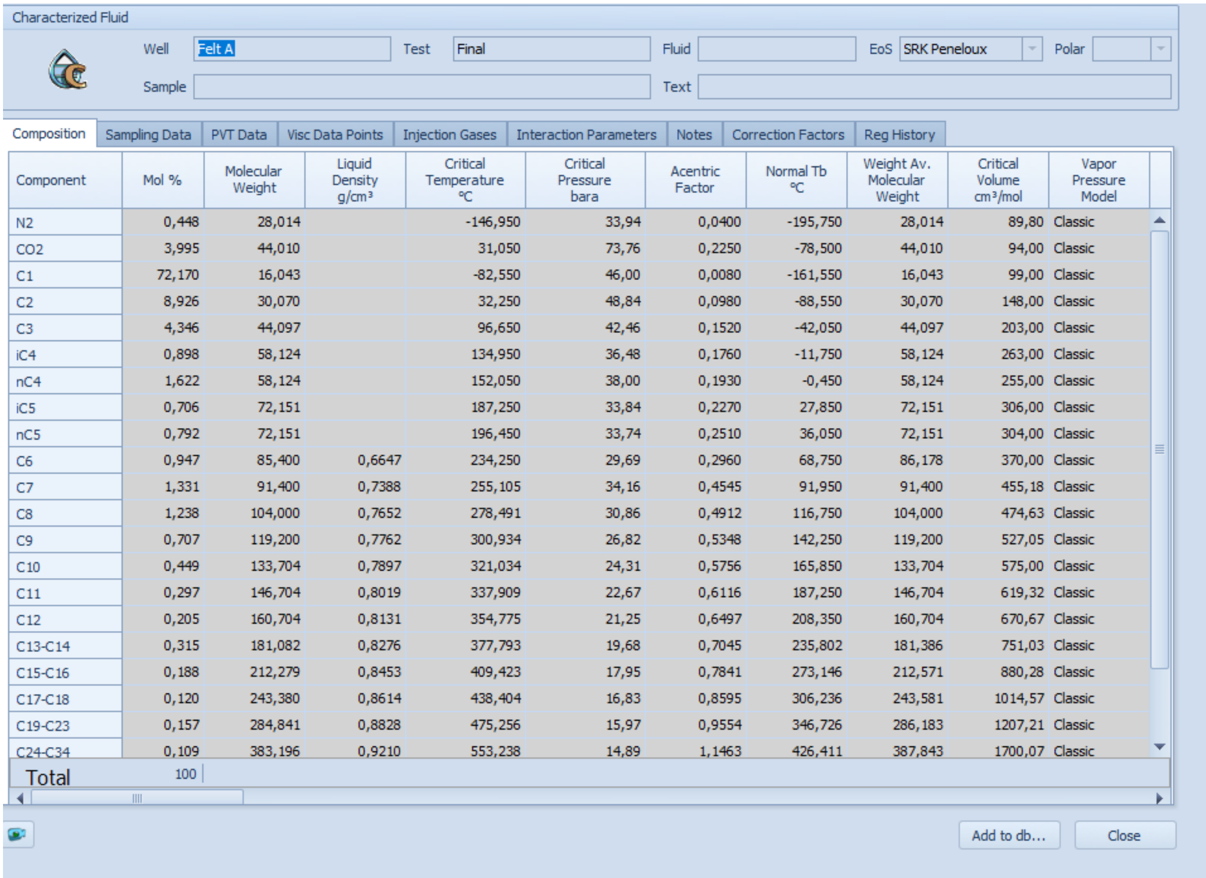

Characterized Fluid

Well: Felt A | Test: Final | Fluid: | EoS: SRK Peneloux | Polar:

Sample: | Text:

Composition | Sampling Data | PVT Data | Visc Data Points | Injection Gases | Interaction Parameters | Notes | Correction Factors | Reg History

Component	Mol %	Molecular Weight	Liquid Density g/cm³	Critical Temperature °C	Critical Pressure bara	Acentric Factor	Normal Tb °C	Weight Av. Molecular Weight	Critical Volume cm³/mol	Vapor Pressure Model
N2	0,448	28,014		-146,950	33,94	0,0400	-195,750	28,014	89,80	Classic
CO2	3,995	44,010		31,050	73,76	0,2250	-78,500	44,010	94,00	Classic
C1	72,170	16,043		-82,550	46,00	0,0080	-161,550	16,043	99,00	Classic
C2	8,926	30,070		32,250	48,84	0,0980	-88,550	30,070	148,00	Classic
C3	4,346	44,097		96,650	42,46	0,1520	-42,050	44,097	203,00	Classic
iC4	0,898	58,124		134,950	36,48	0,1760	-11,750	58,124	263,00	Classic
nC4	1,622	58,124		152,050	38,00	0,1930	-0,450	58,124	255,00	Classic
iC5	0,706	72,151		187,250	33,84	0,2270	27,850	72,151	306,00	Classic
nC5	0,792	72,151		196,450	33,74	0,2510	36,050	72,151	304,00	Classic
C6	0,947	85,400	0,6647	234,250	29,69	0,2960	68,750	86,178	370,00	Classic
C7	1,331	91,400	0,7388	255,105	34,16	0,4545	91,950	91,400	455,18	Classic
C8	1,238	104,000	0,7652	278,491	30,86	0,4912	116,750	104,000	474,63	Classic
C9	0,707	119,200	0,7762	300,934	26,82	0,5348	142,250	119,200	527,05	Classic
C10	0,449	133,704	0,7897	321,034	24,31	0,5756	165,850	133,704	575,00	Classic
C11	0,297	146,704	0,8019	337,909	22,67	0,6116	187,250	146,704	619,32	Classic
C12	0,205	160,704	0,8131	354,775	21,25	0,6497	208,350	160,704	670,67	Classic
C13-C14	0,315	181,082	0,8276	377,793	19,68	0,7045	235,802	181,386	751,03	Classic
C15-C16	0,188	212,279	0,8453	409,423	17,95	0,7841	273,146	212,571	880,28	Classic
C17-C18	0,120	243,380	0,8614	438,404	16,83	0,8595	306,236	243,581	1014,57	Classic
C19-C23	0,157	284,841	0,8828	475,256	15,97	0,9554	346,726	286,183	1207,21	Classic
C24-C34	0,109	383,196	0,9210	553,238	14,89	1,1463	426,411	387,843	1700,07	Classic
Total	100									

Add to db... | Close

6) The figure above is the new fluid characterisation for field A.

Appendix C – Old fluid characterisation

The old fluid characterisation for field A, B and C is shown in the tables below:

Field A - Old characterisation								
Component	Molfrac	NBP	MW	Liq Den	T_c	P_c	V_c	Acentric factor
	-	C	g/mol	kg/m3	C	bara	m3/kmol	-
A - N2*	0.00449	-195.750	28.020	804.000	-146.950	33.944	0.090	0.040
A - CO2*	0.03994	-78.500	44.010	809.000	31.050	73.765	0.094	0.225
A - C1*	0.72172	-161.550	16.040	300.000	-82.550	46.002	0.099	0.008
A - C2*	0.08927	-88.550	30.070	356.700	32.250	48.839	0.148	0.098
A - C3*	0.04346	-42.050	44.090	506.700	96.650	42.455	0.203	0.152
A - iC4*	0.00898	-11.750	58.120	562.100	134.950	36.477	0.263	0.176
A - nC4*	0.01640	-0.450	58.120	583.100	152.050	37.997	0.255	0.193
A - iC5*	0.00688	27.850	72.150	623.300	187.250	33.843	0.306	0.227
A - nC5*	0.00792	36.050	72.150	629.900	196.450	33.741	0.304	0.251
A - C6*	0.00947	68.750	85.400	664.800	234.250	29.688	0.370	0.296
A - C7*	0.01332	91.950	91.400	737.200	272.490	34.020	0.457	0.454
A - C8*	0.01237	116.750	104.100	764.600	295.754	29.233	0.476	0.492
A - C9*	0.00707	142.250	119.100	776.000	320.125	25.495	0.527	0.534
A - C10*	0.00418	165.850	134.000	782.000	341.955	22.599	0.585	0.576
A - C11*	0.00281	187.250	147.000	793.000	359.596	21.018	0.630	0.612
A - C12*	0.00201	208.350	161.000	804.000	377.358	19.693	0.681	0.650
A - C13-C14*	0.00310	236.050	181.570	820.005	401.831	18.296	0.760	0.706
A - C15-C16*	0.00196	273.239	212.662	839.028	435.191	16.763	0.887	0.785
A - C17-C18*	0.00124	306.217	243.657	853.442	468.289	15.666	1.021	0.860
A - C19-C23*	0.00159	346.355	283.294	869.391	504.761	14.721	1.205	0.952
A - C24-C34*	0.00110	425.731	367.157	898.302	574.201	12.967	1.613	1.118
A - C35-C80*	0.00071	550.612	600.203	986.695	745.214	13.353	2.970	1.318

Field B - Old characterisation								
Component	Molfrac	NBP	MW	Liq Den	T_c	P_c	V_c	Acentric factor
	-	C	g/mol	kg/m3	C	bara	m3/kmol	-
B - N2*	0.00691	-195.750	28.020	804.000	-146.950	33.944	0.090	0.040
B - CO2*	0.02402	-78.500	44.010	809.000	31.050	73.765	0.094	0.225
B - C1*	0.81959	-161.550	16.040	300.000	-82.550	46.002	0.099	0.008
B - C2*	0.05805	-88.550	30.070	356.700	32.250	48.839	0.148	0.098
B - C3*	0.03273	-42.050	44.090	506.700	96.650	42.455	0.203	0.152
B - iC4*	0.00487	-11.750	58.120	562.100	134.950	36.477	0.263	0.176
B - nC4*	0.01047	-0.450	58.120	583.100	152.050	37.997	0.255	0.193
B - iC5*	0.00333	27.850	72.150	623.300	187.250	33.843	0.306	0.227
B - nC5*	0.00445	36.050	72.150	629.900	196.450	33.741	0.304	0.251
B - C6*	0.00475	68.750	84.700	667.600	234.250	29.688	0.370	0.296
B - C7*	0.00685	91.950	91.000	738.900	265.226	34.364	0.453	0.453
B - C8*	0.00588	116.750	104.800	762.000	290.199	30.027	0.482	0.494
B - C9*	0.00344	142.250	121.000	768.200	314.967	25.520	0.544	0.540
B - C10-C11*	0.00439	175.504	139.568	786.924	341.455	22.588	0.605	0.593
B - C12*	0.00148	208.350	161.000	804.000	368.325	20.181	0.681	0.650
B - C13-C14*	0.00241	236.371	181.819	820.189	392.675	18.611	0.761	0.706
B - C15-C16*	0.00165	273.401	212.813	839.095	425.270	16.925	0.888	0.785
B - C17-C18*	0.00111	306.254	243.696	853.456	454.795	15.729	1.021	0.860
B - C19-C22*	0.00128	341.698	279.107	867.522	486.545	14.792	1.184	0.942
B - C23-C29*	0.00103	404.299	343.077	890.808	539.121	13.880	1.489	1.074
B - C30-C40*	0.00081	485.030	463.927	925.426	584.513	12.468	2.119	1.258
B - C41-C80*	0.00050	586.846	687.185	1008.297	727.629	13.459	3.434	1.312

Field C - Old characterisation								
Component	Molfrac	NBP	MW	Liq Den	T_c	P_c	V_c	Acentric factor
	-	C	g/mol	kg/m3	C	bara	m3/kmol	-
C - N2*	0.00247	-195.750	28.020	804.000	-146.950	33.944	0.090	0.040
C - CO2*	0.02336	-78.500	44.010	809.000	31.050	73.765	0.094	0.225
C - C1*	0.26983	-161.550	16.040	300.000	-82.550	46.002	0.099	0.008
C - C2*	0.06960	-88.550	30.070	356.700	32.250	48.839	0.148	0.098
C - C3*	0.08610	-42.050	44.090	506.700	96.650	42.455	0.203	0.152
C - iC4*	0.01607	-11.750	58.120	562.100	134.950	36.477	0.263	0.176
C - nC4*	0.05074	-0.450	58.120	583.100	152.050	37.997	0.255	0.193
C - iC5*	0.01810	27.850	72.150	623.300	187.250	33.843	0.306	0.227
C - nC5*	0.02853	36.050	72.150	629.900	196.450	33.741	0.304	0.251
C - C6*	0.03307	68.750	84.900	666.800	234.250	29.688	0.370	0.296
C - C7*	0.05277	91.950	91.100	738.800	274.051	34.306	0.454	0.454
C - C8*	0.05056	116.750	105.100	760.600	299.624	30.166	0.485	0.494
C - C9*	0.03487	142.250	120.200	771.400	324.194	26.329	0.537	0.538
C - C10-C12*	0.07001	185.638	145.555	792.116	361.074	22.444	0.629	0.610
C - C13-C14*	0.03498	236.230	181.709	820.108	404.908	19.410	0.761	0.706
C - C15-C17*	0.03981	281.814	219.983	842.837	446.039	17.528	0.920	0.804
C - C18-C20*	0.02884	324.247	261.749	860.608	485.673	16.166	1.103	0.902
C - C21-C25*	0.02960	372.657	310.352	879.558	528.193	15.246	1.329	1.008
C - C26-C30*	0.01992	427.130	369.879	898.535	575.505	14.554	1.613	1.121
C - C31-C37*	0.01739	476.979	443.996	918.904	631.448	14.095	1.996	1.235
C - C38-C47*	0.01346	534.466	581.660	967.975	773.306	14.726	2.724	1.354
C - C48-C80*	0.00992	632.335	798.965	1053.372	919.284	16.849	4.104	1.237

Appendix D – New fluid characterisation

The new fluid characterisation for field A, B and C is shown in the tables below:

Field A - New characterisation								
Component	Molfrac	NBP	MW	Liq Den	T_c	P_c	V_c	Acentric factor
	-	C	g/mol	kg/m3	C	bara	m3/kmol	-
A - N2*	0.00449	-195.750	28.014	804.000	-146.950	33.944	0.090	0.040
A - CO2*	0.03994	-78.500	44.010	809.000	31.050	73.765	0.094	0.225
A - C1*	0.72172	-161.550	16.043	300.000	-82.550	46.002	0.099	0.008
A - C2*	0.08927	-88.550	30.070	356.700	32.250	48.839	0.148	0.098
A - C3*	0.04346	-42.050	44.097	506.700	96.650	42.455	0.203	0.152
A - iC4*	0.00898	-11.750	58.124	562.100	134.950	36.477	0.263	0.176
A - nC4*	0.01640	-0.450	58.124	583.100	152.050	37.997	0.255	0.193
A - iC5*	0.00688	27.850	72.151	623.300	187.250	33.843	0.306	0.227
A - nC5*	0.00792	36.050	72.151	629.900	196.450	33.741	0.304	0.251
A - C6*	0.00947	68.750	85.400	664.700	234.250	29.688	0.370	0.296
A - C7*	0.01332	91.950	91.400	738.800	255.105	34.156	0.455	0.454
A - C8*	0.01237	116.750	104.000	765.200	278.491	30.856	0.475	0.491
A - C9*	0.00707	142.250	119.200	776.200	300.934	26.823	0.527	0.535
A - C10*	0.00449	165.850	133.704	789.718	321.034	24.312	0.575	0.576
A - C11*	0.00297	187.250	146.704	801.947	337.909	22.673	0.619	0.612
A - C12*	0.00205	208.350	160.704	813.112	354.775	21.246	0.671	0.650
A - C13-C14*	0.00315	235.802	181.082	827.590	377.793	19.676	0.751	0.704
A - C15-C16*	0.00188	273.146	212.279	845.276	409.423	17.949	0.880	0.784
A - C17-C18*	0.00120	306.236	243.380	861.389	438.404	16.835	1.015	0.860
A - C19-C23*	0.00157	346.726	284.841	882.807	475.256	15.970	1.207	0.955
A - C24-C34*	0.00109	426.411	383.196	921.044	553.238	14.890	1.700	1.146
A - C35-C80*	0.00031	492.630	499.174	953.945	630.397	14.402	2.271	1.299

Field B - New characterisation								
Component	Molfrac	NBP	MW	Liq Den	T_c	P_c	V_c	Acentric factor
	-	C	g/mol	kg/m3	C	bara	m3/kmol	-
B - N2*	0.00691	-195.750	28.014	804.000	-146.950	33.944	0.090	0.040
B - CO2*	0.02402	-78.500	44.010	809.000	31.050	73.765	0.094	0.225
B - C1*	0.81959	-161.550	16.043	300.000	-82.550	46.002	0.099	0.008
B - C2*	0.05805	-88.550	30.070	356.700	32.250	48.839	0.148	0.098
B - C3*	0.03273	-42.050	44.097	506.700	96.650	42.455	0.203	0.152
B - iC4*	0.00487	-11.750	58.124	562.100	134.950	36.477	0.263	0.176
B - nC4*	0.01047	-0.450	58.124	583.100	152.050	37.997	0.255	0.193
B - iC5*	0.00333	27.850	72.151	623.300	187.250	33.843	0.306	0.227
B - nC5*	0.00445	36.050	72.151	629.900	196.450	33.741	0.304	0.251
B - C6*	0.00475	68.750	84.800	667.400	234.250	29.688	0.370	0.296
B - C7*	0.00685	91.950	91.000	741.400	254.887	34.580	0.450	0.453
B - C8*	0.00588	116.750	104.600	762.900	278.975	30.456	0.480	0.493
B - C9*	0.00344	142.250	120.200	772.400	301.598	26.308	0.536	0.538
B - C10-C11*	0.00332	176.357	140.082	792.265	329.102	23.254	0.602	0.594
B - C12*	0.00137	208.350	161.000	810.051	354.584	21.046	0.675	0.650
B - C13-C14*	0.00226	236.627	182.018	825.236	378.315	19.469	0.758	0.707
B - C15-C16*	0.00175	274.121	213.486	843.345	410.175	17.781	0.887	0.787
B - C17-C18*	0.00135	306.118	243.550	859.228	438.191	16.736	1.017	0.860
B - C19-C22*	0.00185	342.853	281.231	879.258	471.652	15.957	1.189	0.947
B - C23-C29*	0.00163	403.512	352.417	908.951	528.901	15.072	1.534	1.091
B - C30-C40*	0.00085	477.672	468.563	945.787	612.035	14.474	2.131	1.265
B - C41-C80*	0.00027	577.277	668.668	992.620	743.902	14.384	3.279	1.329

Field C - New characterisation								
Component	Molfrac	NBP	MW	Liq Den	T_c	P_c	V_c	Acentric factor
	-	C	g/mol	kg/m3	C	bara	m3/kmol	-
C - N2*	0.00247	-195.750	28.014	804.000	-146.950	33.944	0.090	0.040
C - CO2*	0.02336	-78.500	44.010	809.000	31.050	73.765	0.094	0.225
C - C1*	0.26983	-161.550	16.043	300.000	-82.550	46.002	0.099	0.008
C - C2*	0.06960	-88.550	30.070	356.700	32.250	48.839	0.148	0.098
C - C3*	0.08610	-42.050	44.097	506.700	96.650	42.455	0.203	0.152
C - iC4*	0.01607	-11.750	58.124	562.100	134.950	36.477	0.263	0.176
C - nC4*	0.05074	-0.450	58.124	583.100	152.050	37.997	0.255	0.193
C - iC5*	0.01810	27.850	72.151	623.300	187.250	33.843	0.306	0.227
C - nC5*	0.02853	36.050	72.151	629.900	196.450	33.741	0.304	0.251
C - C6*	0.03307	68.750	84.900	666.800	234.250	29.688	0.370	0.296
C - C7*	0.05277	91.950	91.000	741.400	254.887	34.580	0.450	0.453
C - C8*	0.05056	116.750	105.000	761.600	279.334	30.211	0.484	0.494
C - C9*	0.03487	142.250	120.300	772.400	301.726	26.282	0.536	0.538
C - C10-C12*	0.06561	187.102	146.479	798.544	337.724	22.533	0.626	0.613
C - C13-C14*	0.03442	236.788	182.144	826.117	378.580	19.500	0.757	0.707
C - C15-C17*	0.04077	282.567	220.685	848.476	417.553	17.547	0.919	0.806
C - C18-C20*	0.03065	324.771	262.240	871.283	455.294	16.378	1.099	0.904
C - C21-C25*	0.03512	373.036	315.460	896.119	500.021	15.518	1.350	1.019
C - C26-C30*	0.02183	426.742	385.107	922.419	552.753	14.900	1.690	1.148
C - C31-C37*	0.01742	475.895	466.712	947.672	610.041	14.564	2.110	1.263
C - C38-C47*	0.01130	533.725	580.175	976.416	684.064	14.434	2.722	1.354
C - C48-C80*	0.00680	626.160	787.354	1017.399	813.772	14.638	3.954	1.254

Appendix E – UniSim model

The figures below illustrate the UniSim model.

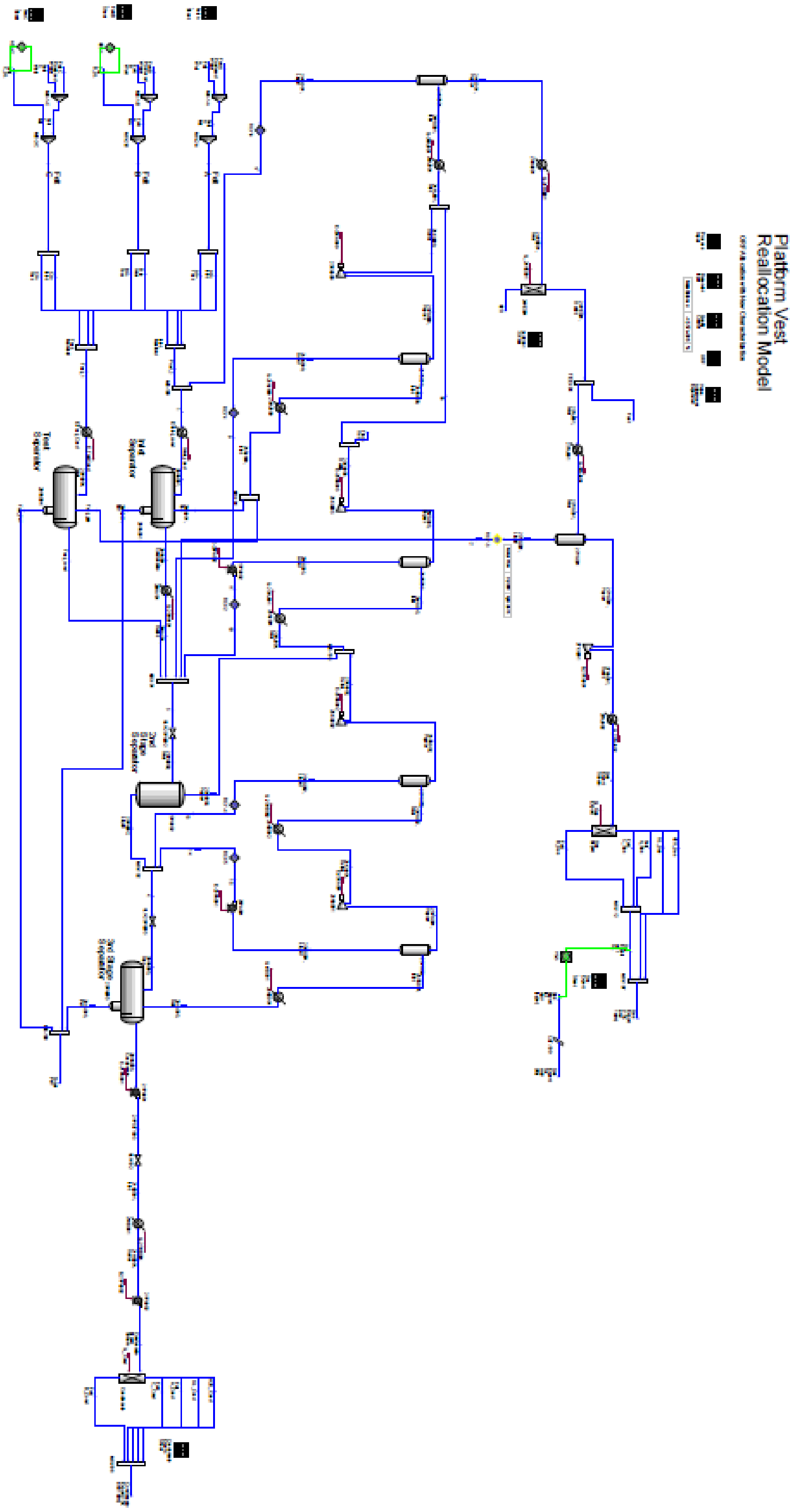

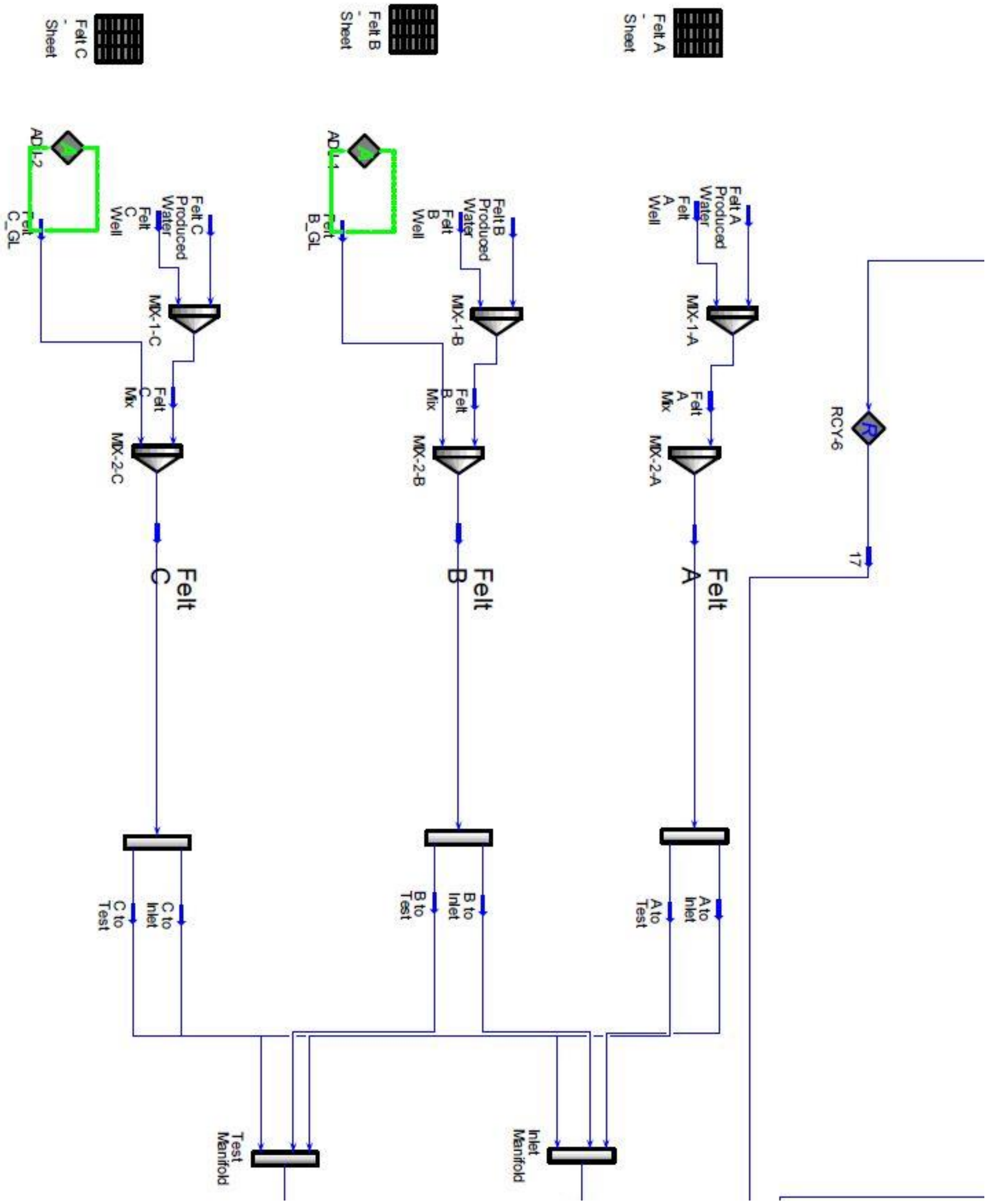
Felt A Sheet
Felt B Sheet
Felt C Sheet
ADJ-1
ADJ-2
Felt A Well
Felt A Produced Water
Felt B Well
Felt B Produced Water
Felt C Well
Felt C Produced Water
Felt B_GL
Felt C_GL
MIX-1-A
MIX-1-B
MIX-1-C
Felt A Mix
Felt B Mix
Felt C Mix
MIX-2-A
MIX-2-B
MIX-2-C
RCY-6
17
Felt A
Felt B
Felt C
A to Inlet
A to Test
B to Inlet
B to Test
C to Inlet
C to Test
Inlet Manifold
Test Manifold

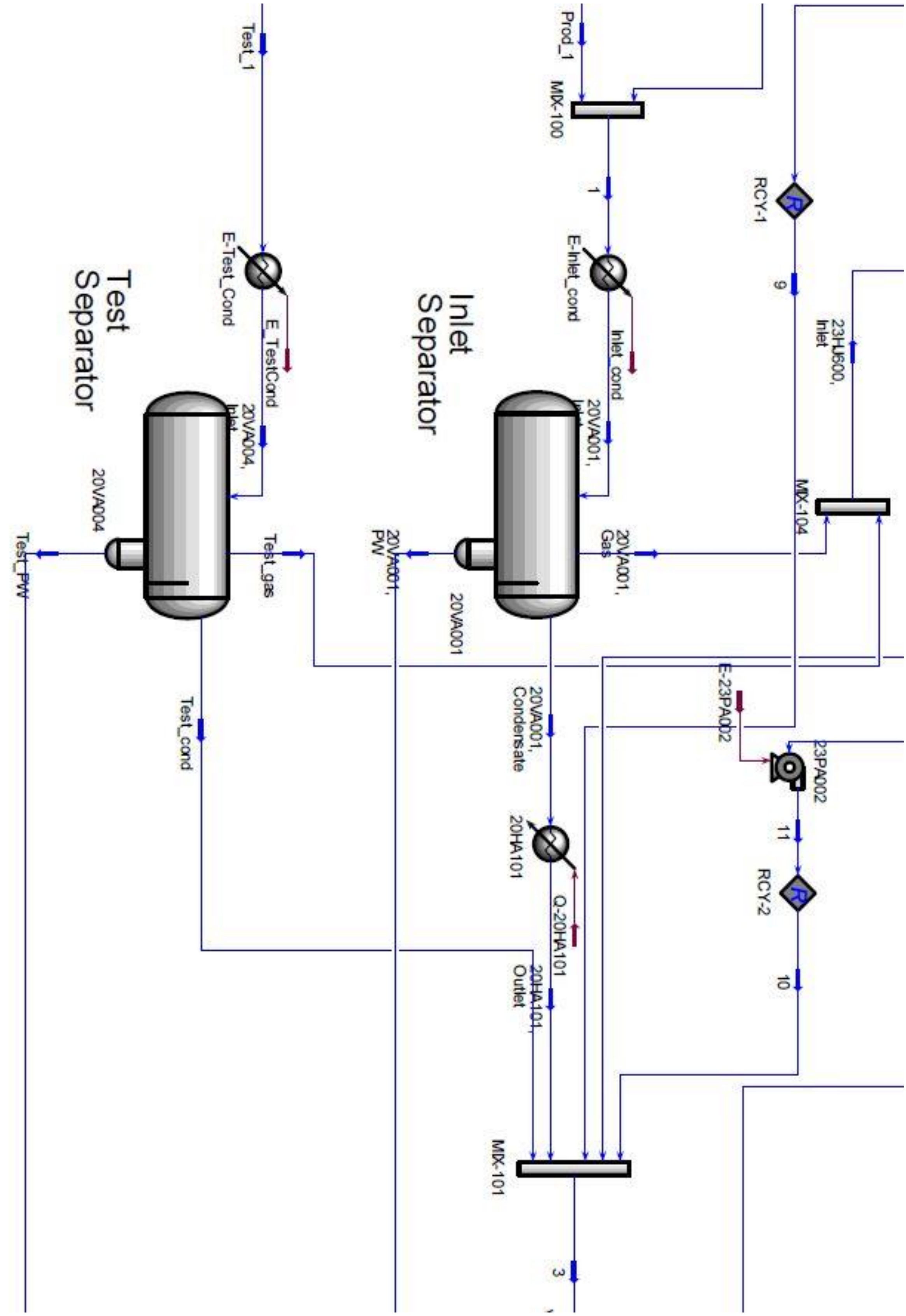
Prod_1
MIX-100
1
E-Inlet_cond
Inlet_cond
20VA001, Inlet
Inlet Separator
20VA001, Gas
20VA001, PW
20VA001
20VA001, Condensate
20HA101
Q-20HA101
20HA101, Outlet
MIX-101
3
Test_1
E-Test_Cond
E_TestCond
20VA004, Inlet
Test Separator
20VA004
Test_gas
Test_PW
Test_cond
RCY-1
9
23HJ600, Inlet
MIX-104
E-23PA002
23PA002
11
RCY-2
10

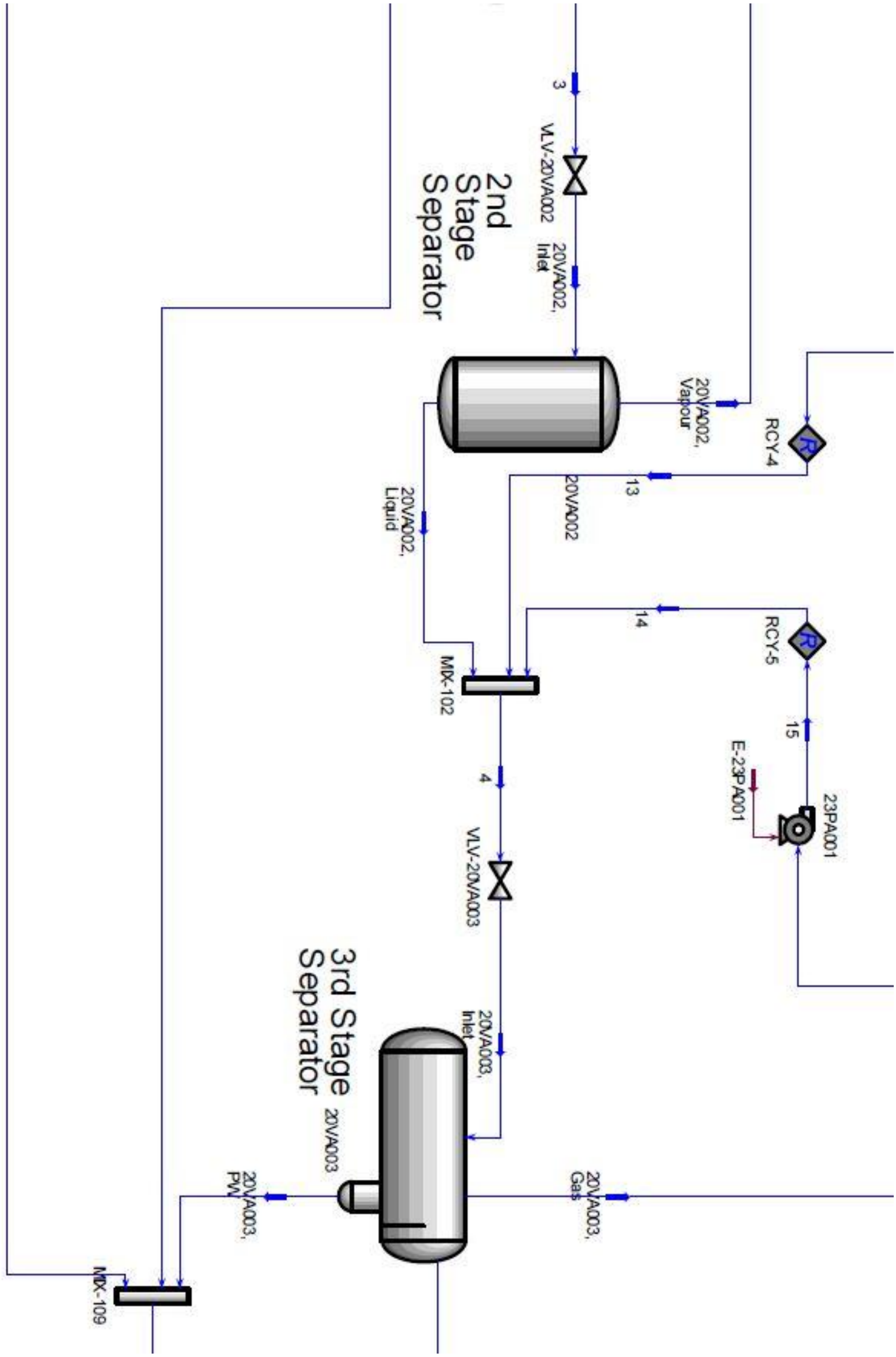
3
VLV-20VA002
2nd Stage Separator
20VA002, Inlet
20VA002, Vapour
RCY-4
13
20VA002
20VA002, Liquid
14
RCY-5
MIX-102
15
E-23PA001
23PA001
4
VLV-20VA003
3rd Stage Separator
20VA003, Inlet
20VA003
20VA003, PW
20VA003, Gas
MIX-109

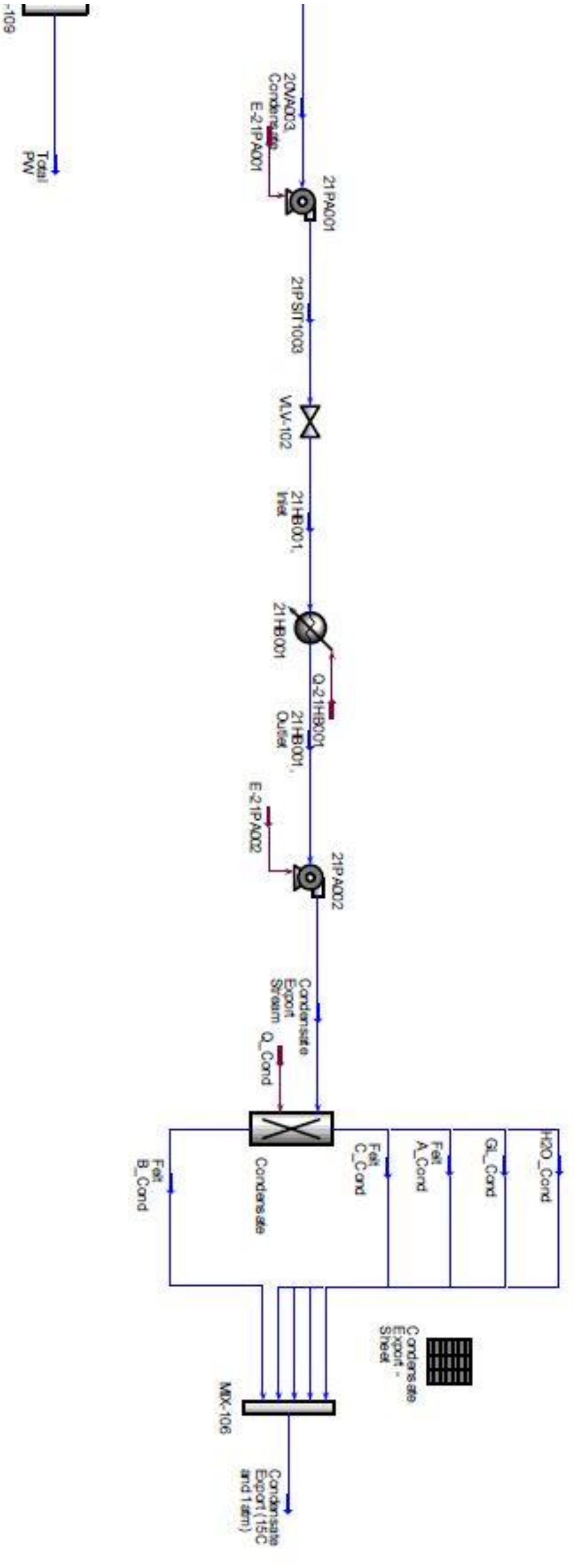
-109
Total PW
20VA003, Condensate
E-21PA001
21PA001
21PSIT1003
VLV-102
21HB001, Inlet
21HB001
Q-21HB001
21HB001, Outlet
E-21PA002
21PA002
Condensate Export Stream
Q_Cond
Condensate
Feil B_Cond
Feil C_Cond
Feil A_Cond
GL_Cond
H2O_Cond
Condensate Export - Sheet
MIX-106
Condensate Export (15C and 1 atm)

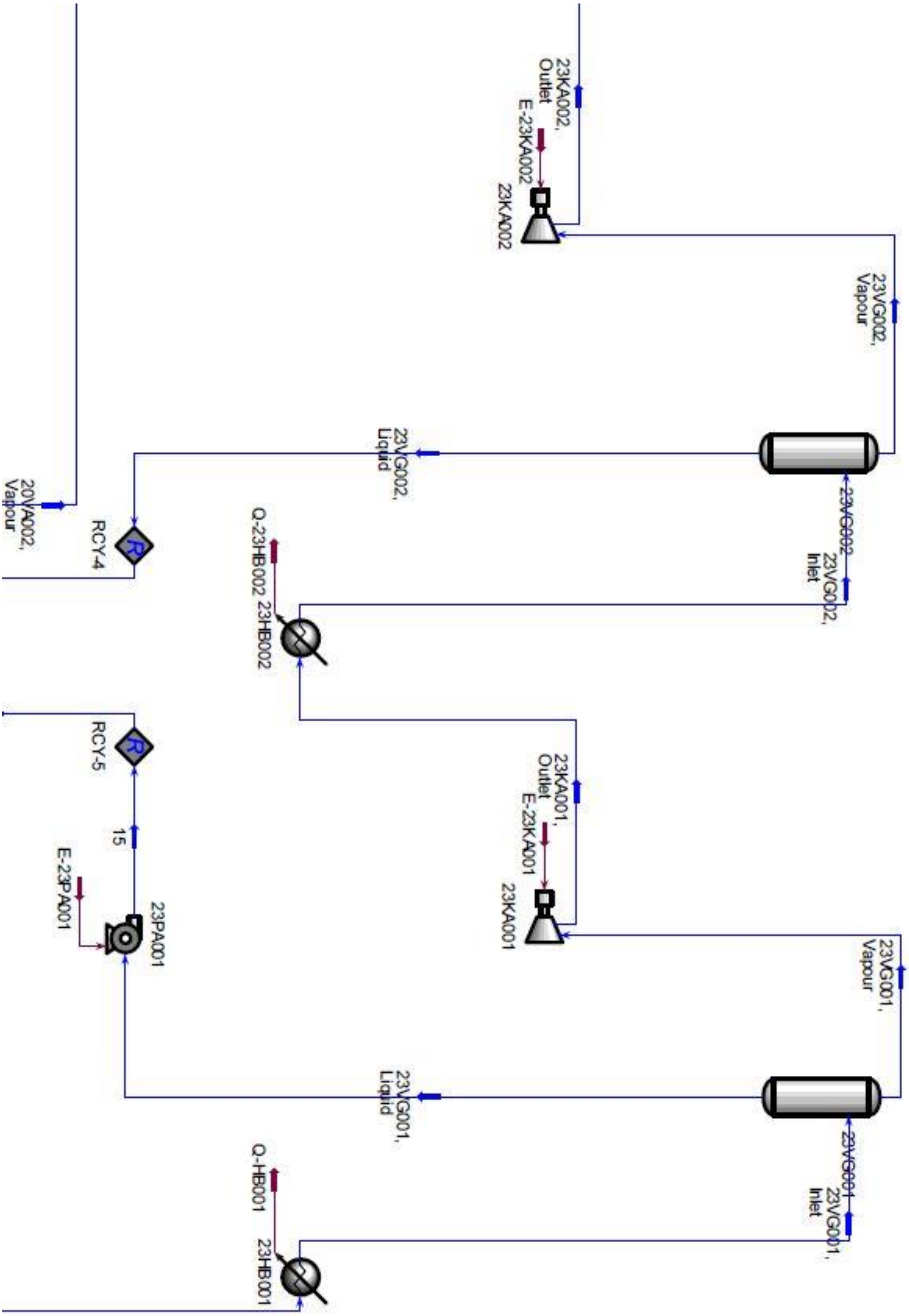
23KA002, Outlet
E-23KA002
23KA002
23VG002, Vapour
23VG002, Liquid
23VG002
23VG002, Inlet
Q-23HB002
23HB002
RCY-4
20VA002, Vapour
RCY-5
15
E-23PA001
23PA001
23KA001, Outlet
E-23KA001
23KA001
23VG001, Vapour
23VG001, Liquid
23VG001
23VG001, Inlet
Q-HB001
23HB001

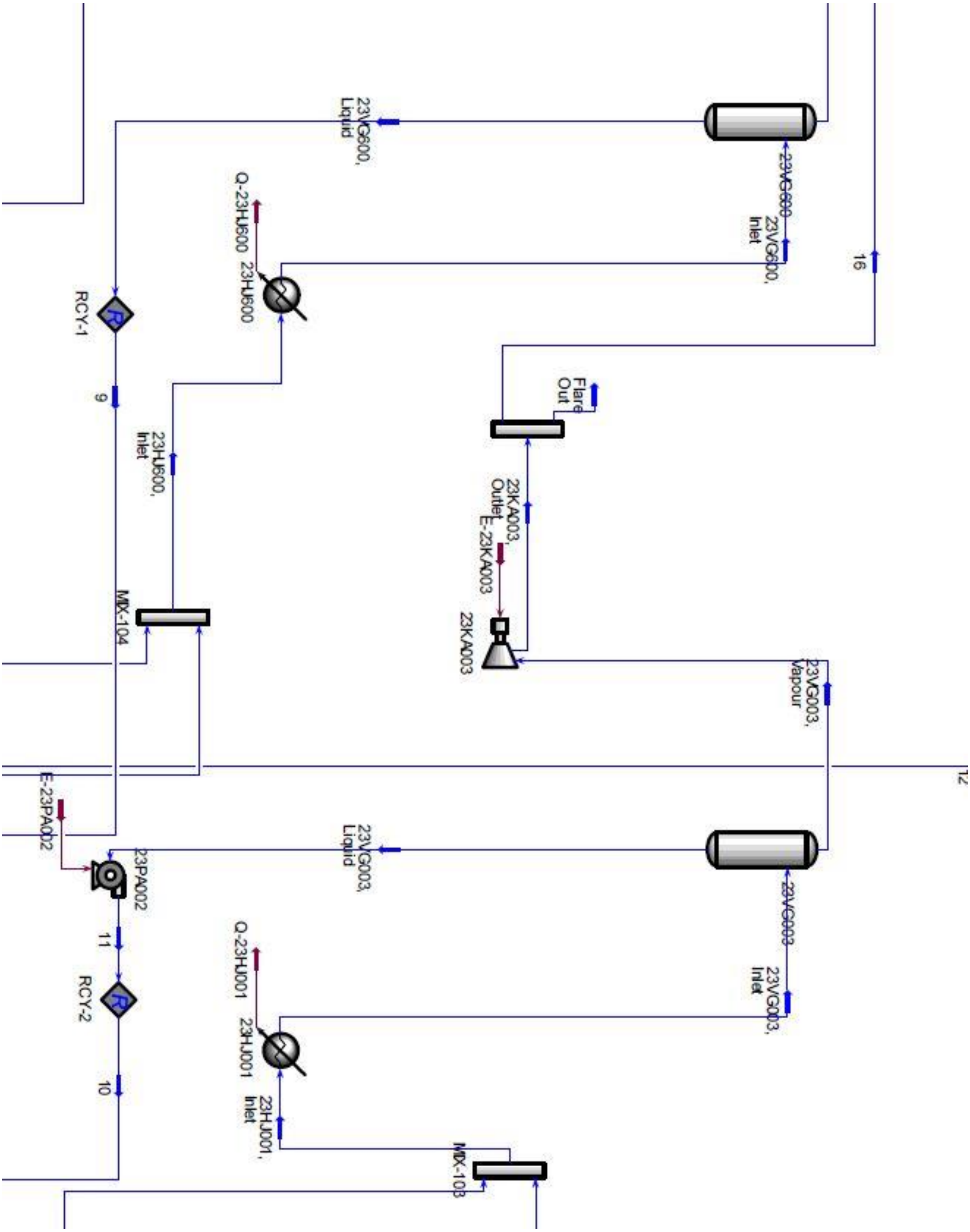
23VG600, Liquid
Q-23HJ600
23HJ600
RCY-1
9
23HJ600, Inlet
MIX-104
23VG600
23VG600, Inlet
16
Flare Out
23KA003, Outlet
E-23KA003
23KA003
23VG003, Vapour
12
E-23PA002
23PA002
23VG003, Liquid
23VG003
23VG003, Inlet
11
RCY-2
10
Q-23HJ001
23HJ001
23HJ001, Inlet
MIX-103

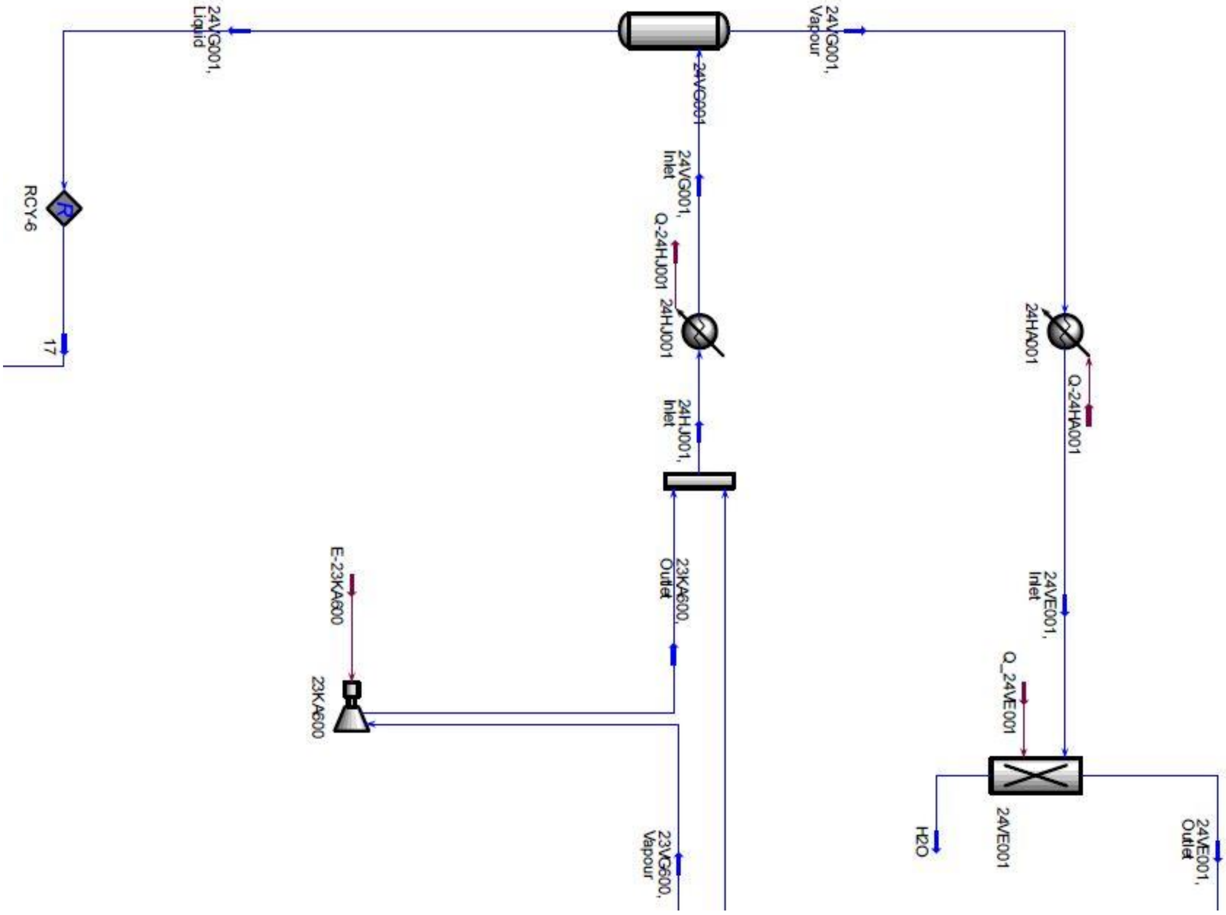
24VG001, Liquid
24VG001, Vapour
24VG001
24VG001, Inlet
Q-24HJ001
24HJ001
24HJ001, Inlet
RCY-6
17
24HA001
Q-24HA001
24VE001, Inlet
Q_24VE001
24VE001
H2O
24VE001, Outlet
23KA600, Outlet
E-23KA600
23KA600
23VG600, Vapour

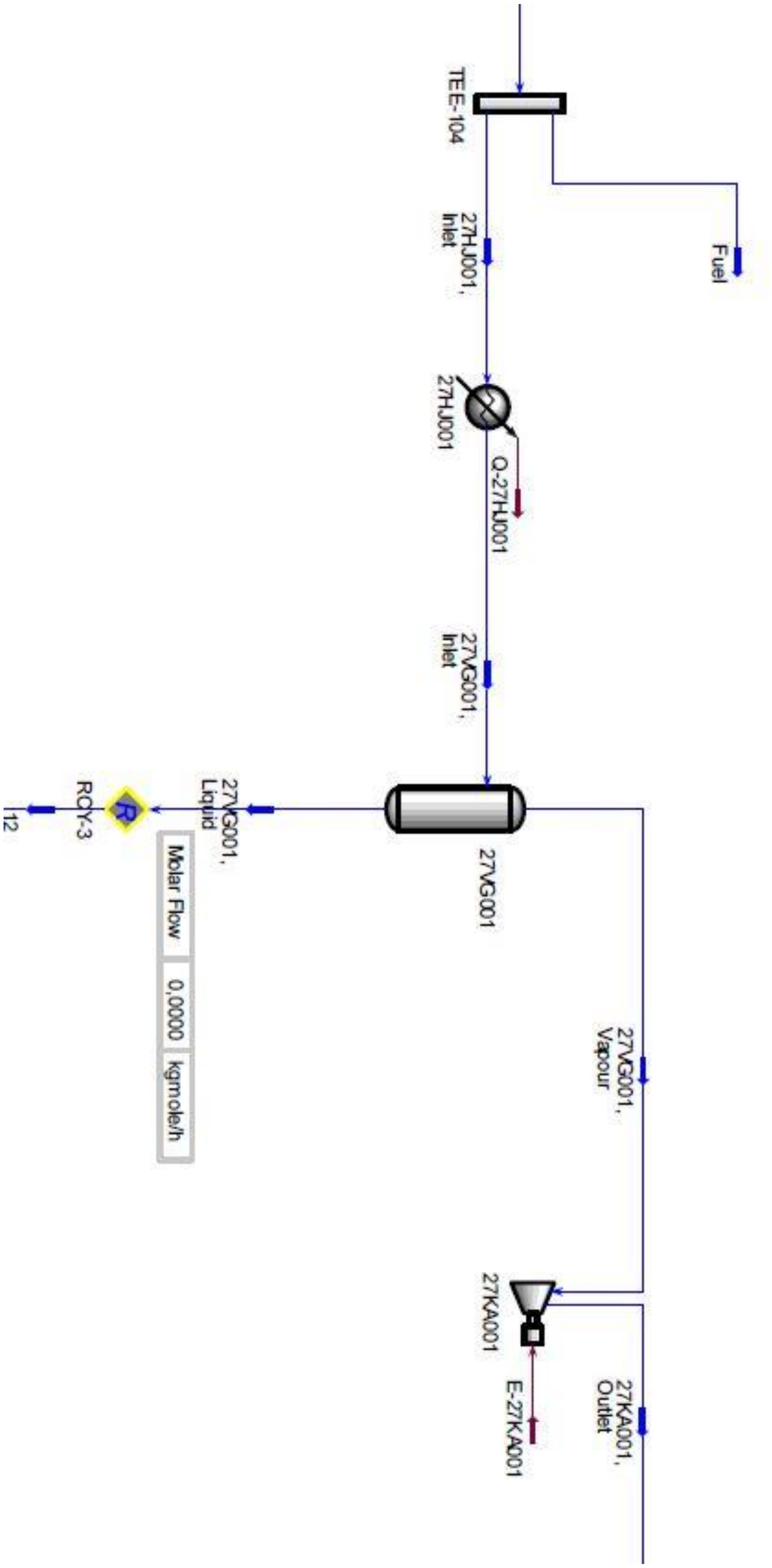
TEE-104
Fuel
27HJ001,
Inlet
27HJ001
Q-27HJ001
27VG001,
Inlet
27VG001
27VG001,
Liquid
RCY-3
12
Molar Flow
0,0000
kgmole/h
27VG001,
Vapour
27KA001
E-27KA001
27KA001,
Outlet

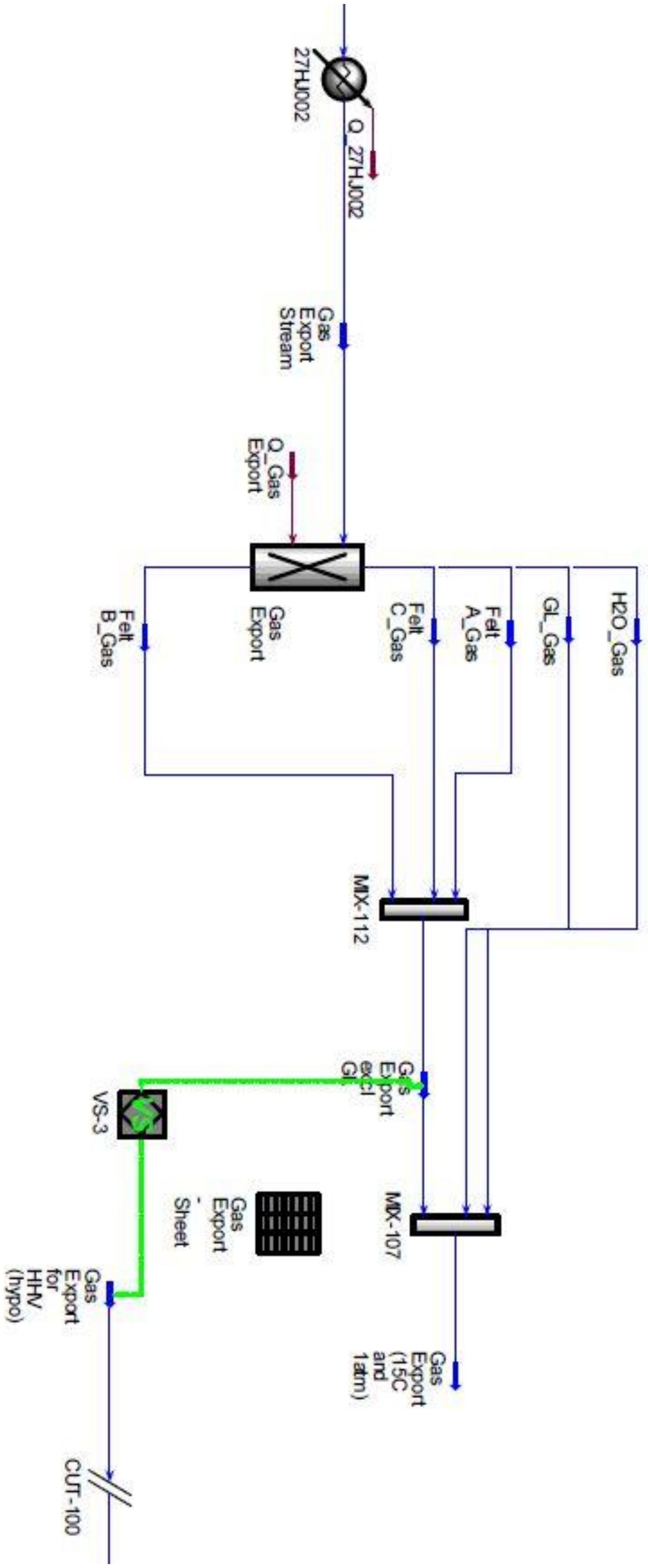
27HJ002
Q_27HJ002
Gas Export Stream
Q_Gas Export
Gas Export
Felt B_Gas
Felt C_Gas
Felt A_Gas
GL_Gas
H2O_Gas
MIX-112
Gas Export excl Gl
VS-3
Gas Export - Sheet
MIX-107
Gas Export for HHV (hypo)
Gas Export (15C and 1atm)
CUT-100

Appendix F – Process equipment input

INPUT Process Input

Unit Name	Stream Name	Temperature, °C	Pressure, bara
20VA001	20VA001, Inlet	47.26	33.74
20VA004	20VA004, Inlet	40.73	32.20
20HA101	20HA101, Outlet	79.49	-
20VA002	20VA002, Inlet	-	23.50
20VA003	20VA003, Inlet	-	2.05
21HB001	21HB001, Outlet	55.13	
23VG001	23VG001, Inlet	30.00	1.86
23KA001	23VG001, Vapour		1.77
	23KA001, Outlet	89.86	7.11
23VG002	23VG002, Inlet	30.00	6.97
23KA002	23VG002, Vapour		6.86
	23KA002, Outlet	97.84	23.57
23VG003	23VG003, Inlet	21.52	23.09
23KA003	23VG003, Vapour		22.73
	23KA003, Outlet	109.88	76.96
23VG600	23VG600, Inlet	21.65	29.50
23KA600	23VG600, Vapour		29.22
	23KA600, Outlet	98.78	75.44
24VG001	24VG001, Inlet	23.70	75.66
24VE001	24VE001, Inlet	28.32	75.19
27VG001	27VG001, Inlet	25.00	73.68
27KA001	27VG001, Vapour		73.51
	27KA001, Outlet	101.41	182.32

Appendix G – Inflow data for reallocation

INPUT Production

Felt A Day Production to Platform Vest Measured tonn/d	Felt B Day Production from MPFM to Platform Vest Measured tonn/d	Felt C Day Production from MPFM to Platform Vest Measured tonn/d
2754.24	10420.36	2578.72

In reservior input

Well Gas Lift from Platform Øst to FELT C kSm3/d (allocated)	Well Gas Lift from Platform Øst to FELT B kSm3/d (allocated)
508.8	943.6

In reservior Input

INPUT

	FELT A	FELT B	FELT C
ARRIVAL TEMP., C	75	60.23	66.8
ARRIVAL PRES., bara	48.46	49.58	44
TO INLET SEPARATOR	NO	YES	YES
TO TEST SEPARATOR	YES	NO	NO
WATER PROD., Sm3/d	2462.1	2428.1	72.6

Appendix H – ProMax model

The figures below illustrate the ProMax model.

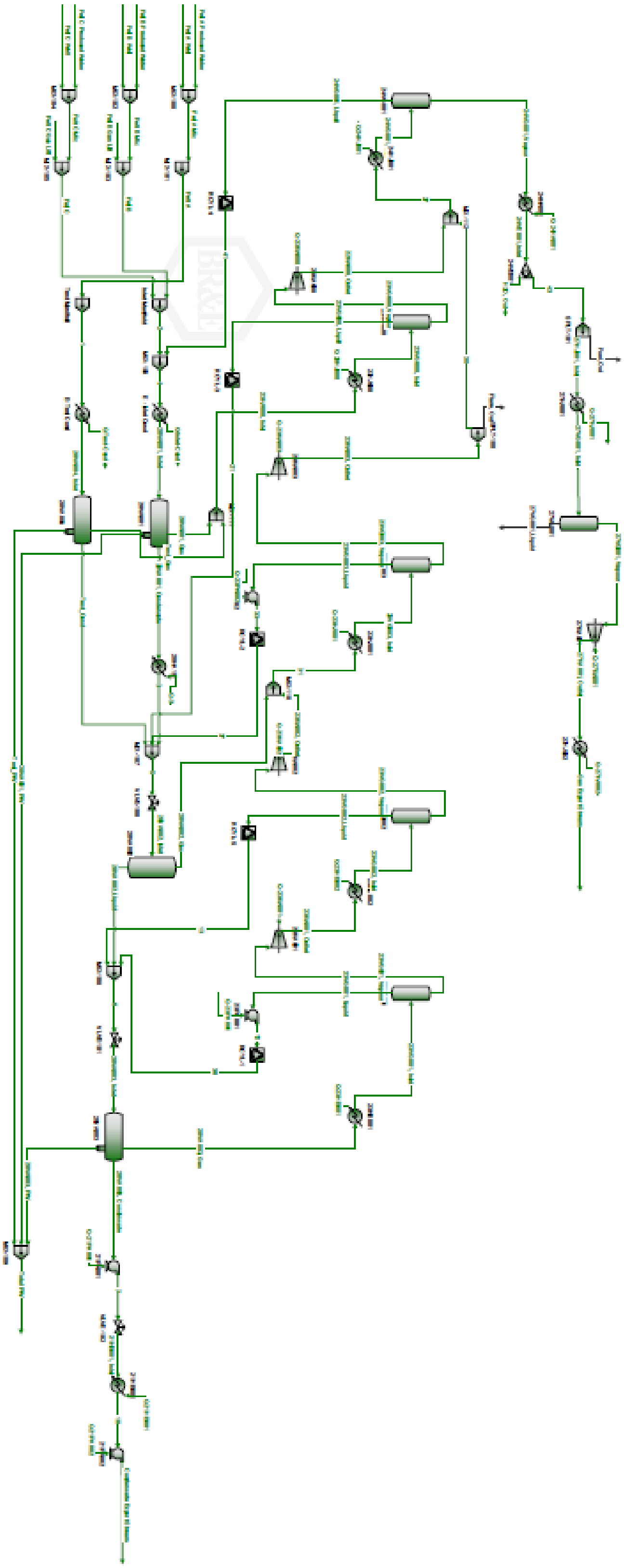

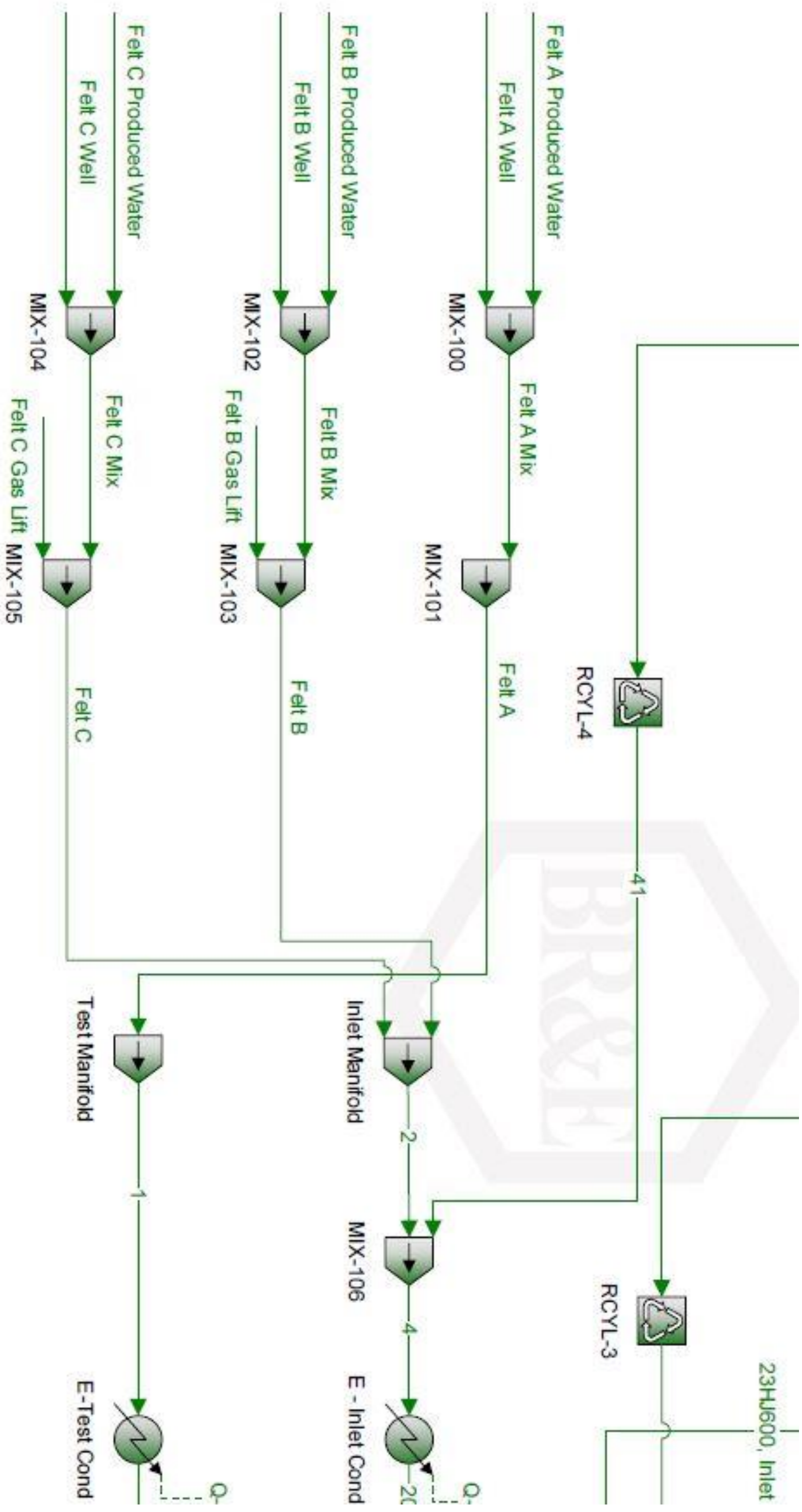
Felt A Produced Water
Felt A Well
MIX-100
Felt A Mix
MIX-101
Felt A
Felt B Produced Water
Felt B Well
MIX-102
Felt B Mix
Felt B Gas Lift
MIX-103
Felt B
Felt C Produced Water
Felt C Well
MIX-104
Felt C Mix
Felt C Gas Lift
MIX-105
Felt C
RCYL-4
41
Inlet Manifold
2
MIX-106
4
E - Inlet Cond
Test Manifold
1
E-Test Cond
RCYL-3
23HJ600, Inlet

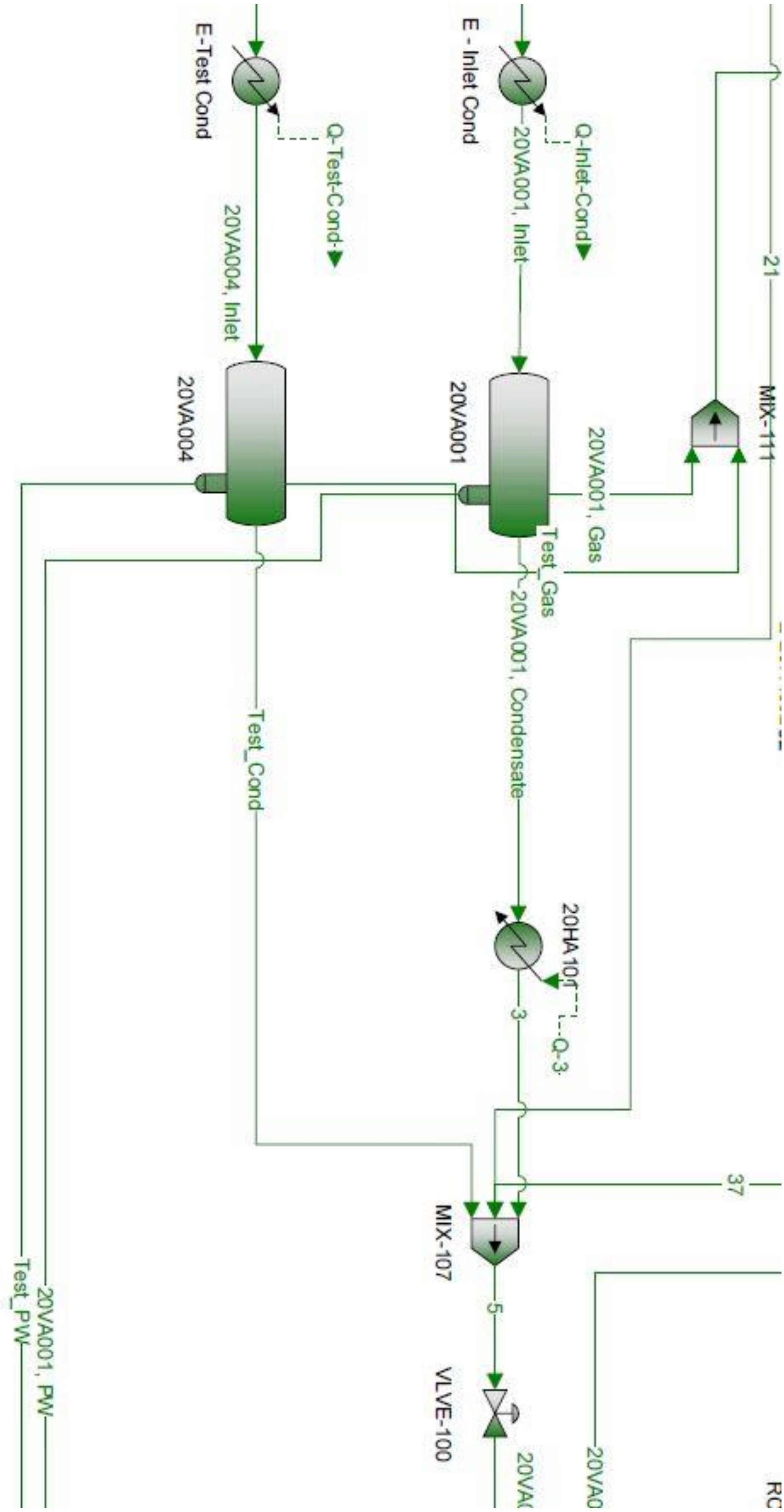
E-Test Cond
E - Inlet Cond
Q-Test-Cond-
Q-Inlet-Cond
20VA001, Inlet
20VA004, Inlet
21
MIX-111
20VA001
20VA004
20VA001, Gas
Test_Gas
20VA001, Condensate
Test_Cond
20HA 101
Q-3
3
37
MIX-107
5
VLVE-100
20VA001, PW
Test_PW

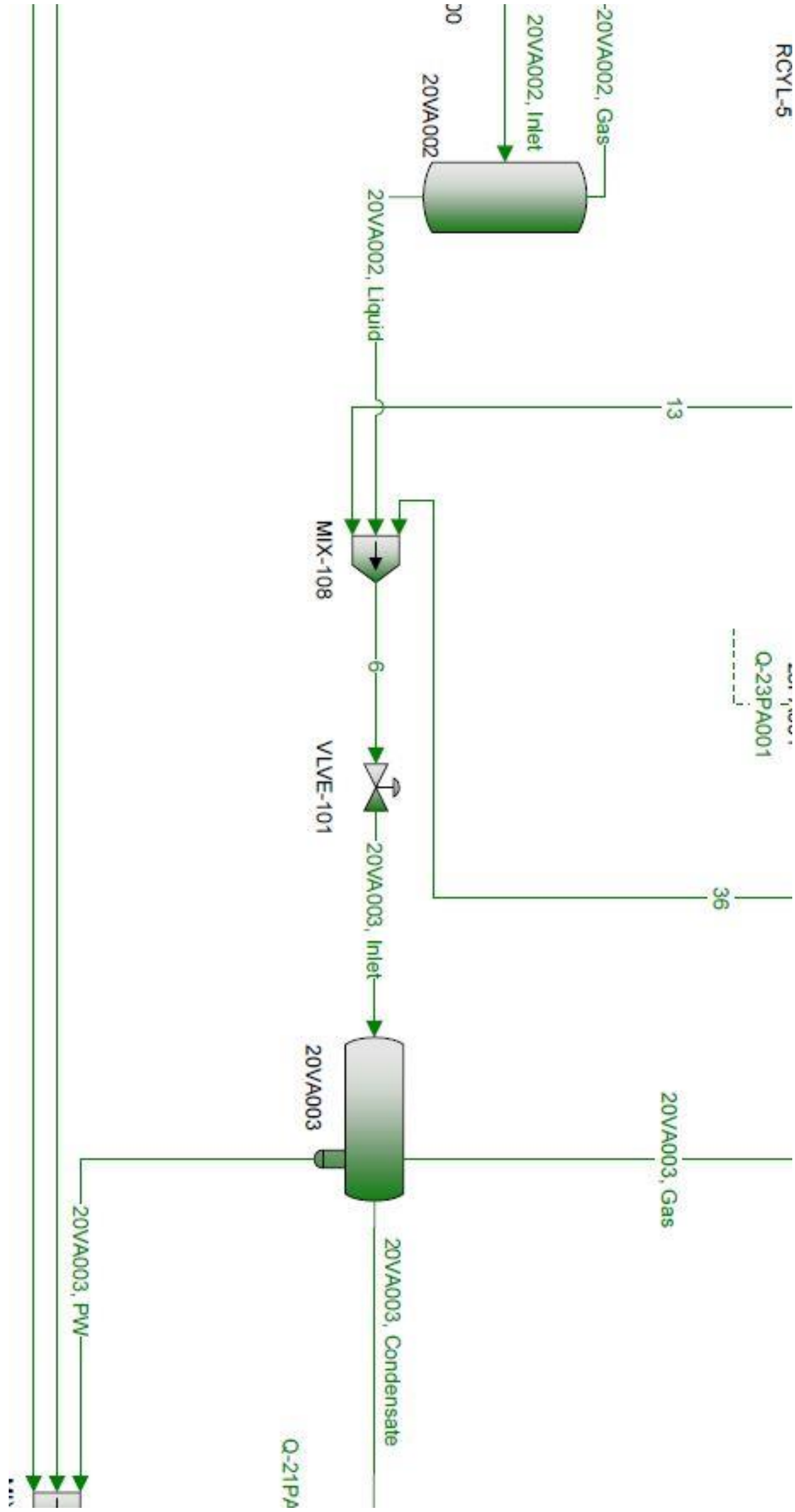
RCYL-5
20VA002, Gas
20VA002, Inlet
20VA002
20VA002, Liquid
13
MIX-108
6
Q-23PA001
VLVE-101
36
20VA003, Inlet
20VA003
20VA003, Gas
20VA003, PW
20VA003, Condensate

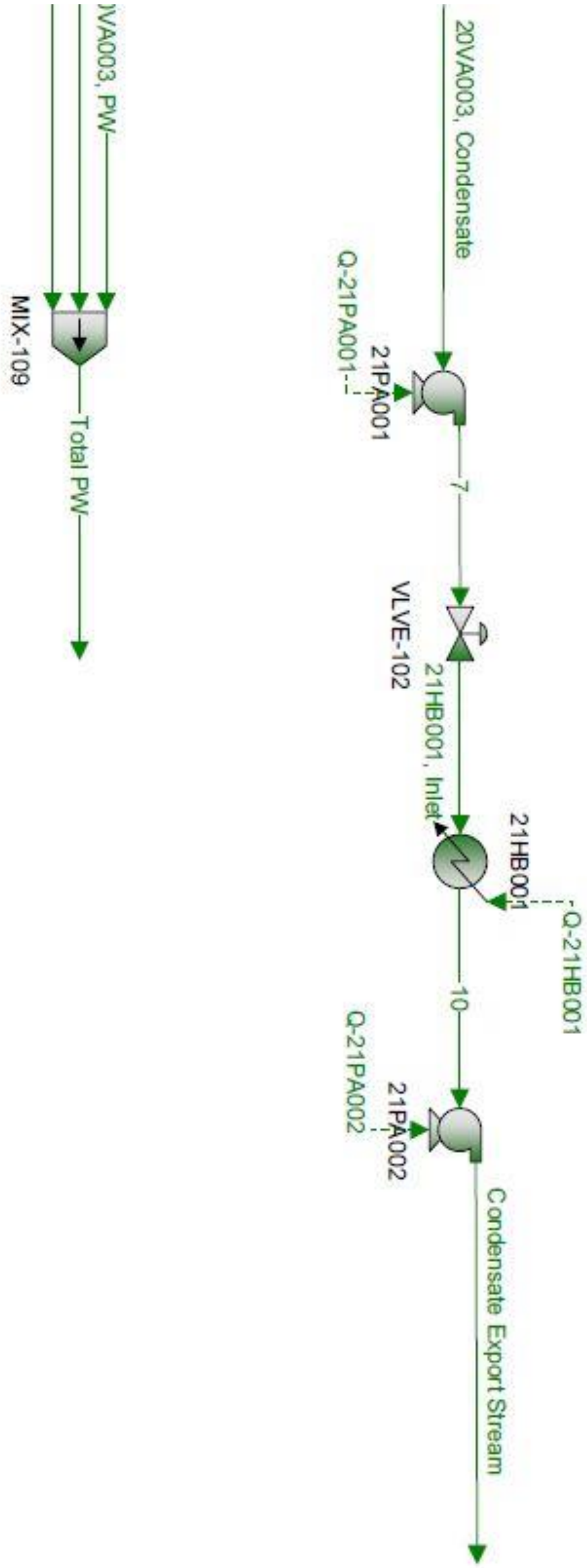
20VA003, Condensate
Q-21PA001
21PA001
7
VLVE-102
21HB001, Inlet
21HB001
Q-21HB001
10
Q-21PA002
21PA002
Condensate Export Stream
VA003, PW
MIX-109
Total PW

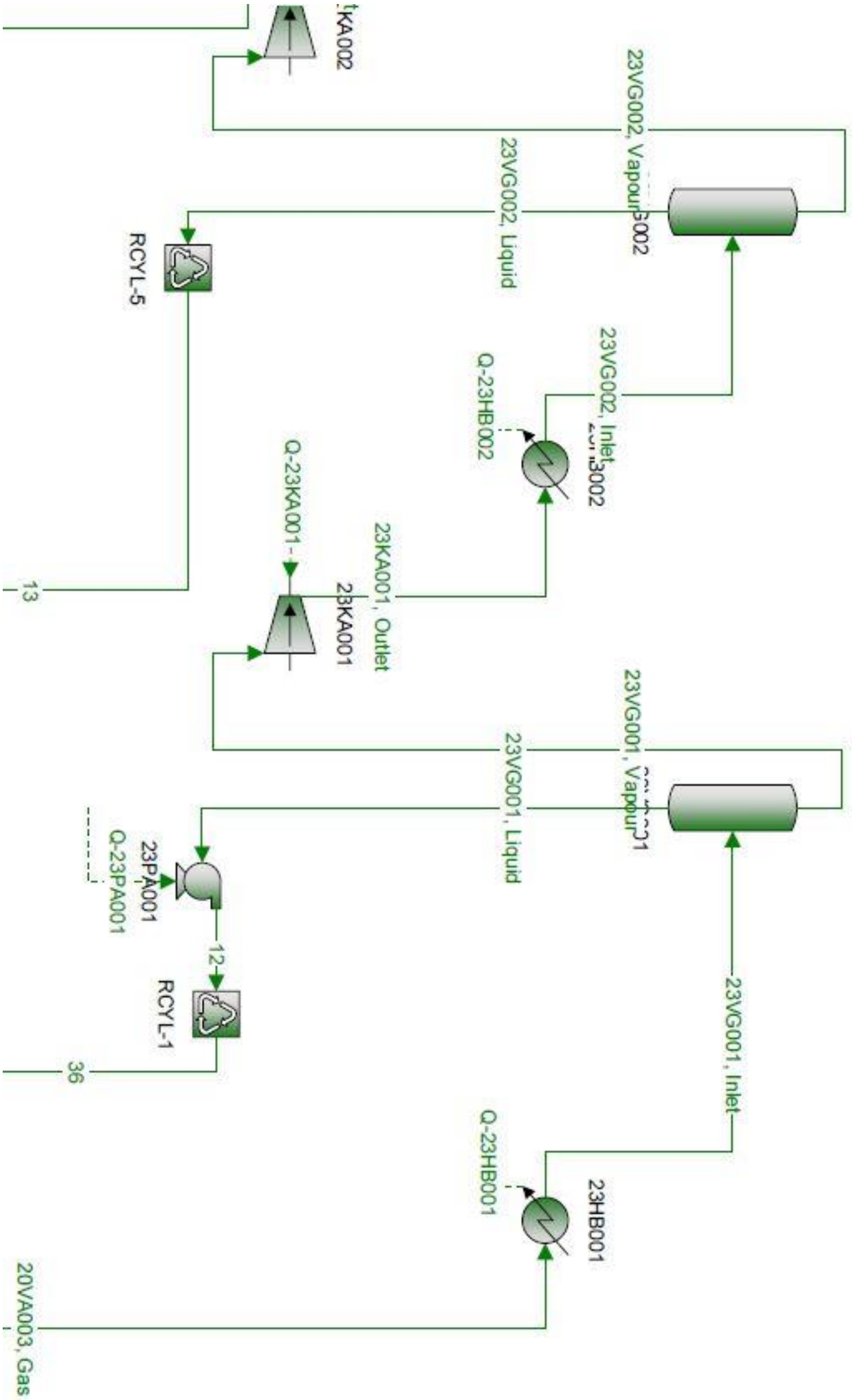
23VG002, Vapour
23VG002, Liquid
RCYL-5
23VG002, Inlet
Q-23HB002
Q-23KA001
23KA001, Outlet
23KA001
13
23VG001, Vapour
23VG001, Liquid
23PA001
Q-23PA001
12
RCYL-1
36
23VG001, Inlet
Q-23HB001
23HB001
20VA003, Gas

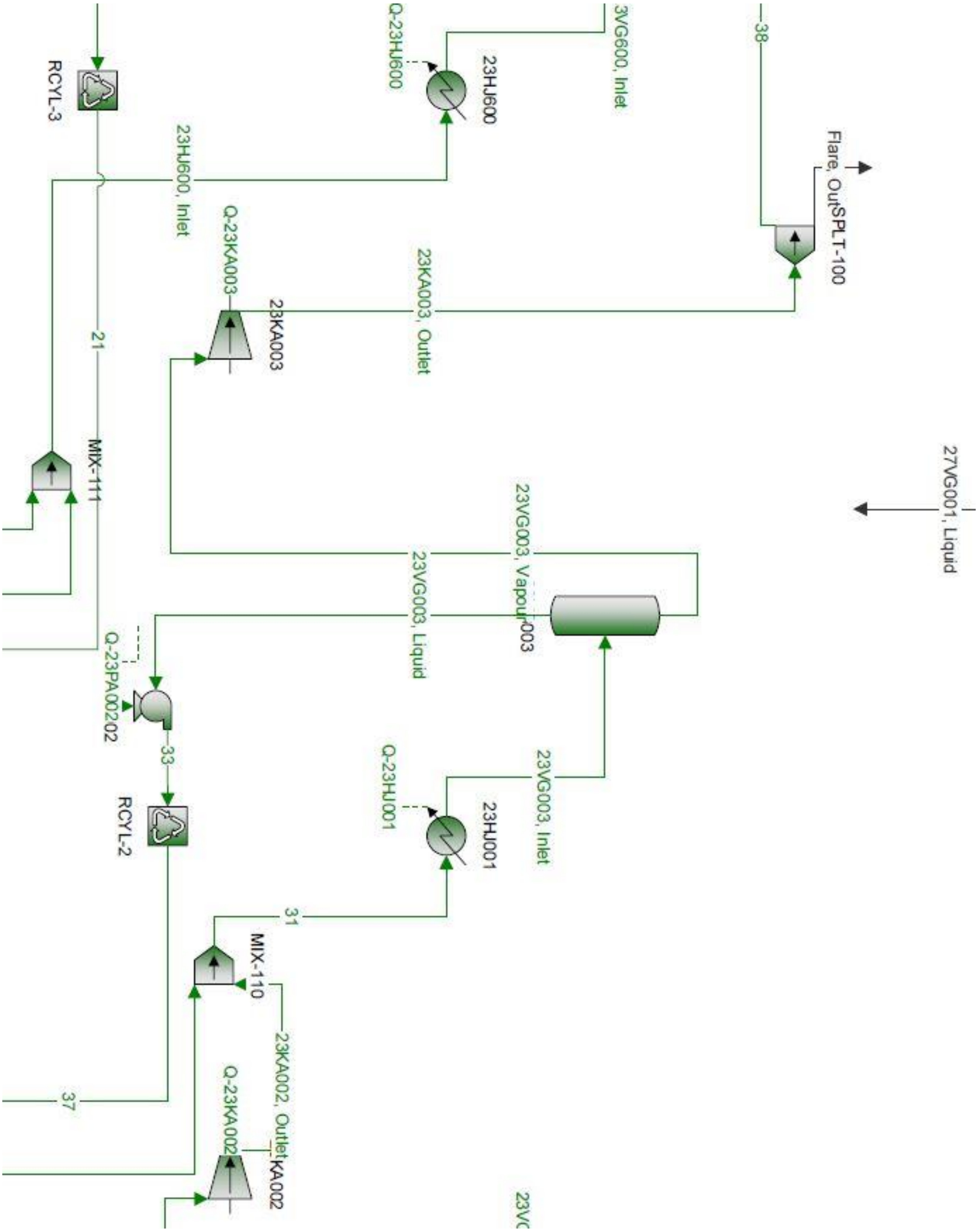

38
3VG600, Inlet
Q-23HJ600
23HJ600
RCYL-3
Flare, Out
SPLT-100
23HJ600, Inlet
Q-23KA003
23KA003
23KA003, Outlet
21
MIX-111
27VG001, Liquid
23VG003, Vapour
23VG003, Liquid
003
Q-23PA002
02
33
RCYL-2
Q-23HJ001
23VG003, Inlet
23HJ001
31
MIX-110
23KA002, Outlet
Q-23KA002
KA002
37
23VC

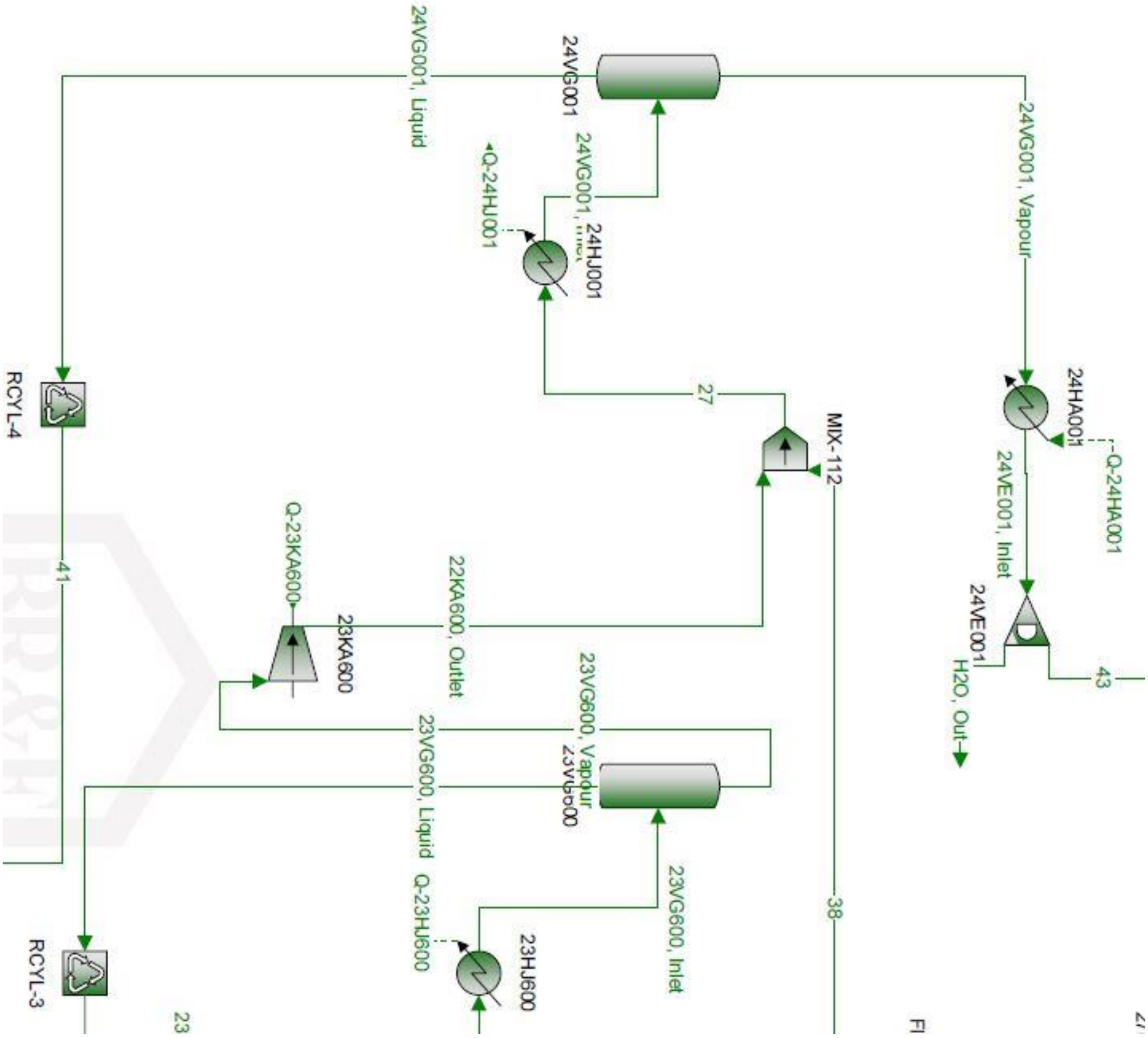
24VG001, Liquid
24VG001
24VG001, Vapour
24HA001
Q-24HA001
24VE001, Inlet
24VE001
H2O, Out
43
Q-24HJ001
24HJ001
27
MIX-112
RCYL-4
41
Q-23KA600
23KA600
22KA600, Outlet
23VG600, Vapour
23VG600, Liquid
Q-23HJ600
23HJ600
23VG600, Inlet
38
RCYL-3

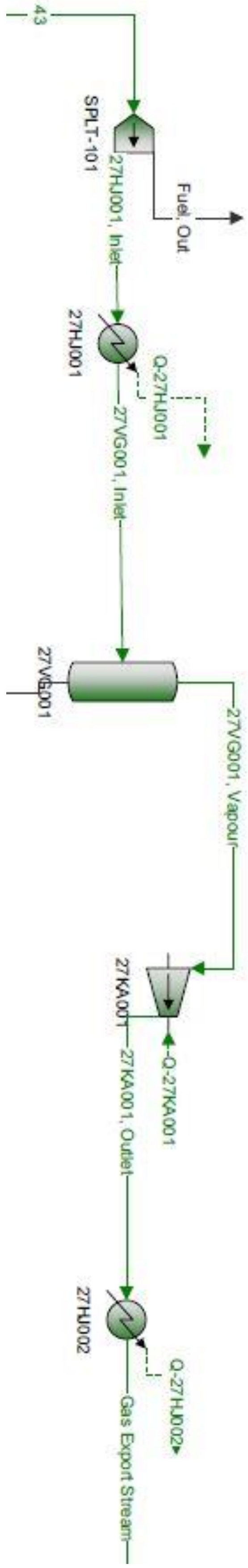
43
SPLT-101
Fuel, Out
27HJ001, Inlet
27HJ001
Q-27HJ001
27VG001, Inlet
27VG001
27VG001, Vapour
27KA001
Q-27KA001
27KA001, Outlet
27HJ002
Q-27HJ002
Gas Export Stream

Appendix I – Building the UniSim model

The procedure for building the UniSim model is as follows:

1) The EOS is set to SRK as shown in the figure below:

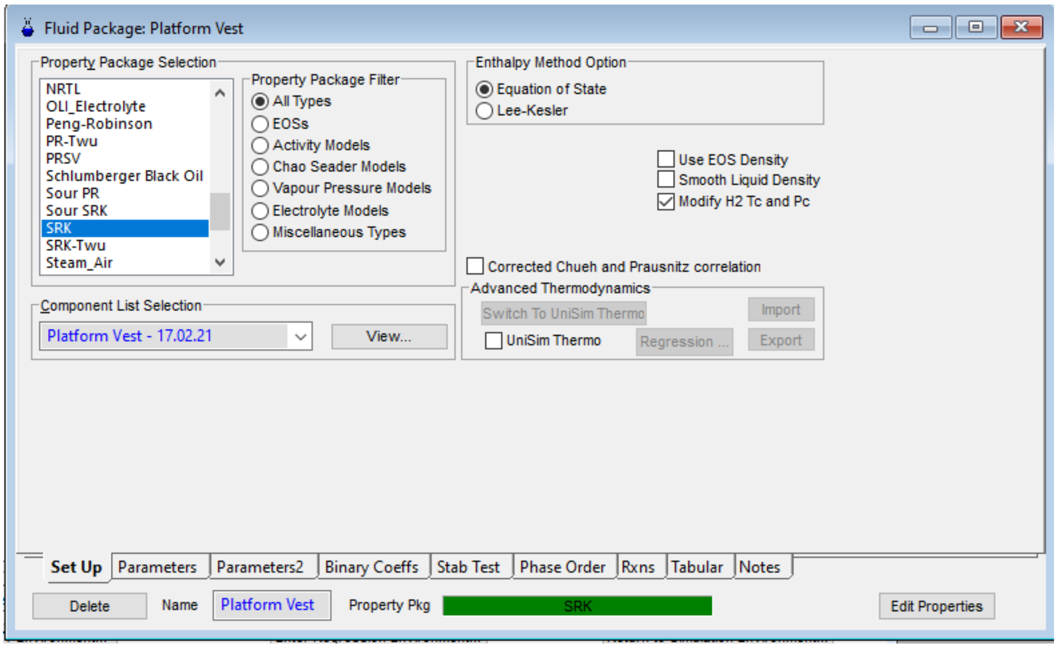

2) The component list is added and named Platform Vest as shown in the figure below:

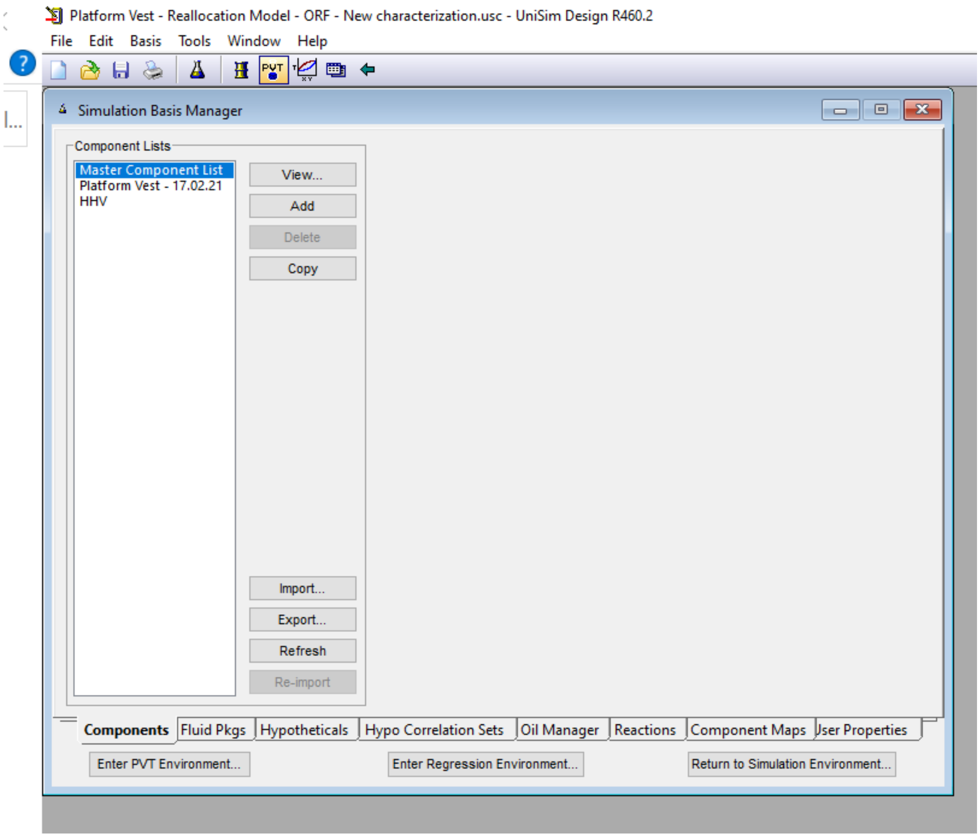

3) Hypothetical components for each field is defined as follows, with the fluid characterisation as the input.

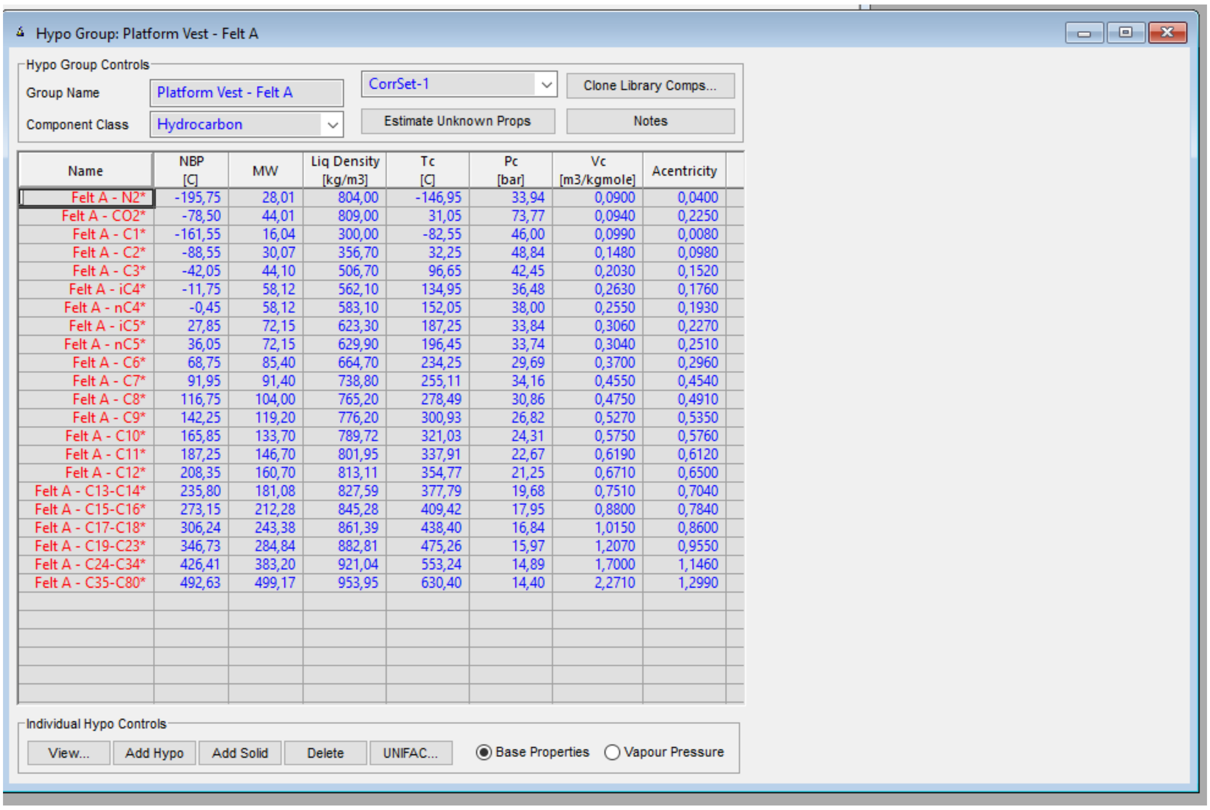

Name	NBP [C]	MW	Liq Density [kg/m3]	Tc [C]	Pc [bar]	Vc [m3/kgmole]	Acentricity
Felt A - N2*	-195,75	28,01	804,00	-146,95	33,94	0,0900	0,0400
Felt A - CO2*	-78,50	44,01	809,00	31,05	73,77	0,0940	0,2250
Felt A - C1*	-161,55	16,04	300,00	-82,55	46,00	0,0990	0,0080
Felt A - C2*	-88,55	30,07	356,70	32,25	48,84	0,1480	0,0980
Felt A - C3*	-42,05	44,10	506,70	96,65	42,45	0,2030	0,1520
Felt A - iC4*	-11,75	58,12	562,10	134,95	36,48	0,2630	0,1760
Felt A - nC4*	-0,45	58,12	583,10	152,05	38,00	0,2550	0,1930
Felt A - iC5*	27,85	72,15	623,30	187,25	33,84	0,3060	0,2270
Felt A - nC5*	36,05	72,15	629,90	196,45	33,74	0,3040	0,2510
Felt A - C6*	68,75	85,40	664,70	234,25	29,69	0,3700	0,2960
Felt A - C7*	91,95	91,40	738,80	255,11	34,16	0,4550	0,4540
Felt A - C8*	116,75	104,00	765,20	278,49	30,86	0,4750	0,4910
Felt A - C9*	142,25	119,20	776,20	300,93	26,82	0,5270	0,5350
Felt A - C10*	165,85	133,70	789,72	321,03	24,31	0,5750	0,5760
Felt A - C11*	187,25	146,70	801,95	337,91	22,67	0,6190	0,6120
Felt A - C12*	208,35	160,70	813,11	354,77	21,25	0,6710	0,6500
Felt A - C13-C14*	235,80	181,08	827,59	377,79	19,68	0,7510	0,7040
Felt A - C15-C16*	273,15	212,28	845,28	409,42	17,95	0,8800	0,7840
Felt A - C17-C18*	306,24	243,38	861,39	438,40	16,84	1,0150	0,8600
Felt A - C19-C23*	346,73	284,84	882,81	475,26	15,97	1,2070	0,9550
Felt A - C24-C34*	426,41	383,20	921,04	553,24	14,89	1,7000	1,1460
Felt A - C35-C80*	492,63	499,17	953,95	630,40	14,40	2,2710	1,2990

4) The library component of H2O is added to the component list as shown in the figure below:

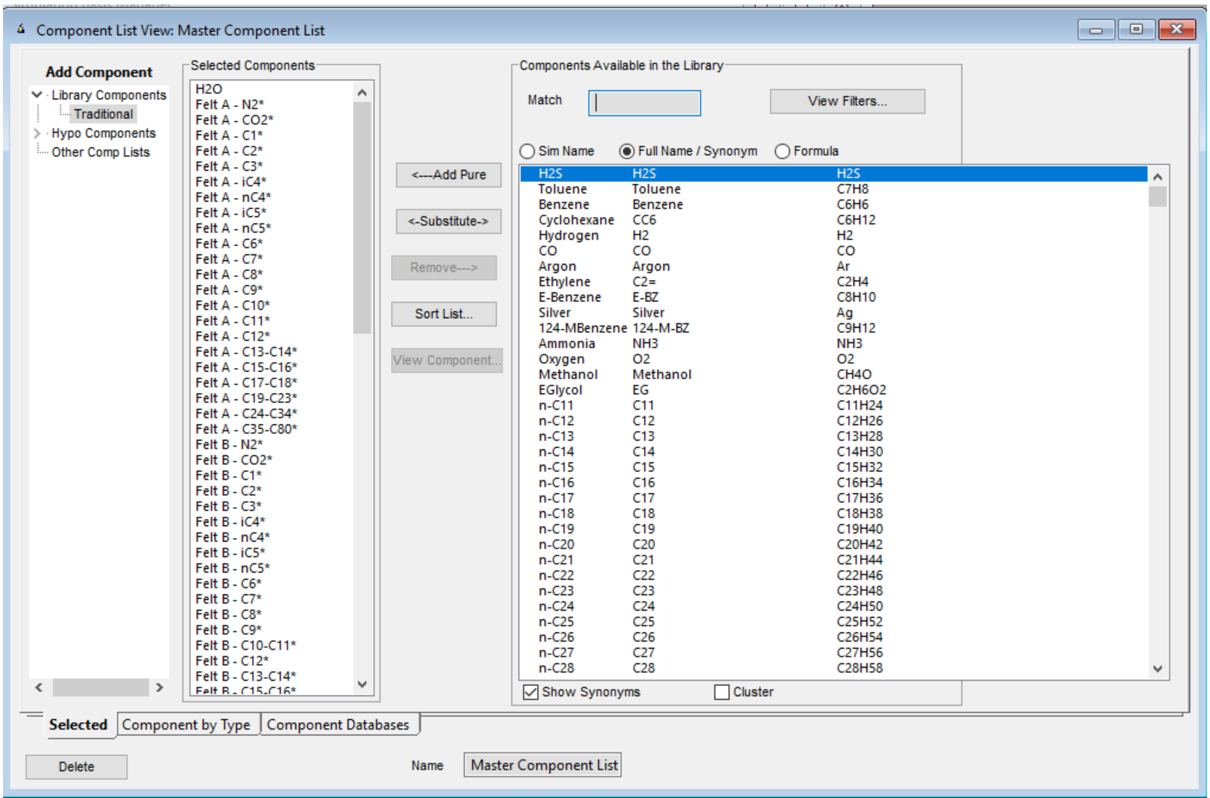

5) When the environment is defined the model can be build by using the equipment shown in the figure below:

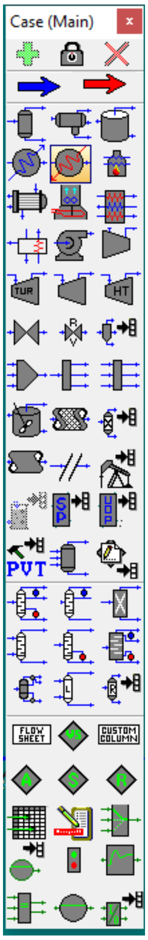

6) The final UniSim model is illustrated in Appendix E – UniSim model.
7) The following spreadsheets are created when the UniSim model is finish built.

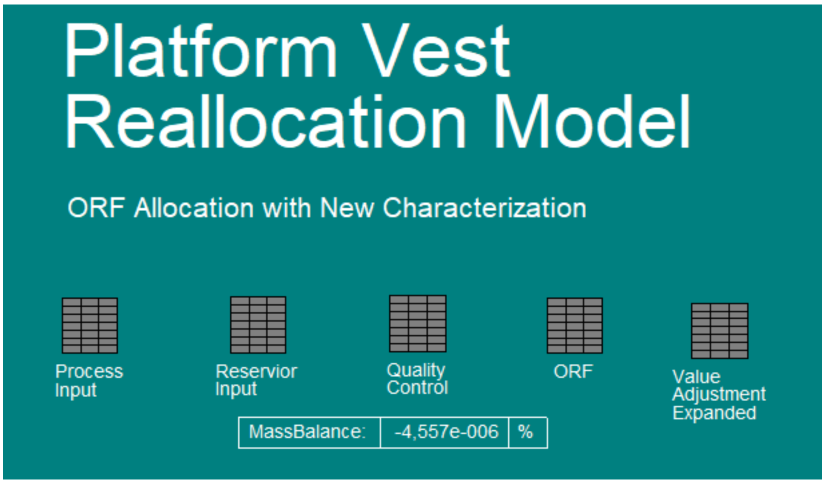

8) The process input sheet is as follows, where the values are incorporated directly into the stream.

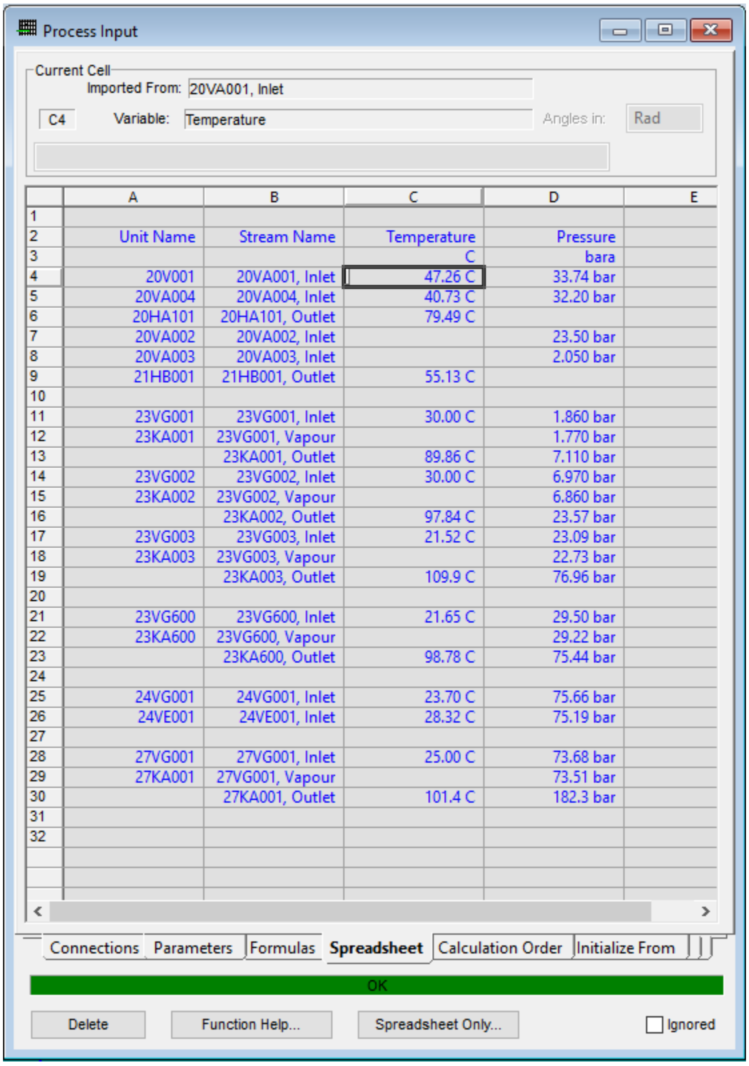

	A	B	C	D	E
1					
2	Unit Name	Stream Name	Temperature	Pressure	
3			C	bara	
4	20V001	20VA001, Inlet	47.26 C	33.74 bar	
5	20VA004	20VA004, Inlet	40.73 C	32.20 bar	
6	20HA101	20HA101, Outlet	79.49 C		
7	20VA002	20VA002, Inlet		23.50 bar	
8	20VA003	20VA003, Inlet		2.050 bar	
9	21HB001	21HB001, Outlet	55.13 C		
10					
11	23VG001	23VG001, Inlet	30.00 C	1.860 bar	
12	23KA001	23VG001, Vapour		1.770 bar	
13		23KA001, Outlet	89.86 C	7.110 bar	
14	23VG002	23VG002, Inlet	30.00 C	6.970 bar	
15	23KA002	23VG002, Vapour		6.860 bar	
16		23KA002, Outlet	97.84 C	23.57 bar	
17	23VG003	23VG003, Inlet	21.52 C	23.09 bar	
18	23KA003	23VG003, Vapour		22.73 bar	
19		23KA003, Outlet	109.9 C	76.96 bar	
20					
21	23VG600	23VG600, Inlet	21.65 C	29.50 bar	
22	23KA600	23VG600, Vapour		29.22 bar	
23		23KA600, Outlet	98.78 C	75.44 bar	
24					
25	24VG001	24VG001, Inlet	23.70 C	75.66 bar	
26	24VE001	24VE001, Inlet	28.32 C	75.19 bar	
27					
28	27VG001	27VG001, Inlet	25.00 C	73.68 bar	
29	27KA001	27VG001, Vapour		73.51 bar	
30		27KA001, Outlet	101.4 C	182.3 bar	
31					
32					

9) The reservoir input sheet is as follows, where the values are incorporated directly into the stream.

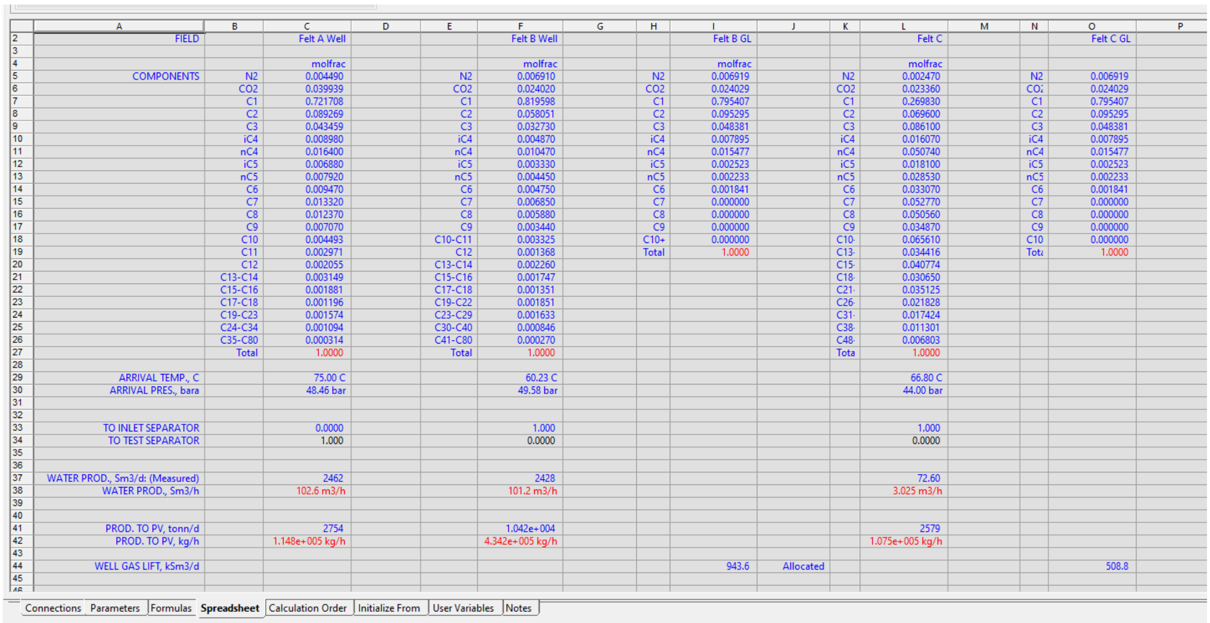

	A	B	C	D	E	F	G	H	I	J	K	L	M	N	O	P
2	FIELD		Felt A Well			Felt B Well			Felt B GL			Felt C			Felt C GL	
3																
4			molfrac			molfrac			molfrac			molfrac				
5	COMPONENTS	N2	0.004490		N2	0.006910		N2	0.006919		N2	0.002470		N2	0.006919	
6		CO2	0.039939		CO2	0.024020		CO2	0.024029		CO2	0.023360		CO:	0.024029	
7		C1	0.721708		C1	0.819598		C1	0.795407		C1	0.269830		C1	0.795407	
8		C2	0.089269		C2	0.058051		C2	0.095295		C2	0.069600		C2	0.095295	
9		C3	0.043459		C3	0.032730		C3	0.048381		C3	0.086100		C3	0.048381	
10		iC4	0.008980		iC4	0.004870		iC4	0.007895		iC4	0.016070		iC4	0.007895	
11		nC4	0.016400		nC4	0.010470		nC4	0.015477		nC4	0.050740		nC4	0.015477	
12		iC5	0.006880		iC5	0.003330		iC5	0.002523		iC5	0.018100		iC5	0.002523	
13		nC5	0.007920		nC5	0.004450		nC5	0.002233		nC5	0.028530		nC5	0.002233	
14		C6	0.009470		C6	0.004750		C6	0.001841		C6	0.033070		C6	0.001841	
15		C7	0.013320		C7	0.006850		C7	0.000000		C7	0.052770		C7	0.000000	
16		C8	0.012370		C8	0.005880		C8	0.000000		C8	0.050560		C8	0.000000	
17		C9	0.007070		C9	0.003440		C9	0.000000		C9	0.034870		C9	0.000000	
18		C10	0.004493		C10-C11	0.003325		C10+	0.000000		C10-	0.065610		C10	0.000000	
19		C11	0.002971		C12	0.001368		Total	1.0000		C13-	0.034416		Tot:	1.0000	
20		C12	0.002055		C13-C14	0.002260					C15-	0.040774				
21		C13-C14	0.003149		C15-C16	0.001747					C18-	0.030650				
22		C15-C16	0.001881		C17-C18	0.001351					C21-	0.035125				
23		C17-C18	0.001196		C19-C22	0.001851					C26-	0.021828				
24		C19-C23	0.001574		C23-C29	0.001633					C31-	0.017424				
25		C24-C34	0.001094		C30-C40	0.000846					C38-	0.011301				
26		C35-C80	0.000314		C41-C80	0.000270					C48-	0.006803				
27		Total	1.0000		Total	1.0000					Tota	1.0000				
28																
29	ARRIVAL TEMP., C		75.00 C			60.23 C						66.80 C				
30	ARRIVAL PRES., bara		48.46 bar			49.58 bar						44.00 bar				
31																
32																
33	TO INLET SEPARATOR		0.0000			1.000						1.000				
34	TO TEST SEPARATOR		1.000			0.0000						0.0000				
35																
36																
37	WATER PROD., Sm3/d: (Measured)		2462			2428						72.60				
38	WATER PROD., Sm3/h		102.6 m3/h			101.2 m3/h						3.025 m3/h				
39																
40																
41	PROD. TO PV, tonn/d		2754			1.042e+004						2579				
42	PROD. TO PV, kg/h		1.148e+005 kg/h			4.342e+005 kg/h						1.075e+005 kg/h				
43																
44	WELL GAS LIFT, kSm3/d								943.6	Allocated					508.8	
45																

10) The quality control sheet is as follows, where the simulated values are compared to the measured values. As well as a mass balance over the total process.

PRODUCTION				
	Simulated Produced Gas	Simulated Produced Gas	Measured Gas Production	Dev. %
	Sm3/h	MSm3/d	MSm3/d	%
Felt A	8.803e+004 STD_m3/h	2.113 STD_m3/h		
Felt B	4.002e+005 STD_m3/h	9.606 STD_m3/h		
Felt C	1.270e+004 STD_m3/h	0.3047 STD_m3/h		
Total production	5.010e+005 STD_m3/h	12.02 STD_m3/h	11.61	3.44 %
	Simulated Prod. Condensate	Simulated Prod. Condensate	Measured Oil Production	Dev. %
	Sm3/h	Sm3/d	Sm3/d	%
Felt A	47.07 m3/h	1130 m3/h		
Felt B	131.1 m3/h	3147 m3/h		
Felt C	106.6 m3/h	2557 m3/h		
Total production	284.7 m3/h	6834 m3/h	5641	17.45 %
MASS BALANCE				
Feed rate		Product rate		
	kmole/h		kg/h	
Felt A	9818 kgmole/h	Gas Export	2.372e+004 kgmole/h	
Felt B	2.503e+004 kgmole/h	Condensate Export	1547 kgmole/h	
Felt C	2061 kgmole/h	Fuel	0.0000 kgmole/h	
		Flare	0.0000 kgmole/h	
		H2O	12.80 kgmole/h	
		Produced Water	1.163e+004 kgmole/h	
Feed rate total	3.691e+004 kgmole/h	Product rate	3.691e+004 kgmole/h	
Imbalance	-0.00 %			

11) The ORF sheet is as follows, where the ORFs are calculated directly into the sheet. (Only A and B in the figure to save space)

	A	B	C	D	E	F	G	H	I	J	K
1											
2	OIL RECOVERY FACTOR, ORF		Felt A Feed	Felt A Cond	Felt A ORF			Felt B Feed	Felt B Cond	Felt B ORF	
3			kg/h	kg/h	%			kg/h	kg/h	%	
4		N2	507.99 kg/h	4.8518e-003 kg/h	9.551e-004		N2	3420.9 kg/h	2.0946e-002 kg/h	6.123e-004	
5		CO2	7099.0 kg/h	10.498 kg/h	0.1479		CO2	18681 kg/h	18.241 kg/h	9.764e-002	
6		C1	46762 kg/h	8.3600 kg/h	1.788e-002		C1	2.3236e+005 kg/h	26.964 kg/h	0.0116	
7		C2	10841 kg/h	75.303 kg/h	0.6946		C2	30848 kg/h	139.75 kg/h	0.4530	
8		C3	7739.9 kg/h	546.54 kg/h	7.061		C3	25506 kg/h	1199.5 kg/h	4.703	
9		iC4	2108.0 kg/h	474.32 kg/h	22.50		iC4	5002.3 kg/h	777.22 kg/h	15.54	
10		nC4	3849.8 kg/h	1219.3 kg/h	31.67		nC4	10754 kg/h	2432.5 kg/h	22.62	
11		iC5	2004.8 kg/h	1108.9 kg/h	55.31		iC5	4245.9 kg/h	1822.8 kg/h	42.93	
12		nC5	2307.8 kg/h	1425.5 kg/h	61.77		nC5	5674.0 kg/h	2799.2 kg/h	49.33	
13		C6	3266.2 kg/h	2702.7 kg/h	82.75		C6	7118.3 kg/h	5239.6 kg/h	73.61	
14		C7	4916.8 kg/h	4624.8 kg/h	94.06		C7	11016 kg/h	9914.0 kg/h	90.00	
15		C8	5195.6 kg/h	5100.4 kg/h	98.17		C8	10869 kg/h	10539 kg/h	96.96	
16		C9	3403.5 kg/h	3390.7 kg/h	99.62		C9	7307.2 kg/h	7260.3 kg/h	99.36	
17		C10+	14748 kg/h	14746 kg/h	99.99		C10+	61359 kg/h	61353 kg/h	99.99	
18		C10	2426.0 kg/h	2424.3 kg/h			C10-C11	8230.5 kg/h	8224.9 kg/h		
19		C11	1760.4 kg/h	1760.1 kg/h			C12	3891.5 kg/h	3891.2 kg/h		
20		C12	1333.5 kg/h	1333.5 kg/h			C13-C14	7269.4 kg/h	7269.3 kg/h		
21		C13-C14	2303.2 kg/h	2303.2 kg/h			C15-C16	6591.4 kg/h	6591.4 kg/h		
22		C15-C16	1612.4 kg/h	1612.4 kg/h			C17-C18	5813.3 kg/h	5813.3 kg/h		
23		C17-C18	1175.1 kg/h	1175.1 kg/h			C19-C22	9201.4 kg/h	9201.4 kg/h		
24		C19-C23	1810.9 kg/h	1810.9 kg/h			C23-C29	10170 kg/h	10170 kg/h		
25		C24-C34	1692.7 kg/h	1692.7 kg/h			C30-C40	7005.1 kg/h	7005.1 kg/h		
26		C35-C80	633.48 kg/h	633.48 kg/h			C41-C80	3186.8 kg/h	3186.8 kg/h		
27											
28		C6+	31530 kg/h	30564 kg/h	96.94	%C6+ in Cond.	C6+	97669 kg/h	94305 kg/h	96.56	%C6+ in Cond.
29		TOT	1.1475e+005 kg/h	35433 kg/h			TOT	4.3417e+005 kg/h	1.0352e+005 kg/h		
30											
31		C6+ fraction		0.8626			C6+ fraction		0.9110		
32		C10+ fraction		0.4162			C10+ fraction		0.5927		
33											

12) The value adjustment sheet is as follows, where the value in NOK/year is calculated directly into the sheet. (only C included in the figure to save space).

N	O	P	Q	R	S	T	U
Felt C						Dollar Price (04.	8.490
	Felt C - iC5*	558.58 kg/h	Naphtha	Tonn/y	Price (USD/y)	Naphtha price (	588.2
	Felt C - nC5*	1009.3 kg/h	17180 kg/h	1.5050e+005 kg/h	8.852e+007	Kerosene price (	455.4
	Felt C - C6*	2053.9 kg/h	Kerosene			Gas oil price (04	537.9
	Felt C - C7*	4295.1 kg/h	15779 kg/h	1.3822e+005 kg/h	6.295e+007	Residue	264.1
	Felt C - C8*	5120.6 kg/h	Gasoil				
	Felt C - C9*	4142.5 kg/h	27943 kg/h	2.4478e+005 kg/h	1.317e+008		
	Felt C - C10-C12*	9548.4 kg/h	Residue				
	Felt C - C13-C14*	6230.2 kg/h	28276 kg/h	2.4770e+005 kg/h	6.541e+007		
	Felt C - C15-C17*	8942.8 kg/h					
	Felt C - C18-C20*	7988.1 kg/h	89178 kg/h				
	Felt C - C21-C25*	11012 kg/h		Total USD/y	3.485e+008		
	Felt C - C26-C30*	8354.6 kg/h		Total MNOK/y	2959		
	Felt C - C31-C37*	8082.1 kg/h					
	Felt C - C38-C47*	6516.1 kg/h					
	Felt C - C48-C80*	5323.2 kg/h					
	Sum	89178 kg/h					

Appendix J – Utility method in UniSim

The utility method is as follows:

1) Add a utility called allocation utility to either the condensate export stream or the gas export stream.
2) In the utility the feed stream is selected as follows:

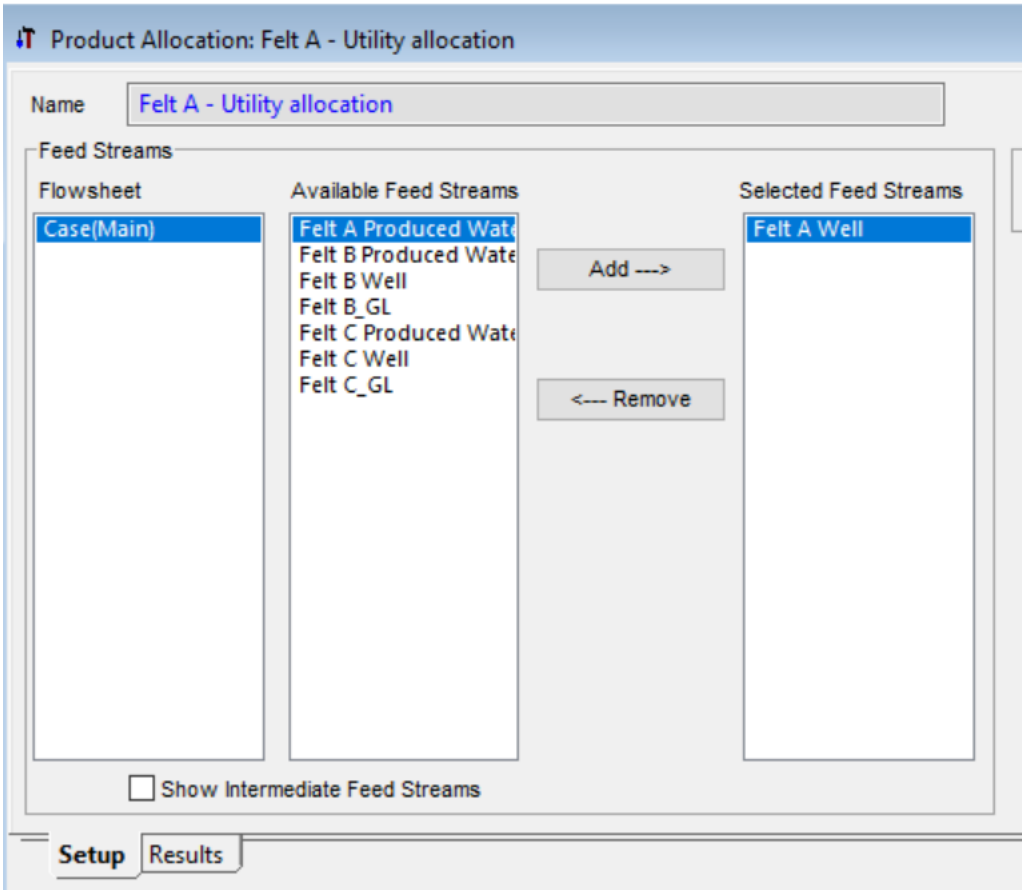

3) In the figure above the A field well is selected as the feed stream.
4) In the result tab the product stream is selected, as follows:

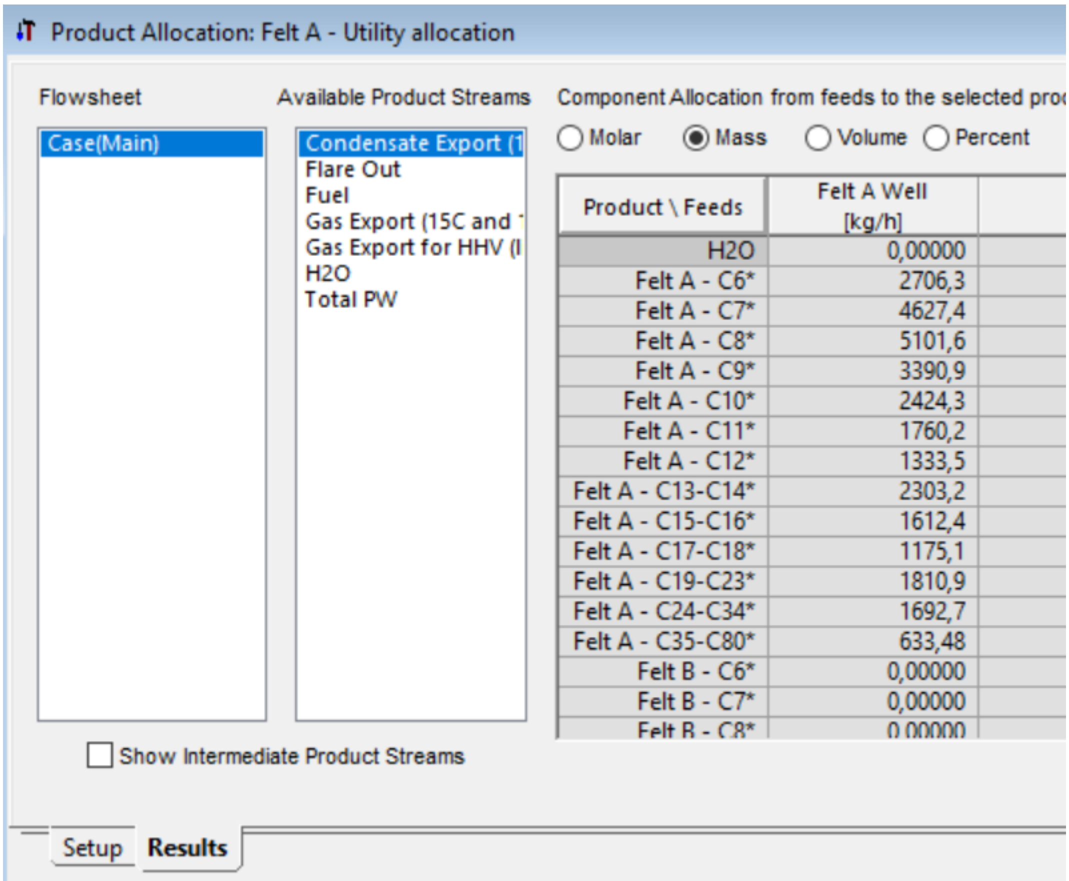

5) The utility will track the components from the selected feed stream to the selected product stream. The results is available in molar, mass or volume flow.

Appendix K – C20+ fluid characterisation

The C20+ fluid characterisation for field A, B and C is shown in the tables below:

Field A - C20+ characterisation								
Component	Molfrac	NBP	MW	Liq Den	T_c	P_c	V_c	Accentricity
	-	C	g/mol	kg/m3	C	bara	m3/kmol	-
Felt A - N2*	0.004	-195.750	28.014	804.000	-146.950	33.944	0.090	0.040
Felt A - CO2*	0.040	-78.500	44.010	809.000	31.050	73.765	0.094	0.225
Felt A - C1*	0.722	-161.550	16.043	300.000	-82.550	46.002	0.099	0.008
Felt A - C2*	0.089	-88.550	30.070	356.700	32.250	48.839	0.148	0.098
Felt A - C3*	0.043	-42.050	44.097	506.700	96.650	42.455	0.203	0.152
Felt A - iC4*	0.009	-11.750	58.124	562.100	134.950	36.477	0.263	0.176
Felt A - nC4*	0.016	-0.450	58.124	583.100	152.050	37.997	0.255	0.193
Felt A - iC5*	0.007	27.850	72.151	623.300	187.250	33.843	0.306	0.227
Felt A - nC5*	0.008	36.050	72.151	629.900	196.450	33.741	0.304	0.251
Felt A - C6*	0.009	68.750	85.400	664.700	234.250	29.688	0.370	0.296
Felt A - C7*	0.013	91.950	91.400	738.800	255.105	34.156	0.455	0.454
Felt A - C8*	0.012	116.750	104.000	765.200	278.491	30.856	0.475	0.491
Felt A - C9*	0.007	142.250	119.200	776.200	300.934	26.823	0.527	0.535
Felt A - C10*	0.004	165.850	133.704	789.718	321.034	24.312	0.575	0.576
Felt A - C11*	0.003	187.250	146.704	801.947	337.909	22.673	0.619	0.612
Felt A - C12*	0.002	208.350	160.704	813.112	354.775	21.246	0.671	0.650
Felt A - C13-C14*	0.003	235.802	181.082	827.590	377.793	19.676	0.751	0.704
Felt A - C15-C16*	0.002	273.146	212.279	845.276	409.423	17.949	0.880	0.784
Felt A - C17-C19*	0.002	311.677	248.729	864.485	443.421	16.705	1.039	0.873
Felt A - C20+*	0.003	411.882	358.140	913.705	540.935	15.141	1.635	1.110

Field B - C20+ characterisation								
Component	Molfrac	NBP	MW	Liq Den	T_c	P_c	V_c	Accentricity
	-	C	g/mol	kg/m3	C	bara	m3/kmol	-
Felt B - N2*	0.007	-195.750	28.014	804.000	-146.950	33.944	0.090	0.040
Felt B - CO2*	0.024	-78.500	44.010	809.000	31.050	73.765	0.094	0.225
Felt B - C1*	0.820	-161.550	16.043	300.000	-82.550	46.002	0.099	0.008
Felt B - C2*	0.058	-88.550	30.070	356.700	32.250	48.839	0.148	0.098
Felt B - C3*	0.033	-42.050	44.097	506.700	96.650	42.455	0.203	0.152
Felt B - iC4*	0.005	-11.750	58.124	562.100	134.950	36.477	0.263	0.176
Felt B - nC4*	0.010	-0.450	58.124	583.100	152.050	37.997	0.255	0.193
Felt B - iC5*	0.003	27.850	72.151	623.300	187.250	33.843	0.306	0.227
Felt B - nC5*	0.004	36.050	72.151	629.900	196.450	33.741	0.304	0.251
Felt B - C6*	0.005	68.750	84.800	667.400	234.250	29.688	0.370	0.296
Felt B - C7*	0.007	91.950	91.000	741.400	254.887	34.580	0.450	0.453
Felt B - C8*	0.006	116.750	104.600	762.900	278.975	30.456	0.480	0.493
Felt B - C9*	0.003	142.250	120.200	772.400	301.598	26.308	0.536	0.538
Felt B - C10*	0.002	165.850	134.000	786.189	320.808	24.039	0.580	0.576
Felt B - C11*	0.002	187.250	147.000	798.664	337.702	22.440	0.624	0.612
Felt B - C12*	0.001	208.350	161.000	810.051	354.585	21.046	0.675	0.650
Felt B - C13-C14*	0.002	236.627	182.018	825.236	378.315	19.469	0.758	0.707
Felt B - C15-C16*	0.002	274.121	213.486	843.345	410.175	17.781	0.887	0.787
Felt B - C17-C19*	0.002	311.880	249.219	862.572	443.513	16.602	1.043	0.874
Felt B - C20+*	0.004	430.133	377.497	920.750	563.383	15.019	1.819	1.133

Field C - C20+ characterisation								
Component	Molfrac	NBP	MW	Liq Den	T_c	P_c	V_c	Accentricity
	-	C	g/mol	kg/m3	C	bara	m3/kmol	-
Felt C - N2*	0.002	-195.750	28.014	804.000	-146.950	33.944	0.090	0.040
Felt C - CO2*	0.023	-78.500	44.010	809.000	31.050	73.765	0.094	0.225
Felt C - C1*	0.270	-161.550	16.043	300.000	-82.550	46.002	0.099	0.008
Felt C - C2*	0.070	-88.550	30.070	356.700	32.250	48.839	0.148	0.098
Felt C - C3*	0.086	-42.050	44.097	506.700	96.650	42.455	0.203	0.152
Felt C - iC4*	0.016	-11.750	58.124	562.100	134.950	36.477	0.263	0.176
Felt C - nC4*	0.051	-0.450	58.124	583.100	152.050	37.997	0.255	0.193
Felt C - iC5*	0.018	27.850	72.151	623.300	187.250	33.843	0.306	0.227
Felt C - nC5*	0.029	36.050	72.151	629.900	196.450	33.741	0.304	0.251
Felt C - C6*	0.033	68.750	84.900	666.800	234.250	29.688	0.370	0.296
Felt C - C7*	0.053	91.950	91.000	741.400	254.887	34.580	0.450	0.453
Felt C - C8*	0.051	116.750	105.000	761.600	279.334	30.211	0.484	0.494
Felt C - C9*	0.035	142.250	120.300	772.400	301.726	26.282	0.536	0.538
Felt C - C10*	0.024	165.850	134.000	786.398	320.842	24.051	0.580	0.576
Felt C - C11*	0.022	187.250	147.000	799.061	337.766	22.462	0.624	0.612
Felt C - C12*	0.020	208.350	161.000	810.621	354.677	21.076	0.675	0.650
Felt C - C13-C14*	0.034	236.788	182.144	826.117	378.580	19.500	0.757	0.707
Felt C - C15-C16*	0.028	274.264	213.620	844.490	410.479	17.823	0.887	0.787
Felt C - C17-C19*	0.034	312.159	249.509	864.100	443.997	16.652	1.043	0.874
Felt C - C20+*	0.102	458.772	413.577	936.366	598.386	14.968	2.098	1.169

Appendix L – C10+ fluid characterisation

The C10+ fluid characterisation for field A, B and C is shown in the tables below:

Field A - C10+ characterisation								
Component	Molfrac	NBP	MW	Liq Den	T_c	P_c	V_c	Accentricity
	-	C	g/mol	kg/m3	C	bara	m3/kmol	-
Felt A -N2*	0.004	-195.750	28.014	804.000	-146.950	33.944	0.090	0.040
Felt A - CO2*	0.040	-78.500	44.010	809.000	31.050	73.765	0.094	0.225
Felt A - C1*	0.722	-161.550	16.043	300.000	-82.550	46.002	0.099	0.008
Felt A - C2*	0.089	-88.550	30.070	356.700	32.250	48.839	0.148	0.098
Felt A - C3*	0.043	-42.050	44.097	506.700	96.650	42.455	0.203	0.152
Felt A - iC4*	0.009	-11.750	58.124	562.100	134.950	36.477	0.263	0.176
Felt A - nC4*	0.016	-0.450	58.124	583.100	152.050	37.997	0.255	0.193
Felt A - iC5*	0.007	27.850	72.151	623.300	187.250	33.843	0.306	0.227
Felt A - nC5*	0.008	36.050	72.151	629.900	196.450	33.741	0.304	0.251
Felt A - C6*	0.009	68.750	85.400	664.700	234.250	29.688	0.370	0.296
Felt A - C7*	0.013	91.950	91.400	738.800	255.105	34.156	0.455	0.454
Felt A - C8*	0.012	116.750	104.000	765.200	278.491	30.856	0.475	0.491
Felt A - C9*	0.007	142.250	119.200	776.200	300.934	26.823	0.527	0.535
Felt A - C10+*	0.019	272.242	195.000	842.000	412.857	19.292	0.964	0.795

Field B - C10+ characterisation								
Component	Molfrac	NBP	MW	Liq Den	T_c	P_c	V_c	Accentricity
	-	C	g/mol	kg/m3	C	bara	m3/kmol	-
Felt B - N2*	0.007	-195.750	28.014	804.000	-146.950	33.944	0.090	0.040
Felt B - CO2*	0.024	-78.500	44.010	809.000	31.050	73.765	0.094	0.225
Felt B - C1*	0.820	-161.550	16.043	300.000	-82.550	46.002	0.099	0.008
Felt B - C2*	0.058	-88.550	30.070	356.700	32.250	48.839	0.148	0.098
Felt B - C3*	0.033	-42.050	44.097	506.700	96.650	42.455	0.203	0.152
Felt B - iC4*	0.005	-11.750	58.124	562.100	134.950	36.477	0.263	0.176
Felt B - nC4*	0.010	-0.450	58.124	583.100	152.050	37.997	0.255	0.193
Felt B - iC5*	0.003	27.850	72.151	623.300	187.250	33.843	0.306	0.227
Felt B - nC5*	0.004	36.050	72.151	629.900	196.450	33.741	0.304	0.251
Felt B - C6*	0.005	68.750	84.800	667.400	234.250	29.688	0.370	0.296
Felt B - C7*	0.007	91.950	91.000	741.400	254.887	34.580	0.450	0.453
Felt B - C8*	0.006	116.750	104.600	762.900	278.975	30.456	0.480	0.493
Felt B - C9*	0.003	142.250	120.200	772.400	301.598	26.308	0.536	0.538
Felt B - C10+*	0.015	326.161	237.000	866.000	463.929	17.547	1.251	0.907

Field C - C10+ characterisation								
Component	Molfrac	NBP	MW	Liq Den	T_c	P_c	V_c	Accentricity
	-	C	g/mol	kg/m3	C	bara	m3/kmol	-
Felt C - N2*	0.002	-195.750	28.014	804.000	-146.950	33.944	0.090	0.040
Felt C - CO2*	0.023	-78.500	44.010	809.000	31.050	73.765	0.094	0.225
Felt C - C1*	0.270	-161.550	16.043	300.000	-82.550	46.002	0.099	0.008
Felt C - C2*	0.070	-88.550	30.070	356.700	32.250	48.839	0.148	0.098
Felt C - C3*	0.086	-42.050	44.097	506.700	96.650	42.455	0.203	0.152
Felt C - iC4*	0.016	-11.750	58.124	562.100	134.950	36.477	0.263	0.176
Felt C - nC4*	0.050	-0.450	58.124	583.100	152.050	37.997	0.255	0.193
Felt C - iC5*	0.019	27.850	72.151	623.300	187.250	33.843	0.306	0.227
Felt C - nC5*	0.029	36.050	72.151	629.900	196.450	33.741	0.304	0.251
Felt C - C6*	0.033	68.750	84.900	666.800	234.250	29.688	0.370	0.296
Felt C - C7*	0.053	91.950	91.000	741.400	254.887	34.580	0.450	0.453
Felt C - C8*	0.051	116.750	105.000	761.600	279.334	30.211	0.484	0.494
Felt C - C9*	0.035	142.250	120.300	772.400	301.726	26.282	0.536	0.538
Felt C - C10+*	0.264	371.024	274.490	889.000	511.099	16.799	1.563	0.989

Appendix M – Future allocation profiles

The future allocation profiles for field A, B and C for year 8, 10 and 12 are shown in the tables below:

Field A - Future allocation						
Year	Gas	Oil	Water	*GOR*	Inlet pressure	Gas Lift
	Sm3/d	Sm3/sd	Sm3/d	*Sm3/Sm3*	bar	kSm3/d
8	2238890	961.95	494.50	*2327*	38	-
10	1604748	632.30	116.30	*2538*	38	-
12	1400900	518.28	118.98	*2703*	32	-

Field B - Future allocation						
Year	Gas	Oil	Water	*GOR*	Inlet pressure	Gas Lift
	Sm3/d	Sm3/sd	Sm3/d	*Sm3/Sm3*	bar	kSm3/d
8	11168145	3 477.07	2 192.08	*3212*	38	300
10	10759291	2 397.68	1 263.41	*4487*	38	100
12	9380462	1 560.74	768.52	*6010*	32	50

Field C - Future allocation						
Year	Gas	Oil	Water	*GOR*	Inlet pressure	Gas Lift
	Sm3/d	Sm3/sd	Sm3/d	*Sm3/Sm3*	bar	MSm^3/d
8	167432	1 342	0	*125*	38	0.05
10	293621	2 373	0	*124*	38	0.14
12	255732	2 075	14	*123*	32	0.32

Appendix N – Future allocation ORF result for year 10 and 12

The following tables shown the ORFs for field A, B and C for the future allocation for year 10 and 12.

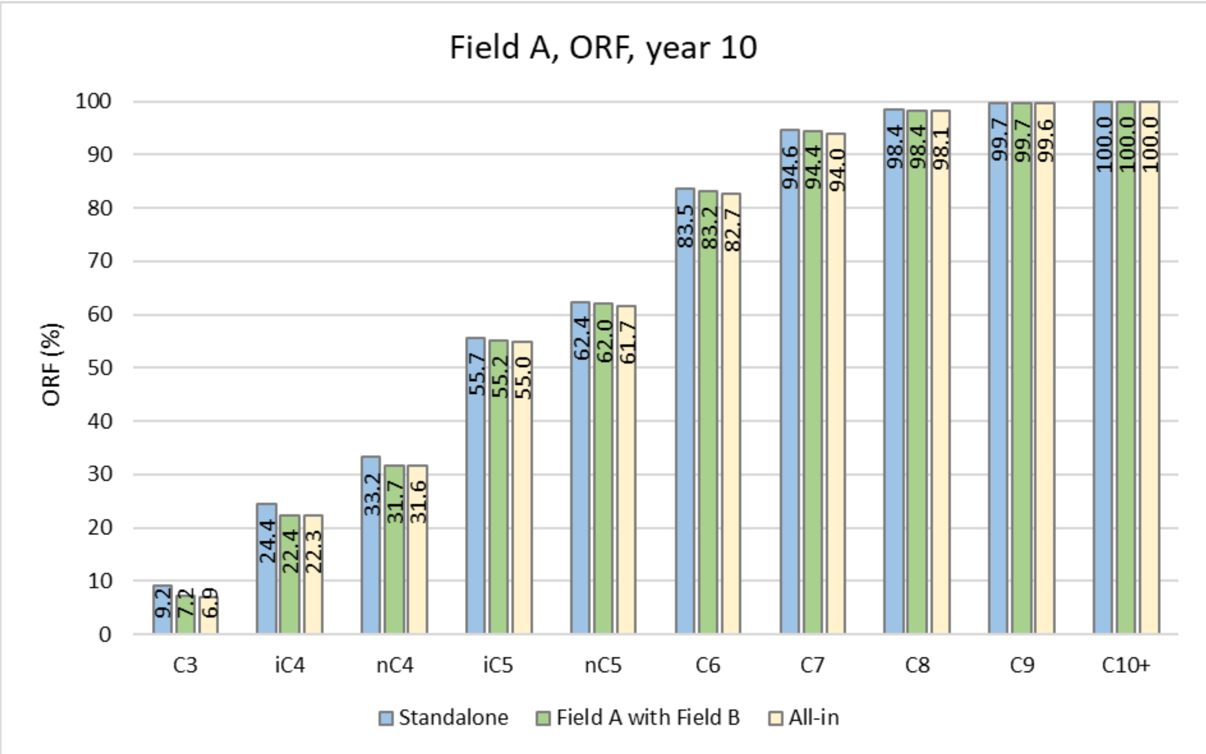

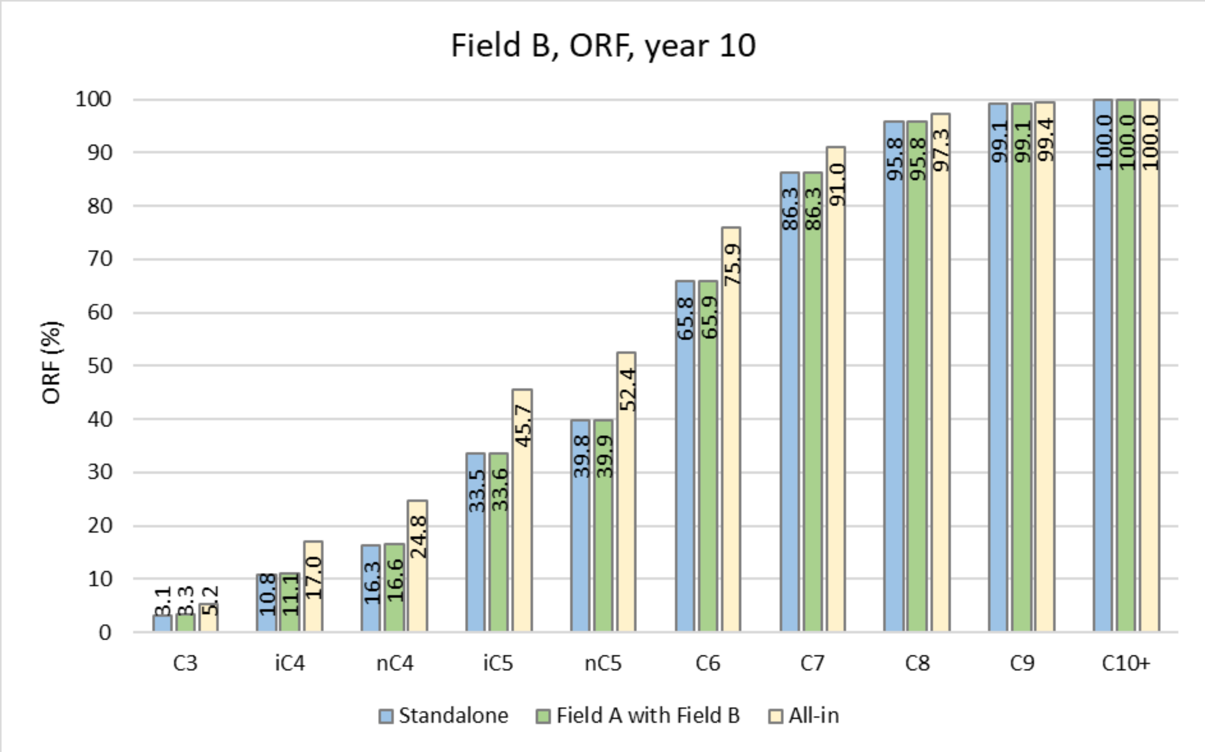
Field B, ORF, year 10
ORF (%)
100
90
80
70
60
50
40
30
20
10
0
3.1
3.3
5.2
10.8
11.1
17.0
16.3
16.6
24.8
33.5
33.6
45.7
39.8
39.9
52.4
65.8
65.9
75.9
86.3
86.3
91.0
95.8
95.8
97.3
99.1
99.1
99.4
100.0
100.0
100.0
C3
iC4
nC4
iC5
nC5
C6
C7
C8
C9
C10+
Standalone
Field A with Field B
All-in

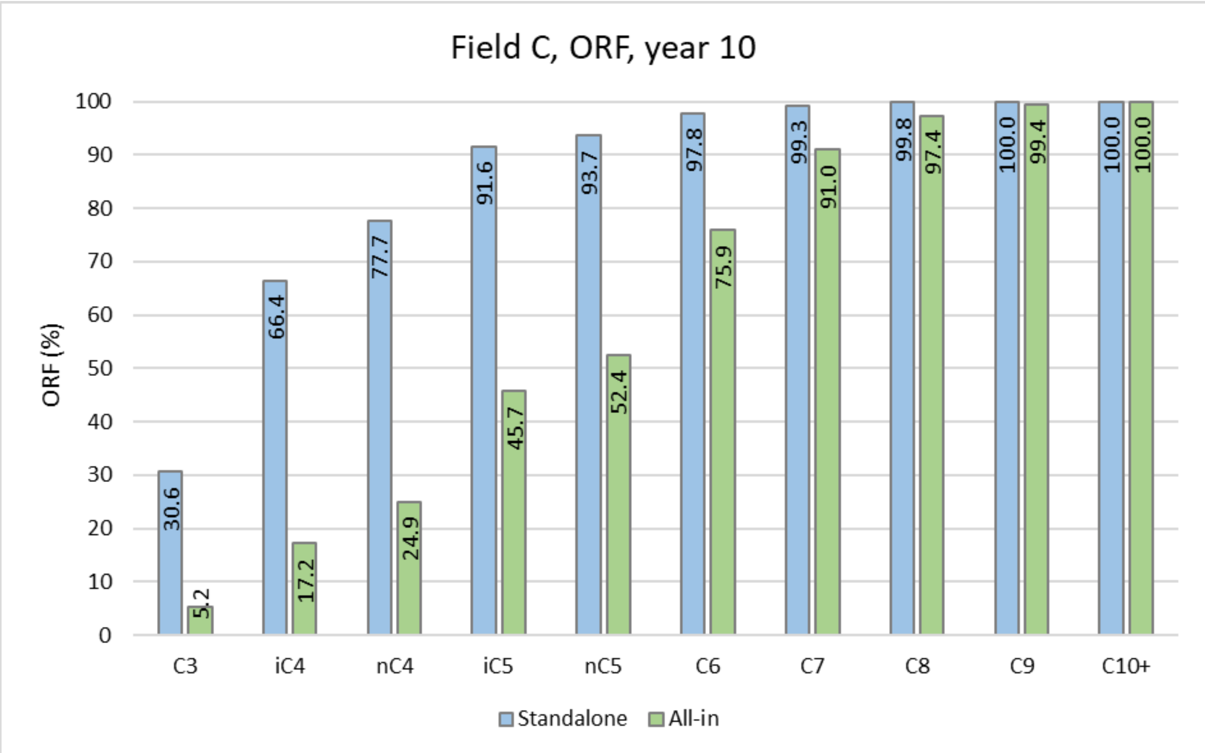
Field C, ORF, year 10
ORF (%)
100
90
80
70
60
50
40
30
20
10
0
30.6
5.2
66.4
17.2
77.7
24.9
91.6
45.7
93.7
52.4
97.8
75.9
99.3
91.0
99.8
97.4
100.0
99.4
100.0
100.0
C3
iC4
nC4
iC5
nC5
C6
C7
C8
C9
C10+
Standalone
All-in

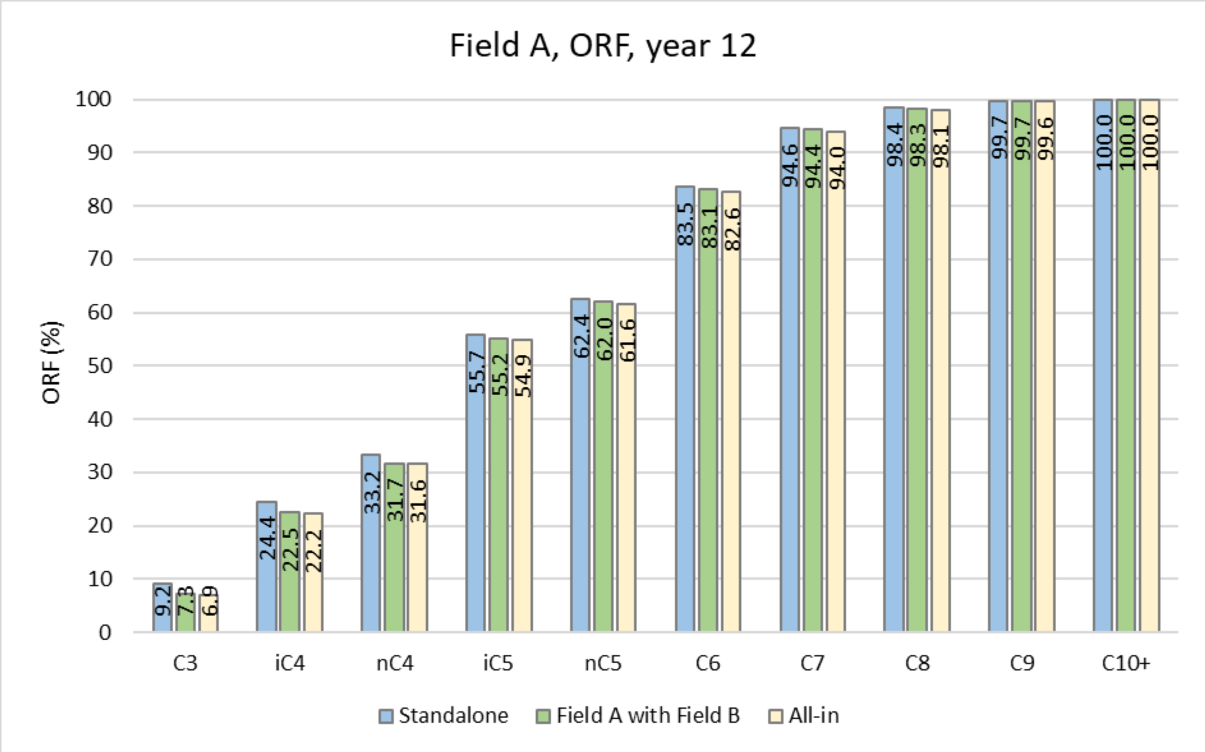
Field A, ORF, year 12
ORF (%)
100
90
80
70
60
50
40
30
20
10
0
C3
iC4
nC4
iC5
nC5
C6
C7
C8
C9
C10+
9.2
7.3
6.9
24.4
22.5
22.2
33.2
31.7
31.6
55.7
55.2
54.9
62.4
62.0
61.6
83.5
83.1
82.6
94.6
94.4
94.0
98.4
98.3
98.1
99.7
99.7
99.6
100.0
100.0
100.0
Standalone
Field A with Field B
All-in

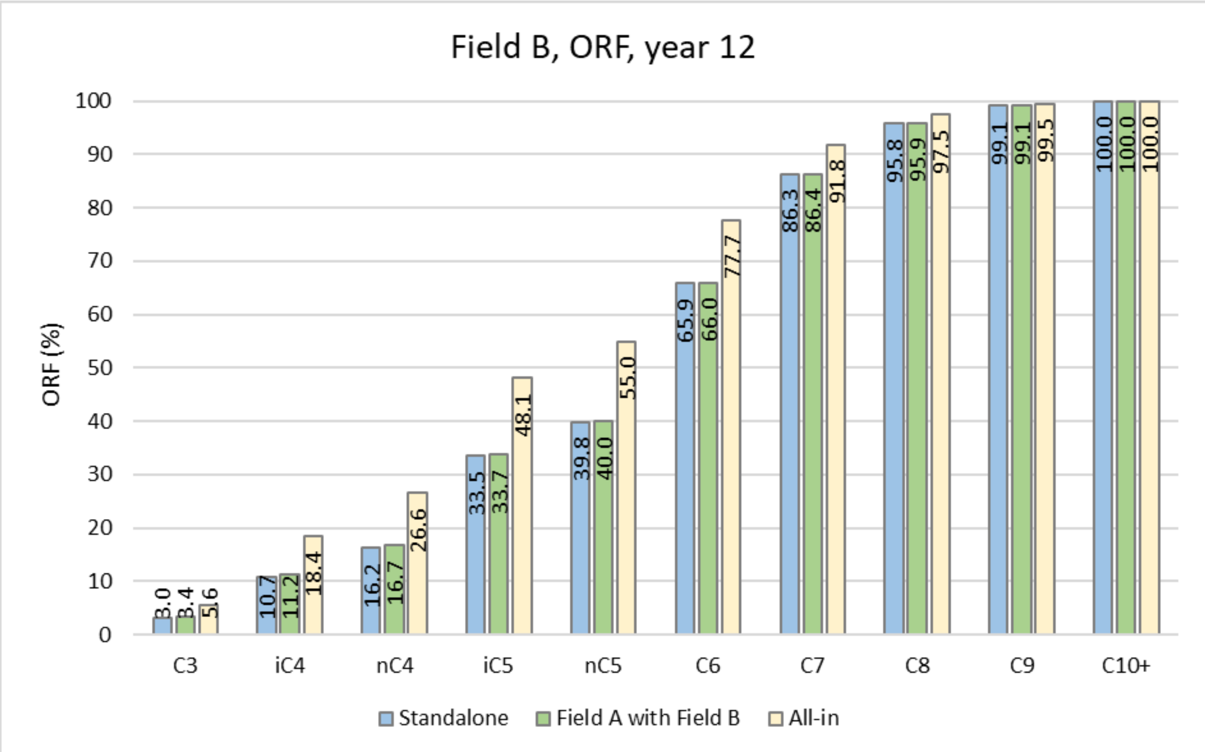
Field B, ORF, year 12
ORF (%)
100
90
80
70
60
50
40
30
20
10
0
C3
iC4
nC4
iC5
nC5
C6
C7
C8
C9
C10+
3.0
3.4
5.6
10.7
11.2
18.4
16.2
16.7
26.6
33.5
33.7
48.1
39.8
40.0
55.0
65.9
66.0
77.7
86.3
86.4
91.8
95.8
95.9
97.5
99.1
99.1
99.5
100.0
100.0
100.0
Standalone
Field A with Field B
All-in

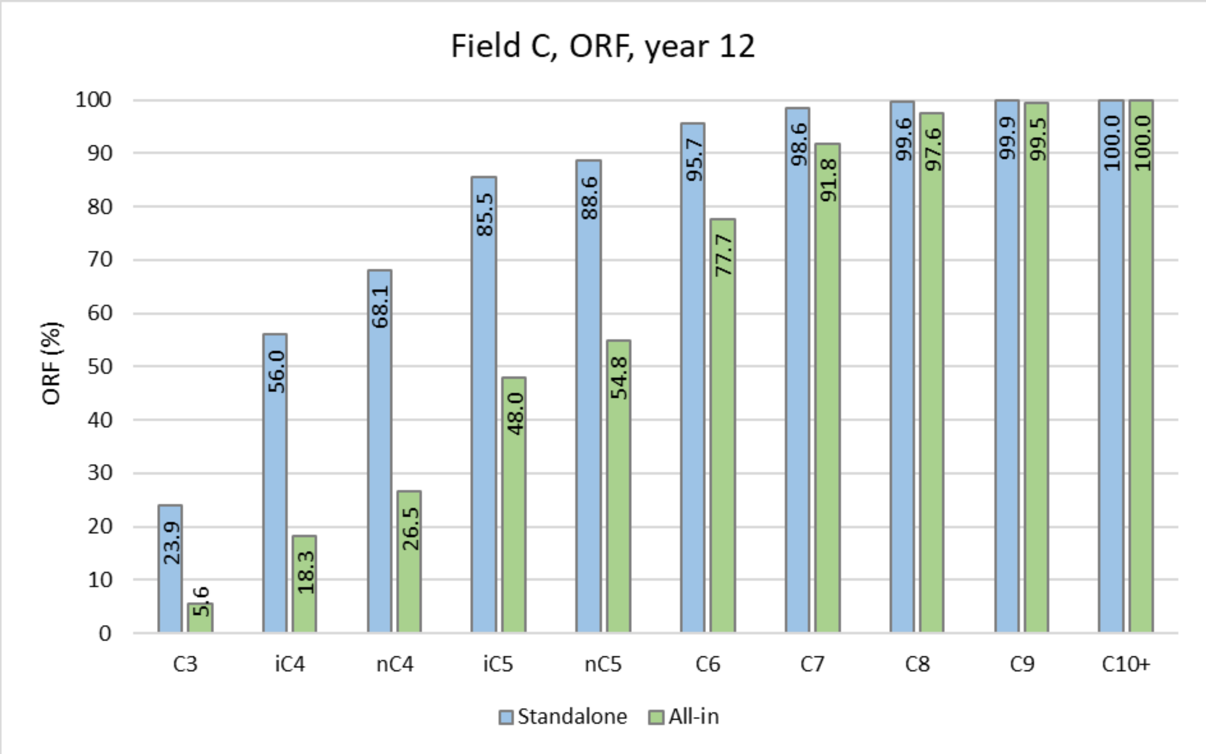
Field C, ORF, year 12
ORF (%)
100
90
80
70
60
50
40
30
20
10
0
C3
iC4
nC4
iC5
nC5
C6
C7
C8
C9
C10+
23.9
5.6
56.0
18.3
68.1
26.5
85.5
48.0
88.6
54.8
95.7
77.7
98.6
91.8
99.6
97.6
99.9
99.5
100.0
100.0
Standalone
All-in

Appendix O – UniSim GOR model

The model for the GOR tuning is developed as follows:

1) A simplified model of the process is created upstream the different fields well inflow. As shown in the figure below:

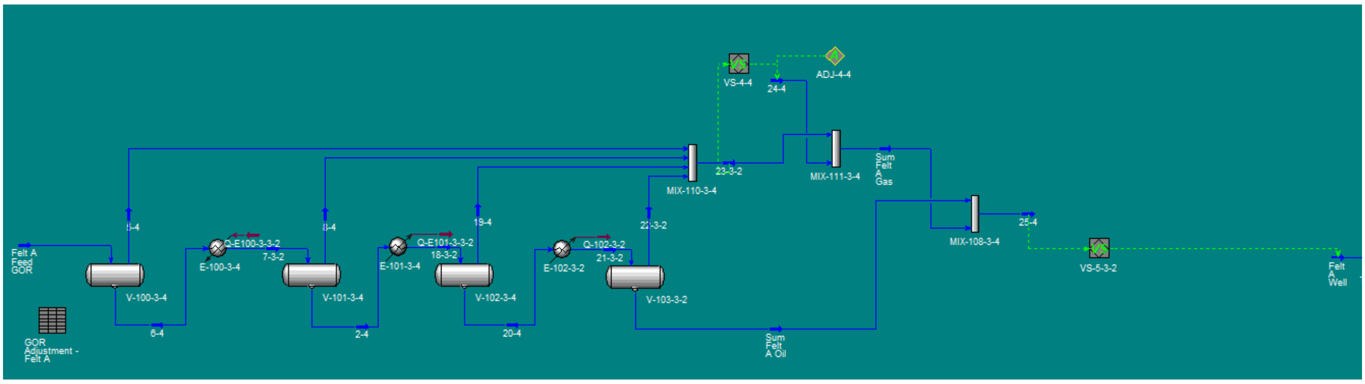

2) A separate sheet is added to tune on the GOR value. This sheet is shown in the figure below:

GOR Adjustment - Felt A

Current Cell

A1 Variable: Angles in: Rad

	A	B	C	D	E
1					
2	CONDENSATE				
3		Simulated Prod. Condensate	Simulated Prod. Condensate	Measured Oil Production	Diff.
4		Sm3/h	Sm3/d	Sm3/d	%
5	Felt A	39.90 m3/h	957.6	961.9	-0.45 %
6					
7	GAS				
8		Simulated Produced Gas	Simulated Produced Gas	Measured Gas Production	Diff.
9		Sm3/h	MSm3/d	MSm3/d	%
10	Felt A	9.285e+004 STD_m3/h	2.228	2.239	-0.47 %
11					
12					
13		Sm3/h	Sm3/d		
14	Simulated Oil (GOR sim)	19.71 m3/h	473.0		
15					
16	Simulated Gas (GOR sim)	4.935e+004 STD_m3/h	1.184e+006		
17					
18					
19		Measured	Simulated	Total Simulated	Diff.
20		Sm3/Sm3	Sm3/Sm3	Sm3/Sm3	%
21	GOR	2327	2504	2327	-0.02 %
22					
23	Simulated Well Feed	5.985e+004 kg/h			
24					
25	Upscaling Factor	2.034			
26					
27	Upscaled feed rate	1.217e+005 kg/h			

Connections | Parameters | Formulas | **Spreadsheet** | Calculation Order | Initialize From | User Variables | Notes

3) The C5 and C10 fields include the simulated gas and condensate production over the total process (not the simplified case). These values are compared to the measured values and the difference is calculated.
   In D21 the GOR for the total process is calculated.
   For the simplified case, the gas and condensate are shown in C14 and C16. The GOR for the simplified model is calculated using these values and are shown in C21.
   The adjuster (ADJ-4-4) on the stream mixed into the gas stream for the simplified case, adjust its flow to match the GOR on the total process to the measured GOR.
   The gas and condensate on the simplified case are mixed, and the composition in this stream is exported to the Field A Well stream.

   The mass flow into the simplified process is guessed in B23. An upscaling factor is calculated using D5/C14. The upscaled feed rate is calculated in B27, and this value is exported as the Felt A Well mass flow.

Appendix P – Building the ProMax model

The procedure for building the ProMax model is as follows:

1) The EOS is set to SRK as shown in the figure below:

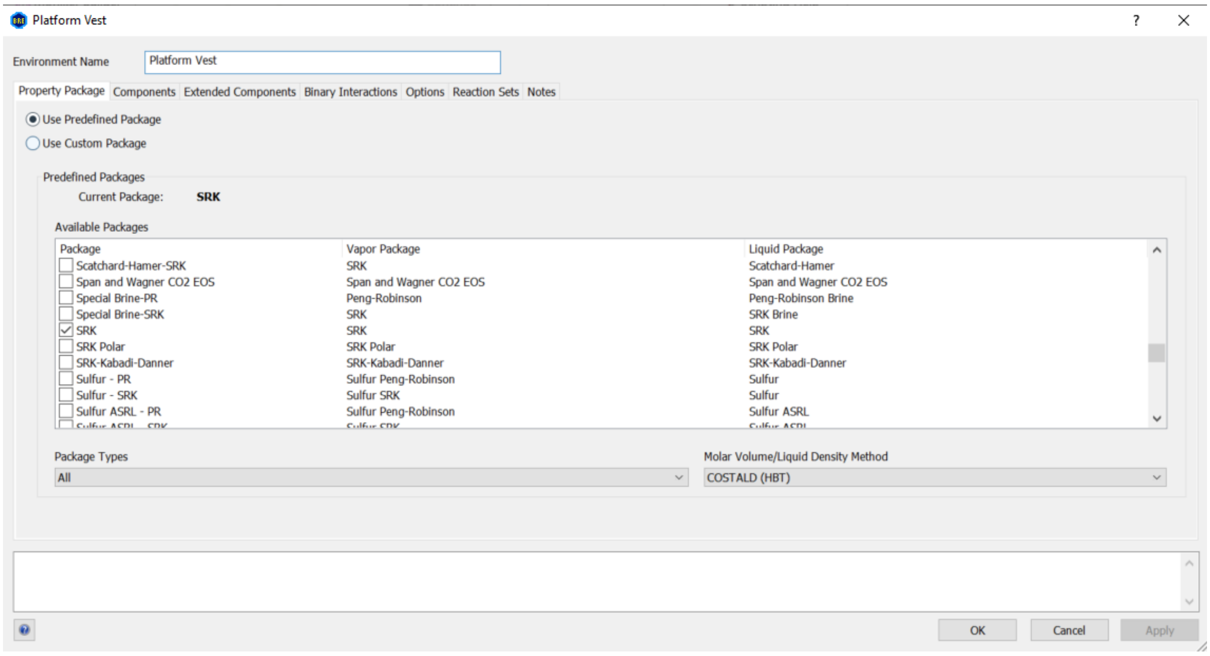

2) The hypothetical components (the C6+ components) are added as single oils as shown in the figure below:

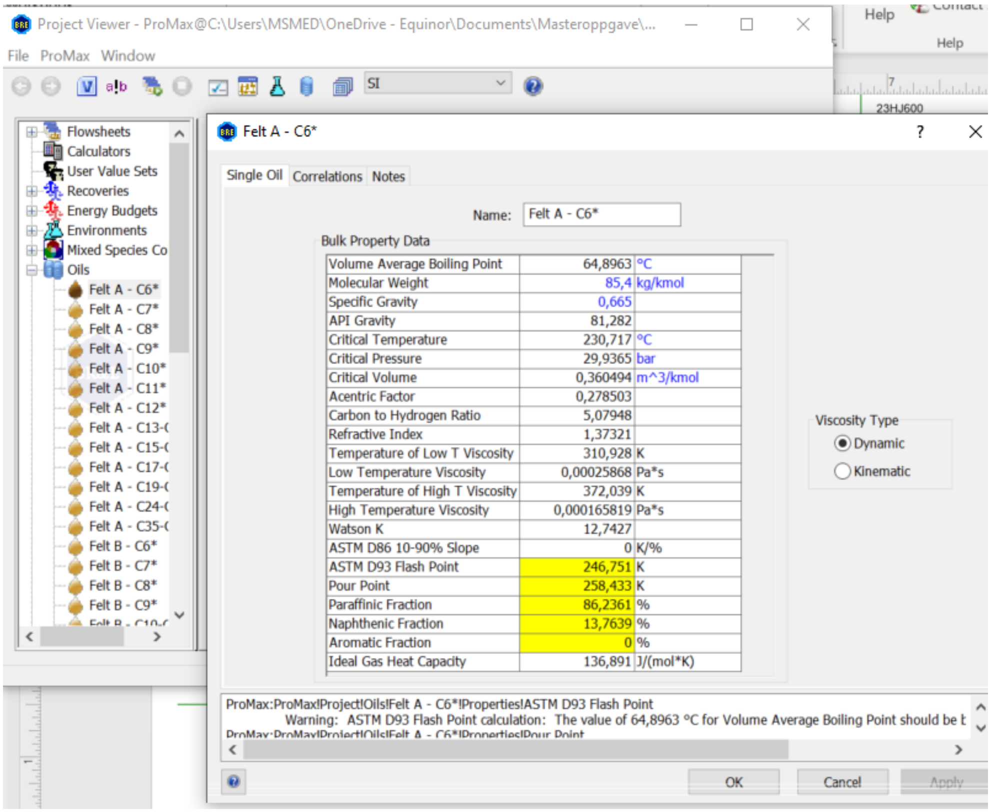

3) The component list is created with library components for components lower than C6, as shown in the figure below:

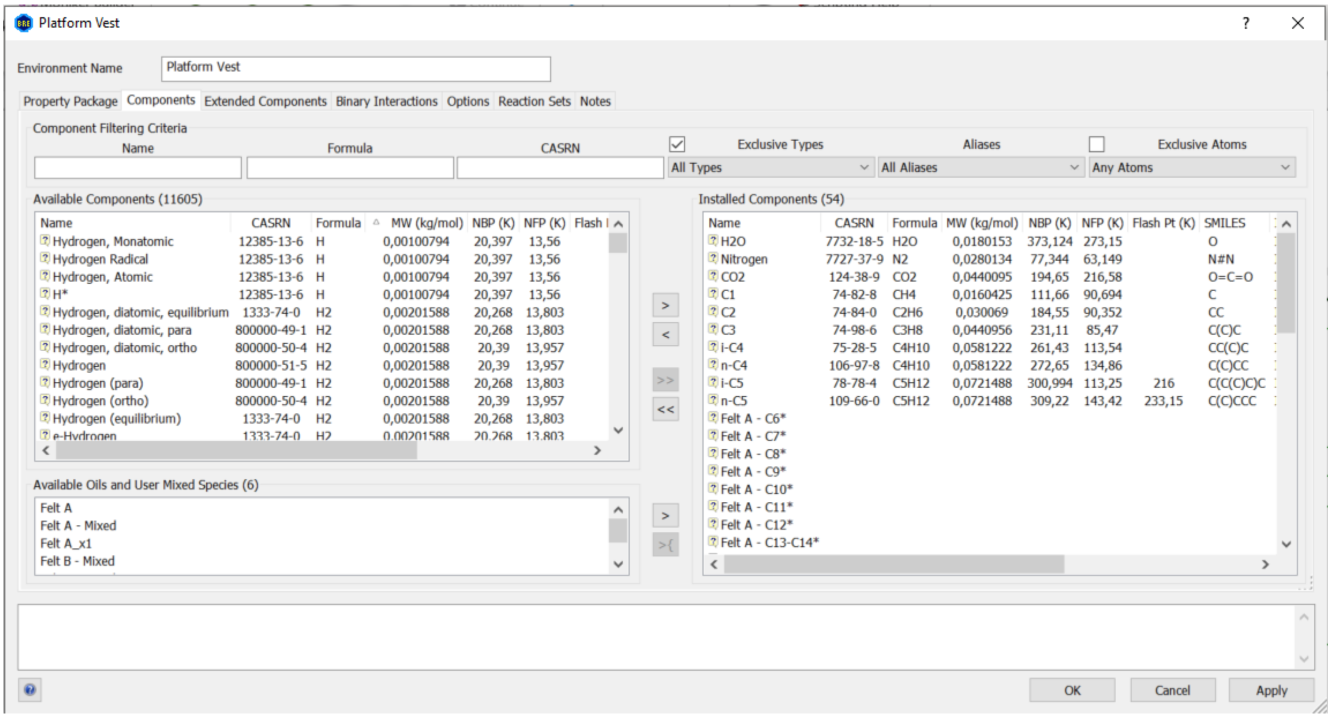

4) The model is built with process equipment using ProMax shapes as shown in the figure below:

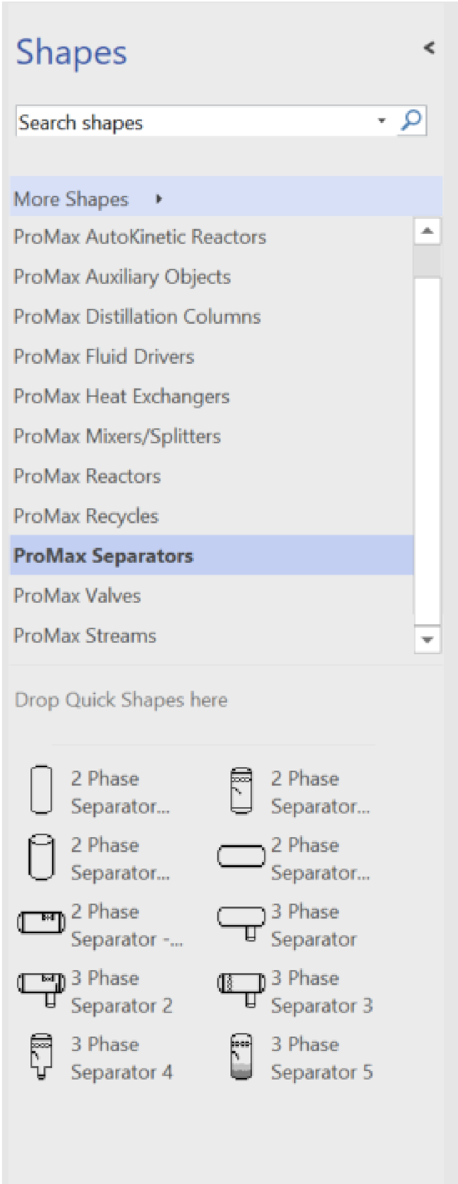

5) The finished model is shown in Appendix H – ProMax model.
6) ProMax comes with a excel interface, but due to time limitation spreadsheets where not made for the ProMax model. Instead, the results were read directly from the different product streams.

Appendix Q – Allocation methods calculation

1) By Difference

By difference	
Inputs	Quantites (ton/d):
Measured export gas (tonne/d)	11012.02
Field B estimate - gas	9271.90
Field A estimate - gas	1586.36
Measured export oil (tonne/d)	4575.28
Field B estimate - oil	2773.69
Field A estimate - oil	721.20
Calculations	
Q - Produced gas	11012.02
Q1 - Produced gas allocated to Field C	153.76
Q - Produced oil	4575.28
Q1 - Produced oil allocated to Field C	1080.38

2) Pro-Rata

Pro rata	
Inputs	Quantites (ton/d):
Measured export gas (tonne/d)	11012.02
Field A estimate - gas	1586.36
Field B estimate - gas	9271.90
Field C estimate - gas	127.70
Gas estimation	10985.96
Measured export oil (tonne/d)	4575.28
Field A estimate - oil	721.20
Field B estimate - oil	2773.69
Field C estimate - oil	1106.62
Oil estimation	4601.51
Calculations	
Field A calculated - gas	1590.12
Field B calculated - gas	9293.89
Field C calculated - gas	128.01
Field A calculated - oil	717.09
Field B calculated - oil	2757.87
Field C calculated - oil	1100.31

3) ORF method

	Year 8		
Standalone ORF	Field A	Field B	Field C
N2	0.0	0.0	0.0
CO2	0.3	0.1	0.9
C1	0.0	0.0	0.1
C2	1.2	0.3	4.1
C3	9.2	3.0	33.2
iC4	24.4	10.7	69.0
nC4	33.2	16.1	79.7
iC5	55.8	33.1	92.7
nC5	62.4	39.5	94.6
C6	83.5	65.6	98.3
C7	94.6	86.1	99.5
C8	98.4	95.8	99.9
C9	99.7	99.1	100.0
C10+	100.0	100.0	100.0

	Year 8		
Inflow, tonn/d	Field A	Field B	Field C
N2	10.2	94.9	0.8
CO2	142.8	518.3	11.7
C1	940.3	6446.7	49.4
C2	218.0	855.8	23.9
C3	155.6	707.6	43.3
iC4	42.4	138.8	10.7
nC4	77.4	298.4	33.6
iC5	40.3	117.8	14.9
nC5	46.4	157.4	23.5
C6	65.7	197.5	32.0
C7	98.9	305.6	54.8
C8	104.5	301.6	60.6
C9	68.4	202.7	47.9
C10+	296.6	1702.3	826.6
SUM	**2307.5**	**12045.5**	**1233.6**

Allocation basis, oil, tonn/d	Year 8		
	Field A	Field B	Field C
N2	0.0	0.0	0.0
CO2	0.4	0.3	0.1
C1	0.3	0.5	0.0
C2	2.6	2.5	1.0
C3	14.3	21.5	14.4
iC4	10.4	14.9	7.4
nC4	25.7	48.2	26.8
iC5	22.5	39.0	13.8
nC5	29.0	62.2	22.2
C6	54.9	129.5	31.5
C7	93.6	263.2	54.5
C8	102.8	288.8	60.5
C9	68.2	200.9	47.9
C10+	296.5	1702.1	826.6
SUM	**721.2**	**2773.7**	**1106.6**

Inputs	Quantites (ton/d)
Measured export gas (tonne/d)	11012.02
Measured export oil (tonne/d)	4575.28
Imbalance, oil	-26.19
Imbalance, Gas	0.70

Allocated values, oil, ton/d:	Year 8		
	Field A	Field B	Field C
SUM	**721.2**	**2755.0**	**1099.2**

Allocation basis, Gas, ton/d:	Year 8		
	Field A	Field B	Field C
SUM	1586.3	9290.5	134.5

Allocated values, Gas, ton/d:	Year 8		
	Field A	Field B	Field C
SUM	**1586.4**	**9291.1**	**134.5**